

Parametric design of a grid shell
roof over existing buildings,
with a focus on connection design

Fiori ISUFI
November 2021

PARAMETRIC DESIGN OF A GRID SHELL ROOF
OVER EXISTING BUILDINGS, WITH A FOCUS ON
CONNECTION DESIGN

A thesis submitted to the Delft University of Technology in partial
fulfillment
of the requirements for the degree of

Master of Science in Building Engineering

by

Fiori Isufi

November 2021



octatube

Fiori Isufi: *Parametric design of a grid shell roof over existing buildings, with a focus on connection design* (2021)

Student number: 5030846

Department of Materials, Mechanics, Management & Design (3MD)
Faculty of Civil Engineering & Geosciences
Delft University of Technology

Supervisors: Dr. ir. HR Roel Schipper - TU Delft
Prof. dr. Mauro Overend - TU Delft
Dr. Florentia Kavoura - TU Delft
Ir. Joey Janssen - Octatube

ABSTRACT

The motivation of the thesis relates to designing grid shells over existing buildings. Grid shell roofs are a way to enclose an existing space structurally efficiently and have minimal interference with the surroundings from an architectural and environmental perspective. The solution results in less material usage than shell structures, and transparency, allowing for more daylight.

Joints play a significant role in the design of grid shells, including structural and economic efficiency. It is common practice in engineering to design rectangular patterned grid shells with rigid joints. A rectangular shape is easy to deform by applying load; hence, it needs stiffness and rigidity. On the other hand, triangular patterned grid shells are designed with pinned joints as the triangular shape is stiff enough and does not need additional stiffness in the joints. Considering these points, the following research question arises:

How can connection stiffness in the parametric design of grid shell roof structures lead to more efficiency for existing buildings?

To answer this research question, the thesis procedure is divided into five steps. First, a literature study provides a clear understanding of grid shell design principles and their joints. Based on the out-of-plane rotational stiffness, a classification system for joints in grid shells is suggested. The Matrix Method is used to find the boundary for rigid stiffness. The boundary for pinned stiffness is found by studying the influence of the stiffness decreasing in a logarithmic scale over the bending moment distribution.

Furthermore, to explore the influence of the stiffness over the design of the grid shell, a parametric model is created. The study investigates the structural behavior of a triangular and rectangular grid pattern. Therefore, a comparison of the influence of the joint between a rigid and non-rigid shape will be made. The design criteria include the Ultimate Limit State (ULS) and Serviceability Limit State (SLS). To quantify the results, a case study is applied. The C30 Shell project, now designed and completed by Octatube, will be used as a reference to apply the theory of this thesis.

Based on the Eurocode checks, conclusions are drawn related to the effect of the stiffness. The grid shell with rectangular pattern is significantly affected in both Ultimate and Serviceability Limit State with alternation of stiffness in logarithmic scale. However, the stiffness decrease was proved to have no significant effect over the maximum displacements (SLS) but only over the stress distribution for the triangular pattern. Therefore, to find the optimal solution for a grid shell with a triangular pattern, only the ULS unity checks need to be compared. On the contrary, for grid shells with a rectangular pattern, a balance needs to be found between ULS and SLS unity checks.

Following this conclusion, the study is focused on the grid shell with a rectangular pattern. Joints are designed for different stiffness to visualize the difference on how to achieve these stiffness in real-life engineering practice. The FEM software IDEA StatiCa is used to design the joints. The joints follow a similar concept with a rectangular hollow section box in the middle where all the joints are connected. While the required stiffness is decreased approaching semi-rigid and pinned, the dimensions of the joint components are also decreased. The reduction of material

used also makes the structure more lightweight and less expensive in terms of material.

Finally, to answer the research question, an optimization procedure has been conducted. Octopus, an optimization algorithm within Grasshopper, is used. The optimization procedure is divided into four steps. The first step was to find an optimal cross-section for each of the stiffness studied. This step focuses on where the solution with the smallest cross-section and lower stiffness can be found. By finding the smallest cross-section, the material used is optimized on a global scale, being one step closer to the smaller self-weight of the roof structure. The second step aims to find the lowest stiffness possible for the cross-section obtained in step 1. This objective is related to design considerations. By lowering the required stiffness, also the dimensions of the components in the joint can be reduced. Thus the material used is decreased on the local scale. In step three, two smaller cross-sections are iterated for different stiffness to verify that the solution obtained is optimal. The last step consisted in giving an optimal design solution for the connections. Other aspects are considered, such as fabrication practicality and transport limitations.

Two types of connections are designed for the grid shell roof. The first connection is designed using only welding and the second connection uses a combination of bolts and welding. The aim is to avoid welding in situ and prefabricate parts of the roof in the factory within the transportation limitations. The fully welded connections allow the prefabrication of roof components off-site. The bolted ones allow connecting these smaller parts in situ.

Based on this investigation, it can be concluded:

The final solution results in a reduction of the total weight of the joints by approximately 50% from fully rigid to optimal stiffness design. Furthermore, an 8% reduction of the self-weight of the structure is achieved by optimizing joint stiffness. Consequently, it results in reduced imposed loading over the existing building and foundation. This reduction is also beneficial for economic and environmental purposes by being more sustainable in terms of material footprint.

Key words: grid shell, existing building, parametric design, joint stiffness, optimization, case study

ACKNOWLEDGEMENTS

Wings are a constraint that makes
it possible to fly.
— Robert Bringhurst

This document marks the final step towards completing my experience as a Master of Science student in Building Engineering, Faculty of Civil Engineering at Delft University of Technology. After two intense and challenging years. I am one step closer to becoming the building engineer I aspire to be. I would like to acknowledge and express my gratitude to the people who have helped me over the last ten months during my thesis:

First of all, I would like to thank the committee members for their supervision and guidance during my thesis. I am thankful for the willingness of Roel Schipper to answer all the questions that were raised during my thesis and my study at TU Delft. I am very grateful for the input, support, and encouragement of Florentia Kavoura. I want to thank Mauro Overend for his interesting conversations. Furthermore, I would like to express my gratitude to my supervisor from Octatube, Joey Janssen, for his interest in the topic. Your comments and observations steered my research in the right direction.

Thanks to all the friends I met during these two years to turn this personal achievement into a life experience.

Finally, my greatest thanks are to my family for supporting me during these last two years, more than ever. Especially without my mom's help, I could never have been where I am today.

Fiori Isufi
Delft, November 2021

CONTENTS

1	INTRODUCTION	1
	Introduction	1
1.1	Research motivation	1
1.1.1	Terminology	1
1.2	Research question	2
1.3	Research objectives	2
1.4	Research methodology	3
2	LITERATURE REVIEW	6
2.1	Grid shells	6
2.1.1	Shells	6
2.1.2	Grid shells	8
2.1.3	Design principles	8
2.1.4	Grid shells over existing building	10
2.1.5	Case study: C30 Shell	12
2.2	Grid shell joints	13
2.2.1	Importance of joint stiffness	13
2.2.2	Joint classification in grid shells	16
2.3	Conclusions	20
3	PARAMETRIC DESIGN	24
3.1	Grid shell model	24
3.2	Structural analysis	26
3.3	Conclusions	30
4	JOINT STIFFNESS INFLUENCE	31
4.1	Joint stiffness classification	31
4.2	Rectangular pattern	32
4.3	Triangular pattern	39
4.4	Conclusions	43
5	DESIGN OF CONNECTIONS	46
5.1	Connection design	46
5.1.1	Connection design examples	48
5.2	Results & Discussions	49
5.3	Conclusions	56
6	OPTIMIZATION	57
6.1	Optimization procedure	57
6.1.1	Step 1. Optimal cross section	58
6.1.2	Step 2. Optimal stiffness	59
6.1.3	Step 3. Verification	59
6.1.4	Step 4. Optimized connection design	59
6.2	Results & Discussions	63
6.3	Conclusions	63
7	CONCLUSIONS & RECOMMENDATIONS	65
7.1	Conclusions	65
7.2	Recommendations	65
A	APPENDIX A. LITERATURE REVIEW	70
A.0.1	Joint classifications	70
A.0.2	Joint stiffness influence	71
B	APPENDIX B. GRASSHOPPER SCRIPT	73
C	APPENDIX C. JOINT STIFFNESS CLASSIFICATION – MATRIX METHOD	78
D	APPENDIX D. JOINT STIFFNESS INFLUENCE	83
E	APPENDIX E. CONNECTION DESIGN	107

E.1	Rigid connection	107
E.2	Semi-Rigid 1 connection	117
E.3	Semi-Rigid 2 connection	128
E.4	Semi-Rigid 3 connection	141
E.5	Pinned connection	153
F	APPENDIX F. OPTIMAL CONNECTION DESIGN	165
F.1	Connection design with optimal cross section and fully rigid stiffness	165
F.2	Connection design with optimal stiffness and cross section	178
F.2.1	Connection with bolts	178
F.2.2	Connection with welding	191

LIST OF FIGURES

Figure 1.1	Research question and the follow up sub-questions	3
Figure 1.2	Methodology	4
Figure 2.1	Effect of surface curvature	6
Figure 2.2	Corbel arch Hoogenboom [2011]	6
Figure 2.3	Corbel dome Hoogenboom [2011]	7
Figure 2.4	Pantheon dome with an oculus	7
Figure 2.5	Grid shell structures	8
Figure 2.6	Grid shell	9
Figure 2.7	Possible grid patterns	9
Figure 2.8	Examples of grid shells over existing buildings	11
Figure 2.9	Solution for grid shells over existing buildings	11
Figure 2.10	Solution for grid shells over existing buildings	12
Figure 2.11	Solution for grid shells over existing buildings	13
Figure 2.12	Examples of the three types of connections	13
Figure 2.13	Influence of connection stiffness on bending moment diagram along a beam	14
Figure 2.14	Output of Von Mises stresses along the beam supported by pinned and rigid connection	14
Figure 2.15	Different behavior of beams supported by pinned and rigid connection	15
Figure 2.16	Requirements for joint design Van der Linden [2015]	16
Figure 2.17	Illustration of scenarios considered in the optimization Grande et al. [2020]	16
Figure 2.18	Basis for classification of stiffness boundaries	17
Figure 2.19	Geometric relations Welleman [2021]	18
Figure 2.20	Geometric relations Welleman [2021]	18
Figure 2.21	Equilibrium equation Welleman [2021]	18
Figure 2.22	Scenario (a)	19
Figure 2.23	Scenario (b)	20
Figure 2.24	Effect of stiffness alternation on bending moment	21
Figure 2.25	Eurocode classification of stiffness	21
Figure 3.1	Parameters	24
Figure 3.2	Triangular and rectangular shape	25
Figure 3.3	Rectangular pattern	25
Figure 3.4	Triangular pattern	26
Figure 3.5	Initial and equilibrium state of a particle spring Eigenraam [2017]	26
Figure 3.6	Snow load coefficients from Eurocode	28
Figure 3.7	Snow load distribution	28
Figure 3.8	Wind load	29
Figure 3.9	Maximum global deflection	30
Figure 4.1	Result for rectangular pattern	31
Figure 4.2	Result for triangular pattern	32
Figure 4.3	Procedure	33
Figure 4.4	Maximum displacements for serviceability limit state load combination 1	33
Figure 4.5	Maximum displacements for serviceability limit state load combination 1	33
Figure 4.6	Maximum bending stresses for ultimate limit state load combination 1	34

Figure 4.7	Maximum bending stresses for ultimate limit state load combination 1	34
Figure 4.8	Maximum axial stresses for ultimate limit state load combination 1	35
Figure 4.9	Maximum combined stresses for ultimate limit state load combination 1	35
Figure 4.10	Maximum displacements for serviceability limit state load combination 2	36
Figure 4.11	Maximum displacements for serviceability limit state load combination 2	36
Figure 4.12	Maximum bending stresses for ultimate limit state load combination 2	37
Figure 4.13	Maximum bending stresses for ultimate limit state load combination 2	37
Figure 4.14	Maximum axial stresses for ultimate limit state load combination 2	38
Figure 4.15	Maximum combined stresses for ultimate limit state load combination 2	38
Figure 4.16	Governing unity checks for rectangular pattern	38
Figure 4.17	Maximum displacements for serviceability limit state load combination 1	39
Figure 4.18	Maximum displacements for serviceability limit state load combination 1	39
Figure 4.19	Maximum bending stresses for ultimate limit state load combination 1	40
Figure 4.20	Maximum bending stresses for ultimate limit state load combination 1	40
Figure 4.21	Maximum axial stresses for ultimate limit state load combination 1	40
Figure 4.22	Maximum combined stresses for ultimate limit state load combination 1	41
Figure 4.23	Maximum displacements for serviceability limit state load combination 2	41
Figure 4.24	Maximum displacements for serviceability limit state load combination 2	42
Figure 4.25	Maximum bending stresses for ultimate limit state load combination 2	42
Figure 4.26	Maximum bending stresses for ultimate limit state load combination 2	42
Figure 4.27	Maximum axial stresses for ultimate limit state load combination 2	42
Figure 4.28	Maximum combined stresses for ultimate limit state load combination 2	43
Figure 4.29	Governing unity checks for triangular pattern	43
Figure 5.1	Component method explained	46
Figure 5.2	Example	47
Figure 5.3	Examples of connection designed by Octatube	48
Figure 5.4	Location of governing node in ULS 2	49
Figure 5.5	3D model of rigid connection	50
Figure 5.6	Stress distribution of rigid connection	50
Figure 5.7	3D model of semi rigid 1 connection	51
Figure 5.8	Stress distribution of semi rigid 1 connection	52
Figure 5.9	3D model of semi rigid 2 connection	52
Figure 5.10	Stress distribution of semi rigid 2 connection	53
Figure 5.11	3D model of semi rigid 3 connection	54
Figure 5.12	Stress distribution of semi rigid 3 connection	54

Figure 5.13	3D model of pinned connection	55
Figure 5.14	Stress distribution of pinned connection	55
Figure 6.1	Methodology	57
Figure 6.2	Optimization procedure	57
Figure 6.3	Optimization plug-in	58
Figure 6.4	Optimization in Octopus	59
Figure 6.5	Design of the grid shell roof	60
Figure 6.6	3D model of optimal connection with bolts	60
Figure 6.7	Stress distribution of optimal connection with bolts	61
Figure 6.8	3D model of optimal connection welded	62
Figure 6.9	Stress distribution of optimal connection with bolts	62
Figure 6.10	Optimization results	63

LIST OF TABLES

Table 3.1	Material properties of steel S235	27
Table 3.2	Serviceability Limit State (SLS) load combinations	29
Table 3.3	Ultimate Limit State (ULS) load combinations	29
Table 4.1	Joint stiffness classification	32
Table 6.1	Optimal cross section for each stiffness	58

1

INTRODUCTION

1.1 RESEARCH MOTIVATION

Why study grid shells?

Grid shells are known for their geometrical complexity and architectural value. They are an eye-catcher and can turn any building into a point of attraction. From an engineer's point of view, if designed smartly, they can make a structurally efficient solution. They have been used in the past for notable buildings such as exhibitions and pavilions. In some cases, the unique shapes can lead to non-economical solutions due to increased member size or node design. Frei Otto is known for using physical modeling in the preliminary design phases. Since then, computational modeling has advanced giving more possibilities to explore. Almost every shape is possible to design, including non-standard patterns and free form geometry.

Why study grid shells over existing buildings?

Previously are built many open court-yards for buildings. However, every year is seen an increase in demand for more closed space. This is due to lack of space and also due to the weather conditions during the year. Glazed grid shell roofs are a way to enclose an existing space structurally efficiently and have minimal interference with the surrounding from an architectural and environmental perspective. In many of the projects briefly discussed in the following chapter, grid shells are used to create more space, such as offices, libraries, shopping streets, museums.

Why study joints?

Joints play a significant role in the design of grid shells, including structural and economic efficiency. Nevertheless, an optimal connection design of grid shells has not been studied as thoroughly as form-finding methods. It is common practice in engineering to design rectangular patterned grid shells with rigid joints. A rectangular shape is easy to deform by applying load; hence, it needs stiffness and rigidity. On the other hand, triangular patterned grid shells are designed with pinned joints as the triangular shape is stiff enough and does not need additional stiffness in the joints. Additional studies could be conducted on the influence of joint stiffness in the design of a grid shell. Considering that the motivation and focus of this thesis will be on grid shells designed over existing buildings, the main objective is to optimize the stiffness of the joints to have a lighter-weight roof—consequently, smaller superimposed loading on the existing building and foundation.

1.1.1 Terminology

A brief definition of the keywords in the title is given below.

Parametric design in Civil Engineering:

Generation of geometrical shapes by using algorithms driven by input parameters as a digital design means to assess engineering problems. [Van der Linden \[2018\]](#)

Shell:

A three-dimensional double-curved structure that forms an enclosure. The essential features include structural continuity, curvature, and small thickness compared to the radius. Continuity makes it possible to transmit forces in infinitely different

directions. The curvature makes it possible to distribute external loads by in-plane forces. Finally, the small thickness in comparison to span makes these structures lightweight. [Miura and Pelligrino \[2001\]](#)

Grid shell:

A structure that originates from shells, but the material is removed so that a grid pattern is created. Less material usage provides the benefit of a more efficient structure and increases the internal space. [Schober \[2015\]](#)

The function of grid shells is to serve as roof structures, canopy, or full building enclosure. [Patterson \[2011\]](#)

Connection:

The set of physical components that are used to fasten the connected elements mechanically. When the interaction of the connected elements is considered, the concept “joint” is used. [Jaspart and Weynand \[2016\]](#)

1.2 RESEARCH QUESTION

Considering the points mentioned, the research questions in this study will be:

How can connection stiffness in the parametric design of grid shell roof structures lead to more efficiency for existing buildings?

The definition of efficiency in this thesis relates to achieving smaller structural weight of the grid shell, thus resulting in smaller superimposed loading over the existing building and foundation.

1.3 RESEARCH OBJECTIVES

The objective of this Master Thesis is to identify the effect of rotational, out-of-plane joint stiffness in the grid shell design and optimize to obtain a more lightweight roof over existing buildings. To be able to answer the research question and the follow-up sub-questions, the thesis will have the following objectives:

Objective 1. Provide sufficient literature review on the design of shells and grid shells. The focus will be on design approaches and structural performance to have an accurate study in the follow-up stages of the thesis.

- What is a grid shell structure, and what are its structural principles?
- What are the design principles for grid shells over existing structures?

Objective 2. Study of the classification of joint stiffness in steel structures and grid shell structures.

- What is the importance of joint stiffness in a grid shell design according to the literature?
- How can the boundaries between the categories: rigid, semi-rigid, pinned be obtained for a grid shell?
- What is the influence of joint stiffness in a grid shell in terms of ultimate limit state and serviceability limit state?

Objective 3. Design of structural joint models with different stiffness.

- What are the design requirements for joints in grid shell structures?
- How would structural joints of grid shells look in real-life engineering to obtain the different stiffness?

Objective 4. Optimization of cross-section and joint stiffness.

- How can connection stiffness be optimized to have a lighter-weight grid shell roof structure over the existing building?
- What does the optimal joint design look like?

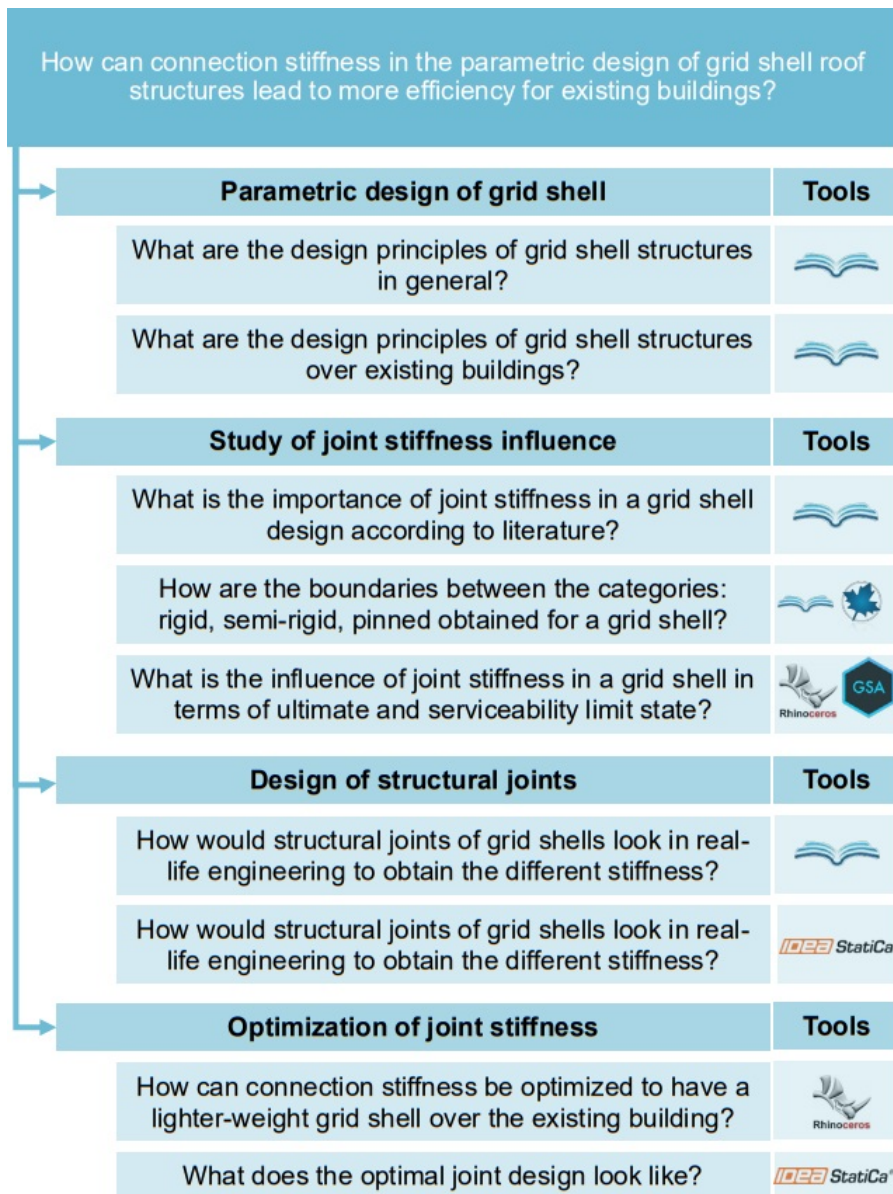


Figure 1.1: Research question and the follow up sub-questions

1.4 RESEARCH METHODOLOGY

In order to solve the research questions and objectives, the thesis is arranged in four steps. An overview of the methodology is given in Figure 1.2.

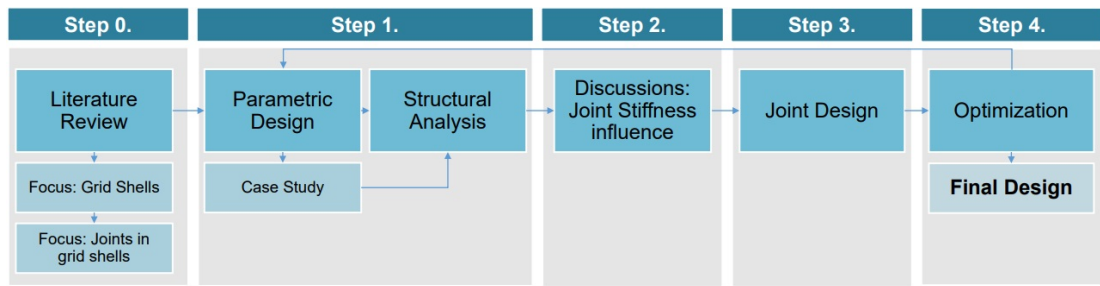


Figure 1.2: Methodology

Step 0. Literature review.

Previous to each step, firstly, one must understand the studies related to the topic. The corresponding sub-questions related to design guidelines of grid shells and joints will be answered. The importance of joint stiffness in standard steel structures such as frames is explained, followed by their influence on grid shells.

Step 1. Parametric model of grid shell roof.

A parametric model will be made in Grasshopper. The parameters include dimensions in x and y directions, divisions of the pattern in the x and y-axis, and rectangular and triangular patterns. The geometry is obtained by using form-finding methods.

After obtaining a geometry that is used to have a double-curved grid shell, the geometry design loop is closed. The structural analysis is also parametrical through linking the Grasshopper model with Oasys GSA. This choice is crucial for the thesis as structural parameters such as the cross-section of members and joint stiffness will change continuously. Thus, performing multiple iterations is less time-consuming. This process was possible by using Geometry Gym plug-ins in Grasshopper.

Step 2. Study of joint stiffness influence.

First, a study and application of classification methods for both structures are conducted. The process is explained in detail, based on the Matrix Method. Afterward, a parametrical study follows to study the influence of alternation of joint stiffness in logarithmic scale in the grid shell design. The basis of the influence is on the structural performance considering serviceability limit state and ultimate limit state conditions. At the end of this step, the choice will be made whether it is essential to continue studying both grid patterns, rigid and non-rigid shapes.

Step 3. Design of connections.

The third step will introduce the use of IDEA StatiCa in this thesis. The FEM software for designing joints is used to design the joints with different stiffness firstly. Then, the design stage is followed by a structural performance for the ultimate limit state. The last stage consists of running a rotational stiffness analysis based on the Eurocode Component method. The result of this analysis verifies whether the aimed stiffness is reached. Finally, the obtained results are discussed to compare the designs on how to achieve the different stiffness and give some practical details of the fabrication.

Step 4. Optimization

The last step of the thesis will end the design with an optimization. The optimization process is conducted in two stages. An optimal design for this thesis is considered to result in the smallest self-weight as a first objective and followed by secondary objectives that consider the practicality and fabrication aspect of the design to make it more realistic and increase the application possibility.

- Stage 1. The cross-section is optimized for the studied stiffness. These results will give some limitations to possible design. The stiffness range where the smallest cross-sections are obtained will follow in the second stage.
- Stage 2. The stiffness is optimized to obtain the smallest possible stiffness. This will result in smaller dimensions required for the joint, thus smaller self-weight. Some other aspects will be considered to validate the design as optimal such as practicality.
- Stage 3. Verification if there is no other optimal solution for a smaller cross-section.
- Stage 4. The final design of joints with the optimal stiffness.

2 | LITERATURE REVIEW

2.1 GRID SHELLS

2.1.1 Shells

As grid shell structures originate from shells, it is essential to understand first the behavior of shell structures. Shells are curved surface elements, which derive their strength from this feature. The essential features of shells include structural continuity, curvature, and small thickness compared to the radius. Continuity makes it possible to transmit forces in infinitely different directions. The curvature makes it possible to distribute external loads by in-plane forces. Since extensional stiffness is always much greater than bending stiffness, even a very thin shell can be very stiff. This form of behavior is described as membrane theory. Finally, the small thickness in comparison to span makes these structures lightweight. [Schueller \[1983\]](#)

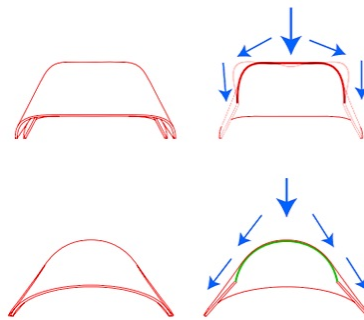


Figure 2.1: Effect of surface curvature

These advantages have been used in ancient Greece civilization in the form of corbel dome tombs. Corbels are created easily from blocks piled over each other, slightly shifted to create the shape of an arch without form-work. The downside of this type of construction was that the height would increase significantly despite no theoretical limitations of the arch dimensions for large spans. Nevertheless, some of the tombs built with this principle in Greece still exist. One of them spans 14.5 m with a radius of 16 m and thickness of 0.8 m. [Hoogenboom \[2011\]](#)

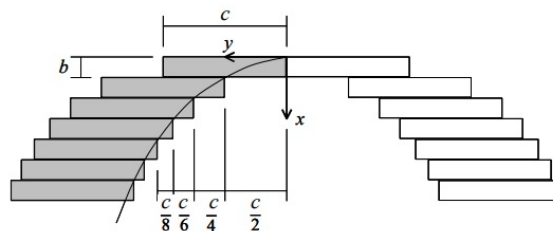


Figure 2.2: Corbel arch [Hoogenboom \[2011\]](#)

The first known shell is the Pantheon in Rome 126 BC, made out of concrete. It is a 43 m diameter and 1.2 m thick dome with an oculus. For centuries after, many large diameter masonry domes were part of major Gothic cathedrals and Renaissance churches. In modern times, shells have seen remarkable growth due to the



Figure 2.3: Corbel dome [Hoogenboom \[2011\]](#)

availability of new materials and the development of structural and manufacturing technologies. [Schueller \[1983\]](#)



Figure 2.4: Pantheon dome with an oculus

2.1.2 Grid shells

History of grid shells

Grid shells can provide an aesthetical and material-efficient solution, which is a demanding task for architectural design, structural design, and manufacturing.

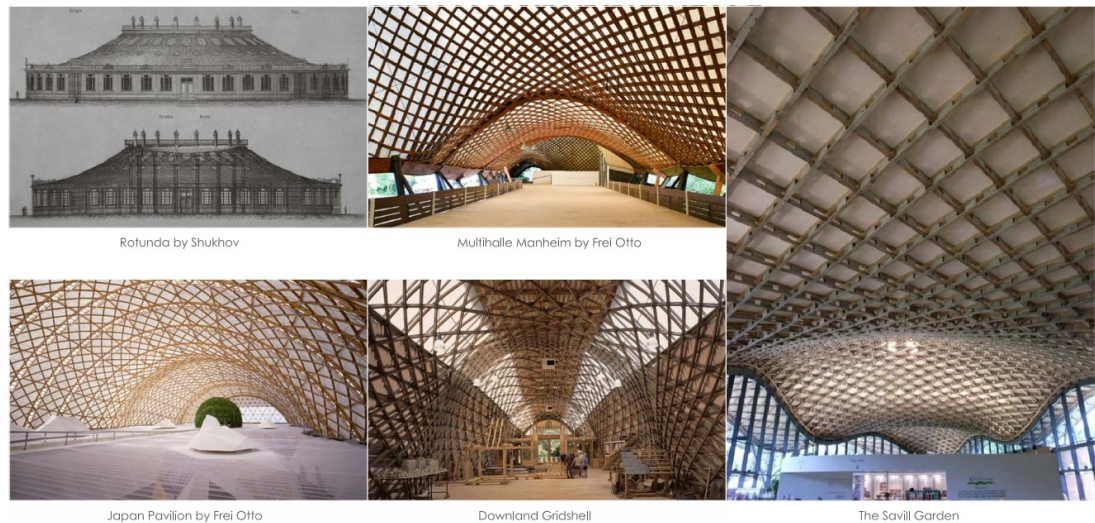


Figure 2.5: Grid shell structures

The Rotunda by Vladimir Shukhov is known as the world's first double-curved steel grid shell. It was constructed in 1895 as a pavilion for All-Russia Exhibition. He was an inspiration later for the German engineer Frei Otto, who in 1975 designed a multifunctional hall in Mannheim, Germany. It was originally built as a temporary structure for an exhibition. Another grid shell structure designed by Frei Otto is the Japan Pavilion built in Hannover Expo 2000. An example of alternative design choices is the Weald and Downland Grid shell, constructed of green oak. The design of grid shells nowadays still follows a similar workflow to Frei Otto's work. It starts with the grid geometry definition and is followed by form-finding. Otto developed physical form-finding by using scale models with different shapes and forms to study behavior. [Winslow et al. \[2008\]](#)

The Savill Building in England, designed by Buro Happold, serves as a visitor entrance center to the garden of the same name. The brief was for 'an environmentally sensitive building that would nevertheless leave a dramatic mark on the landscape. The grid shell follows a three-domed sinusoidal shape with a squared 1 m grid. The structure is supported on a steel tubular ring beam. Buro Happold designed the exact form of the roof to be structurally efficient by creating their own software. [Harris et al. \[2008\]](#)

2.1.3 Design principles

Grid shell results from removing the material from a shell in order to create a pattern. They obtain the essential feature of shells that is the strength due to curvature. However, instead of surface continuity, they consist of straight members connected by joints. This characteristic makes the most significant difference compared to shells. Grid shells lose the surface continuity and consequently the ability to transfer hoop forces internally. It can only transmit loads in the direction of members. [Van der Linden \[2015\]](#)



Figure 2.6: Grid shell

Removal of material in a grid pattern provides a lighter-weight solution and transparency for daylight. Usually, there is also a distinction in the material. Shells are made out of masonry, reinforced concrete, while grid shells are often from steel, timber, or aluminum. Factors affecting the grid shell's structural behavior are the geometry of the grid shell, the layout of the pattern, the cross-section of the members, and the type of joints. [Van der Linden \[2015\]](#)

Pattern

The development in design optimization tools and fabrication methods allows for numerous possibilities for the pattern of a grid shell roof structure. The more standard ones are triangular and rectangular. However, also hexagonal, kagome and free-form are possible. The choice for the pattern depends on the architectural and structural requirements for the design. The different patterns will lead to different structural behavior as visualized later on in the thesis. Additionally, different fabrication methods and joint design possibilities need to be considered.

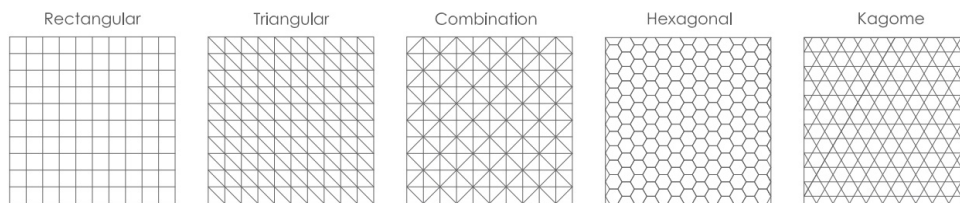


Figure 2.7: Possible grid patterns

Geometry definition

The geometry of the grid shell can be assigned in different computational or physical methods from the engineer. Computational methods include defining the geometry through equations such as elliptical paraboloid, sine equation, a combination of equations, or specific algorithm designed for the case.

Physical models include hanging models. These models can be achieved through candle waxing or cutting fabrics. An important discovery in the development of shells was made by Robert Hooke in the second half of the 17th century: "*As hangs a flexible cable, so inverted, stand the touching pieces of an arch*". A chain hanging between two supports will adopt a catenary or funicular shape due to its self-weight only. [Hoogenboom \[2011\]](#)

For standard gravity loading conditions, the cable funicular shapes are catenary and parabola. When these shapes are "frozen" and inverted, they transform into funicular arches responding in pure compression. The gravity load needs to result only in compression as the moments in the arch will be developed by live loading only. A parabola is a funicular arch under a uniform load acting on a horizontal roof projection. Under uniform, vertical load action, there is no bending and shear along

the arch. The forces are resisted in a purely axial manner. This moment less arch is a funicular arch. A catenary arch is a funicular for the gravity load. [Schueller \[1983\]](#)

Antoni Gaudí is a famous architect who made use of a network of hanging chains to analyze his designs. His best-known work has become the design of the Sagrada Familia in Barcelona, Spain. Gaudi used the principle of reversing the model; consequently, it becomes loaded in compression instead of tension. By using this method, elegant shapes can be found which make very efficient use of material. [Schueller \[1983\]](#)

Form-finding is a developed computational method comparable to the physical methods used previously. Chris Williams defines form-finding: "Form Finding is the process of establishing a structural geometry for a mechanism to carry a particular load." It is related to finding the equilibrium shape of structures such as cable-nets, membranes, and shells. These types of structures are classified as form-active (the structure's geometry affects the distribution of forces) or surface-active structures (the distribution of forces is affected by surface resistance and particular surface). Some form-finding methods include particle spring, soap film, force density, and dynamic relaxation. [Coenders \[2008\]](#)

Structural analysis

Structural calculation of complex geometries (grid shells) is possible through structural software such as Oasys GSA. Arup has developed a program for the static analysis of three-dimensional structures composed of skeletal elements. The static analysis makes it possible to find the displacement, u , of a linear system of equations with a given load as a vector f . The elements are represented by their stiffness K . So the system of equations is:

$$K u = f$$

After the software conducts the analysis, two unity checks will be made. The first check relates to the strength and resistance of the elements (Ultimate Limit State). The maximum calculated stresses of elements should not exceed the yield strength of the steel. The second check relates to stiffness (Serviceability Limit State). The maximum deflection of steel elements should not exceed $L/250$, where L is the span of the grid shell. This check is specific to the design of grid shells.

In order to conduct the analysis in Oasys GSA parametrically, the model in Rhino (Grasshopper) needs to be linked with the structural software. A transfer mechanism without losing the advantage of parametric design is possible through Geometry Gym. It is a plug-in in Grasshopper developed by Jon Mirtschin.

2.1.4 Grid shells over existing building

When designing grid shells over existing structures, a few other aspects need to be considered. The existing building and foundation have already been calculated to withstand a significant load. The additional load that can be added is limited, especially when the building was designed over 50 years ago. The Great Court in the British Museum (Fig. 2.8.) is an example of a complex parametric design used for grid shell roof structures over an existing building. The roof was added due to the need for more library space. The design team introduced dynamic relaxation as a form-finding method which at the time was an innovation for grid shell design. One of the constraints in the design was to avoid horizontal reaction forces in the existing building. For this reason, it is supported on sliding bearings through the perimeter and horizontally restrained only in the corners. [Stansfield \[1999\]](#)

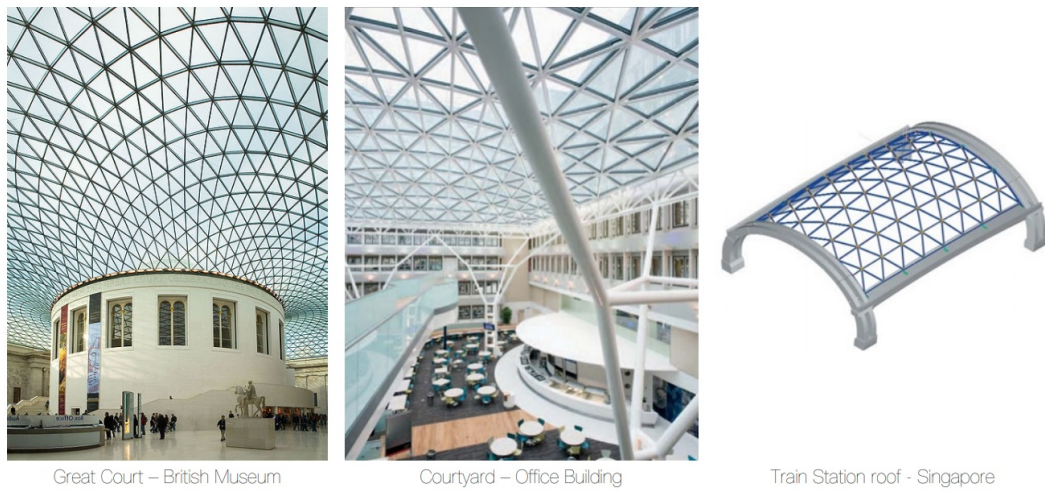


Figure 2.8: Examples of grid shells over existing buildings

Fig. 2.8 shows a double-curved wide-span steel and glass roof over a courtyard between four separate office buildings. The grid shell is constructed from circular hollow steel sections and a perimeter ring beam in the form of a structural gutter. The gutter provides the required stiffness to resist the spread of the arched steel members. One of the requirements in the design was to avoid connections to the building. The new roof is a structurally independent, complex geometric form-fitted to four buildings built at different periods. One of the many challenges was the accuracy needed for a roof structure that can move yet also fit within the space created by the existing buildings. The roof is laterally restrained by one of the buildings at the fourth-floor level and supported by “tree structures” in the edges to achieve structural stability. [Maunsell \[2007\]](#)

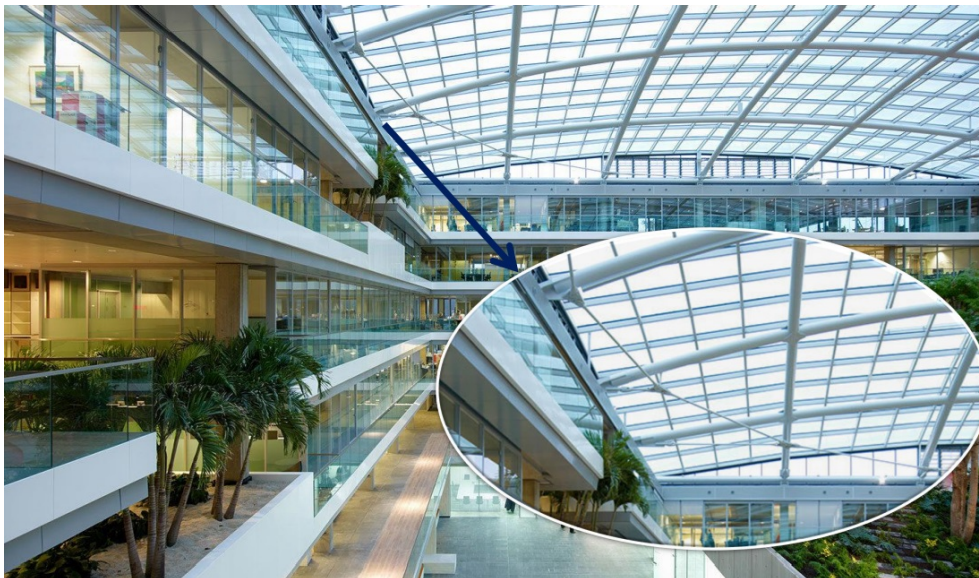


Figure 2.9: Solution for grid shells over existing buildings

Fig. 2.8 shows the glazed steel roof structure that was designed for the extension of Boon Lay’s existing station in Singapore. The requirements included “cost-effectiveness, aesthetically pleasing and harmonious, easy to build and possible to adopt for future elevated stations in Singapore”. Different concepts were compared by Life Cycle Analysis. The shown scheme was considered the best design with the challenge to the designer to ensure steel nodes that are simple and standardized

to achieve optimal constructability. The grid shell structure provided not only an aesthetical appearance but also structural efficiency in vertical load capacity.

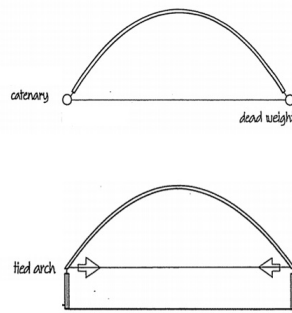


Figure 2.10: Solution for grid shells over existing buildings

Two possible solutions are given in this thesis from the literature review regarding solutions for additional horizontal loading. The first solution is applied in the case study designed by Octatube, explained in the following sub-section 2.1.5. The second solution is an example used in the Ministry of Finance building located in The Hague, Netherlands. Both of them transmit the horizontal forces through cables or steel rods/bars within the grid shell roof. Considering that the design of these members is outside of the focus of this thesis, the solutions are not discussed extensively and are not included in the parametric design due to being out of the scope of the thesis. However, to achieve the same result, the grid shell will be supported by a pin on both sides to avoid sliding and represent the solution. This way, the horizontal reactions will be transmitted in the steel rods, not the existing building.

2.1.5 Case study: C30 Shell

In order to quantify the approaches studied in this thesis, a case study will be applied. C30 Shell is a grid shell designed and completed by Octatube in 2020. It is designed over an existing building completed in 1916. The dome consists of a double-curved steel grid of approximately 30x30 meters. The steel construction behaves like a three-dimensional arch construction. [Winkel and Fritzsche \[2021\]](#)

Although Octatube has designed multiple grid shells, this case study is selected because the simple plan geometry allows the focus of the study on the joints.

The connection between old and new brought several constructive issues. Only low tensile forces are allowed in the old building, and no horizontal tensile forces may arise. To prevent damage from the deformation of the roof, it is held in the horizontal plane separate from the underlying masonry. They have a sliding connection and can therefore move freely horizontally. Each side of the edge beam has one fixed horizontal support in the middle of the facade plane to keep the roof in place. The tie rods that hold the edge beams together also play a role: they catch the occurring horizontal movement. The edge bar functions as a rigid element to transfer the forces to the tie rods. [Winkel and Fritzsche \[2021\]](#)

The double-curved roof contains the largest possible welded prefab frames, which are bolted together in situ. These connections are not rigid but also not pinned. The stiffness of the connection determines the distribution of the forces over the roof. The challenge was how stiff these bolted connections had to be. More stiffness implies greater forces (and thus greater dimensions), but less stiffness implies more chance of instability of the whole structure. [Winkel and Fritzsche \[2021\]](#)

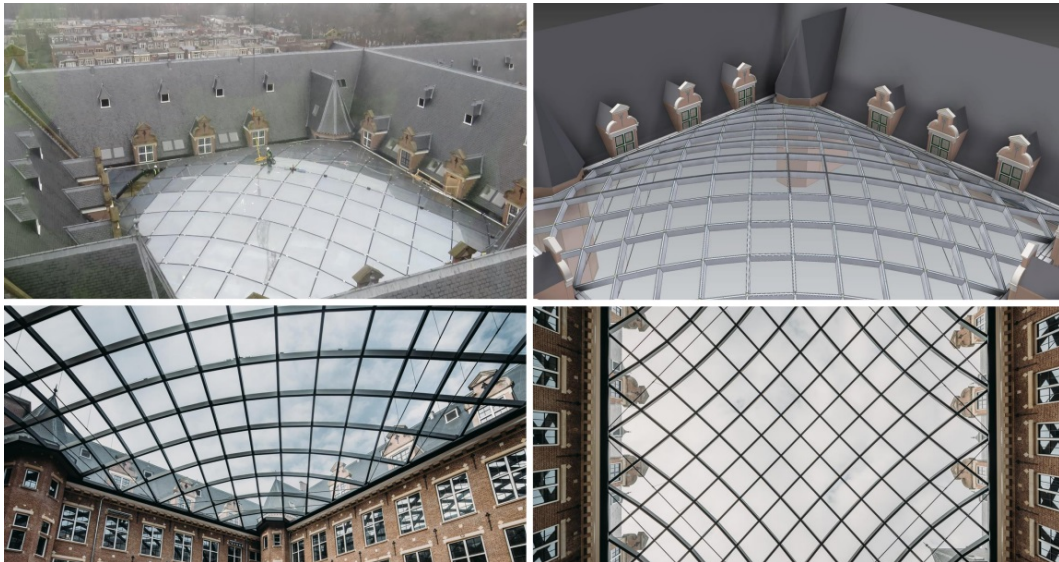


Figure 2.11: Solution for grid shells over existing buildings

2.2 GRID SHELL JOINTS

2.2.1 Importance of joint stiffness

Why is the study of joint stiffness important?

In structural design projects, engineers focus primarily on global behavior and the ability of the structure to withstand the ultimate and serviceability limit state. Connection stiffness of members is sometimes neglected, although it can be used to improve design efficiency. The design procedure is usually limited to assigning the type of connection: rigid, semi-rigid, pinned, relying only on the ability to distribute bending moments or not. Kubicek [2021b]

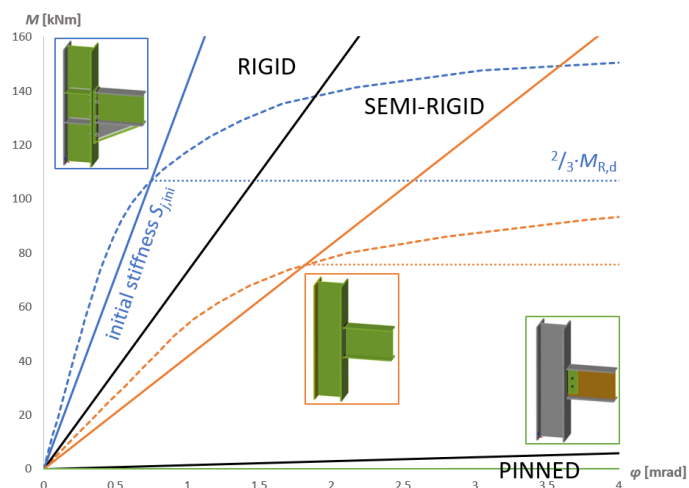


Figure 2.12: Examples of the three types of connections

In global structural analysis, mostly the groups of rigid or pinned joints are used. However, in real engineering practice, these connections sometimes behave as semi-rigid. Joints considered as pinned will transmit some bending moments into connected members. Likewise, rigid joints could not be rigid enough. That could be due to manufacturing or assembly reasons. Most engineers argue that this inaccu-

racy is on the safe side; thus, it does not lead to problems. However, the study of joint stiffness is necessary because there is no reason to increase the rigidity of a connection, when in fact, it does not lead to a more efficient solution. Kubicek [2021b]

In Eurocode EN 1993-1-8, the joints are classified according to initial stiffness as:

- Pinned - joint does not transmit any bending moments, but rotation is allowed, characterized by low bending stiffness.
- Semi-rigid - joint transfers some bending moments, and its behavior needs to be considered in global analysis.
- Rigid - joint does not affect the analysis; members are rigidly connected to each other. As a result, the nodes are characterized by high bending stiffness.

The example can illustrate the effect of joint bending stiffness in Figure 2.13. This is a beam of length L_b with a moment of inertia of the cross-section I_b of material with elastic modulus E . The beam is loaded with a constant continuous load q . The beam is attached to the columns by connections with a stiffness $S_{j, ini}$. Kubicek [2021b]

The stiffness of the joint can be classified according to EN 1993-1-8 by engineering estimation or by reference to the stiffness of the connected beam. The dimensionless stiffness k_b is defined as:

$$k_b = \frac{S_{j, ini} \cdot L_b}{I_b \cdot E} \quad (2.1)$$

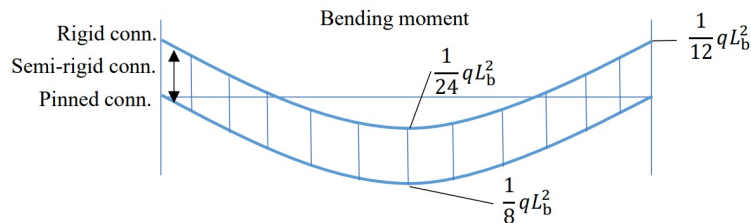


Figure 2.13: Influence of connection stiffness on bending moment diagram along a beam

For semi-rigid joints, determining the stiffness for the moment derivation along the beam is essential for its design. Contrary, for rigid and pinned beams, the exact determination of stiffness is not significant. With increasing or decreasing stiffness, the moment does not change substantially.

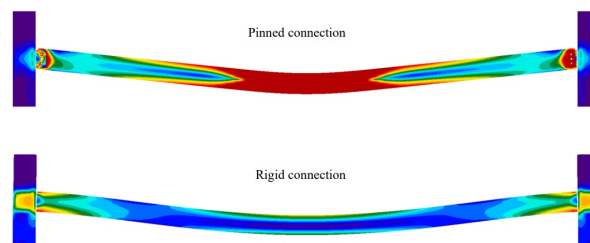


Figure 2.14: Output of Von Mises stresses along the beam supported by pinned and rigid connection

Changing the joint stiffness causes the bending moments to be redistributed in the attached member. Even a significant change in stiffness at a rigid or pinned

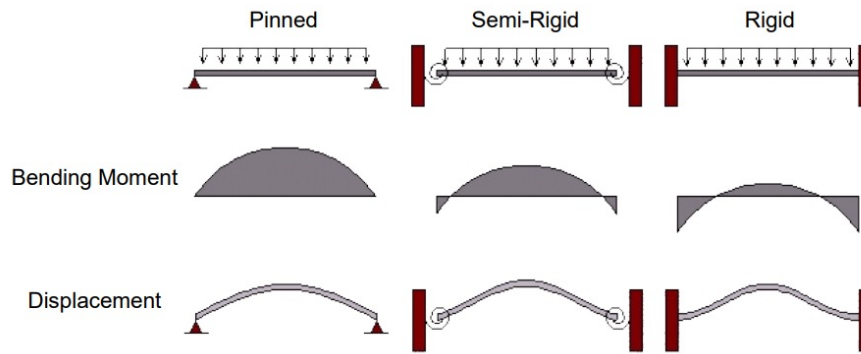


Figure 2.15: Different behavior of beams supported by pinned and rigid connection

joint only causes a slight redistribution. Changing stiffness is quite essential when designing semi-rigid joints.

What is the importance of joint stiffness in a grid shell design according to the literature?

Engineers have studied the effect of the stiffness of joints both experimentally and numerically for some time. In the Appendix A is given a detailed summary of the available literature review related to the influence of joint stiffness on-grid shells. Research available in the literature proved that joint stiffness affects the stability and load-bearing capacity of grid shells. Earlier studies by See (1983) and Fathelbab (1987) verified the effect of stiffness on the load-displacement behavior of a structure. Previous studies have also focused on material and cost savings due to the effect of joint properties. Wang et al. [2016] Studies from El-Sheikh, Chenaghloou, and Nooshin have concluded that the bending stiffness of connections influences the behavior of a structure and the failure mode. Fan et al. [2011]

Feng, Yao, and Ye studied the stability of grid shell roofs and the factors that influence them. Among the factors, they concluded that joint stiffness plays a role in the ultimate bearing capacity of the structure. They studied the behavior of the structure with stiffness altering in a logarithmic scale from 1×10 to 1×10^7 N/m\$. Feng, Yao, and Ye concluded that the critical load would also decrease with the decrease of joint stiffness. Additionally, it was noted that the ultimate load-bearing capacity is 10% lower in grid shells with in-plane pin and out-of-plane rigid compared to fully rigid. Feng et al. [2012] Another study by Ye and Lu proposes an optimal dome design against instability by considering the effect of joint stiffness. Ye and Lu [2020]

Van der Linden has included an overview of requirements to be taken into account during the joint design. Among the requirements, the ability to transfer bending moment and the out-of-plane stiffness will be the most relevant to the thesis. The requirements include: Van der Linden [2015]

In the paper "Optimization Strategies for Grid shells: The Role of joints," the authors explore three optimization approaches combining member sizing optimization and stiffness configuration of joints. The aim was to propose a strategy in obtaining a lighter structure compared to only member sizing optimization. The main constraints of the optimization problem are the global buckling and stresses of members. The parameters include the number of joints in the preliminary solution and the member diameter. Grande et al. [2020]

The first approach is "Pinned-Rigid" joints, which considers the possibility of varying the configuration of some joints from pinned to rigid. As a result, the

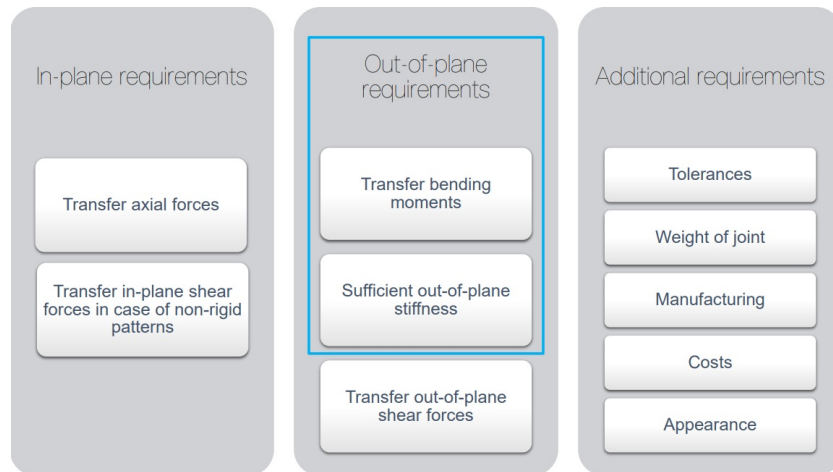


Figure 2.16: Requirements for joint design Van der Linden [2015]

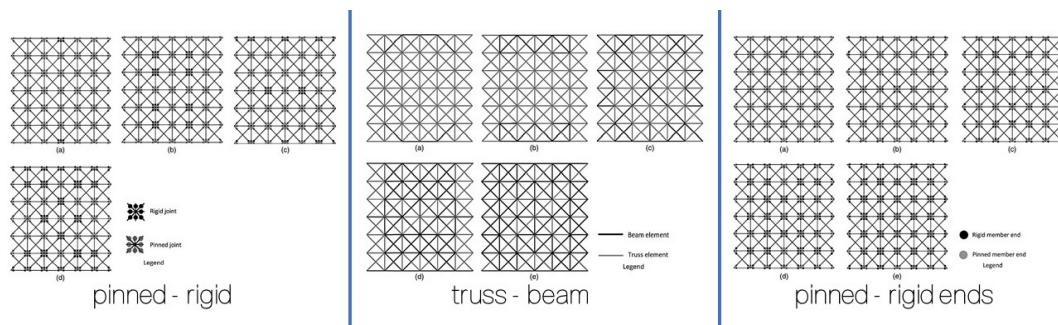


Figure 2.17: Illustration of scenarios considered in the optimization Grande et al. [2020]

whole joint would be either pinned or rigid but could be different for both ends of the member. The second approach is “Truss-Beam” members, where some of the members can alter from truss elements to beam elements. Truss elements can transfer only axial forces without bending moments or shear forces. Different from the first approach, the conversion from truss to beam would lead to variation from pinned to rigid connection for both ends of the element. The third approach is “Pinned-Rigid ends”. The final solution of this technique would result in joints that may behave as rigid for some members they are connected to and pinned for others. In the outcome of this study, the authors underline that the member’s diameter influences both the stress and global buckling behavior, while the joint stiffness alternation mostly affects the global buckling. Grande et al. [2020]

The available literature proves that there is an effect of joint stiffness on the global behavior of grid shells. They have been mainly focused on the influence on the buckling or critical load of grid shells. However, engineers design grid shells based on serviceability limit state and ultimate limit state in most situations. Considering the available research and the scope of this thesis, the main objective is to optimize the stiffness of the joints to have a more lightweight, consequently less additional loading on existing buildings.

2.2.2 Joint classification in grid shells

How can the boundaries between the joint stiffness categories: rigid, semi-rigid, pinned be obtained for a grid shell?

The paper by Fan, Ma, Can & Shen in 2011 [Fan et al. \[2011\]](#) proposes a classification system for joints of spatial structures, taking into consideration stiffness and moment capacity of joints and structural behavior of grid shells.

Joint classification based on the stiffness k

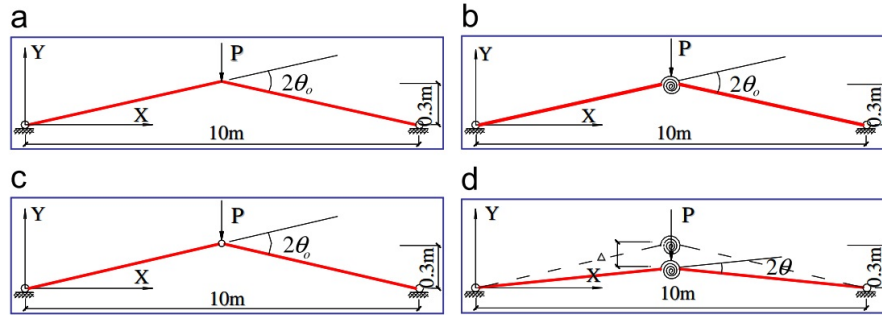


Figure 2.18: Basis for classification of stiffness boundaries

The system is based on a simplified structure composed of 2 members. In the Figure, scheme (a) represents a rigidly jointed structure; scheme (b) a structure connected with a semi-rigid joint, which they classify as flexible joint with stiffness k ; scheme (c) represents a pinned jointed structure and scheme (d) the deformed state of the structures under the vertical load P , where the angle between the members and the horizontal direction changes from θ_0 to θ . [Fan et al. \[2011\]](#)

The paper provided the basis for the classification system used in this thesis. A detailed summary of the paper and the procedure they followed is given in the Appendix A. The objective is to determine the moments at the top of the structures in relation to the angle θ_0 and θ . In order to derive these moment equations, the Matrix Method is used. [Fan et al. \[2011\]](#)

The matrix method is a numerical procedure, considered as a form of the finite element method. It will result in a form $f=k*a$, where f are the internal forces in the element, k is the element stiffness matrix, and a are the unknown displacements. In structural systems, the unknown displacements include axial extensions, transverse deflections, and rotations. While f collects the corresponding axial forces, shear forces, and bending moments. [Simone \[2011\]](#)

The members taken into account in this study are referred to as the Euler-Bernoulli beam, the classical formulation for bending beams.

The f , k , and a matrices are derived from the fourth-order ordinary differential equation relating the element stiffness, displacement, and applied load for beams in bending. The differential equation derivation for the Euler-Bernoulli beam is explained below: [Welleman \[2021\]](#)

Differential equation method applied in Matrix Method:

- Geometric relations

$$\begin{aligned} \Delta\varphi &= \frac{\Delta s}{R} \approx \frac{\Delta x}{R} \Rightarrow \frac{1}{R} = \frac{\Delta\varphi}{\Delta x} \\ \lim_{\Delta x \rightarrow 0} \frac{\Delta\varphi}{\Delta x} &= \frac{d\varphi}{dx} = \kappa \end{aligned} \quad (2.2)$$

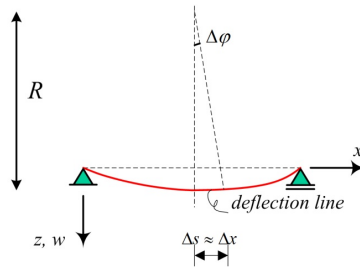


Figure 2.19: Geometric relations Welleman [2021]

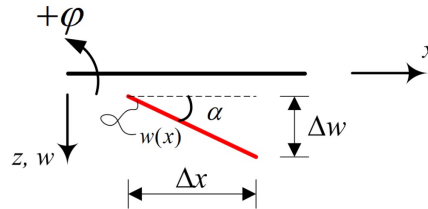


Figure 2.20: Geometric relations Welleman [2021]

$$\tan \alpha \approx \alpha = \lim_{\Delta x \rightarrow 0} \frac{\Delta w}{\Delta x} = \frac{dw}{dx} \quad (2.3)$$

$$\alpha = -\varphi \quad (2.4)$$

- Constitutive relation based on Hooke's Law: $M = EI \cdot \kappa$
- Equilibrium equations

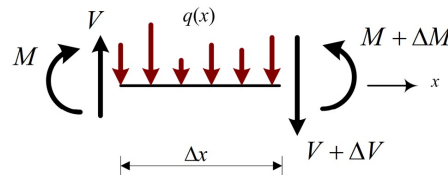


Figure 2.21: Equilibrium equation Welleman [2021]

The following equations are considered:

$$\begin{aligned} \varphi &= -\frac{dw}{dx}; & \kappa &= \frac{d\varphi}{dx}; \\ M &= EI\kappa & (\text{Hooke}) & \\ \frac{dV}{dx} &= -q; & \frac{dM}{dx} &= V \end{aligned} \quad (2.5)$$

These relations result in the following ODE:

$$\begin{aligned} EI \frac{d^4 w}{dx^4} &= q \\ V &= -EI \frac{d^3 w}{dx^3}; & M &= -EI \frac{d^2 w}{dx^2}; & \varphi &= -\frac{dw}{dx} \end{aligned} \quad (2.6)$$

In order to solve the fourth-order differential equation, four boundary conditions are needed, which could relate to bending moment, shear force, vertical displacement, or rotation.

To obtain the general stiffness matrix for the Euler-Bernoulli beam, the following boundary conditions are given:

$$w(0) = w_1, \phi(0) = \phi_1, w(L) = w_2, \phi(L) = \phi_2$$

$$\begin{bmatrix} V_1 \\ M_1 \\ V_2 \\ M_2 \end{bmatrix} = \begin{bmatrix} \frac{12EI}{L^3} & \frac{6EI}{L^2} & -\frac{12EI}{L^3} & \frac{6EI}{L^2} \\ \frac{6EI}{L^2} & \frac{4EI}{L} & -\frac{6EI}{L^2} & \frac{2EI}{L} \\ -\frac{12EI}{L^3} & -\frac{6EI}{L^2} & \frac{12EI}{L^3} & -\frac{6EI}{L^2} \\ \frac{6EI}{L^2} & \frac{2EI}{L} & -\frac{6EI}{L^2} & \frac{4EI}{L} \end{bmatrix} \begin{bmatrix} v_1 \\ \theta_1 \\ v_2 \\ \theta_2 \end{bmatrix} \quad (2.7)$$

The calculations to find the boundaries of rigid stiffness in this thesis are computed in Maple, which are included in the Appendix C. Firstly, situation (a) is considered, consisting of finding the moment at the top of the structures in the case of rigidly joined members. The following boundary conditions are applied to obtain the element stiffness matrix:

X=0: The design restricts the support as pinned; thus no horizontal displacement is possible, but rotation is allowed ($w = 0, \phi = \phi_1$).

X=L/2: Rigid jointed members allow for no rotation, but horizontal displacement is possible which is noted as delta ($w = w_2 = \Delta, \phi = 0$).

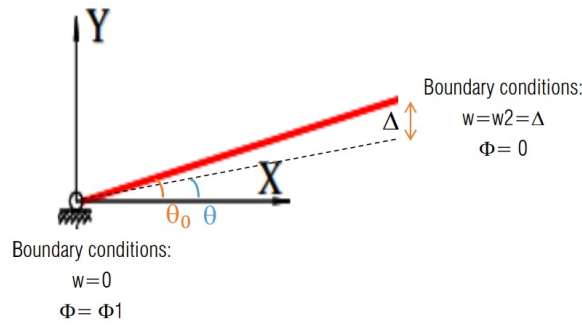


Figure 2.22: Scenario (a)

By applying these conditions, the stiffness matrix is obtained as follows:

$$K_{sys} = \begin{bmatrix} 0 & -\frac{6EI}{L^2} & -\frac{12EI}{L^3} & 0 \\ 0 & \frac{4EI}{L} & \frac{6EI}{L^2} & 0 \\ 0 & \frac{6EI}{L^2} & \frac{12EI}{L^3} & 0 \\ 0 & \frac{2EI}{L} & \frac{6EI}{L^2} & 0 \end{bmatrix} \quad (2.8)$$

To find the moment at the second node, the last row of components are needed. They are multiplied with the given rotation ϕ_1 and displacement Δ . The displacement delta is taken as an upper boundary: $L/250$, the serviceability limit for grid shells, where L is the span of the grid shell. The displacement Δ is given in relation to the angles θ_0 and θ . The rotation ϕ_1 is equal to the difference between these two angles. Finally, the displacement is rotated from the local to the global axis. The moment equation obtained is:

$$M_{zr} = \frac{2EI}{L_0} (\theta_0 - \theta) + \frac{3EI}{L_0} (\tan \theta_0 - \tan \theta) \cos \theta \quad (2.9)$$

The same procedure is followed for the semi-rigid or flexible jointed members. The only difference is in the boundary condition for node 2 where rotation is allowed $\phi = \phi_2$.

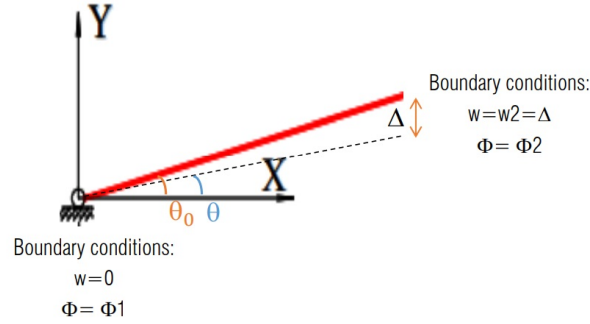


Figure 2.23: Scenario (b)

Additionally, the member stiffness EI/L is substituted with k , as this k is the stiffness that we are trying to find. These conditions result in the following stiffness matrix:

$$K_{sys} := \begin{bmatrix} 0 & -6k & -12k & -6k \\ 0 & 4k & 6k & 2k \\ 0 & 6k & 12k & 6k \\ 0 & 2k & 6k & 4k \end{bmatrix} \quad (2.10)$$

By applying the known displacements, we can find the moment at node 2:

$$M_{zs} = 2k(\theta_0 - \theta) + 3k(\tan \theta_0 - \tan \theta) \cos \theta + 2k(2\theta_0 - 2\theta) \quad (2.11)$$

By stating $M_{zr} = M_{zs}$ in order to find the minimal stiffness required to obtain a rigid joint, result in the rigid boundary stiffness:

$$k = \frac{EI * (3 * \cos(\theta) * \tan(\theta_0) - 3 * \cos(\theta) * \tan(\theta) - 2 * \theta + 2 * \theta_0)}{L * (3 * \cos(\theta) * \tan(\theta_0) - 3 * \cos(\theta) * \tan(\theta) - 10 * \theta + 10 * \theta_0)} \quad (2.12)$$

A parametric study is needed to find the stiffness boundary of pinned joints to visualize the effect of alternation of stiffness in a logarithmic scale. A study related to the influence of joint stiffness in beams in frames will be used as a basis for comparison. In Figure 2.24, the blue curve shows the bending moment at the joints and the red curve bending moment in the beam mid-span. According to the Eurocode classification, this graph assigns the value $k=25EI/L$ as the rigid boundary and $k=0.5EI/L$ for the pinned boundary (Figure 2.24). The internal forces nearly do not change in the pinned and rigid region but change rapidly in the semi-rigid region. Also, the difference in rotational stiffness is given in a logarithmic scale. It means that the stiffness may change even 100 times, and it will have a negligible effect if the joint stays in the rigid or pinned region.

2.3 CONCLUSIONS

In this chapter, the following sub-questions are answered:

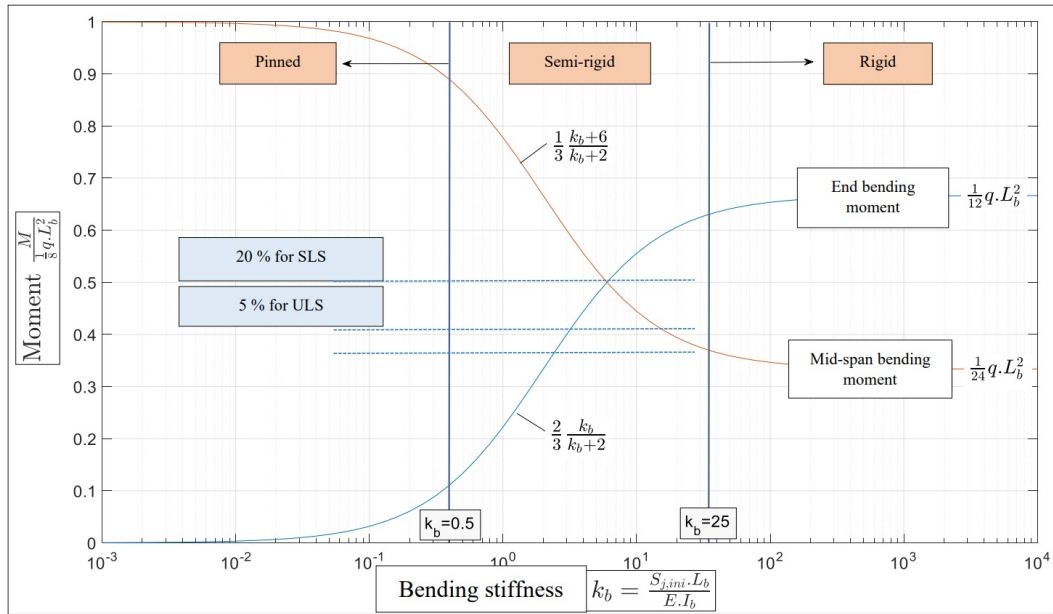


Figure 2.24: Effect of stiffness alternation on bending moment

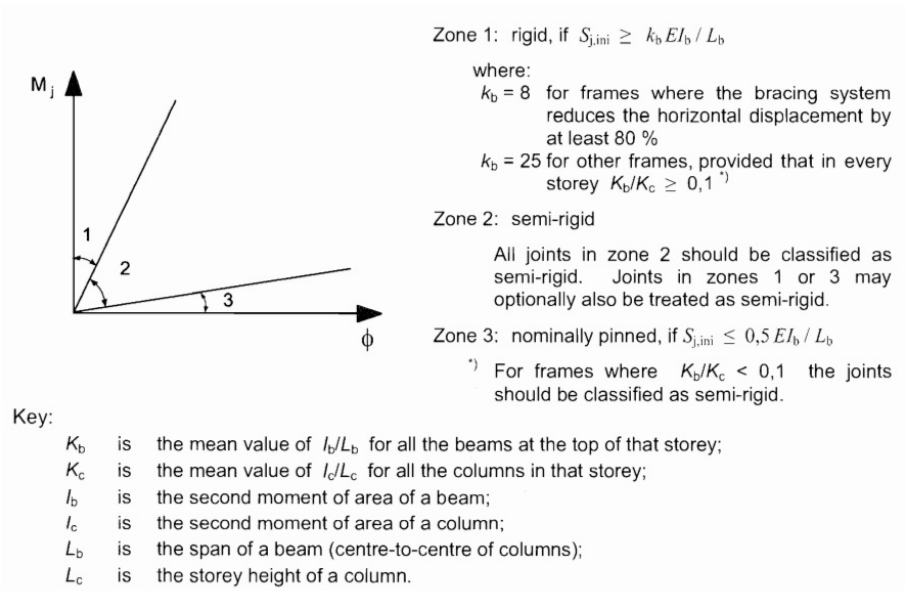


Figure 2.25: Eurocode classification of stiffness

What is a grid shell structure, and what are its structural principles?

Grid shells are structures originating from shell structures. They obtain the essential feature of shells that is the strength due to in-plane structural actions. However, instead of surface continuity, they consist of straight members, which are connected by joints. Removal of material in a grid pattern provides a lighter-weight solution and transparency for daylight.

Different materials can be used for the design of the structure e.g., steel, aluminum, wood. Factors affecting the grid shell's structural behavior are the geometry of the grid shell, the layout of the pattern, the cross-section of the members, and the type of joints. [Van der Linden \[2015\]](#)

What are the design principles for grid shells over existing structures?

When designing grid shells over existing structures, a few other aspects need to be considered. The existing building and foundation have already been calculated to withstand a significant load. The additional load that can be added is often limited, especially when the building was designed over 50 years ago.

Two possible solutions are given in this thesis from the literature review regarding additional horizontal loading. The first solution is applied in the case study designed by Octatube. The second solution is an example used in the Ministry of Finance building located in The Hague, Netherlands. Both of them transmit the horizontal reaction forces through cables or steel rods/bars within the grid shell roof. However, the solutions are not discussed extensively and are not included in the parametric design due to being out of the scope of the thesis.

What is the importance of joint stiffness in a grid shell design according to the literature?

Joints play an essential role in the structural behavior of grid shell structures. Research available in the literature proved that joint stiffness affects the stability and load-bearing capacity of grid shells. [Feng, Yao, and Ye \(2012\)](#) concluded that the critical load would also decrease with the decrease of joint stiffness. Additionally, it was noted that the ultimate load-bearing capacity is 10% lower in grid shells with in-plane pin and out-of-plane rigid compared to fully rigid. [Feng et al. \[2012\]](#)

However, this thesis focuses on the effect that out-of-plane rotational stiffness has on global deformations and maximum stresses in the grid shell. There was a lack of studies related to the effect on the serviceability limit state and ultimate limit state, which will be investigated in the thesis.

How can the boundaries between the joint stiffness categories: rigid, semi-rigid, pinned be obtained for a grid shell?

The boundaries between rigid, semi-rigid, and pinned for joints in a grid shell are obtained based on a method found in the literature review. The matrix method is used to find the moment in a two-member, representing a simplified grid shell. These calculations result in a formula for the stiffness k related only to member properties; length of the beam and angles to the horizontal axis. These variables make the formula applicable to different scenarios. By proper substitution, the value k obtained is the boundary for minimal stiffness to behave as rigid.

In order to obtain the boundary for pinned stiffness, a parametric design followed. The objective was to visualize the effect over the bending moment distribution of alternation of stiffness in logarithmic scale. The boundary for pinned stiffness is ver-

ified by comparing this effect with a study based on the Eurocode joint classification for beams in frames.

3 | PARAMETRIC DESIGN

3.1 GRID SHELL MODEL

Parametric design

In order to achieve the objective of the thesis, the first step is creating a parametric model and structural analysis of a grid shell. The model is scripted in Rhino 6 (Grasshopper) and the summary of the script can be found in Appendix B. The parameters used in the model relate to the plane geometry, a quadrangle with dimensions in x and y direction and the divisions of the grid in x and y-direction. These parameters allow for the possibility of adopting the model in the future to another design and finding the optimal solution by changing the parameters. One of the parameters is changed, the pattern and shape will generate automatically.

Other parameters in the model are related to the structural aspect. The cross-section of the members and the stiffness of the joints are a variable in this thesis. Consequently, the releases of the member ends are a parameter.

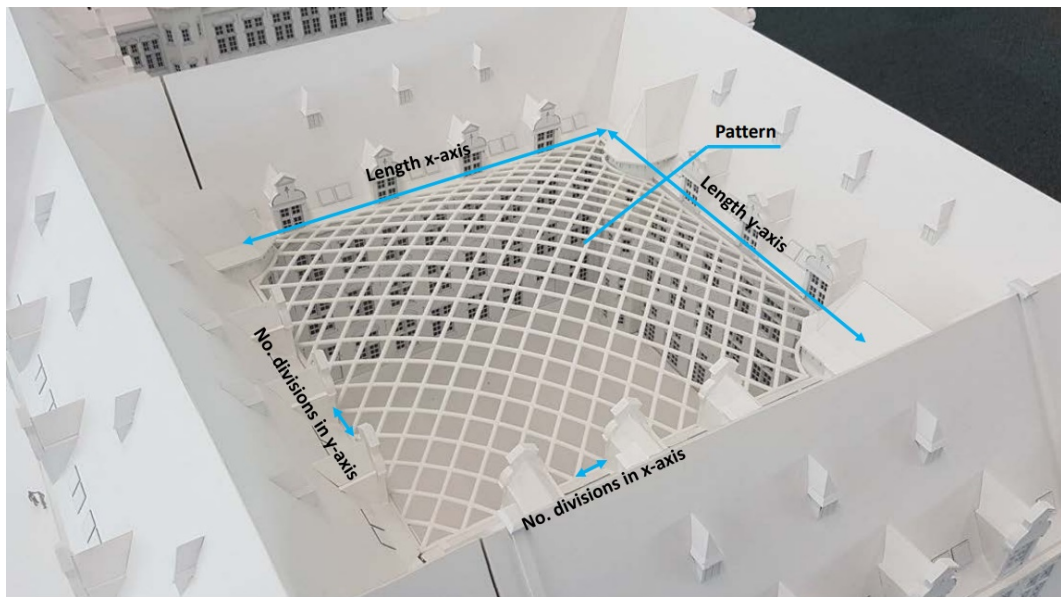


Figure 3.1: Parameters

Pattern

Regarding the grid pattern, triangular and rectangular will be considered. The reasoning behind this choice is related to the scope and focus of the thesis, which is the joint stiffness influence. By applying these patterns, both rigid (triangular) and non-rigid (rectangular) patterns and the difference between them will be investigated. As visualized in Figure 3.2, the rectangular shape will deform easily under loading. However, the triangular pattern will hold its shape.

The rectangular pattern will be at an angle so that in the four corners, we have a triangle instead of a rectangle. The choice is made for structural purposes. By

ending the beam at the edge, the forces are better distributed.

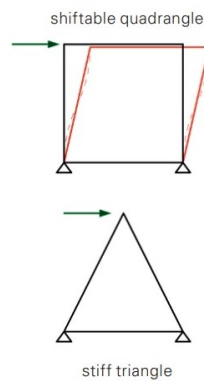


Figure 3.2: Triangular and rectangular shape

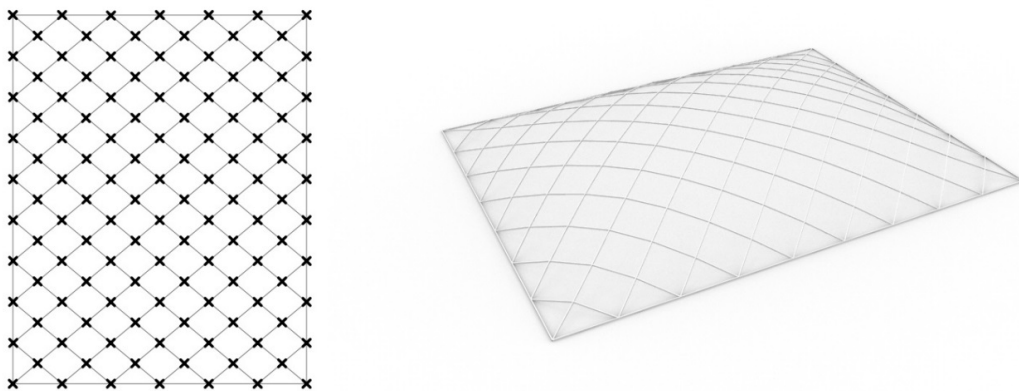


Figure 3.3: Rectangular pattern

Geometry definition

A catenary shape is chosen for the curvature of the grid shell. It is similar looking to a parabola, but there is a difference in the behavior. The parabola will result in mainly axial forces in case of uniformly distributed load along the projection of the arch. However, a catenary shape will result in no bending and shear in the case of uniformly distributed load along the arch. As in grid shell, we deal with the self-weight the latter solution is more suitable.

In practice, the grid shell's self-weight is less significant in the structural analysis as grid shells are considered lightweight. More influence will have live loads such as wind and snow. However, in this situation, the bending moments will be introduced by live load only because they could be asymmetrical.

The catenary shape is achieved through form-finding. The method used is Particle Spring, applied in Kangaroo, a plug-in within Grasshopper. A particle is considered a point mass which means it has no other properties than mass. A particle behaves according to Newton's second law, which states that the sum of forces acting on an object is equal to the product of its mass and acceleration. Springs are considered weightless and linearly elastic with constant stiffness. The springs span between the particles. Figure 3.5 shows a simple setup of a particle spring system. In the initial setup, the middle particle is out of balance due to the applied force. The particle acceleration results in velocity. After one iteration or time step, the particle has displaced. The connecting spring extends, resulting in a force. The system

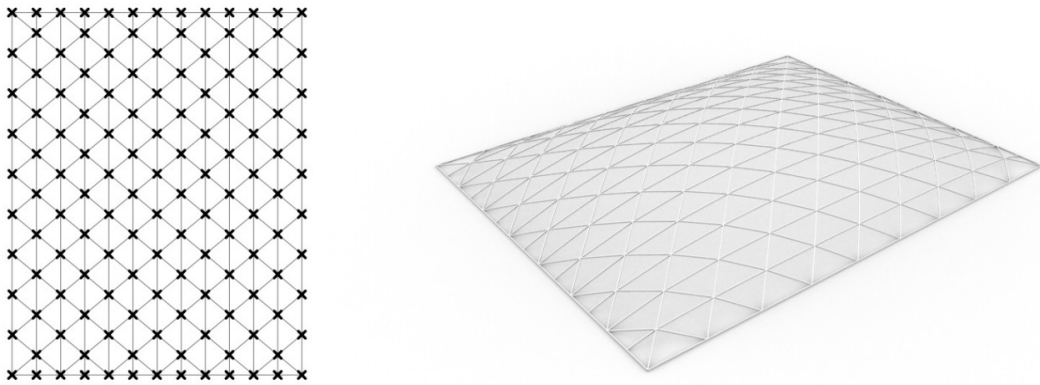
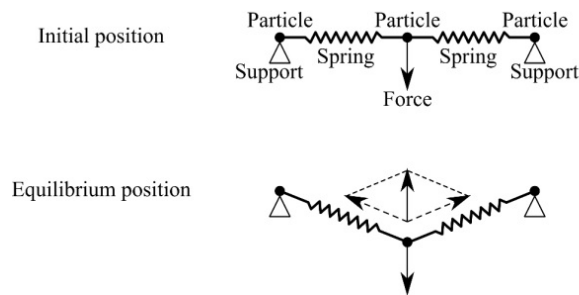


Figure 3.4: Triangular pattern

moves as long as there is no equilibrium. [Eigenraam \[2017\]](#)

Figure 3.5: Initial and equilibrium state of a particle spring [Eigenraam \[2017\]](#)

3.2 STRUCTURAL ANALYSIS

A list of applied Eurocodes in the structural analysis:

- EN 1990 – Basis of structural design
- EN 1991-1-3 – Eurocode 1: Actions on structures – Part 1-3: General actions – Snow loads
- EN 1991-1-4 – Eurocode 1: Actions on structures – Part 1-4: General actions – Wind loads
- EN 1993-1-1 – Design of steel structures – Part 1-1: General rules and rules for buildings

Material properties

When the pattern and geometry are finalized, a structural performance needs to be conducted. Material properties are assigned, choosing steel S235. The cross-section of the members is chosen rectangular hollow sections (RHS).

Load assumptions

The loads considered in the analysis are the self-weight of the steel grid, the dead load of the glass units, and live loads. For live loads, both snow and wind are

Material property	Value
Density ρ	7850 kg/m ³
Unit weight γ	78.5kN/m ³
Modulus of elasticity E (Young's modulus)	210000MPa
Shear modulus G	81000MPa
Yield strength f_y	235MPa
Ultimate strength f_u	360MPa
Poisson's ratio in elastic range ν	0.30
Coefficient of linear thermal expansion α	$12 \times 10^{-6} \text{K}^{-1}$

Table 3.1: Material properties of steel S235

considered. Despite that other types of loads such as maintenance load and asymmetric snow load may occur, they will not be included, as they are considered out of the scope of the thesis.

The calculations below are specific to the case study due to the need to quantify the corresponding coefficients. However, by having a parametric model, the loading could be easily changed to any case study.

(a) Self-weight structural steel

The gravity load is calculated within the software in kN/m² by applying material properties and cross-section dimensions in Geometry Gym components in Grasshopper. The structural analysis software Oasys GSA takes into consideration gravity acceleration of 9.81 m/s².

(b) Self-weight glass units

The roof is loaded with glass units with a weight of 25 kN/m³. It is assumed a panel of three glass sheets with a thickness of 6 mm. The distributed load acting on the steel beams is analyzed from the size of the panels in the Grasshopper model.

(c) Snow load

The design snow load in the design is 0.56 kN/m². It is calculated as follows according to the Eurocode EN 1991-1-3:

$$s = \mu_i * c_e * c_t * s_k \quad (3.1)$$

Where μ_i is the snow load shape coefficient, s_k is the characteristic values of snow load on the ground, c_e is the exposure coefficient, c_t is the thermal coefficient.

$S_k=0.7$ kN/m² (National annex)

$C_e=1.0$ (National annex)

$C_t=1.0$ (National annex)

The start angle of the roof is smaller than 30° for both situations with rigid and non-rigid patterns. At the top of the grid shell, the angle is 0°. Thus according to Eurocode, $\mu_i = 0.8$. Additionally, 0.8 is the smallest allowed coefficient in the case that obstructions prevent the snow from sliding off the roof. This could be the case for a grid shell surrounded by existing walls or structures.

Due to the thesis's scope, only the case of uniformly distributed over the surface of the grid shell is considered. The load is assumed to act vertically (global

(2) The values given in Table 5.2 apply when the snow is not prevented from sliding off the roof. Where snow fences or other obstructions exist or where the lower edge of the roof is terminated with a parapet, then the snow load shape coefficient should not be reduced below 0,8.

Table 5.2: Snow load shape coefficients

Angle of pitch of roof α	$0^\circ \leq \alpha \leq 30^\circ$	$30^\circ < \alpha < 60^\circ$	$\alpha \geq 60^\circ$
μ_1	0,8	$0,8(60 - \alpha)/30$	0,0
μ_2	$0,8 + 0,8 \alpha/30$	1,6	--

Figure 3.6: Snow load coefficients from Eurocode

z-direction) and refers to a horizontal projection of the roof area. As the model consists of the grid members, the load is calculated to be uniformly distributed over the beams.

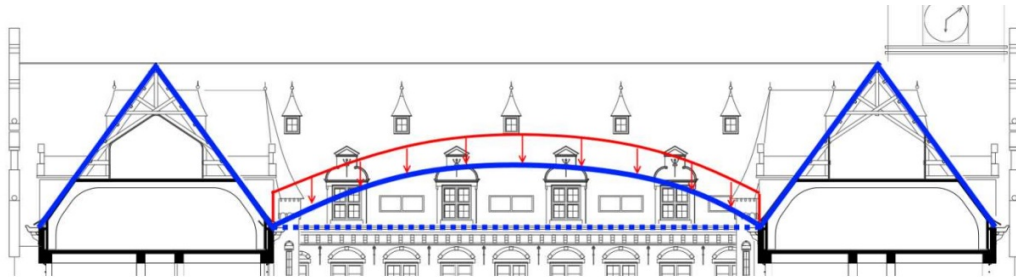


Figure 3.7: Snow load distribution

(d) Wind load

The design wind load is considered from one direction only due to the symmetry of the roof. According to Eurocode it is calculated as follows:

$$p_{\text{wind}} = c_s c_d * c_p * q_p \quad (3.2)$$

Where c_s, c_d is the structural factor to take into account the effect on wind actions from the non-simultaneous occurrence of peak wind pressures on the surface (c_s) together with the effect of the vibrations of the structure due to turbulence (c_d). In this situation, the factor is taken as 1.

c_p is the pressure coefficient for the internal pressure. The height at the top of the building, according to Octatube data, is $z_e = h_t o p = 20.7$ m. The basic wind load in this area is $q_{pz} = 0.91$ kN/m².

The shape factors as suggested in the Eurocode are:

$$c_{pA} = 1.3$$

$$c_{pB} = -0.9$$

$$c_{pC} = -0.5$$

Thus, wind load in the design is divided into three zones: A with 1.19 kN/m², B with -0.82 kN/m², and C with -0.46 kN/m².

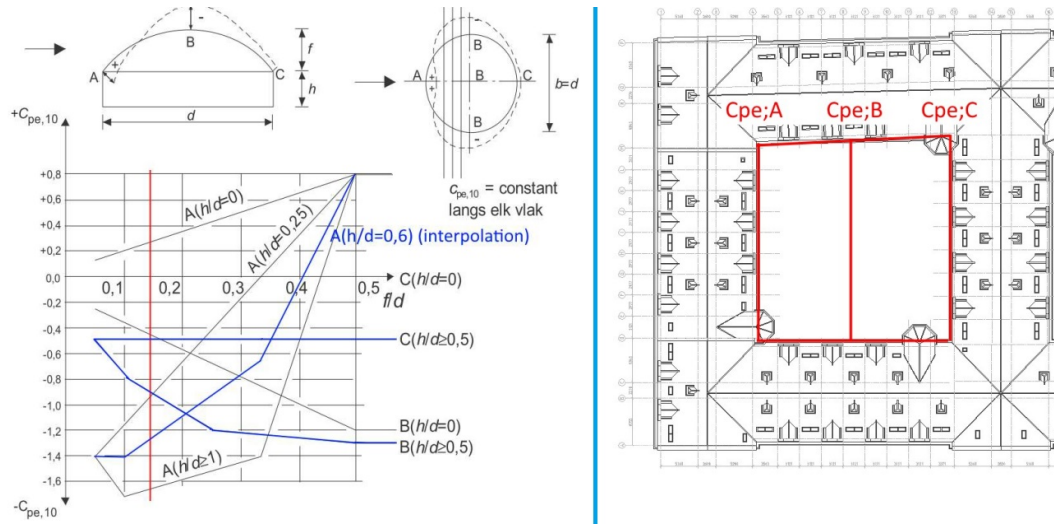


Figure 3.8: Wind load

SLS combination	Self-weight + Snow (SLS 1)	Self-weight + Wind (SLS 2)
Self-weight steel	1	1
Snow (equal distributed)	1	
Wind, zone A, B & C		1

Table 3.2: Serviceability Limit State (SLS) load combinations

The wind load acts on the local z-direction. The uniformly distributed load over the surface is calculated in a uniformly distributed load over the beams due to modeling of grid shells in grid members.

Load combinations

(a) Serviceability Limit State (SLS)

Serviceability Limit State load combinations will be used for deformation checks of the elements.

(b) Ultimate Limit State (ULS)

Ultimate Limit State load combinations will be used for the strength of the elements checks. To study the stresses and internal forces, the ultimate limit state load cases are considered, with consequence class CC2 and reference period of 50 years:

Design criteria

(a) Serviceability Limit State (SLS)

Deflection of steel elements must be in line with requirements for Serviceability Limit State (SLS). Deflection of the beams resulting from load combinations SLS 1

ULS combination	Self-weight + Snow (ULS 1)	Self-weight + Wind (ULS 2)
Self-weight steel	1, 2	1, 2
Snow (equal distributed)	1, 5	
Wind, zone A, B & C		1, 5

Table 3.3: Ultimate Limit State (ULS) load combinations

and SLS 2 must not exceed:

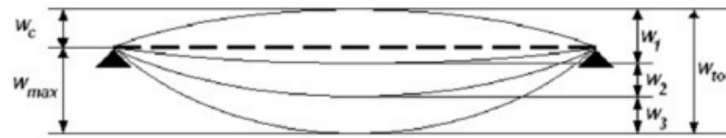


Figure 3.9: Maximum global deflection

The deflection limitation is a global boundary; for this reason, it is compared to the span of the grid shell. In the case study: $W_{allowed} = 30\text{m} / 250 = 0.12\text{m}$

(b) Ultimate Limit State

The resulting design strength of elements E_d from ULS 1 and ULS 2 must not exceed resistance strength R_d . $E_d < R_d$ The governing stress value is compared to the yielding strength of steel 235 MPa.

3.3 CONCLUSIONS

This chapter provides the basis for the parametrical design and the assumptions considered to perform the structural analysis. The regulations presented are found in the Eurocode. Different load combinations are analyzed, including self-weight, snow, and wind loading. The main difference between the two load combinations is that one is uniformly distributed and the other asymmetrical. This will allow the study of joint stiffness influence over the grid shell in different scenarios.

4 | JOINT STIFFNESS INFLUENCE

4.1 JOINT STIFFNESS CLASSIFICATION

A new classification system for the joint stiffness in grid shells is introduced in the literature review (Chapter 2). It resulted in an equation where rotational stiffness k is given in relation with the member properties, length, and angle with the horizontal axis. By substituting the values specific to the case study on equation 2.12, the following stiffness for the rigid boundary is obtained:

$$k = 0.389 \frac{EI}{L_0} \quad (4.1)$$

By using this value as the boundary for rigidity, the stiffness is decreased in a logarithmic scale. The following two graphs are obtained specific to the case study, comparable with Figure 2.24. The graphs in the figures below also indicate the rigid and pinned boundaries in the Eurocode EN 1993-1-8 for frames. Specifically, the values are $k=25EI/L$ as the rigid boundary and $k=0.5EI/L$ for the pinned boundary. These values are within the rigid range, proving that they cannot be used in this case study as they do not give the necessary insight. The proposed method seems to give more insight.

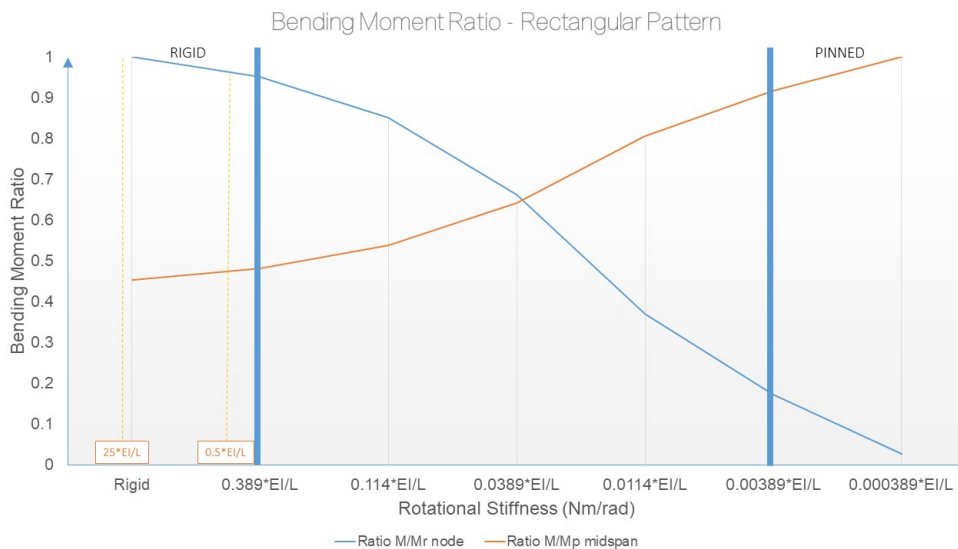


Figure 4.1: Result for rectangular pattern

The blue curve shows the ratio between the actual bending moment to the bending moment of the fully rigid joint. The bending moments are located at the node of the members. Within the rigid stiffness, this ratio can decrease until approximately 0.9. When the pinned region is reached, the ratio decreases to approximately 0.1. On the contrary, the red curve shows the ratio of the actual bending moment to the bending moment of a simply supported beam. These moments are located in the mid-span of the beam. The ratio within the rigid region ranges between 0.4 to

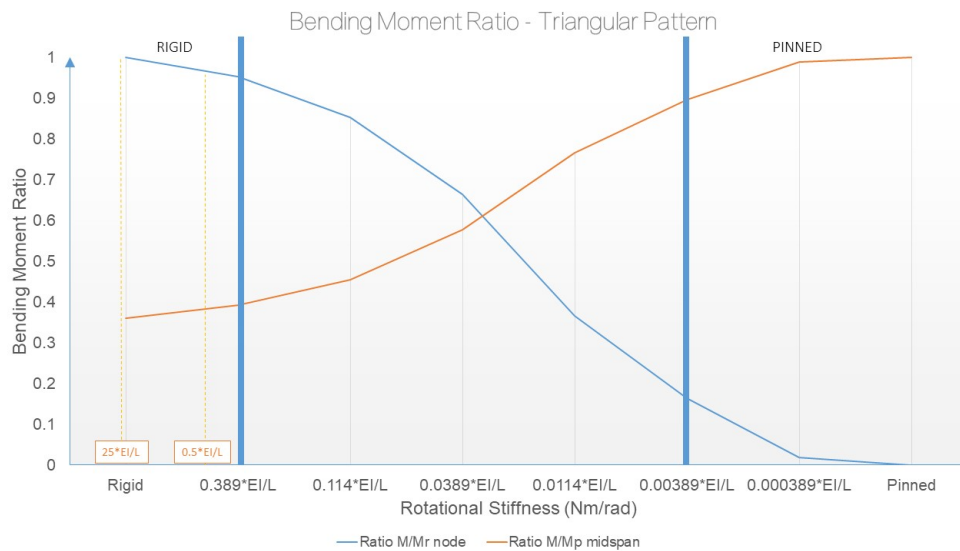


Figure 4.2: Result for triangular pattern

Joint stiffness	Notation in thesis
Fully rigid	Rigid
$0.389 * EI/L$	Rigid Boundary
$0.114 * EI/L$	Semi-rigid 1
$0.0389 * EI/L$	Semi - rigid 2
$0.0114 * EI/L$	Semi - rigid 3
$0.00389 * EI/L$	Pinned Boundary
$0.000389 * EI/L$	Pinned
Pinned	Pinned

Table 4.1: Joint stiffness classification

0.5. Contrary, in the pinned boundary, it lowers to approximately 0.9. These ratios are comparable to the study conducted for the joint stiffness classification in the Eurocode EN 1993-1-8 (Figure 2.24). As expected, the internal forces do not change significantly in pinned and rigid regions but change rapidly in the semi-rigid region. From this parametrical study of the stiffness, the pinned boundary in this case study is $k=0.00389EI/L$.

The joint stiffness that will be investigated in the following sections of the thesis are noted below:

Fully rigid stiffness indicates that the maximum capacity for bending moment transfer is reached. Pinned stiffness indicates there is no bending moment transfer.

In order to investigate the influence the rotational stiffness has on the design of the grid shell, the same cross-section is chosen. The cross-section chosen for both patterns is RHS 150x100x10. The joint stiffness will alter between the values noted in Table 4.1.

4.2 RECTANGULAR PATTERN

The analysis started with studying the grid shell with a rectangular pattern with different node stiffness. The graphs below visualize the effect of the joint stiffness over the ultimate and serviceability limit state checks. Firstly the study is done for

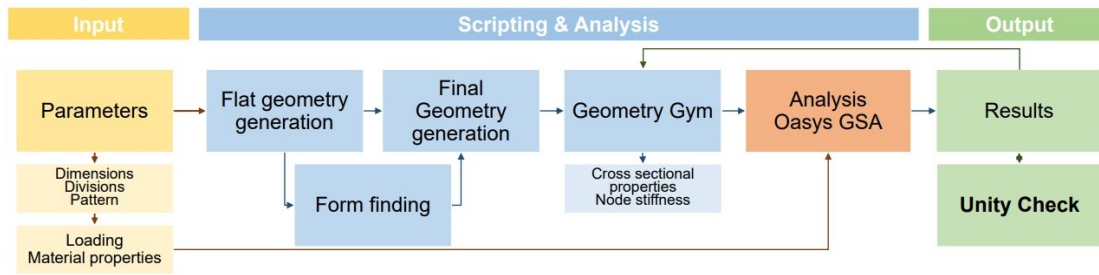


Figure 4.3: Procedure

the uniformly distributed load combination.

The first graph below shows the maximum displacement of the grid shell for load combination SLS 1. This maximum value is reached at the node located in the middle of the geometry, as expected. The graph ranges from 0 to 0.12 m displacement, where the latter one is the maximum allowed displacement. As can be seen from the graph, the stiffness reduction does not significantly affect the results. The reason for that is that the roof is only loaded with the self-weight and snow load. This loading scenario is uniformly distributed. The drastic increase of the displacement value, exceeding the allowed values, is seen closer to the pinned configuration. This has to do with the fact that the pattern is not a rigid shape. Thus with the decrease of stiffness, it will lose the shape, and for fully pinned nodes, the analysis will no longer run.

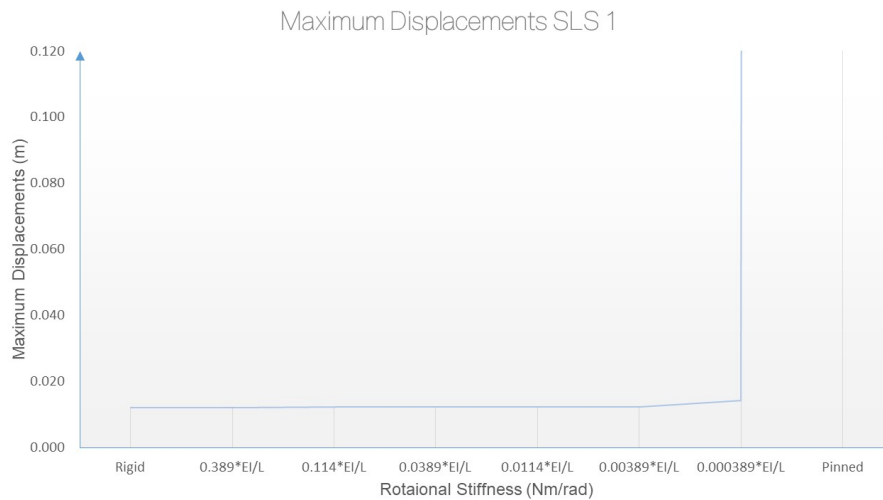


Figure 4.4: Maximum displacements for serviceability limit state load combination 1

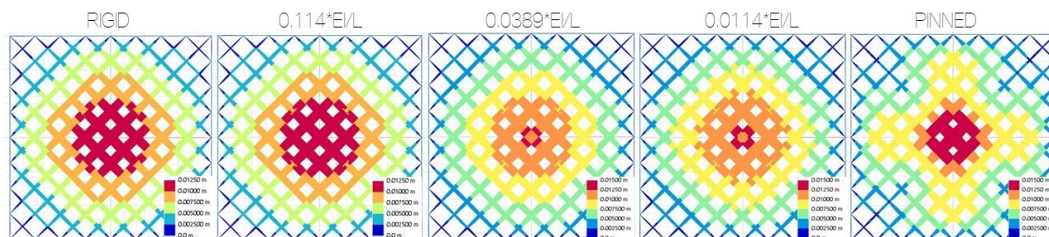


Figure 4.5: Maximum displacements for serviceability limit state load combination 1

The results from GSA show that the maximum displacement is located near the center at all configurations, as expected. The legend in each image shows that the maximum displacements are increased slightly.

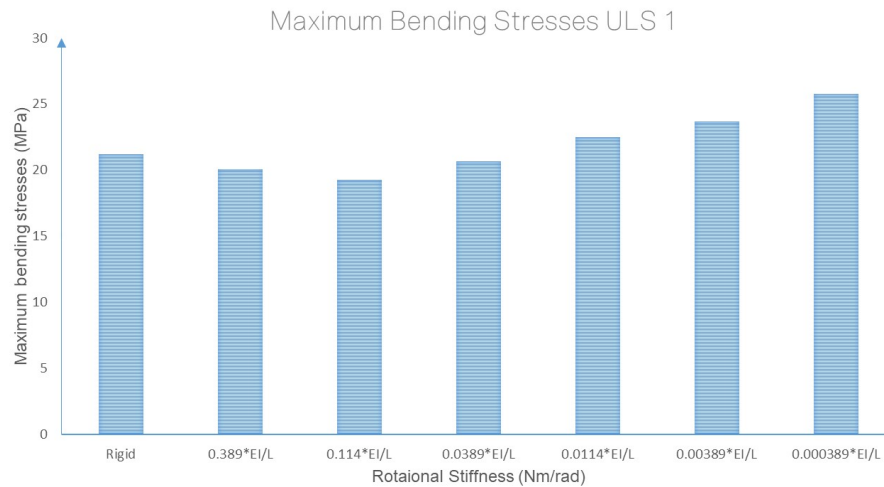


Figure 4.6: Maximum bending stresses for ultimate limit state load combination 1

The graph of maximum values reached for the bending stresses does not give a straightforward relation between the stiffness and bending stresses. As can be seen, the maximum value decreases going from rigid connection to semi-rigid 1 node with stiffness $k=0.114EI/L$. From this point on, the maximum values increase again. This shift is related to the location where the maximum values are reached on the beam. For the three first stiffness: rigid, semi-rigid 1, and semi-rigid 2, these maximum peaks are reached at the nodes. From that point on, the peaks are reached at the mid-span of the beams.

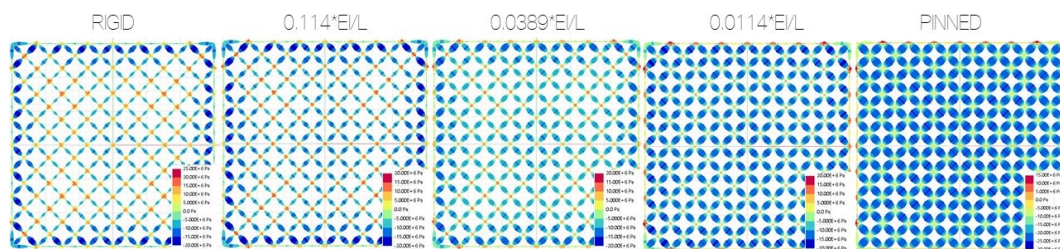


Figure 4.7: Maximum bending stresses for ultimate limit state load combination 1

Results from GSA give insight into where the peaks are reached. It is clear that going from the fully rigid to the pinned boundary stiffness, the stresses reduce at the nodes and increase at the mid-span of the beams.

In the case of uniformly distributed load, the axial stresses are lower going towards a pinned node. However, these values are not governing for the load combination. The governing stresses are a combination of the axial and bending ones.

As the grid shell structure is loaded both in bending and axial stresses due to the double-curved geometry, the combination of these stresses needs to be accounted for. The software GSA calculates the combination of bending and axial force at the top and bottom fiber of the cross-section. The output shows how these values in-

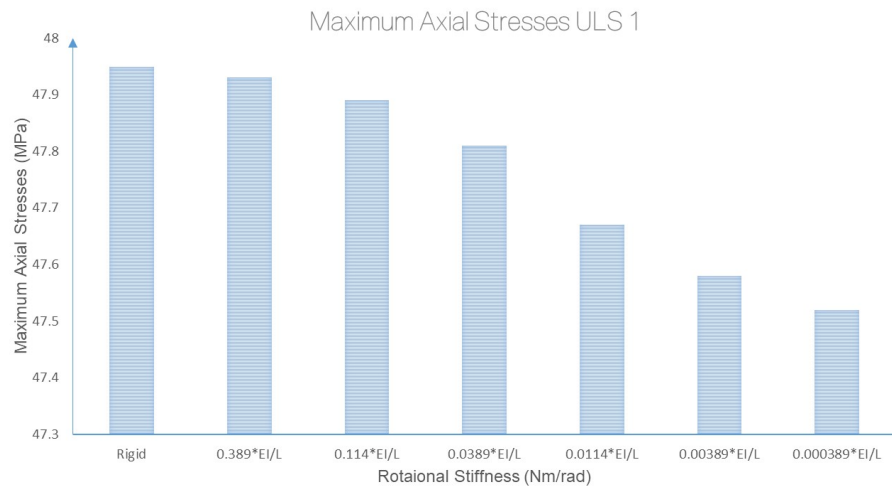


Figure 4.8: Maximum axial stresses for ultimate limit state load combination 1

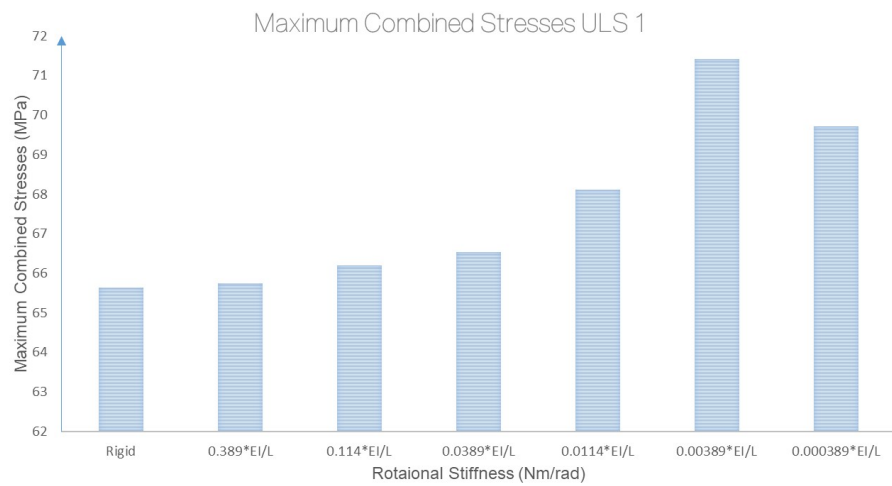


Figure 4.9: Maximum combined stresses for ultimate limit state load combination 1

crease going towards the pinned node.

The uniformly distributed load combination gives insight into how the structure behaves with different stiffness. However, the governing load combination for this design and grid shells, in general, is non uniformly distributed load combination. Below are shown the results for this scenario.

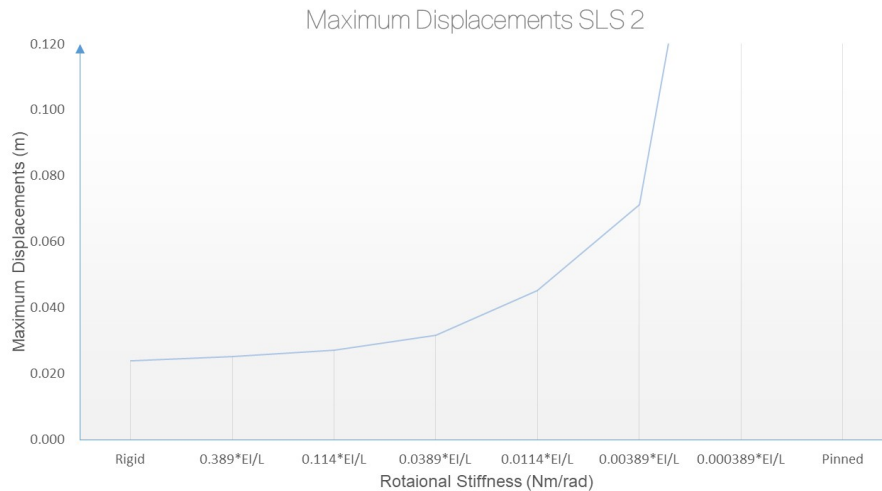


Figure 4.10: Maximum displacements for serviceability limit state load combination 2

The graph for maximum displacements under SLS 2 has a more steep increase in values than SLS 1. It shows that the node stiffness has a more significant influence on the maximum displacements for a non-uniformly distributed load.

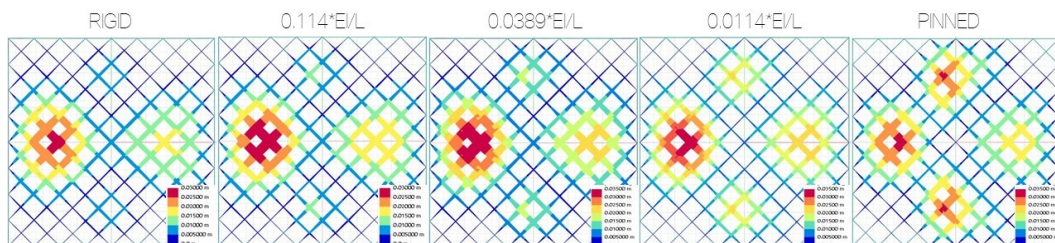


Figure 4.11: Maximum displacements for serviceability limit state load combination 2

This study proves that in a grid shell with a rectangular (non-rigid) pattern when all nodes are released in the $-yy$ and $-zz$ direction, the structural analysis will not run due to the model's failure. Additionally, it was visible that the displacements are increased with a decrease in rotational stiffness until they went above the serviceability limit state. From this graph alone, it can be understood that a rectangular pattern is more efficient with a rigid joint while considering serviceability limit state only. However, the ultimate limit state design needs to be verified as well.

Results from GSA give an understanding of the location of the maximum displacements. These values are reached closer the perimeter beams. That is due to the asymmetrical loading, being higher in some areas and deforming the double curvature of the grid shell.

The graph above visualizes how the maximum bending stresses decrease at the nodes while the stiffness decreases. Furthermore, the maximum bending stresses

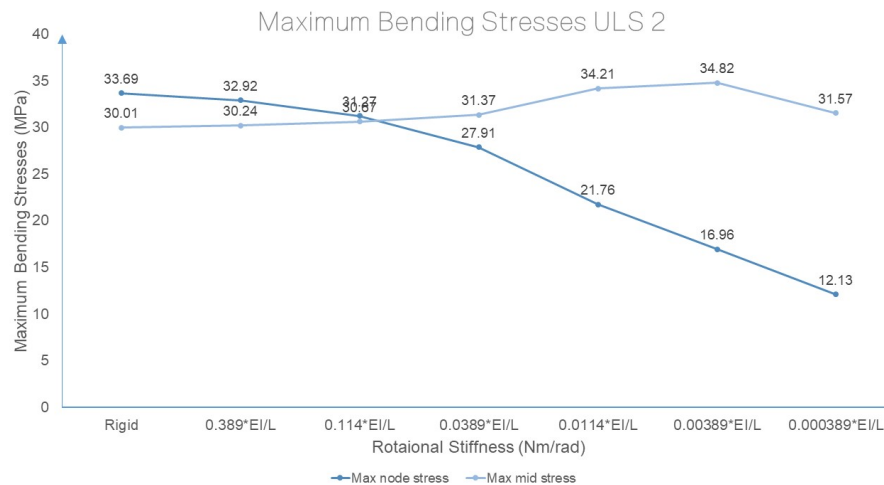


Figure 4.12: Maximum bending stresses for ultimate limit state load combination 2

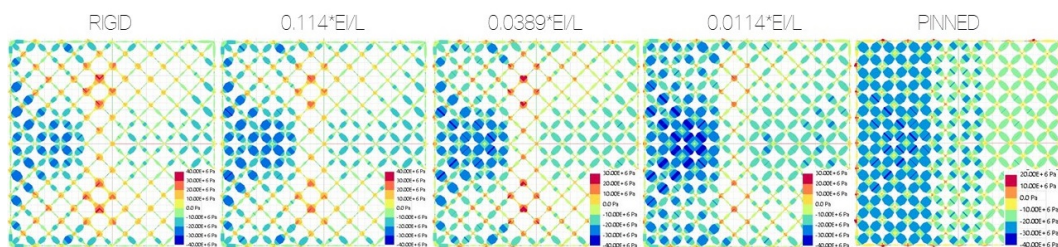


Figure 4.13: Maximum bending stresses for ultimate limit state load combination 2

increase at the mid-span, with the decrease of stiffness. This was expected and comparable with the behavior of beams in frames altering from fixed-fixed to pinned-pinned configuration. The graph also visualizes a point of interest at stiffness with $k=0.114EI/L$, belonging to semi-rigid 1. From that point on, the maximum bending moment has shifted from the nodes to the mid-span of the beams.

Due to the form and curvature of grid shells, axial stresses are generated and mainly govern compared to the bending stresses. It is noticed that these stresses start to decrease with the decrease of stiffness. However, the rate of the decrease is insignificant for this study as it is approximately 2-3% from fully rigid to pinned.

The combination of axial and bending stresses is governing for the ultimate limit state. The unity checks for these values together with maximum displacements will result in the choice of the cross-section.

The smallest unity checks are reached with stiffness k between $0.389EI/L$ and $0.0389EI/L$. These boundaries give limitations to the optimization in the following chapters of the thesis. Considering that when an optimal cross-section is found, both bending stresses and displacement will be influenced depending on the cross-section dimensions, not only stiffness k , additional study is needed for the optimal design.

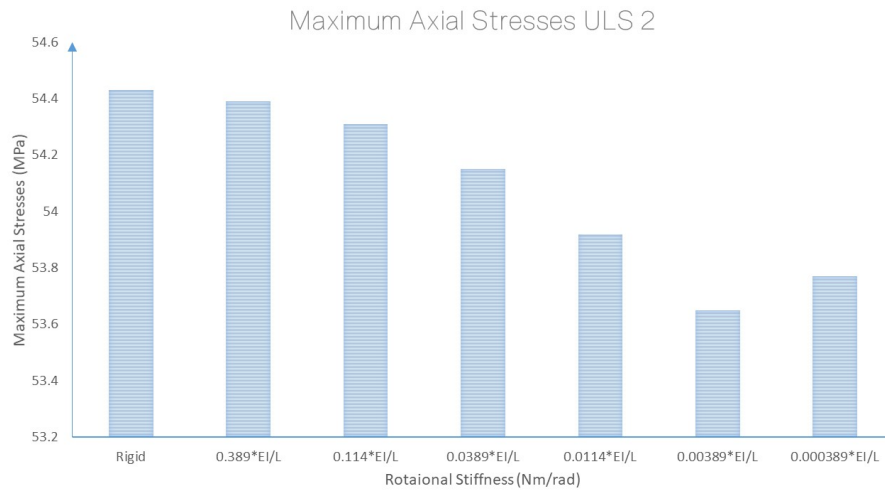


Figure 4.14: Maximum axial stresses for ultimate limit state load combination 2

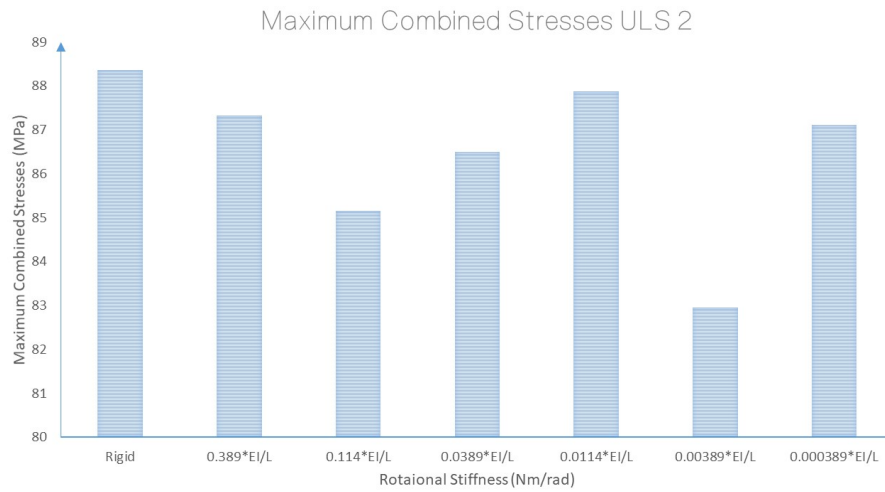


Figure 4.15: Maximum combined stresses for ultimate limit state load combination 2

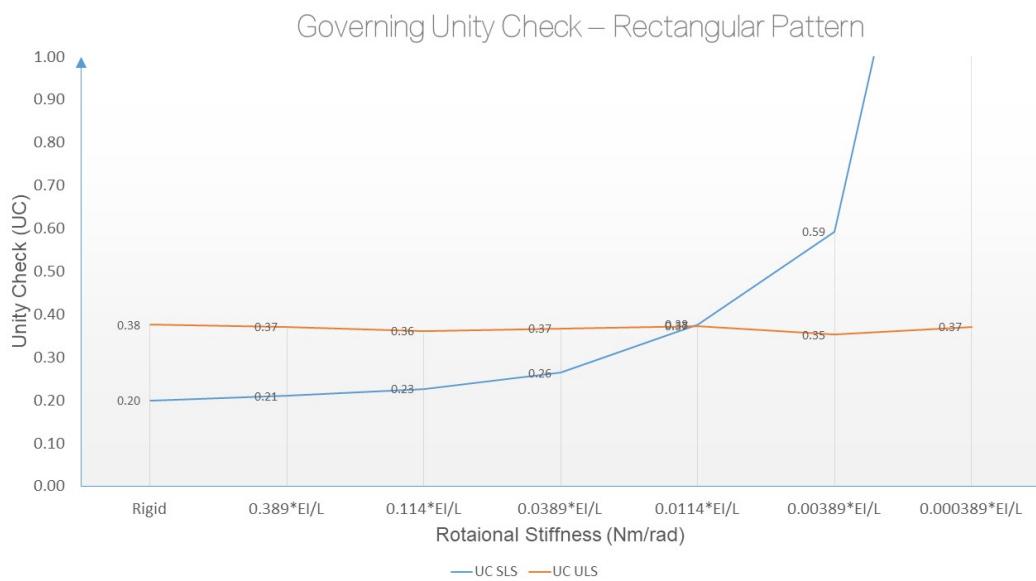


Figure 4.16: Governing unity checks for rectangular pattern

4.3 TRIANGULAR PATTERN

A similar study is conducted for the grid shell with a triangular pattern. The alternation of stiffness gives a different impact compared to the grid shell with a rectangular pattern, which is explained in detail below.

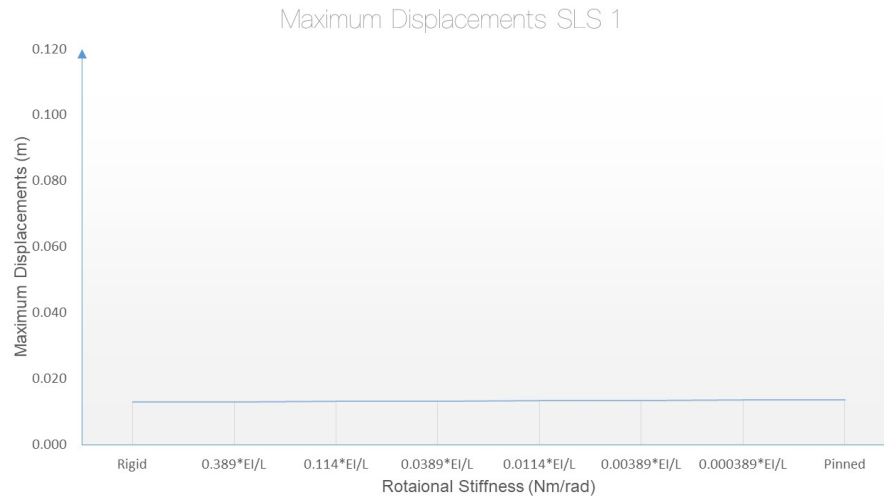


Figure 4.17: Maximum displacements for serviceability limit state load combination 1

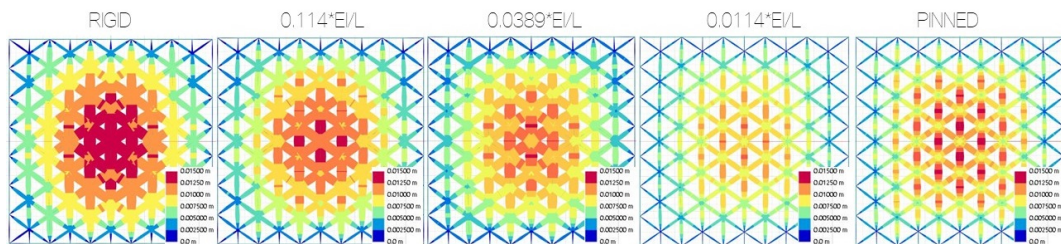


Figure 4.18: Maximum displacements for serviceability limit state load combination 1

Different from the rectangular pattern, the maximum displacements are not influenced by the changes in rotational stiffness. Decreasing the stiffness from rigid to pinned gives almost the same maximum displacement. It can also be observed here that in the situation with pinned nodes, the structure is still working. Thus, the rigidity of the triangular shape allows for minimal shift and displacement, allowing the application of pinned nodes.

Results from GSA show how the maximum displacement is concentrated in the middle of the grid shell. The main difference between these results is related to the fact that in the pinned nodal configuration, beams deflect at the mid-span more than near the nodes.

In the case of symmetrical load distribution, the behavior related to bending stresses is comparable for both structures. That is due to the relation with simple beams. The bending stresses decrease from rigid to semi-rigid 1 stiffness. After that, the maximum values shift from the nodes to the mid-span and start to increase.

The combination of axial and bending stresses will give the governing stresses for a uniformly distributed load. These stresses are lower for rigid nodes, thus giving

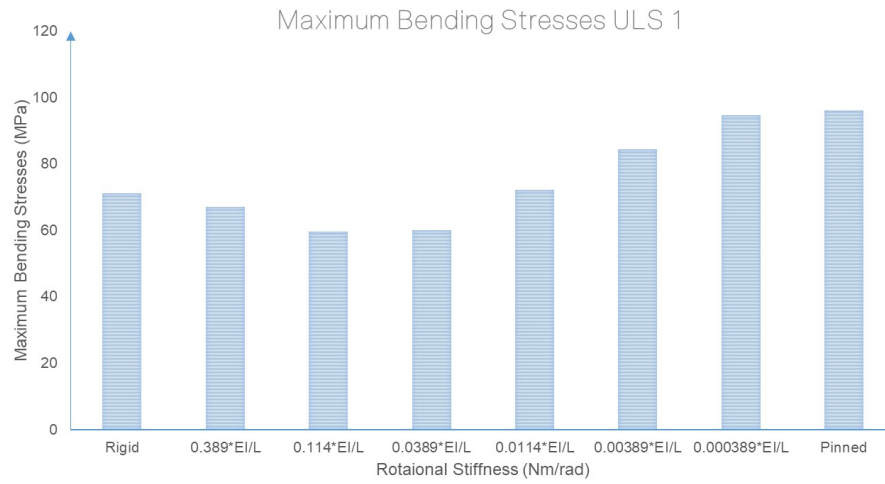


Figure 4.19: Maximum bending stresses for ultimate limit state load combination 1

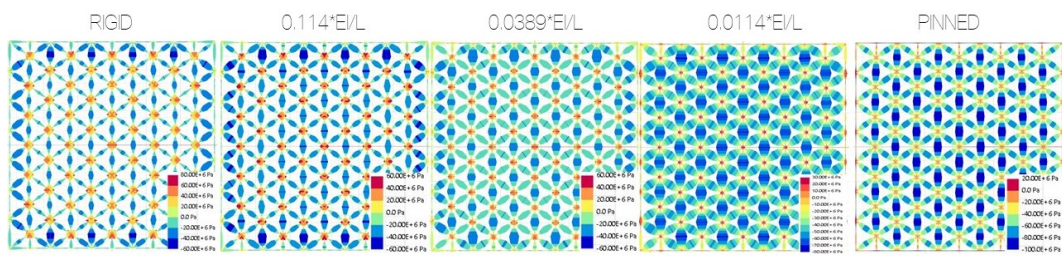


Figure 4.20: Maximum bending stresses for ultimate limit state load combination 1

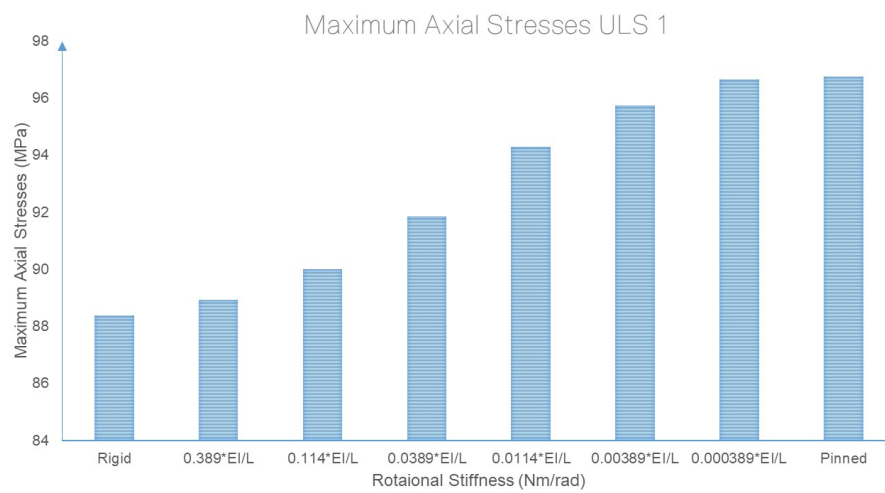


Figure 4.21: Maximum axial stresses for ultimate limit state load combination 1

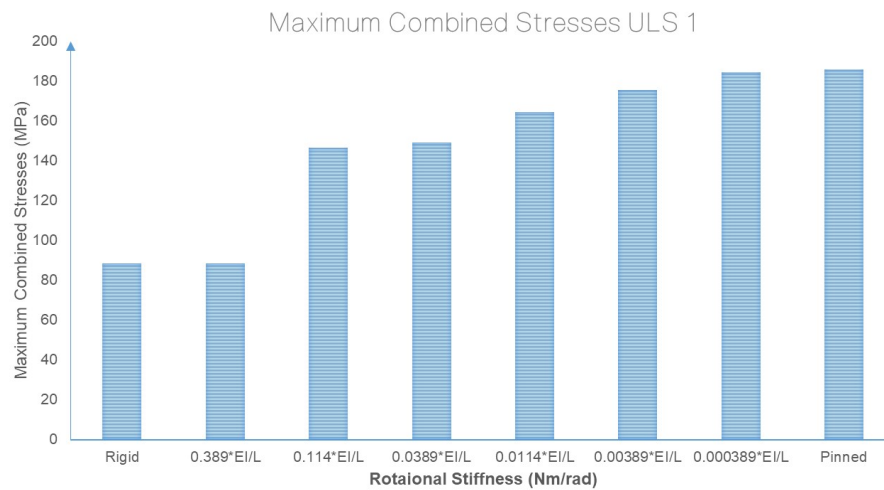


Figure 4.22: Maximum combined stresses for ultimate limit state load combination 1

the idea that it would be more optimal.

Despite the fact uniformly distributed load combinations give practical insight into the behavior of the grid shell, the governing values are again in the asymmetrical loading combination.

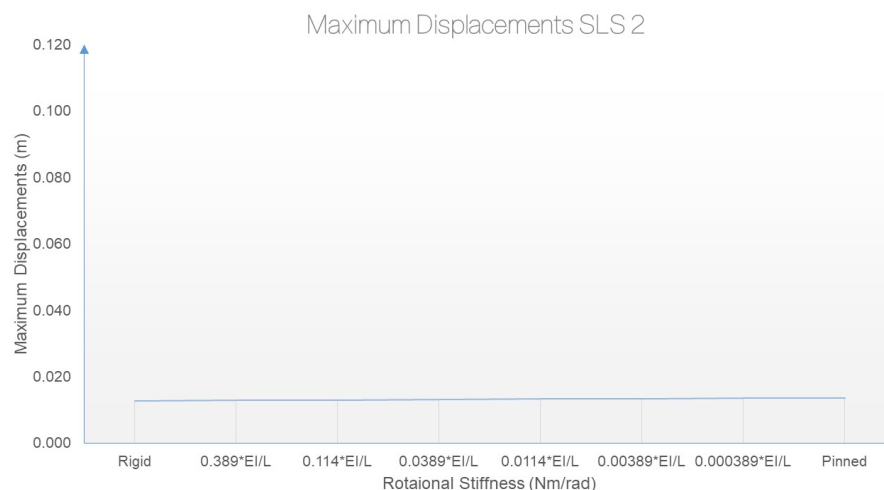


Figure 4.23: Maximum displacements for serviceability limit state load combination 2

For the triangular pattern, it can be concluded that the stiffness alternation does not affect the maximum displacements. After also studying the non-uniformly distributed load, the design criteria will focus on the ultimate limit state.

The changes in bending stresses are similar to the rectangular pattern. They decrease in the nodes up to a point where equal node and mid-span stresses are reached. After that, the opposite occurs. While for the axial stresses, an increase is seen with the decrease of stiffness by approximately 8.5%.

The combined stresses are again governing for the ultimate limit state. A slight difference is seen with alternation of stiffness, where the smaller values are in the semi-rigid 1 nodal configuration. Thus, the optimal cross-section can be found by

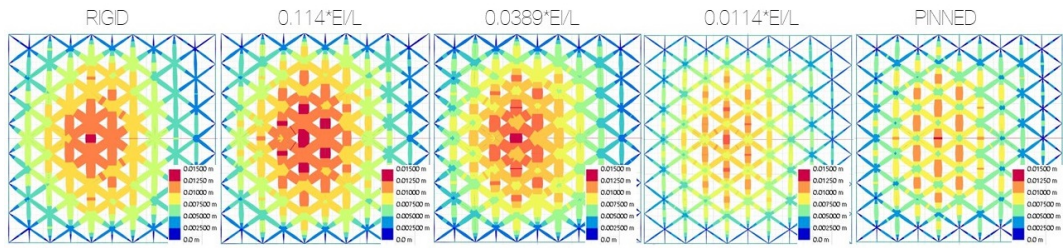


Figure 4.24: Maximum displacements for serviceability limit state load combination 2

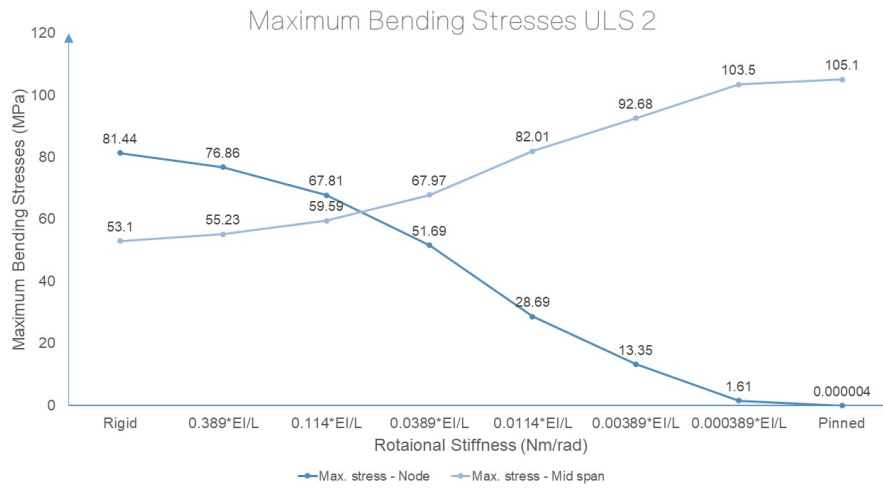


Figure 4.25: Maximum bending stresses for ultimate limit state load combination 2

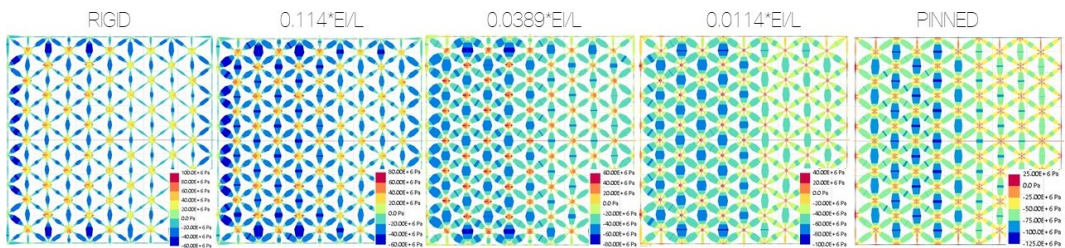


Figure 4.26: Maximum bending stresses for ultimate limit state load combination 2

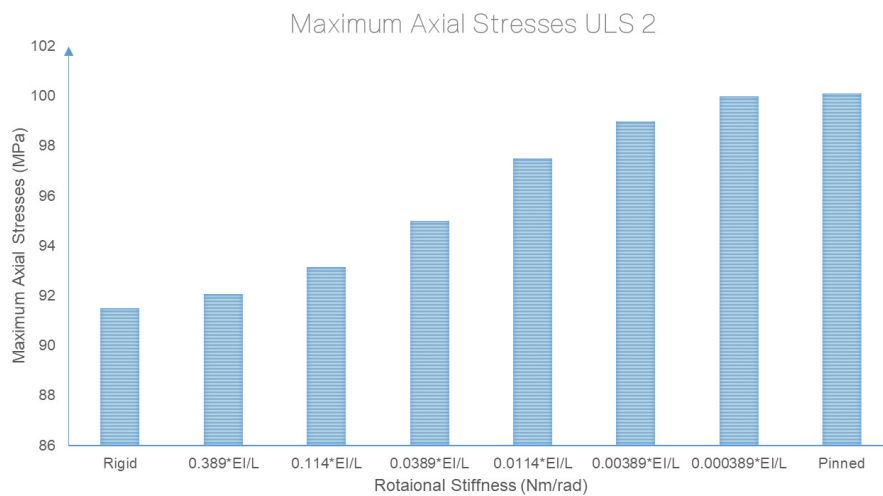


Figure 4.27: Maximum axial stresses for ultimate limit state load combination 2

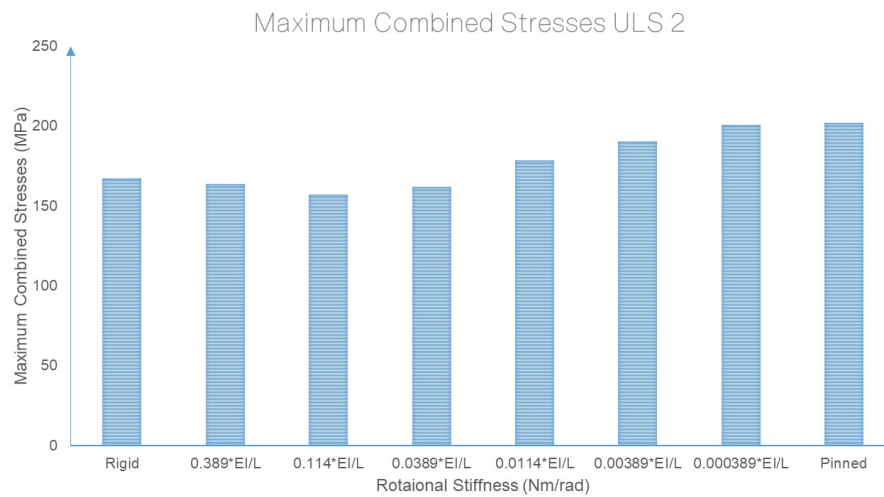


Figure 4.28: Maximum combined stresses for ultimate limit state load combination 2

applying the stiffness corresponding to semi-rigid 1.

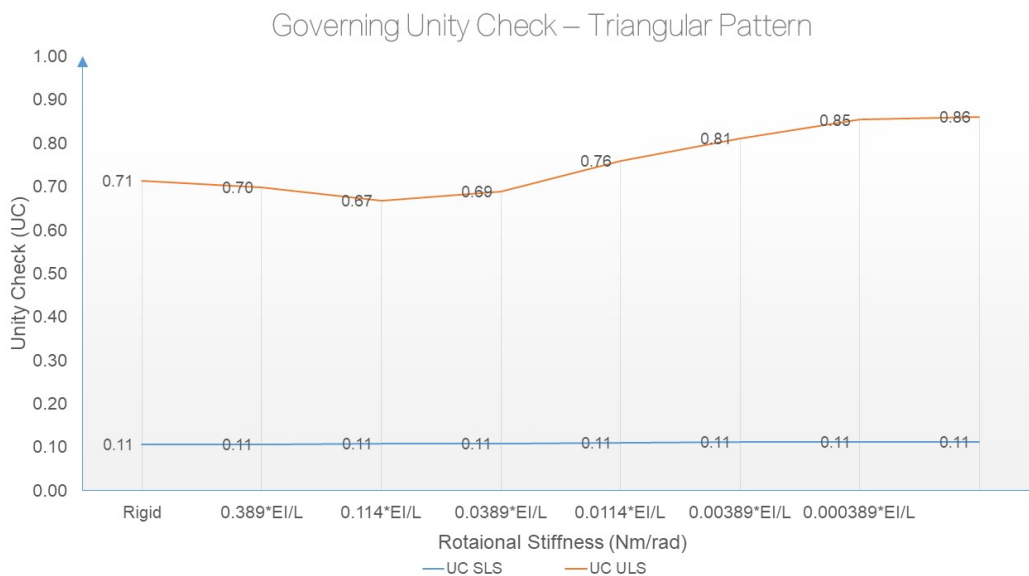


Figure 4.29: Governing unity checks for triangular pattern

From this graph, it can be concluded that the rotational stiffness has a less significant impact on a grid shell with a triangular pattern. Due to the rigid triangular shape, the maximum displacements and consequently the SLS unity checks are almost equal. Therefore, to find the optimal solution for a grid shell with a triangular pattern, only the ULS unity checks need to be compared. On the contrary, for grid shells with a rectangular pattern, a balance needs to be found between ULS and SLS unity checks. For this reason, in the following chapters, only the grid shell with a rectangular pattern will be studied.

4.4 CONCLUSIONS

From this chapter, the following conclusions are obtained:

What is the influence of joint stiffness in a grid shell in terms of ultimate limit state and serviceability limit state?

The influence of joint stiffness on the Ultimate Limit State and Serviceability Limit State was investigated using a parametric design. The study is conducted for grid shells with rectangular (non-rigid) and triangular (rigid) patterns. The parameters related to plane dimensions are fixed according to the case study, and pattern divisions are fixed according to glass pane limitations. The cross-section is RHS 150x100x50 for all scenarios so that only the influence of joint stiffness can be checked. The stiffness investigated are: fully rigid, rigid boundary, semi-rigid 1, semi-rigid 2, semi-rigid 3, pinned boundary, and pinned.

*Regarding the grid shell with the **rectangular pattern**, the following conclusions can be stated:*

- With the decrease of stiffness, the maximum deflections increased rapidly, especially in the asymmetrical load combination, until they exceeded the allowed values, approaching pinned stiffness. Consequently, approaching pinned stiffness, the structure would fail, and the analysis would no longer run. The maximum displacement from fully rigid to pinned boundary stiffness is increased by approximately 35%.

- With the decrease of stiffness, the bending stresses at the nodes decrease, and the bending moment and the mid-span increase reaching a cross-over moment near semi-rigid 1 with stiffness $k=0.114*EI/L$. This cross-over is expected and easily explained with the analogy of beams in frames.

- With the decrease of stiffness, the axial stresses decrease in a small ratio. Thus, the stiffness alternation has a limited effect over the axial stresses, which is expected as the axial stresses are related to the grid shell shape.

- The governing unity check for the ultimate limit state is related to the combination of maximal bending and axial stresses at the top and bottom fiber of the cross-section.

- The balance between ULS and SLS unity checks will be investigated in the following chapter to find an optimal solution.

*Regarding the grid shell with the **triangular pattern**, the following conclusions can be stated:*

- With the decrease of stiffness, the maximum deflections are approximately the equivalent in both load combinations. The variation on rotational stiffness does not influence the maximum deflections in the case of a rigid-shaped pattern, such as the triangular one.

- With the decrease of stiffness, the bending stresses at the nodes decrease, and the bending moment and the mid-span increase reaching a cross-over point between stiffness semi-rigid 1 with $k=0.114EI/L$ and semi-rigid 2 with stiffness $k=0.0389EI/L$. This cross-over is similar to the situation in the grid shell with a rectangular pattern.

- With the stiffness decrease, the axial stresses increase with a difference of approximately 8.5% from fully rigid to fully pinned stiffness.

- The governing unity check for the ultimate limit state is related to the combination of maximal bending and axial stresses at the top and bottom fiber of the

cross-section.

- To find the optimal solution for the triangular pattern with alternation of rotational stiffness, only the ultimate limit state needs to be considered. The lowest unity check is reached near semi-rigid 1, which would lead to the most efficient design.

A conclusion from this chapter is the continuance of research for the grid shell with the rectangular pattern only, as it shows to be affected more by the alternation of rotational stiffness in both ULS and SLS criteria. The rotational stiffness has a less significant impact on a grid shell with a triangular pattern. Due to the rigid triangular shape, the maximum displacements and consequently the SLS unity checks are almost equal. Therefore, to find the optimal solution for a grid shell with a triangular pattern, only the ULS unity checks need to be compared. On the contrary, for grid shells with a rectangular pattern, a balance needs to be found between ULS and SLS unity checks.

5 | DESIGN OF CONNECTIONS

5.1 CONNECTION DESIGN

Component method

IDEA StatiCa is the software used in this thesis to design the connections. The software bases the analysis on the component method (CM) included in the Eurocode EN 1993-1-8 to design steel joints. The component method solves the joint as a system of interconnected items, noted as components and modeled as springs. The forces and stresses are determined for each component, as visualized in Figure 5.1. The components are checked separately using corresponding formulas.

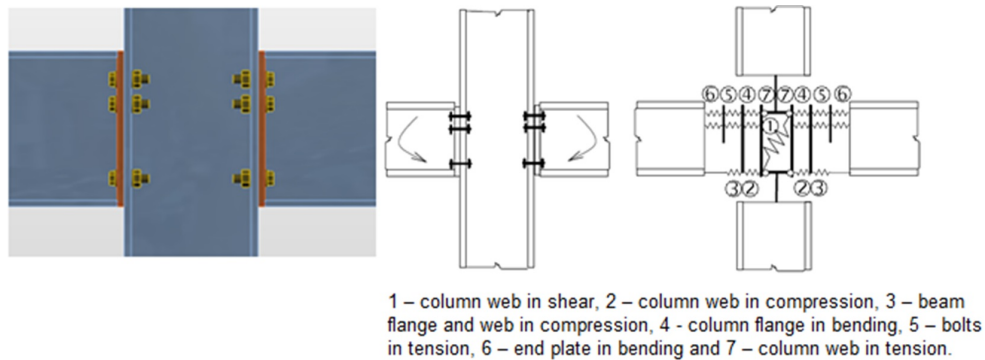


Figure 5.1: Component method explained

IDEA StatiCa has created a Component Based Finite Element Model (CBFEM) to implement in the 3D joint models. The elastic-plastic analysis is required, as the steel usually yields in the structure. Both webs and flanges of connected members are modeled using shell elements. Bolts are modeled by interpolation links between the shank nodes and holes edge nodes. The deformation stiffness of the plates distributes the forces between the bolts and simulates the adequate bearing of the plate. [Kubicek \[2021a\]](#)

The design procedure starts with obtaining data from the global analysis. Joints of members are modeled as massless points when analyzing global structure in Oasys GSA. Equilibrium equations are assembled in joints, and internal forces on beam ends are determined. These internal forces will be applied as loading in the joint model. The resultant of the forces from all members connected in the joint is zero – the whole joint is in equilibrium. [Kubicek \[2021a\]](#)

Based on the CBFEM method, two analyses are conducted in IDEA StatiCa. Strength analysis is the first analysis carried. Strain and stress checks of the components according to the Eurocode checks are performed by elastic-plastic analysis. The analysis of joints is materially non-linear. The load increments are applied gradually, and the state of stress is searched. The stresses in the steel components are compared to their yield strength, according to EN 1993-1-1. The strength of the welding is checked according to the Eurocode EN 1993-1-8 Cl. 4.5.3 check [Kubicek \[2021a\]](#):

$$\sigma_{w,Ed} = \sqrt{\sigma_{\perp}^2 + 3(\tau_{\perp}^2 + \tau_{\parallel}^2)} \quad (5.1)$$

$$\sigma_{w,Rd} = \frac{f_u}{\beta_w \gamma_{M2}} \quad (5.2)$$

The equations result in a weld utilization of:

$$U_t = \min \left\{ \frac{\sigma_{w,Ed}}{\sigma_{w,Rd}}, \frac{\sigma_{\perp}}{0.9f_u/\gamma_{M2}} \right\} \quad (5.3)$$

The second analysis carried is the stiffness analysis. The CBFEM method of IDEAS StatiCa enables the calculation of the connection stiffness. When bending moment M_y is defined, the rotational stiffness about the y-axis is analyzed. The analysis output (Figure 5.2) shows the obtained rotational stiffness compared to the boundaries of rigid and pinned. [Kubicek \[2021a\]](#)

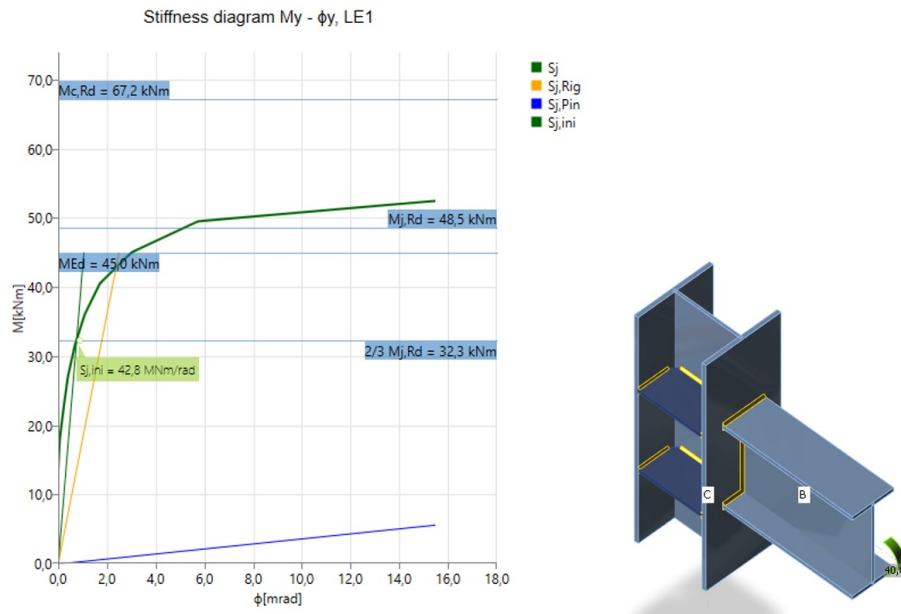


Figure 5.2: Example

A theoretical length is defined for each connected member. According to the software manual, this length is the span of the beam between two columns. In the case study with grid shells, this length relates to the distance between two nodes in the global model.

The deformation capacity/ductility δ_{Cd} belongs with the resistance and the stiffness to the three basic parameters describing the behavior of connections. In moment-resistant connections, the ductility is achieved by a sufficient rotation capacity ϕ_{Cd} . The deformation/rotation capacity is calculated for each connection in the joint separately. The software estimates the deformation capacity as a point where one of the following conditions is achieved [Kubicek \[2021a\]](#):

- Bolt or anchor resistance in tension, shear, or tension/shear interaction is reached.
- Weld resistance is reached.

- Plastic strain in plates is 15 %.

A summary of the design procedure can be given in a few steps:

- Material steel grades are assigned. In this case study, two steel grades are used, S235 and S355.
- Geometry of the joint is designed. For the case study, a similar design is chosen for the connections to make the comparison between them more straightforward.
- Load values are given for axial shear force, bending torsional moments.
- Design iterations including operations for welding, end plates, stiffeners, openings, ribs, until the unity checks are within the allowed limits and the required rotational capacity is reached.
- Stress-strain analysis is conducted, resulting in a deformed shape.
- Stiffness analysis is conducted to calculate.
- Report including the detailed output of both analyses conducted.

5.1.1 Connection design examples

Figure 5.3 shows examples of connections designed by Octatube. These examples will be a baseline for the design in this thesis. The principles that are mostly followed relate to the beam members' openings to input the one-sided bolts. Thus, one side of the threads inside the stiffening box will be welded there. Further, the other part of the bolt will be placed through the opening of the member. These openings allow the usage of tools to place the bolts. As the highest forces in the joints in this case study are axial forces and bending moments, not shear forces, removing material in the members' sides will not significantly impact the stresses. Another design choice is the approach of having a box where the members are connected.

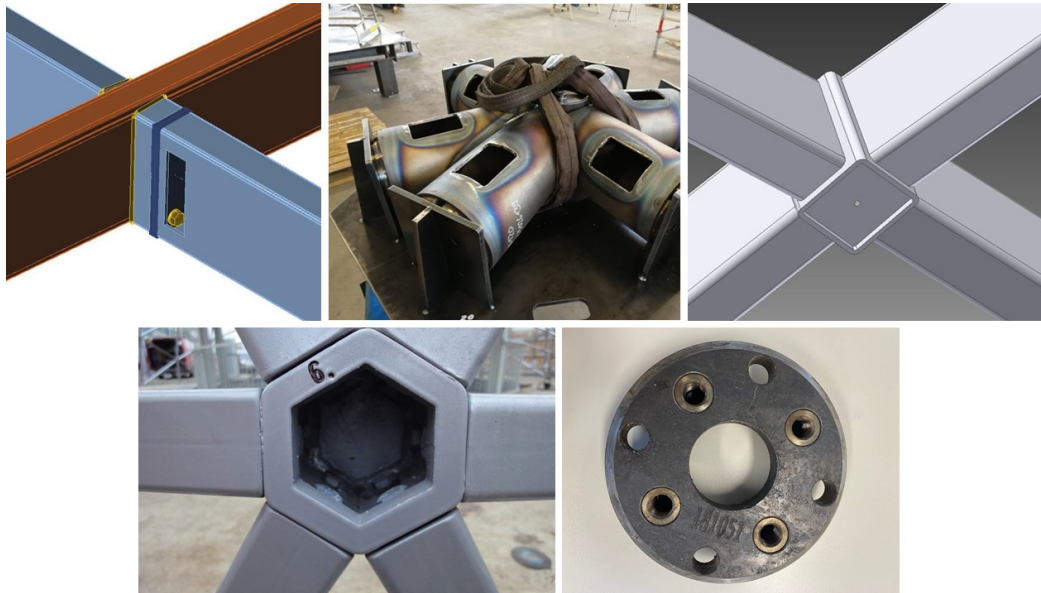


Figure 5.3: Examples of connection designed by Octatube

5.2 RESULTS & DISCUSSIONS

For the analysis in IDEA Statica, the node with the highest combination of axial force N_x and bending moment M_y is considered, corresponding to ULS 2 (non-uniformly distributed wind load). It is highlighted in the top view visualized in Figure 5.4. The full reports resulting from IDEA StatiCa can be found in Appendix E.

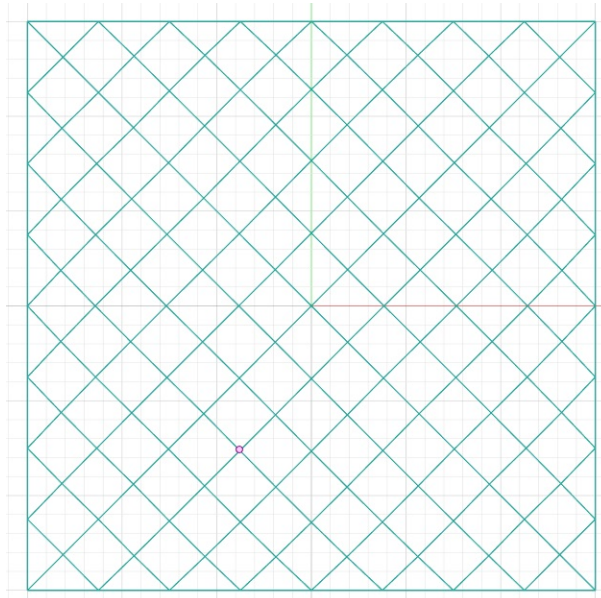


Figure 5.4: Location of governing node in ULS 2

Rigid connection

In order to obtain the stiffness $k=0.38*EI/L$ for the rigid boundary, a welded connection was necessary. The loading applied consists of a moment of 4.4 kNm and an axial force of 160 kN, obtained from the global analysis. The loading is identical for all the members as the node is in equilibrium. The connected members are rotated and tilted according to the global model made in Grasshopper, corresponding to the double curvature of the grid shell. A square hollow section SHS 150x150x16 is created in the middle of the members to weld them together. Top and bottom plates with a thickness of 12 mm are placed on the box. These plates act as stiffeners, decreasing the possible rotation of the connection and increasing thus the rotational stiffness.

The connected members are assigned a steel strength of S235, as in the global analysis. The stiffening box has a steel strength of S355 for both the square hollow section, as well as the top and bottom plates. The welds have a throat thickness of 4 mm and a strength of S235. The strength of the weld is the same as the member with the smallest strength it is connected. The highest stresses in the connection are reached in the stiffening box with a value of 144.4 MPa. These values are located near the corners. The resulting unity check is $UC=0.61$, indicating the connection can be optimized. However, the dimensions of the components cannot be decreased due to the required rotational stiffness. Additionally, the maximum stresses of the beams are located at the bottom, near the connection with the joint. This has to do with the moment force, pushing the members downwards and leading to the deformation. The stiffness calculated by IDEA StatiCa is 41.9 MNm/rad.

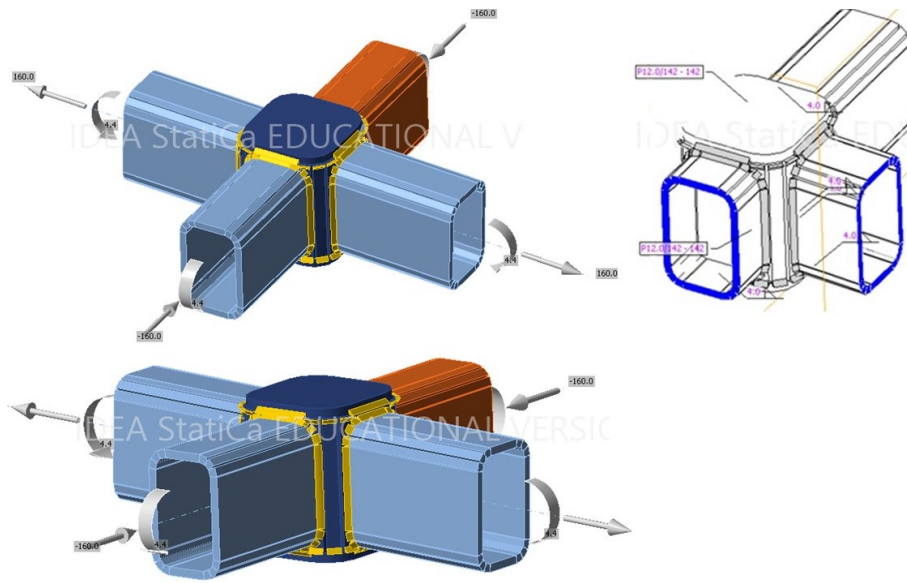


Figure 5.5: 3D model of rigid connection

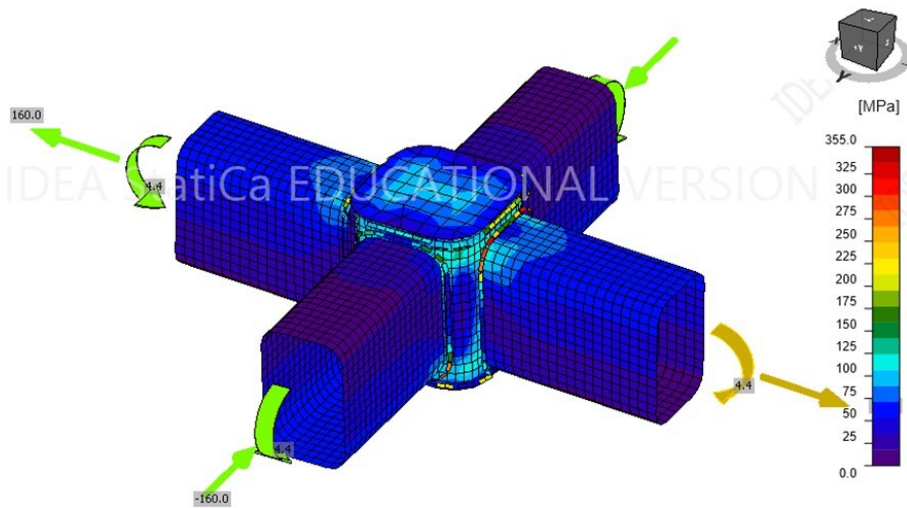


Figure 5.6: Stress distribution of rigid connection

Semi-Rigid 1 connection

In order to design a connection with stiffness $k=0.114*EI/L$, using only bolts was still not possible. For this reason, a welded connection similar to the rigid one is used. As a result of the lower required rotational stiffness, some of the dimensions are reduced. Firstly, the cross-section of the box is reduced to SHS 150x150x12.5, and the top and bottom plates have a thickness of 5 mm. The welds used have a throat thickness of 4 mm and a strength of S235. The axial force applied is the same as in rigid connection 160 kN, while there is a slight reduction of the moment 4.3 kNm.

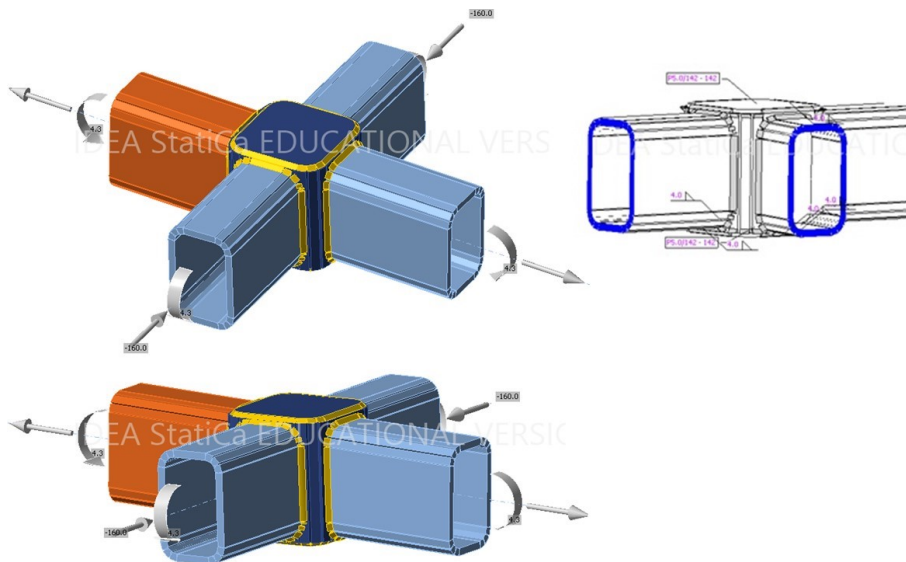


Figure 5.7: 3D model of semi rigid 1 connection

The highest stresses are reached in the stiffening box, which makes the distribution of the moment possible between the members. The maximum value reached is 251.8 MPa, which is found in the top and bottom of the webs welded to the members. Additionally, the top and bottom plates covering the box have maximum stress values of 241.6 MPa and 243.9 MPa at their centers. These maximum values correspond to the locations where the bending moment is transferred within the connected members. The welds reach a utilization rate of 0.98. The governing unity check of the components in the design is 0.71, while the rotational stiffness calculated by IDEA StatiCa is 13.2 MNm/rad.

Semi-Rigid 2 connection

The connection design with a stiffness $k=0.038*EI/L$ is realized using bolts. The box has a cross-section SHS 160x160x16 and the top and bottom plate have a thickness of 10 and 16 mm, respectively. The cross-section of the stiffening box in the middle is increased again from Semi-rigid 1 to Semi-rigid 2. The dimension increase is due to the use of bolts instead of welding. Four rows of bolts M12 10.9 are placed in two columns. The name of the bolts is related to their properties. Thus, the diameter of the bolts is 12 mm, and the ultimate force f_u is 1000 MPa. One row of bolts is outside the cross-section, increasing the lever arm. The choice allows for the distribution of moments and limits the rotation. The endplates have a thickness of 12 mm and steel strength of S355.

The applied bending moment for joint Semi-Rigid 2 is 3.8 kNm. The maximum stresses are found in the endplate, reaching 327.2 MPa. The other end plates reach

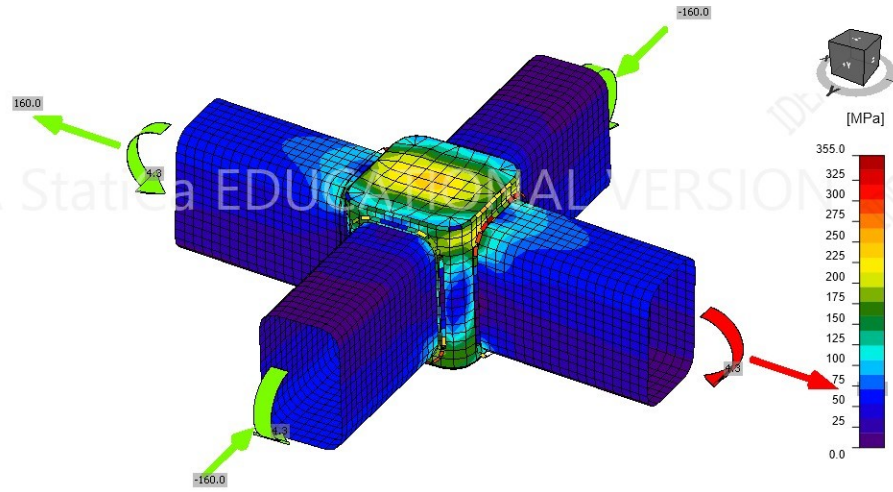


Figure 5.8: Stress distribution of semi rigid 1 connection

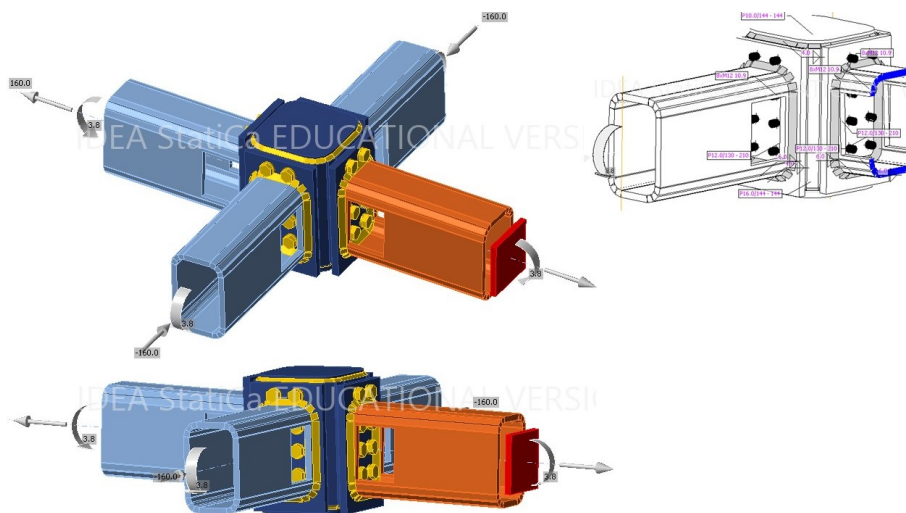


Figure 5.9: 3D model of semi rigid 2 connection

maximum values of 101.4 MPa, 309.8 MPa, and 101.9 MPa. A high value is also reached on the stiffening box, approximately 319 MPa. These values are located near the openings where bolts are placed. From the stress distribution graphs, it can also be noticed that the members have higher stresses near the openings. However, these values are within the limit reaching a maximum of 183.1 MPa. The governing unity check in the design is 0.92.

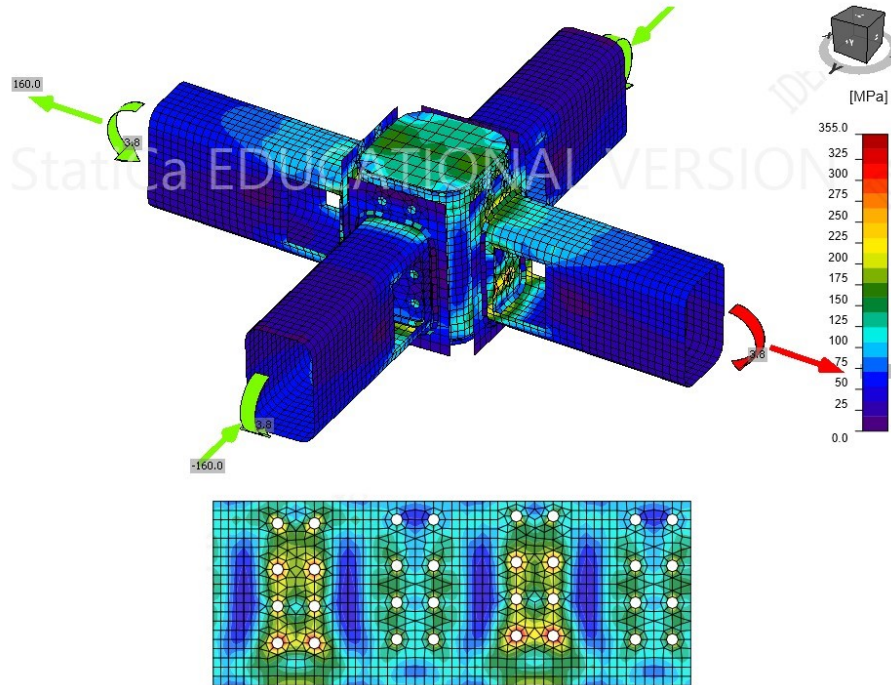


Figure 5.10: Stress distribution of semi rigid 2 connection

Finally, the strength of the welds is checked. The welds are designed with a throat thickness of 4 mm and a strength of S235. The maximum values are reached at the connection point of the stiffening box to the bottom cover plate with a value of 215 MPa in the perpendicular direction.

The resulting rotational stiffness calculated by IDEA StatiCa is 3.8 MNm/rad.

Semi-Rigid 3 connection

For a stiffness $k=0.0114*EI/L$, a connection with bolts similar to Semi-Rigid 2 is applied. The box has the same cross-section SHS 160x160x16 and the top and bottom plate have a thickness of 10 mm both. The rotational stiffness required is smaller for Semi-Rigid 2; thus, the row of bolts at the top of the beam is removed. Consequently, the height of the stiffening box is reduced, resulting in less material use. Two rows of bolts M12 10.9 are placed in two columns. The endplates in this connection have a thickness of 14 mm.

The applied loads include an axial force of 159 kN and a bending moment in the y-direction of 1.7 kNm. Maximal values of stresses are reached in the stiffening member at approximately 343 MPa. The endplates are loaded with maximum stresses, respectively 320.2, 87.1, 324.6, and 85.9 MPa. These maximum stresses are located near the openings for the bolts. The welds have a throat thickness of 4 mm for the stiffening member connected to the bottom and endplates. The welds connecting the member webs to the endplates have a throat thickness of 6 mm. The

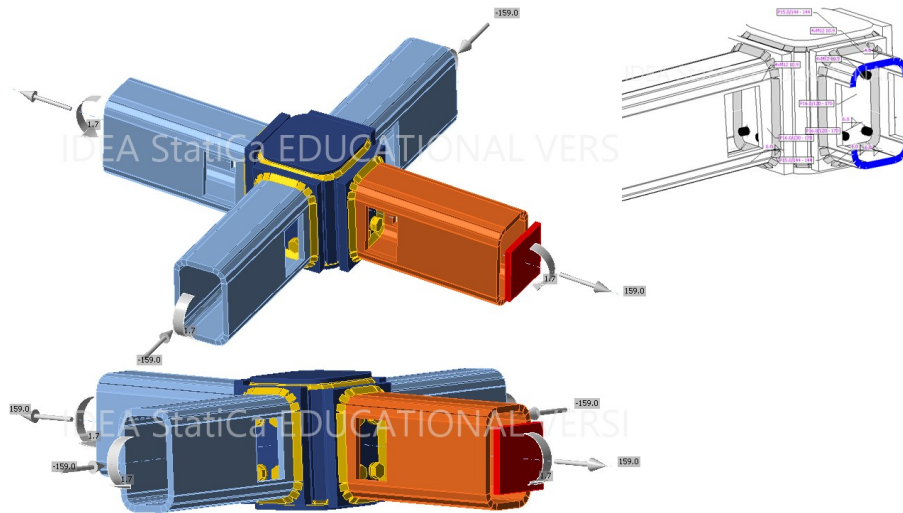


Figure 5.11: 3D model of semi rigid 3 connection

maximum stresses in the principal direction are 174 MPa, where the stiffening box is welded to the bottom covering plate. The utilization of steel reaches about 97

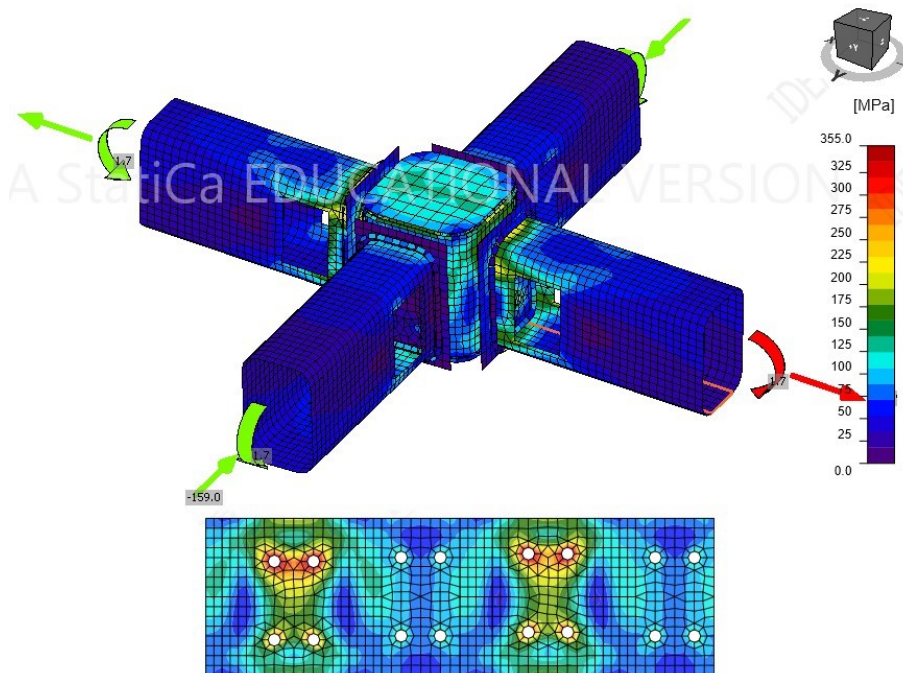


Figure 5.12: Stress distribution of semi rigid 3 connection

Pinned connection

For the pinned connection with stiffness $k=0.0038 \cdot EI/L$, a connection with bolts is applied. The box has the same cross-section SHS 160x160x16 and the top and bottom plate have a thickness of 10 mm both. Two rows of bolts M12 10.9 are placed in two columns. The lever arm between the bolts is decreased compared to Semi-Rigid 3 design due to lower bending moments. The endplates have a thickness of 10 mm.

The applied loads are axial force 84.9 kN and bending moment in y-direction 1.2 kNm. The maximum stresses are reached at the endplates with a value is as high as 327 MPa. The maximum stress at the stiffening box is 222.9 MPa, located near

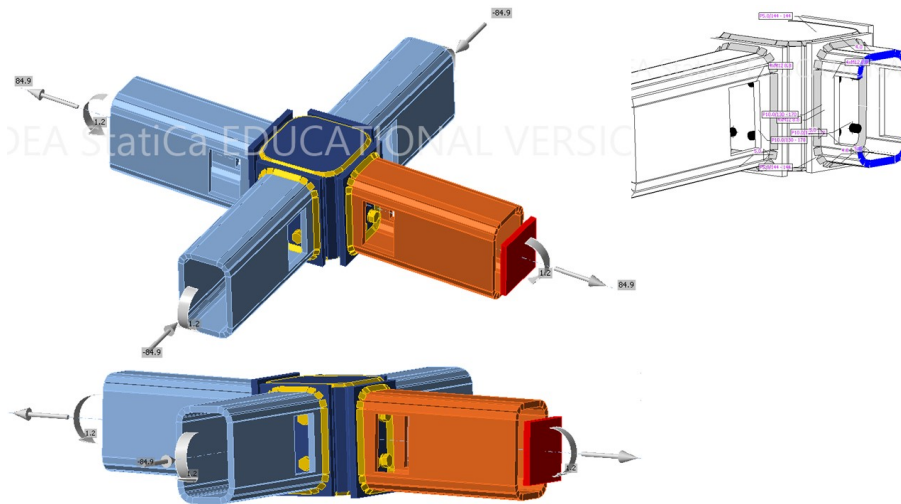


Figure 5.13: 3D model of pinned connection

the openings of the bolts. There are high bending stresses near the openings for the connected members as the stiffening elements are reduced. The welds have a throat thickness of 4 mm for the stiffening box connected to the bottom and top plate. In comparison, the endplates have a welding with a throat thickness of 6 mm. The maximum stresses of the welds reach 185 MPa in a perpendicular direction located at the endplates.

The rotational stiffness calculated in the software is 1.0 MNm/rad. The required rotational stiffness for a pinned joint is smaller. However, by increasing the dimensions of the stiffening member and end plates to withstand the loaded stresses, the rotational stiffness is also increased.

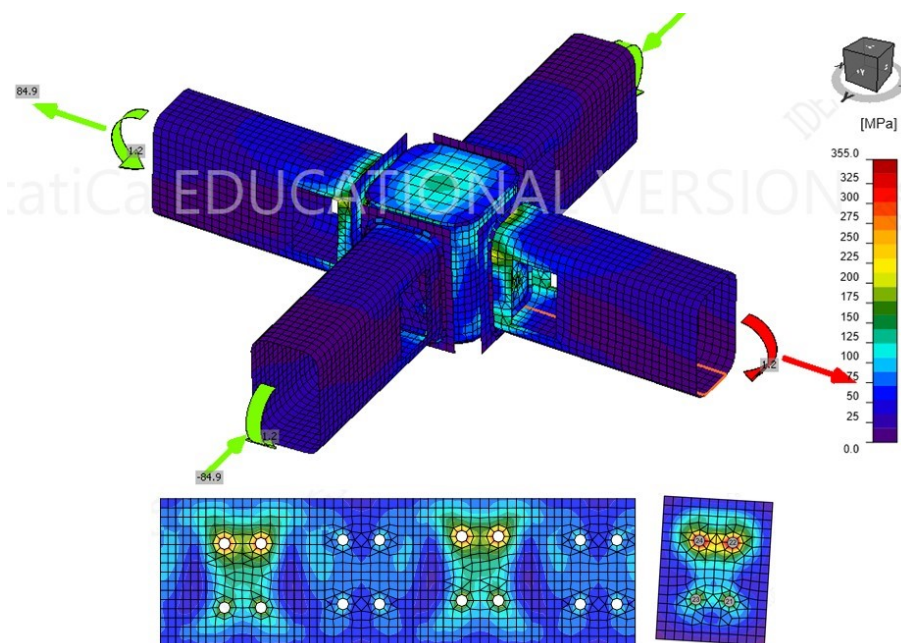


Figure 5.14: Stress distribution of pinned connection

5.3 CONCLUSIONS

What are the design requirements for joints in grid shell structures?

Considering the scope of the thesis, the grid shell joints' requirements are mainly focused on the out-of-plane requirements: the ability to transfer bending moment, sufficient out-of-plane stiffness. However, due to the presence of axial forces in the grid shell related to the shape generated, the ability to transfer axial forces is also necessary. Additional considerations in the design include fabrication, the weight of the joint, and appearance.

The design of joints is based on two analyses conducted in IDEA StatiCa: strength analysis and stiffness analysis. Strength analysis is the first analysis performed as the joint needs to meet each component's allowable stresses requirements. The analysis is based on the Component Method (CM) stated in EN 1993-1-8: Eurocode 3: Design of steel structures – Part 1-8: Design of joints. IDEA StatiCa, a FEM software, has adopted this method to be applicable for 3D models of joints as Component Based Finite Element Model (CBFEM).

Stiffness analysis is run afterward to verify if the required stiffness is achieved. The calculation of rotational stiffness in IDEA StatiCa is based on the ratio of bending moment with rotation.

How would structural joints of grid shells look in real-life engineering to obtain the different stiffness?

The design of the structural joints is based on examples from Octatube. The principles followed include having a steel box where the grid members are connected. This will allow the possibility to design similar joints with different stiffness so that the difference in achieving these stiffness is clear. Another principle followed is the opening in the beams near the joint so that one-sided bolts can be placed.

The designs for Rigid and Semi-Rigid 1 joint are achieved through a fully welded connection. The difference between these two designs is in reducing the thickness of the steel box and covering plates. The Semi-Rigid 2 joint was possible to achieve through using a combination of welded and bolted connection. The Semi-Rigid 3 joint is achieved by removing the row of bolts at the member's top due to the bending moments' decrease. The pinned joint is achieved by decreasing the lever arm between the row of bolts in the Semi-Rigid 3 joint, as there is less need to transfer bending moments.

6 | OPTIMIZATION

6.1 OPTIMIZATION PROCEDURE

To solve the research question, an optimization of connection design focusing on the rotational stiffness is necessary. As visualized in Figure 6.1, the optimization will concentrate on the latter part of the script (analysis). The analysis will run in Oasys GSA through Geometry Gym plug-ins, and the results will be visible in Grasshopper. These results are saved within Octopus.

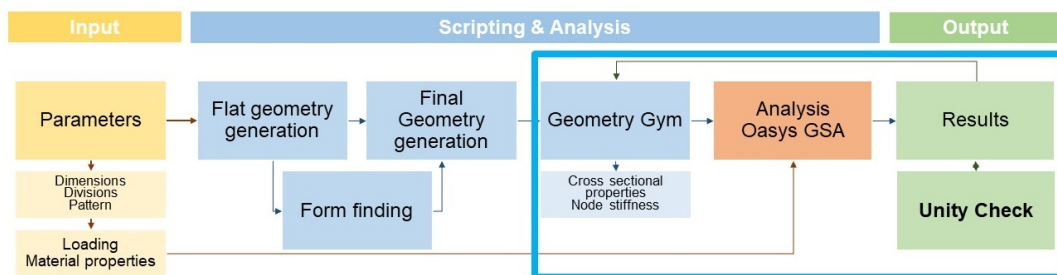


Figure 6.1: Methodology

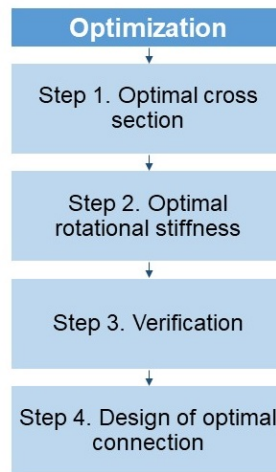


Figure 6.2: Optimization procedure

Octopus is an optimization algorithm within Grasshopper, created by Robert Vierlinger. It is initially made for Multi-Objective Evolutionary Optimization. As an evolutionary simulator, it can approach optimal solution sets through iterative tests and constant self-adaptation. The difference between Galapagos, a similar plug-in in Grasshopper, is that it allows simultaneously searching for many parametric inputs. Additionally, it allows to input multiple objectives instead of just one. Once Octopus has collected data, it begins to map the information on a coordinate grid that is set up based on the objectives set. The grid makes it possible to access the full range of data and separate the solutions that fall in the favorable median. [Hen-](#)

Notation	Rotational Stiffness (Nm/rad)	UC SLS	UC ULS	Cross-section
Fully Rigid	Rigid	0.73	0.93	RHS 100 × 60 × 8
Rigid Boundary	$0.389EI/L$	0.77	0.92	RHS 100 × 60 × 8
Semi-rigid 1	$0.114EI/L$	0.85	0.90	RHS 100 × 60 × 8
Semi-rigid 2	$0.0389EI/L$	0.88	0.87	RHS 120 × 60 × 6.3
Semi-rigid 3	$0.0114EI/L$	0.97	0.53	RHS 120 × 60 × 10
Pinned	$0.00389EI/L$	0.86	0.54	RHS 150 × 100 × 6.3

Table 6.1: Optimal cross section for each stiffness

riksen [2017]

The parameters connected to Octopus in this case study are the cross-section of members and the joint stiffness. The objectives are connected to the unity checks for SLS and ULS to achieve a value close to 1. By definition, the objectives are minimized, and a Boolean can be assigned in Grasshopper to limit the solutions. In this situation, the limit is $UC=1$.

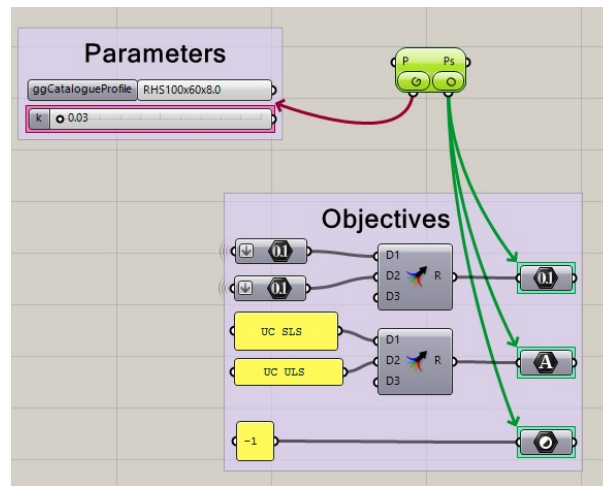


Figure 6.3: Optimization plug-in

The combination of all possible cross-sections and joint stiffness will give a significant number of solutions. Thus to speed up the process, the optimization procedure will follow a few steps (Figure 6.2), explained in the following section.

6.1.1 Step 1. Optimal cross section

The first step is finding an optimal cross-section while applying the rotational stiffness studied in Chapter 4 (Fully Rigid, Rigid Boundary, Semi-Rigid 1, Semi-Rigid 2, Semi-Rigid 3, Pinned). From these results, the smallest cross-section found will give some limitations to the parameter's range.

The table above gives the unity checks for each cross-section and stiffness combination. The optimization algorithm aimed to find a cross-section where the unity checks would be approximately 1, yet smaller than 1. It can be seen that the smallest possible cross-section is reached for Fully Rigid, Rigid Boundary, and Semi-Rigid 1. Specifically, the required cross-section in these three scenarios is RHS 100x60x8.0.

Although the cross-sections are identical and weigh the same, the joints would not have the same weight. As visualized in Chapter 5, the sizes of the joint components could be decreased, while the required rotational stiffness was smaller. Thus

the structural weight of the joints, and consequently the total structural weight of the roof can be optimized by decreasing the required rotational stiffness.

6.1.2 Step 2. Optimal stiffness

The second step of the optimization will start with a fixed cross-section, resulting from step 1: RHS 100x60x8. Additionally, as this step's objective is to find the smallest stiffness possible for this cross-section, the rotational stiffness parameter will be limited between Semi-Rigid 1 and Semi-Rigid 2.

The optimization process is conducted again with the use of Octopus in Grasshopper. The iteration results in a grid of values corresponding to the objectives from running the Octopus plug-in as visualized in Figure 6.3. As a result, the optimal solution is found when applying rotational stiffness $k=0.045EI/L$. The Unity Checks in this situation are $UC=1$ for SLS and $UC=0.86$ for ULS.

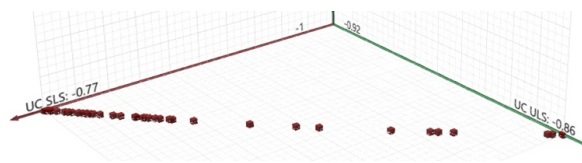


Figure 6.4: Optimization in Octopus

6.1.3 Step 3. Verification

In order to verify there is no other optimal solution, the plug-in is rerun for two other smaller cross-sections for a broader range of stiffness. The cross-sections, in this case, are RHS 100x60x6.3 and RHS 100x50x8. All results obtained (Appendix F) give combinations of Unity Checks where at least one is bigger than 1. By definition, in the Eurocode, it is not allowed. This verifies that indeed the optimal solution is found for cross-section RHS 100x60x8 with rotational stiffness $k=0.045EI/L$.

6.1.4 Step 4. Optimized connection design

Following the result obtained from Octopus, the connections are designed in IDEA StatiCa for members with cross-section RHS 100x60x8 and rotational stiffness $k=0.045EI/L$. Two connections are designed for the grid shell roof. The first connection is designed using only welding and the second connection uses a combination of bolts and welding.

The objective is to use connections welded in a factory for the majority of the joints. This will allow prefabrication of the grid shell in components. Next, they will be transported to the location of the site. The bolted connections will be used to join together these components of the roof. The concept is visualized in Figure 6.4. This solution is found as the most optimal considering also the fabrication aspect. Welding on site is usually avoided due to specific weather conditions and permits required.

The sizing of the components is limited to the transportation possibilities. In the European Union, the maximum legal dimensions of a trailer are a length of 12 meters, a height up to 4 meters, and a width of 2.55 meters. [BTInternational \[2021\]](#)

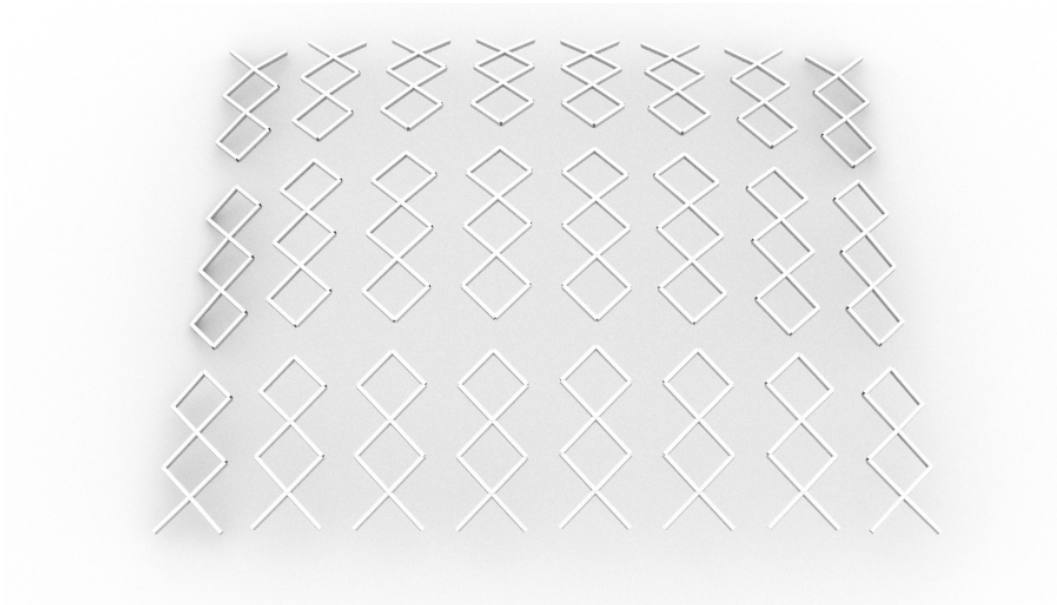


Figure 6.5: Design of the grid shell roof

Connection with bolts

Figure 6.6 of the 3D model shows the two different sides of the connection. Two member ends are welded in the factory, and the other two are bolted in situ.

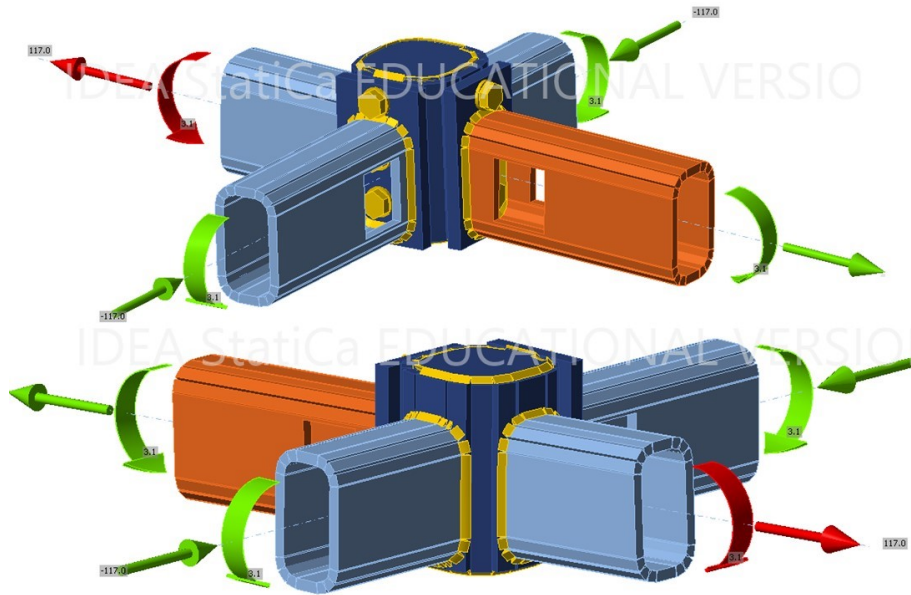


Figure 6.6: 3D model of optimal connection with bolts

The box has a cross-section SHS 120x120x16 and the top and bottom plate have a thickness of 2 and 3 mm, respectively. The additional stiffness from these plates is unnecessary for the design with the optimal stiffness as it is significantly reduced. However, these plates allow the distribution of stresses from the box connecting the members. Three rows of bolts M12 10.9 are placed in one column. The increased strength of bolts was necessary due to the high-stress concentration in the endplates. Similar to the designs in Chapter 5, the member openings allow the placement of one-sided bolts connecting the endplates to the box. The endplates have a thickness of 12 mm. The steel material of the stiffening box and all the connected plates is

S355. The strength of the welds is S355 connecting the box to the top and bottom plates. The welding connecting the endplates to the members has a strength S235, the same as the members.

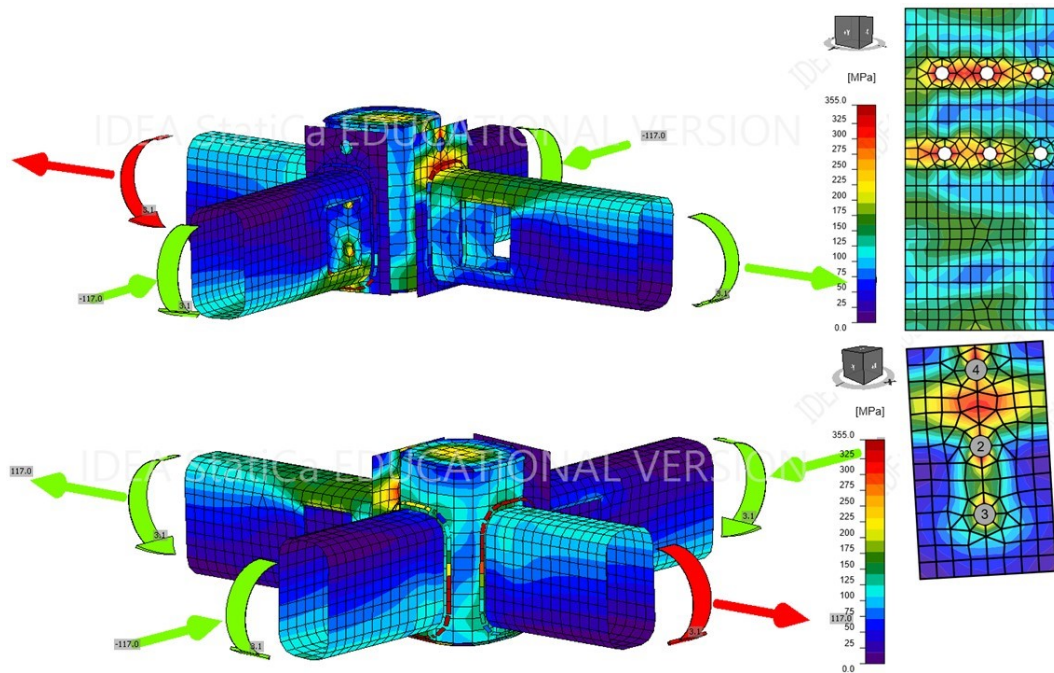


Figure 6.7: Stress distribution of optimal connection with bolts

The maximum stresses are reached in the stiffening box and the bottom plate. The values are 353.1 and 355.0 MPa, respectively. The maximum stress reached in the endplates is 325.5 MPa. It is located near the openings of the bolts, going towards the edge. Thus $UC=1$ is reached in the design, in the bottom plate of the stiffening box. For the members, there are high bending stresses near the openings as the stiffening elements are reduced. The welds have a throat thickness of 3 mm and reach a maximum utilization rate of $UC=0.98$.

The rotational stiffness calculated is 3.3 MNm/rad. The required rotational stiffness for the joint is smaller. However, the dimensions of the connection cannot be reduced to achieve a smaller rotational stiffness as $UC=1$ for the stresses is reached.

Welded connection

The box has a cross-section SHS 100x100x10, and the top and bottom plate have a thickness of 3 mm both. The steel material of the stiffening box and the covering plates is S355. The components are welded together with a throat thickness of 3 mm. The strength of the welding is S355 connecting the box to the top and bottom plates. While the connection of the box to the member is achieved with welding with strength S235.

The maximum stresses are reached at the stiffening box and the bottom covering plate with a value of 355.0 MPa. Thus, the $UC=1$ for the stresses is reached. These values are located near the edges of the stiffening box due to the bending moment and resulting rotation.

The welds have a throat thickness of 3 mm and result in a maximum utilization rate of 0.99. The maximum principal stresses are located at the connection of the

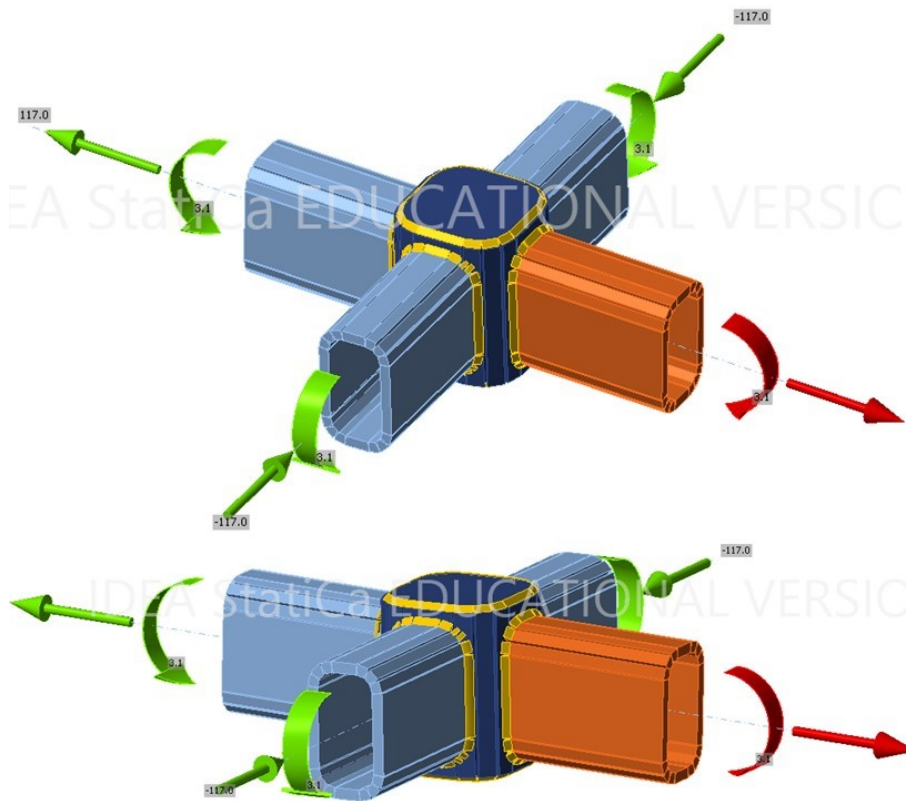


Figure 6.8: 3D model of optimal connection welded

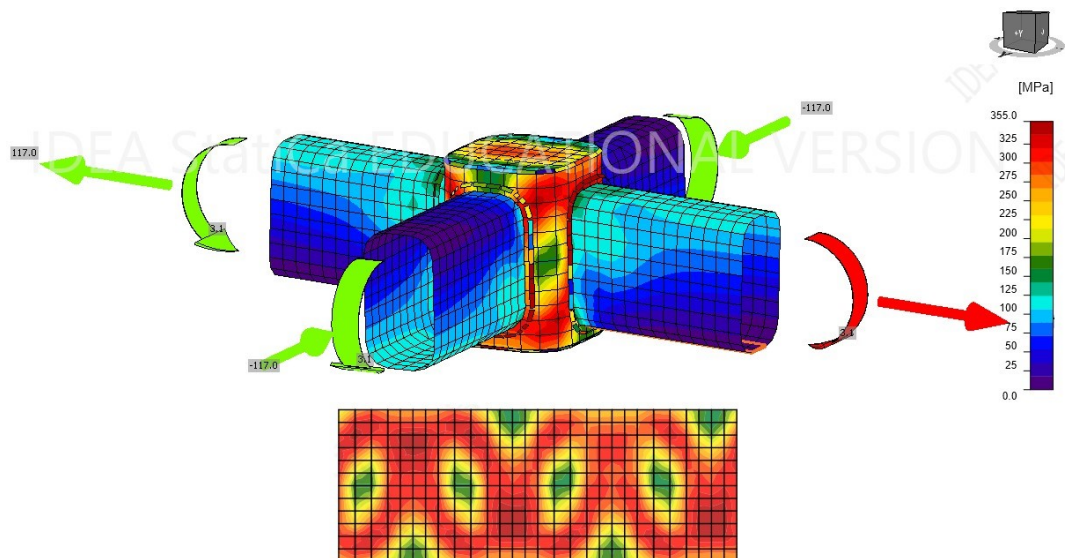


Figure 6.9: Stress distribution of optimal connection with bolts

web of members to the stiffening box. The rotational stiffness calculated is 4.1 MN-m/rad. The required rotational stiffness for the joint is smaller, approximately 0.9 MNm/rad. However, by decreasing the rotational stiffness, the maximum stresses were affected and exceeded the allowable values.

6.2 RESULTS & DISCUSSIONS

Each optimization step resulted in a design closer to the optimal solution, as defined in the research question. The first step concluded from step 1 that the smallest cross-section could be obtained applying Fully Rigid, Rigid Boundary, and Semi-Rigid 1 joint stiffness. The cross-section that could be used for the three scenarios was RHS 100x60x8. Thus, in the global aspect, the grid shell would result in the same structural weight. The second step resulted in the lowest stiffness possible to still be able to assign the cross-section. Consequently, after designing the joints with the optimal stiffness, the structural weight can be reduced. A fully rigid joint with the same cross-section is designed to quantify the advantage of using the joints with the optimal stiffness (included in the Appendix F).

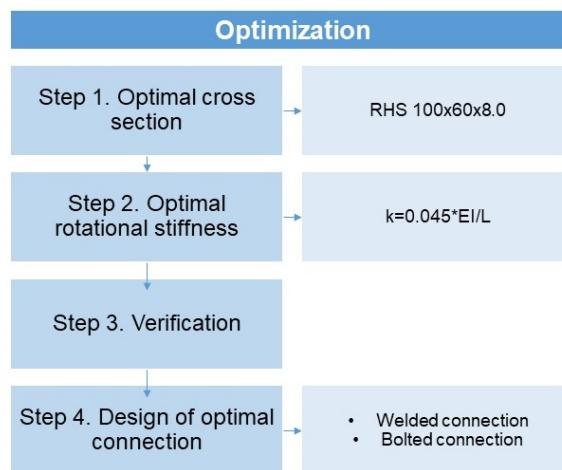


Figure 6.10: Optimization results

With the structural weight calculated within IDEA StatiCa, it was concluded that the total weight of the joints is decreased approximately 50% from Fully Rigid (2343.6 kg) to joints with optimal stiffness (1199.44 kg). Consequently, the total structural weight of the grid shell is decreased by approximately 8% from 14537.43 kg to 13393.27 kg. This reduction is beneficial for structural, economic, and environmental purposes.

6.3 CONCLUSIONS

How can connection stiffness be optimized to have a lighter-weight grid shell roof structure over the existing building?

Octopus is an optimization algorithm within Grasshopper that was used for the optimization procedure. The procedure followed with four steps. The first step consists of finding the optimal cross-section for the stiffness investigated: Fully Rigid, Rigid Boundary, Semi-Rigid 1, Semi-Rigid 2, Semi-Rigid 3, Pinned. For this case study, the smallest cross-section is obtained for stiffness: Fully Rigid, Rigid Bound-

ary, Semi-Rigid 1.

In the second step, the optimal stiffness for this cross-section is obtained. Optimal stiffness in this thesis is considered the smallest stiffness as it would lead to a lighter-weight joint design and consequently a smaller total weight of the grid shell roof. Thus, the stiffness in this step is limited between Semi-Rigid 1 and Semi-Rigid 2. The optimization algorithm reruns the structural analysis until the lowest stiffness is found while maintaining Unity Checks for SLS and ULS smaller than 1. The optimal stiffness found for this case study is $k=0.045EI/L$.

In step three, two smaller cross-sections are iterated for different stiffness to verify that the solution obtained is optimal. In all results, the unity checks were bigger than 1 for at least one of the limit states, thus verifying there is no other solution. The last step consisted in giving a design solution for the connections. Other aspects are considered, such as fabrication practicality and transport limitations.

What does the optimal joint design look like?

Two types of connections are designed for the grid shell roof. The first connection is designed using only welding and the second connection uses a combination of bolts and welding. The aim is to avoid welding in situ and prefabricate parts of the roof in the factory within the transportation limitations. The welded connections are designed with a rectangular hollow section box in between the members. The bolted connections follow similar logistics. However, two sides of the connection allow using bolts to connect with the member through endplates. In contrast, the other two sides are welded with the members in the factory. The fully welded connections allow prefabrication of roof components off-site, and the bolted ones allow connecting these smaller parts in situ.

7

CONCLUSIONS & RECOMMENDATIONS

7.1 CONCLUSIONS

In this section, the final answer to the research question is given:

"How can connection stiffness in the parametric design of grid shell roof structures lead to more efficiency for existing buildings?"

Connection stiffness was proven to significantly affect both Serviceability and Ultimate Limit State for non-rigid (rectangular) pattern grid shells and only on the Ultimate Limit State for rigid (triangular) pattern grid shells. The rectangular patterned grid shell was studied thoroughly, including how the joints with different stiffness could be designed in practice.

The objective of the thesis was to reduce the self-weight of the grid shell, taking into consideration joint stiffness. It is achieved by optimizing both the cross-section and the joint stiffness. By lowering the required stiffness, also the dimensions of the components in the joint can be reduced. Thus the material used is decreased.

Two types of connections are designed for the grid shell roof. The first connection is designed using only welding and the second connection uses a combination of bolts and welding. This design choice allows prefabricating parts of the roof and connecting them in situ.

Finally, using the optimal stiffness in the design of the joints, the total weight of the grid shell roof was reduced by approximately 8%, compared to using fully rigid joints, which is the common practice when designing non-rigid (rectangular) patterned grid shells. The weight of the structural joints was reduced approximately 50% from rigid to the optimal solution. Consequently, the superimposed loading over the existing building and foundation is reduced.

Two considerations need to be taken about the reduction percentage:

- The reduction percentage is specific for this case study. In another design, the reduction could have a higher or lower impact.
- In the final design in IDEA StatiCa, the stresses in the joint were governing compared to the required rotational stiffness. Thus, to stay within the allowed stresses, the dimensions of the joint components were increased, consequently increasing the stiffness higher than $k=0.045EI/L$. Therefore, a different design of the joint could allow for both the allowed stress conditions to be met and the rotational stiffness to be close to the boundary.

7.2 RECOMMENDATIONS

In this section, recommendations concerning further research opportunities are given.

Recommendations for engineers:

- Consider studying the joint stiffness in the design of grid shells. It will benefit in optimal structural utilization, reduction of self-weight, and consequently super-imposed loading over the building and foundation.
- Although the thesis was motivated by grid shells over existing buildings, the parts of the thesis could be relevant to apply for the design of grid shells in general.
- Increase the use of parametrical design and optimization procedures during the structural design. As a result, material savings lead to economic and environmental benefits, which both the client and engineers aim.

Recommendations for educational research:

- Chapter 2 presented a method that could be applied to find the boundaries of joint stiffness in grid shells instead of the Eurocode method applied in frames. Furthermore, this method could be tested parametrically for more complex case studies to obtain more general rules on the method's limitations.
- In future research, a more thorough structural analysis can be conducted by considering more practical and realistic load combinations such as snow load with accumulation at edges. This part was neglected due to the focus being the influence of stiffness. However, it will give more accurate results for the structural performance of grid shells. Additionally, the wind load that was governing was specific to the area where the case study is located.
- The geometrical parameters were set to unchangeable dimensions when the case study was applied. Using parameters gives more general results for the effect joint stiffness has over the grid shell behavior.
- The optimization procedure was conducted in Grasshopper by using Octopus, an optimization algorithm in 3 steps. The data from one step to the other was transmitted manually. This procedure can be fully automated in order to be easily used and adopted in other projects.
- Design possibilities and integration in a parametrical model of the cables and/or steel rods transmitting the horizontal forces within the grid shell could be considered.
- Investigation in detail the axial and shear deformation of the rectangular patterned grid shell to have specific argumentation on the different behavior between the triangular and rectangular pattern.

Future research possibilities:

- The reduction of structural weight also has benefits in the economic aspect and the environmental footprint. These two aspects would be interesting to investigate in future research. Other aspects could be considered in the optimization process, such as the economic and environmental aspects. These aspects were left out of the scope due to time limitations.
- A study on the assembly and disassembly possibilities of the connections can be conducted, so that the structure can be re-used.

- Optimization of joints has been in focus related to design procedure and fabrication. Future research could be done on joint design optimization, including the methodology related to the joint stiffness boundaries for grid shells.
- Application of the stiffness optimization of joints could be combined with 3D printed joints. As a result, the material used could be reduced even more.
- A study of joint stiffness influence can be conducted for timber grid shells, where the assembly of the elements follows another procedure, and consequently, the structural behavior is not alike; thus, the effect that joints have on the grid shells is different.
- Extensive cost analysis and environmental impact of the solution where joint stiffness optimization is applied.

BIBLIOGRAPHY

- BTAInternational (2021). Equipment and trailer dimensions.
- Coenders, J. (2008). Reader of ct5251: Structural design - special structures.
- Eigenraam, P. (2017). Unit ffo1 form finding - particle spring method.
- Fan, F., Ma, H., Cao, Z., and Shen, S. (2011). A new classification system for the joints used in lattice shells. *Thin-walled structures*, 49(12):1544–1553.
- Feng, R. Q., Yao, B., and Ye, J. H. (2012). The stability of elliptic paraboloid grid shell lighting roofs with semi-rigid joints. In *Advanced Materials Research*, volume 374, pages 2148–2151. Trans Tech Publ.
- Feng, R.-q., Ye, J., and Zhu, B. (2015). Behavior of bolted joints of cable-braced grid shells. *Journal of Structural Engineering*, 141(12):04015071.
- Grande, E., Imbimbo, M., and Tomei, V. (2020). Optimization strategies for grid shells: The role of joints. *Journal of Architectural Engineering*, 26(1):04019028.
- Harris, R., Haskins, S., and Roynon, J. (2008). The savill garden gridshell: design and construction. *The Structural Engineer*, 86(17):27–34.
- Henriksen, R. (2017). Optimisation vs. adaptation: Multi-parameter optimisation.
- Hoogenboom, P. (2011). Notes on shell structures. *DUo Technology (Ed.)*, pages 30–32.
- Jaspart, J.-P. and Weynand, K. (2016). *Design of joints in steel and composite structures: Eurocode 3: Design of steel structure, Part 1-8-Design of joints; Eurocode 4: Design of composite steel and concrete structures, Part 1-1-general rules and rules for building*. Brussels: ECCS, 2016.
- Kubicek, J. (2021a). Idea statica connection theoretical background.
- Kubicek, J. (2021b). Why bother with connection stiffness.
- López, A., Puente, I., and Serna, M. A. (2007). Numerical model and experimental tests on single-layer latticed domes with semi-rigid joints. *Computers & structures*, 85(7-8):360–374.
- Maunsell, F. (2007). Gridshell covers courtyard formed by historic buildings. *Structural engineer*, 85:20–22.
- Miura, K. and Pelligrino, S. (2001). Structural concepts and their theoretical foundations. *Unpublished booklet*.
- Patterson, M. (2011). *Structural glass facades and enclosures*. John Wiley & Sons.
- Schober, H. (2015). *Transparent shells: Form, topology, structure*. John Wiley & Sons.
- Schueller, W. (1983). *Horizontal-span building structures*. Wiley.
- Simone, A. (2011). An introduction to the analysis of slender structures.
- Stansfield, K. (1999). British museum: the great court. *Structural Engineer*, 77(6):10–12.
- Van der Linden, L. (2015). Innovative joints for gridshells.

- Van der Linden, L. (2018). *Parametric Engineering*.
- Venuti, F. and Bruno, L. (2018). Influence of in-plane and out-of-plane stiffness on the stability of free-edge gridshells: A parametric analysis. *Thin-Walled Structures*, 131:755–768.
- Wang, X., Feng, R.-q., Yan, G.-r., Liu, F.-c., and Xu, W.-j. (2016). Effect of joint stiffness on the stability of cable-braced grid shells. *International Journal of Steel Structures*, 16(4):1123–1133.
- Welleman, H. (2021). Lecture notes for cie4190 - analysis of slender structures.
- Winkel, J. and Fritzsche, K. (2021). Modern grid tussen oude muren.
- Winslow, P., Pellegrino, S., Sharma, S., and Happold, B. (2008). Free form grid structures. *Structural Engineer*, 86(3):19–20.
- Ye, J. and Lu, M. (2020). Design optimization of domes against instability considering joint stiffness. *Journal of Constructional Steel Research*, 169:105757.

A.o.1 Joint classifications

The paper by Fan, Ma, Can & Shen proposes a classification system for joints of spatial structures. In their system the stiffness, moment capacity of joints and structural behavior of lattice shell. [Fan et al. \[2011\]](#)

Joint classification based on the stiffness k

The system is based on a simplified structure composed of 2 members. In the Figure, scheme (a) represents a rigidly jointed structure; scheme (b) a structure with flexible joint, whose stiffness is k; scheme (c) represents a pinned jointed structure; scheme (d) the deformation equilibrium of the structures under the vertical load P, when the angle between the members and the horizontal direction changes from θ_0 to θ .

The equations (1) & (2) relating the bending moment and the angle θ at the top are given for the deformed configuration:

$$M_{zr} = \frac{4EI}{L_0} \times (\theta_0 - \theta) + \frac{6EI}{L_0} \times \cos \theta (\sin \theta_0 - \sin \theta)$$

$$M_{zs} = k \times 2(\theta_0 - \theta)''$$

M_{zr} is the equation for the rigidly jointed structure, while M_{zs} for the flexible jointed structure. L_0 is the length of the members; E represents Young's modulus; I is the moment of inertia of the members; θ_0 is the initial angle between the members and the horizontal axis; θ is the angle between the member in the deformed structure and horizontal axis. When the stiffness of the flexible joint is increased to ensure $M_{zr}=M_{zs}$, the following equation is obtained:

$$k = \frac{2EI}{L_0} + \frac{3EI}{L_0} \times \cos \theta$$

The authors took an approximation of $\cos \theta = 1$, however for the case study considered in this thesis these values are different for the rectangular and triangular pattern (will be detailed in the following sections). Hence the smallest stiffness they obtained for a rigid joint is:

$$k = \frac{5EI}{L_0}$$

Where EI/L_0 is the stiffness of the members in the structure. The coefficient of stiffness α is defined as:

$$\alpha = \frac{k}{EI/L_0}$$

This coefficient is correlated with the stiffness of the joints, the geometric parameters of the structure and the section properties of the members. A parametric analysis is conducted from the authors to arrive to the classification below:

Categories	Determination coefficient α
Rigid	$\alpha > 5$
Semi-rigid	$5 > \alpha > 0.05$
Pinned	$\alpha < 0.05$

Joint classification based on the stiffness k and moment capacity $M_{j,u}$

The mechanical behavior of the connections includes both the stiffness and moment capacity. The curves with the same stiffness but different moment capacity lead to different behavior of the structure. To investigate the effect of the moment capacity of joints on the mechanical behavior, the determination coefficient of moment capacity β is defined as:

$$\beta = \frac{M_{j,u}}{M_{e,u}}$$

where $M_{j,u}$ is the moment capacity of the joint; $M_{e,u}$ is the plastic moment capacity of the member connected. After conducting a similar analysis to the previous section, the authors came to the following boundaries:

Categories	Determination coefficient α and β
Rigid	$\alpha > 5$ and $\beta \geq 0.5$
Semi-rigid	$5 > \alpha > 0.05$ and $0.01 \leq \beta < 0.5$
Pinned	$\alpha < 0.05$ or $\beta < 0.01$

A.o.2 Joint stiffness influence

Engineers have studied the effect of the stiffness of joints both experimentally and numerically for some time. Earlier studies by See (1983) and Fathelbab (1987) verified the effect of stiffness on the load-displacement behavior of a structure. Previous studies have also focused on material and cost savings due to the effect of joint properties. Wang et al. [2016] Studies from El-Sheikh, Chenaghlou, and Nooshin have concluded that the behavior of a structure and the failure mode is influenced by the bending stiffness of connections. Fan et al. [2011]

Feng, Yao, and Ye studied the stability of grid shell roofs and the factors that influence it. Among the factors, they concluded that joint stiffness plays a role in the ultimate bearing capacity of the structure. They studied the behavior of the structure with stiffness altering from 1×10 to $1 \times 10^7 N/m$. The authors noticed that for stiffness from 10 to 10^4 , the critical load remains the same. For higher stiffness, critical load increases. This is the case for joints with an in-plane pin, out-plane rigid stiffness, where the ultimate load-bearing capacity is 10% lower than a structure with fully rigid joints. Feng et al. [2012]

In another study by Feng, Ye, and Zhu investigated the mechanical behavior of bolted joints used in cable-braced grid shells considering in-plane and out-of-plane rotational stiffness and strength, compared to fully rigid joints. They noticed that failure of the joints differs and the out-of-plane behavior was similar to semi-rigid, while in-plane closer to pinned joints. Feng et al. [2015]

Authors Wang, Feng, Yan, Liu, and Xu researched the stability of cable-braced grid shells considering different joint stiffness to provide minimal stiffness. They concluded that with a decrease of joint stiffness, the compression stresses of the grid shell, buckling load as well as the utilization rate of steel members decreased. From the stability analysis, it was noted that stiffness alternations, affect eigenvalue buckling mode, non-linear buckling mode, and structural internal forces. With low stiffness, the eigenvalue buckling mode showed local deformation. Wang et al. [2016]

Lopez, Puente, Serna point out that single-layer shells are prone to geometric non-linearity, compared to double-layered structures. Therefore, they studied the influence of joint rigidity on the global behavior of structure both numerically and experimentally. Noticeable variations in the behavior of the structure were present in load-displacement curves and snap-through instability, local failure at joints. Due to high rigidity snap-through of nodes could be avoided. López et al. [2007]

Venuti and Bruno focused on the influence of in-plane and out-of-plane stiffness on the stability of grid shells. However, their study was specific to the case of a "Partial Grid shell", where one side of it is cut by an arch. In particular, was

investigated its sensitivity to the flexural stiffness of the boundary structure and to the shear stiffness of the grid shell. [Venuti and Bruno \[2018\]](#)

In more recent studies available, related to grid shell connection include the one from Van der Linden, where he proposed additive manufacturing for an optimal design of joints. [Van der Linden \[2015\]](#) Another study by Ye and Lu, proposes an optimal dome design against instability by considering the effect of joint stiffness. [Ye and Lu \[2020\]](#)

In the paper "Optimization Strategies for Grid shells: The Role of joints", the authors explore three optimization approaches combining member sizing optimization and stiffness configuration of joints. The aim was to propose a strategy in obtaining a lighter structure in comparison to only member sizing optimization. The main constraints of the optimization problem are the global buckling and stresses of members. The parameters include the number of joints in the preliminary solution and the member diameter. [Grande et al. \[2020\]](#)

The first approach is "Pinned-Rigid" joints, which considers the possibility of varying the configuration of some joints from pinned to rigid. As a result, the whole joint would be either pinned or rigid but could be different for both ends of the member. The second approach is "Truss-Beam" members, where some of the members can alter from truss elements to beam elements. Truss elements can transfer only axial forces, without bending moments or shear forces. Different from the first approach, the conversion from truss to beam would lead to variation from pinned to rigid connection for both ends of the element. The third approach "Pinned-Rigid ends". The final solution of this technique would result in joints that may behave as rigid for some members they are connected to and pinned for others. In the outcome of this study, the authors underline that the member's diameter influences both the stress and global buckling behavior, while the joint stiffness alternation affects mostly the global buckling. [Grande et al. \[2020\]](#)

B | APPENDIX B. GRASSHOPPER SCRIPT

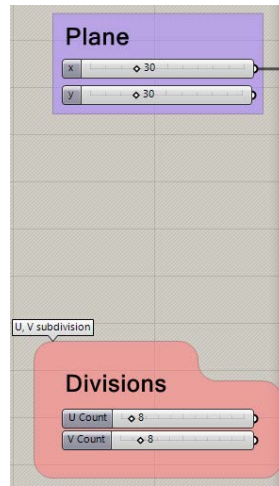


Figure 1. Parameters

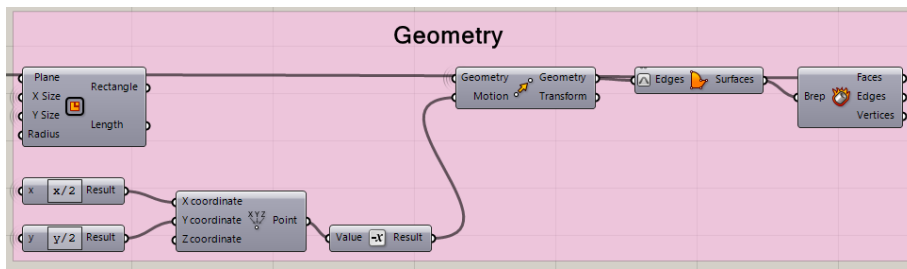


Figure 2. Plane geometry

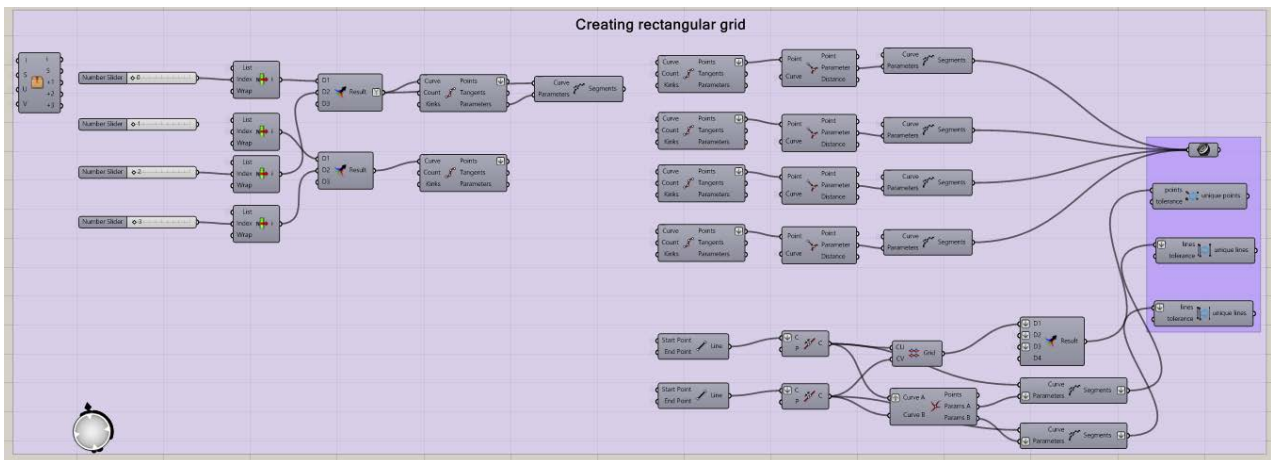


Figure 3. Grid pattern

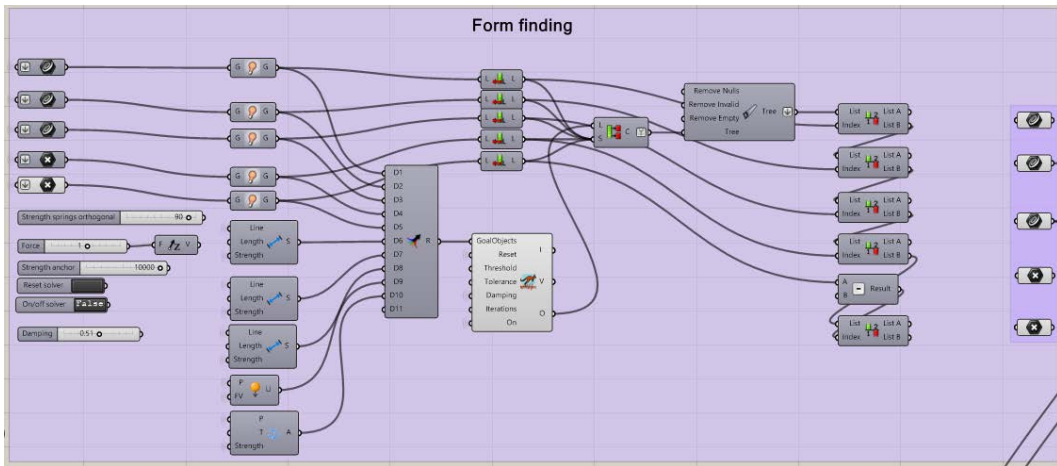


Figure 4. Form finding

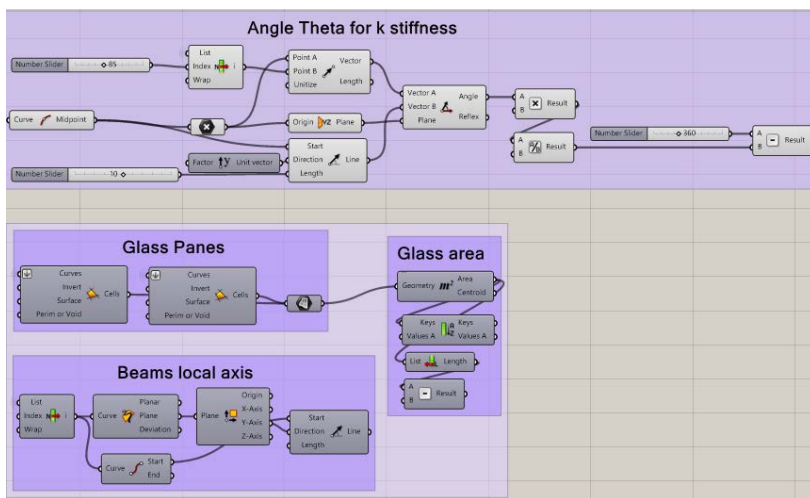


Figure 5. Output from the geometry iteration

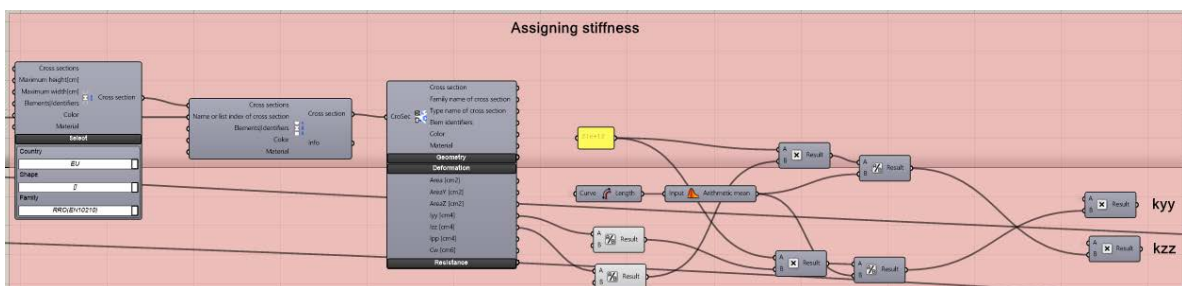


Figure 6. Assigning stiffness k with Geometry Gym

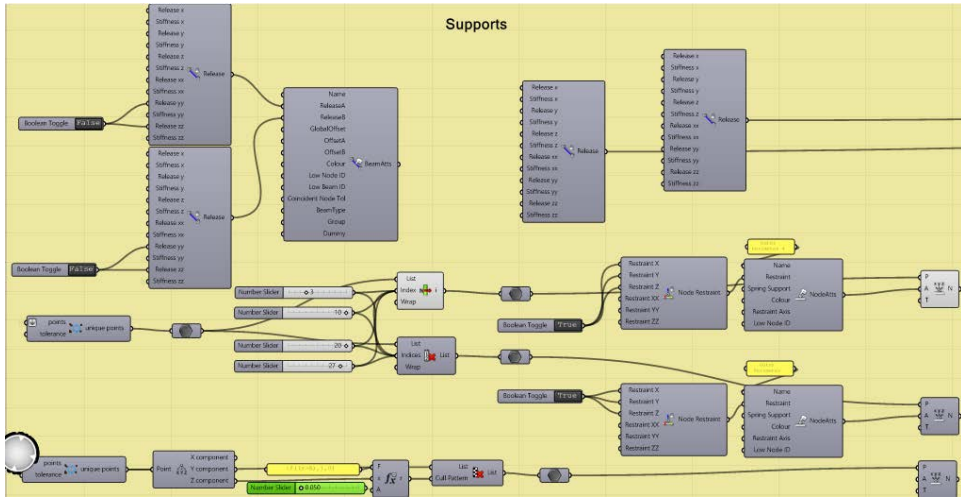


Figure 7. Assigning supports

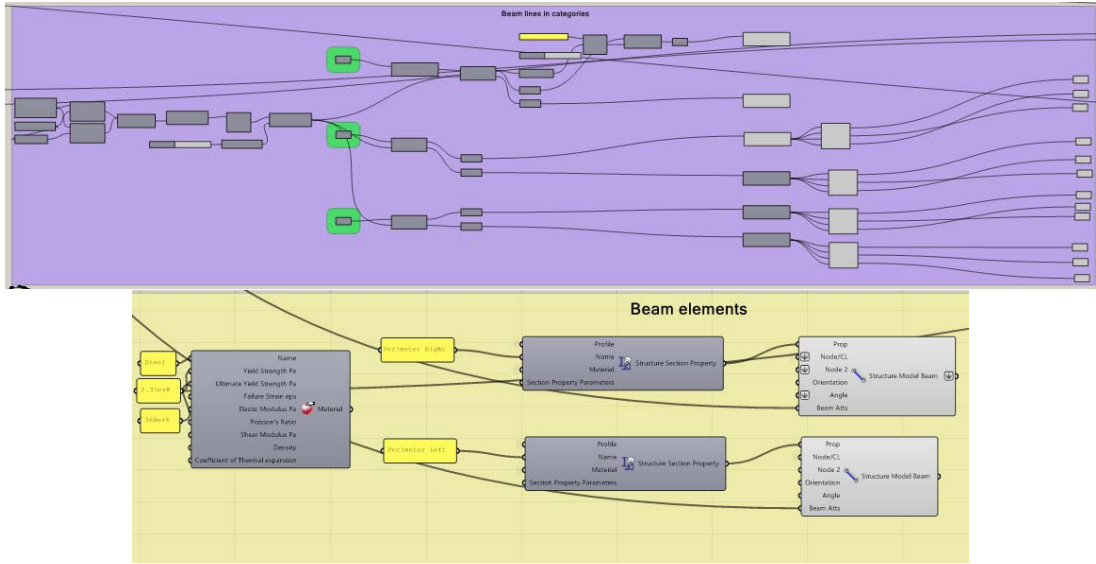


Figure 8. Assigning properties to beam elements

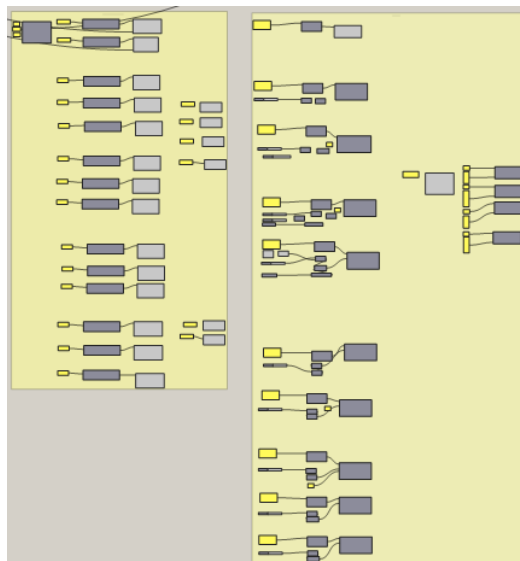


Figure 9. Loads and load combinations

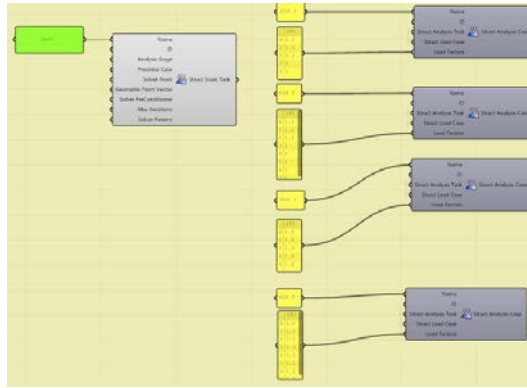


Figure 10. Load combinations

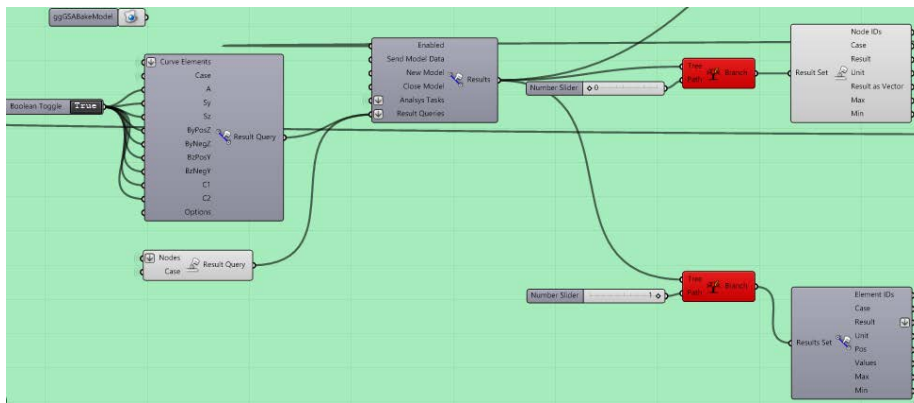


Figure 11. Link between Grasshopper and Oasys GSA

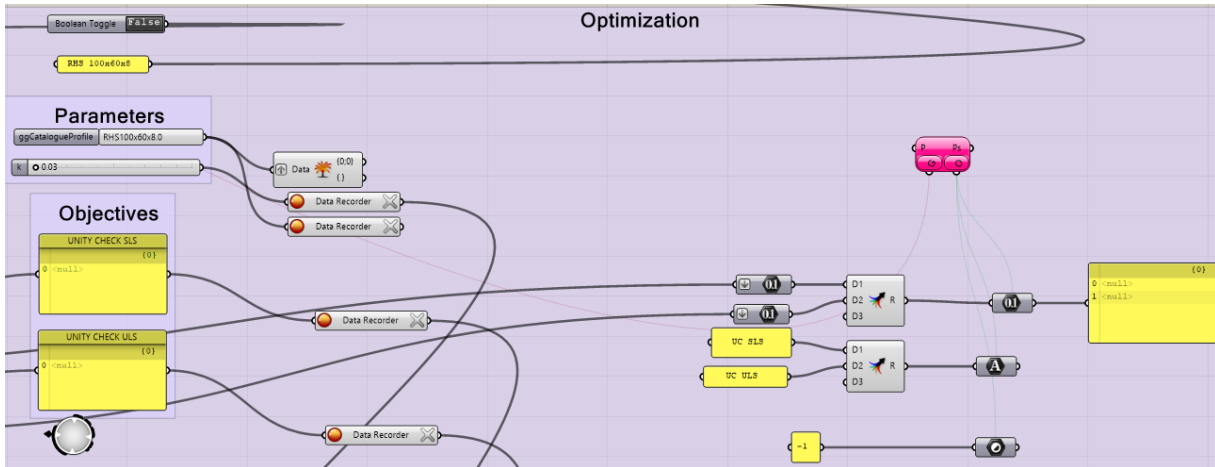
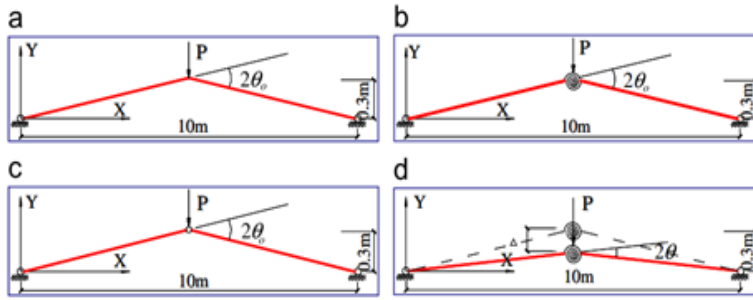


Figure 12. Optimization script

C | APPENDIX C. JOINT STIFFNESS CLASSIFICATION - MATRIX METHOD

> restart;



(a) Moment of the structure with rigid joint:

> ODE := EI·diff(w(x), x\$4) = 0;

$$ODE := EI \left(\frac{d^4}{dx^4} w(x) \right) = 0 \quad (1)$$

> w := rhs(dsolve(ODE, w(x))) :

> phi := -diff(w, x) :

> kappa := diff(phi, x) :

> M := EI·kappa : V := diff(M, x) :

>

> x := 0 : eq1 := w = 0 : eq2 := phi = phi1 :

> x := L : eq3 := w = w2 : eq4 := phi = 0 :

> sol := solve({eq1, eq2, eq3, eq4}, {_C1, _C2, _C3, _C4}) : assign(sol); x := 'x':

> x := 0 : Fz1 := -simplify(V) : Ty1 := -simplify(M) :

> x := L : Fz2 := simplify(V) : Ty2 := simplify(M) :

> k11 := coeff(collect(Fz1, w1), w1) : k12 := coeff(collect(Fz1, phi1), phi1) : k13 :=
coeff(collect(Fz1, w2), w2) : k14 := coeff(collect(Fz1, phi2), phi2) :

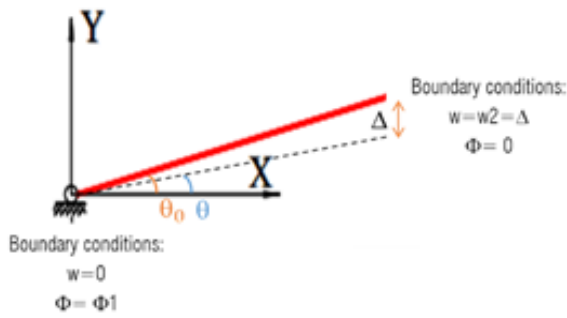
> k21 := coeff(collect(Ty1, w1), w1) : k22 := coeff(collect(Ty1, phi1), phi1) : k23 :=
coeff(collect(Ty1, w2), w2) : k24 := coeff(collect(Ty1, phi2), phi2) :

> k31 := coeff(collect(Fz2, w1), w1) : k32 := coeff(collect(Fz2, phi1), phi1) : k33 :=
coeff(collect(Fz2, w2), w2) : k34 := coeff(collect(Fz2, phi2), phi2) :

> k41 := coeff(collect(Ty2, w1), w1) : k42 := coeff(collect(Ty2, phi1), phi1) : k43 :=
coeff(collect(Ty2, w2), w2) : k44 := coeff(collect(Ty2, phi2), phi2) :

> Ksys := Matrix(4, 4, [[k11, k12, k13, k14], [k21, k22, k23, k24], [k31, k32, k33, k34], [k41,
k42, k43, k44]]);

$$K_{sys} := \begin{bmatrix} 0 & -\frac{6EI}{L^2} & -\frac{12EI}{L^3} & 0 \\ 0 & \frac{4EI}{L} & \frac{6EI}{L^2} & 0 \\ 0 & \frac{6EI}{L^2} & \frac{12EI}{L^3} & 0 \\ 0 & \frac{2EI}{L} & \frac{6EI}{L^2} & 0 \end{bmatrix} \quad (2)$$



> $w1 := 0 : \phi1 := \theta_0 - \theta : w2 := \frac{L}{2} \cdot (\tan(\theta_0) - \tan(\theta)) \cdot \cos(\theta) : \phi2 := 0 :$

$R_{sys} := \text{Matrix}(4, 1, [[w1], [\phi1], [w2], [\phi2]])$;

$$R_{sys} := \begin{bmatrix} 0 \\ \theta_0 - \theta \\ \frac{L (\tan(\theta_0) - \tan(\theta)) \cos(\theta)}{2} \\ 0 \end{bmatrix} \quad (3)$$

>

Moment at the top:

> $M_{Zr} := k41 \cdot w1 + k42 \cdot \phi1 + k43 \cdot w2 + k44 \cdot \phi2$

$$M_{Zr} := \frac{2 EI (\theta_0 - \theta)}{L} + \frac{3 EI (\tan(\theta_0) - \tan(\theta)) \cos(\theta)}{L} \quad (4)$$

> restart;

(b) Moment of the structure with flexible joint:

> $ODE := EI \cdot \text{diff}(w(x), x\$4) = 0$;

$$ODE := EI \left(\frac{d^4}{dx^4} w(x) \right) = 0 \quad (5)$$

> $w := \text{rhs}(\text{dsolve}(ODE, w(x)))$:

> $\phi := -\text{diff}(w, x)$:

> $\kappa := \text{diff}(\phi, x)$:

> $M := EI \cdot \kappa : V := \text{diff}(M, x)$:

>

> $x := 0 : eq1 := w = 0 : eq2 := \phi = \phi1$:

> $x := L : eq3 := w = w2 : eq4 := \phi = \phi2$:

> $sol := \text{solve}(\{eq1, eq2, eq3, eq4\}, \{_C1, _C2, _C3, _C4\}) : \text{assign}(sol) ; x := 'x'$:

> $x := 0 : Fz1 := -\text{simplify}(V) : Ty1 := -\text{simplify}(M)$:

> $x := L : Fz2 := \text{simplify}(V) : Ty2 := \text{simplify}(M)$:

> $k11 := \text{coeff}(\text{collect}(Fz1, w1), w1) : k12 := \text{coeff}(\text{collect}(Fz1, \phi1), \phi1) : k13 := \text{coeff}(\text{collect}(Fz1, w2), w2) : k14 := \text{coeff}(\text{collect}(Fz1, \phi2), \phi2)$:

> $k21 := \text{coeff}(\text{collect}(Ty1, w1), w1) : k22 := \text{coeff}(\text{collect}(Ty1, \phi1), \phi1) : k23 := \text{coeff}(\text{collect}(Ty1, w2), w2) : k24 := \text{coeff}(\text{collect}(Ty1, \phi2), \phi2)$:

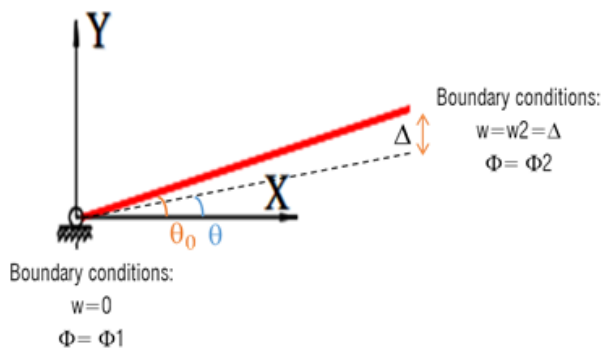
> $k31 := \text{coeff}(\text{collect}(Fz2, w1), w1) : k32 := \text{coeff}(\text{collect}(Fz2, \phi1), \phi1) : k33 := \text{coeff}(\text{collect}(Fz2, w2), w2) : k34 := \text{coeff}(\text{collect}(Fz2, \phi2), \phi2)$:

> $k41 := \text{coeff}(\text{collect}(\text{Ty2}, w1), w1) : k42 := \text{coeff}(\text{collect}(\text{Ty2}, \text{phi1}), \text{phi1}) : k43 := \text{coeff}(\text{collect}(\text{Ty2}, w2), w2) : k44 := \text{coeff}(\text{collect}(\text{Ty2}, \text{phi2}), \text{phi2}) :$
 > $K_{\text{sys}} := \text{Matrix}(4, 4, [[k11, k12, k13, k14], [k21, k22, k23, k24], [k31, k32, k33, k34], [k41, k42, k43, k44]]) ;$

$$K_{\text{sys}} := \begin{bmatrix} 0 & -\frac{6EI}{L^2} & -\frac{12EI}{L^3} & -\frac{6EI}{L^2} \\ 0 & \frac{4EI}{L} & \frac{6EI}{L^2} & \frac{2EI}{L} \\ 0 & \frac{6EI}{L^2} & \frac{12EI}{L^3} & \frac{6EI}{L^2} \\ 0 & \frac{2EI}{L} & \frac{6EI}{L^2} & \frac{4EI}{L} \end{bmatrix}$$

(6)

> $K_{\text{sys}} := \begin{bmatrix} 0 & -6k & -12k & -6k \\ 0 & 4k & 6k & 2k \\ 0 & 6k & 12k & 6k \\ 0 & 2k & 6k & 4k \end{bmatrix} :$



> $w1 := 0 : \text{phi1} := \text{theta0} - \text{theta} : w2 := \frac{L}{2} \cdot (\tan(\text{theta0}) - \tan(\text{theta})) \cdot \cos(\text{theta}) : \text{phi2} := 2 \cdot (\text{theta0} - \text{theta}) : R_{\text{sys}} := \text{Matrix}(4, 1, [[w1], [\text{phi1}], [w2], [\text{phi2}]]) ;$

$$R_{\text{sys}} := \begin{bmatrix} 0 \\ \theta_0 - \theta \\ \frac{L (\tan(\theta_0) - \tan(\theta)) \cos(\theta)}{2} \\ 2\theta_0 - 2\theta \end{bmatrix}$$

(7)

> **Moment at the top:**

> $\text{theta} := 0.259189 : \text{theta0} := 0.26635 :$

> $M2 := k41 \cdot w1 + k42 \cdot \text{phi1} + k43 \cdot w2 + k44 \cdot \text{phi2} ;$

$$M2 := \frac{0.09387803084 EI}{L}$$

(8)

> $Msr := \text{algsubs}\left(\frac{EI}{L} = k, M2\right);$

$$Msr := 0.09387803084 k \quad (9)$$

> $M1 := \frac{2 EI (\theta_0 - \theta)}{L} + \frac{3 EI (\tan(\theta_0) - \tan(\theta)) \cos(\theta)}{L}$

$$M1 := \frac{0.03659003084 EI}{L} \quad (10)$$

> $eq1 := Msr = M1;$

$$eq1 := 0.09387803084 k = \frac{0.03659003084 EI}{L} \quad (11)$$

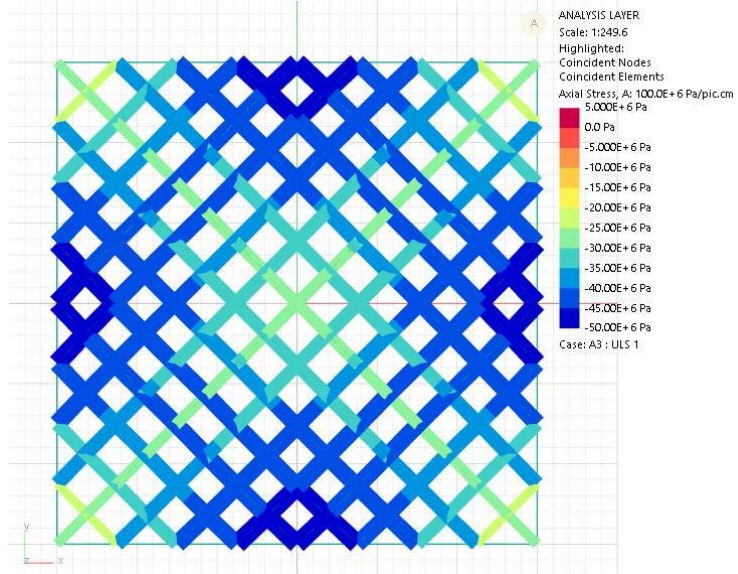
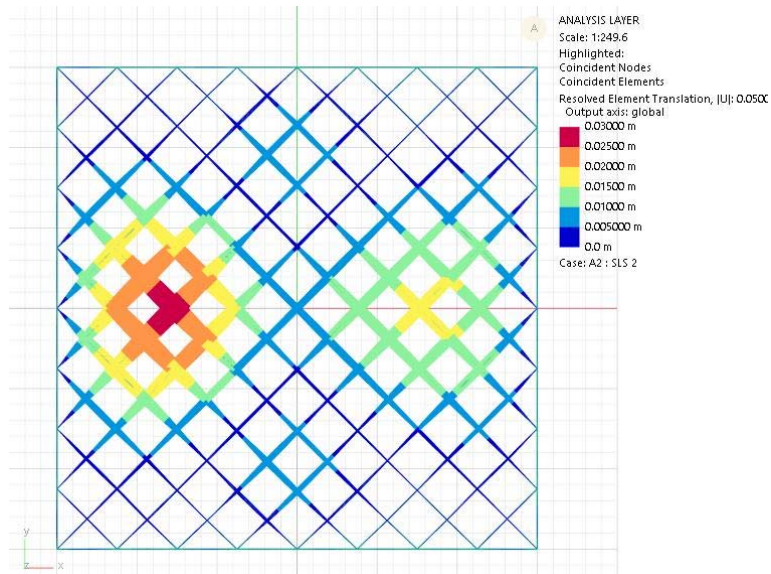
> $sol := \text{solve}(eq1, k);$

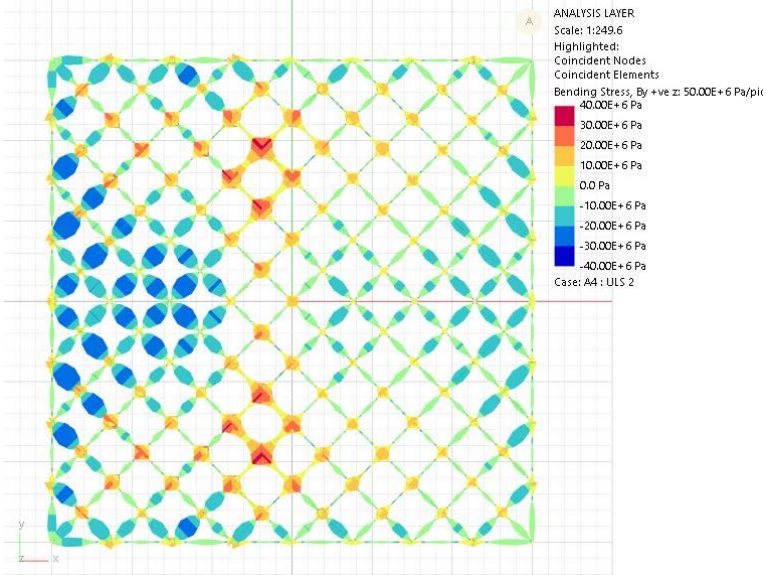
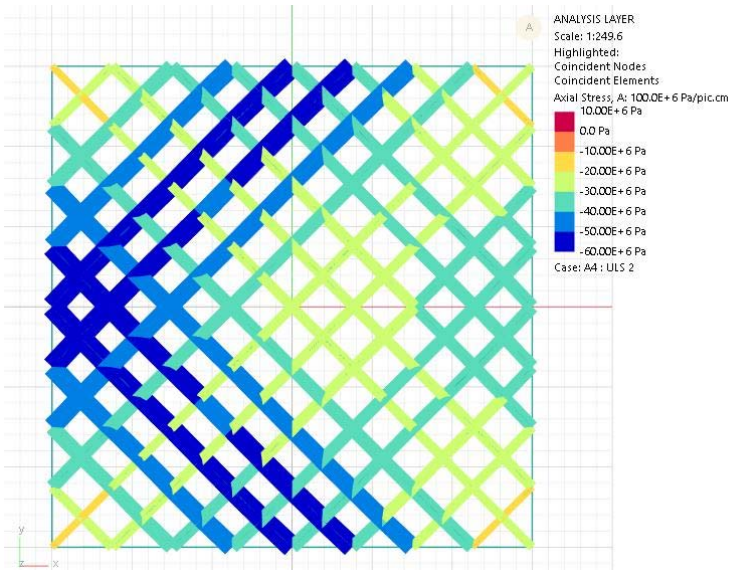
$$sol := \frac{0.3897613799 EI}{L} \quad (12)$$

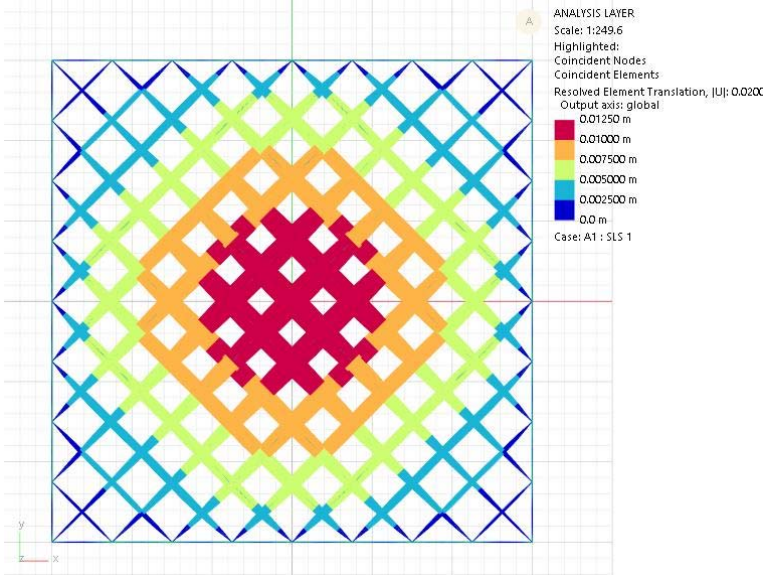
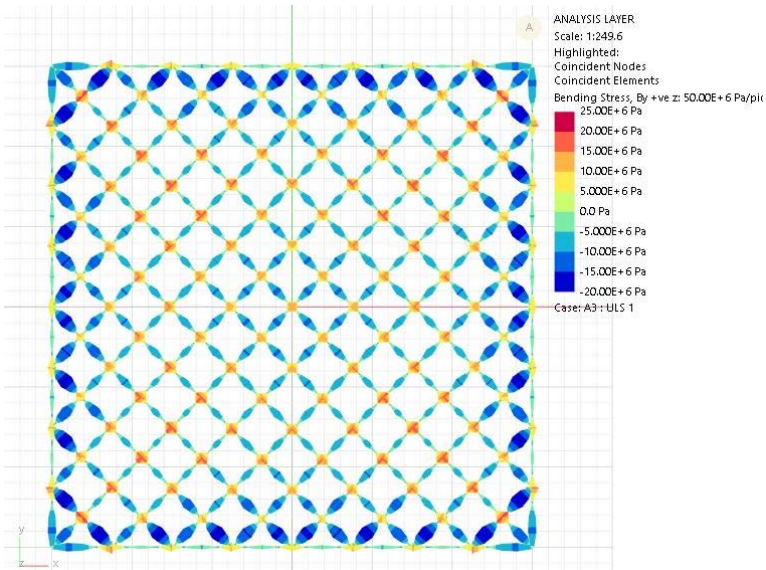
D | APPENDIX D. JOINT STIFFNESS INFLUENCE

Rectangular pattern

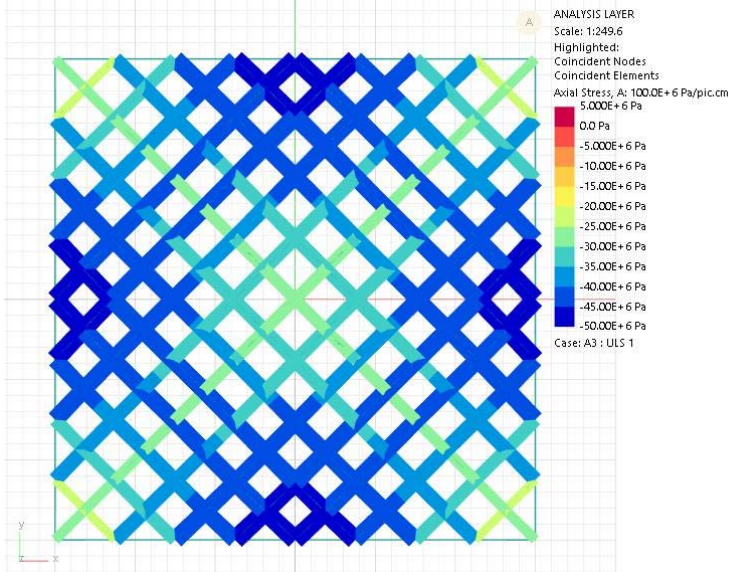
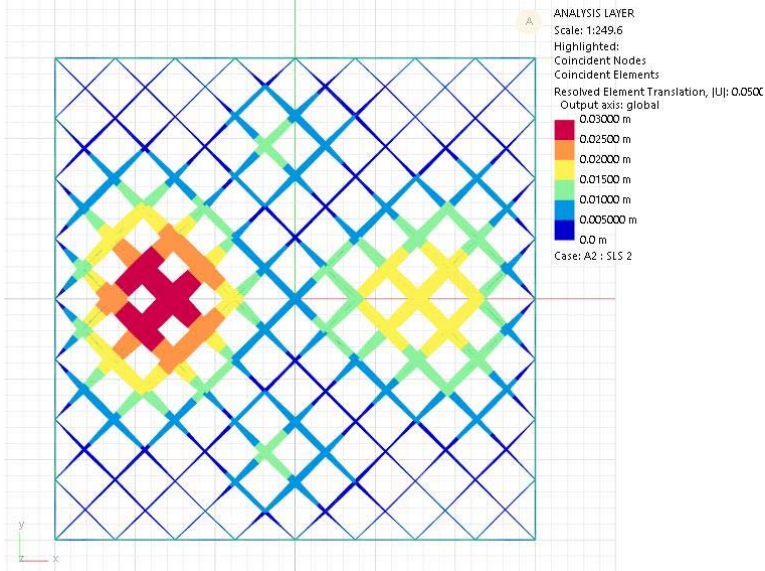
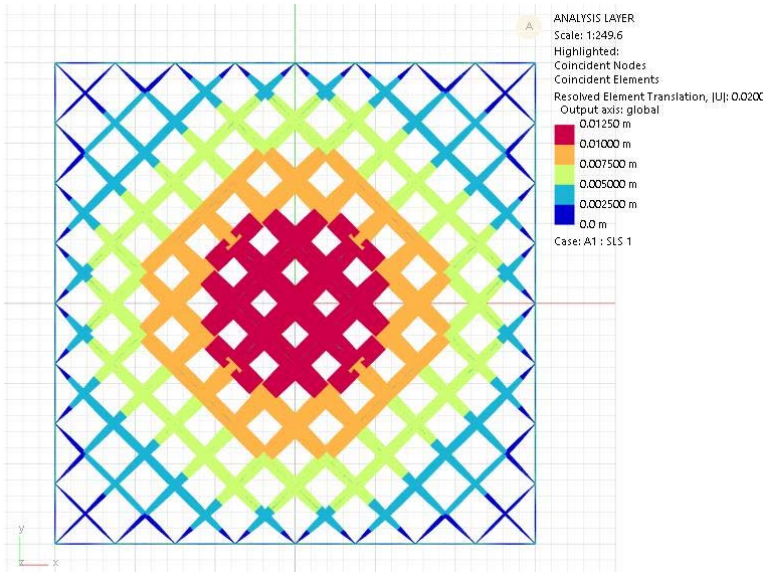
Rigid:

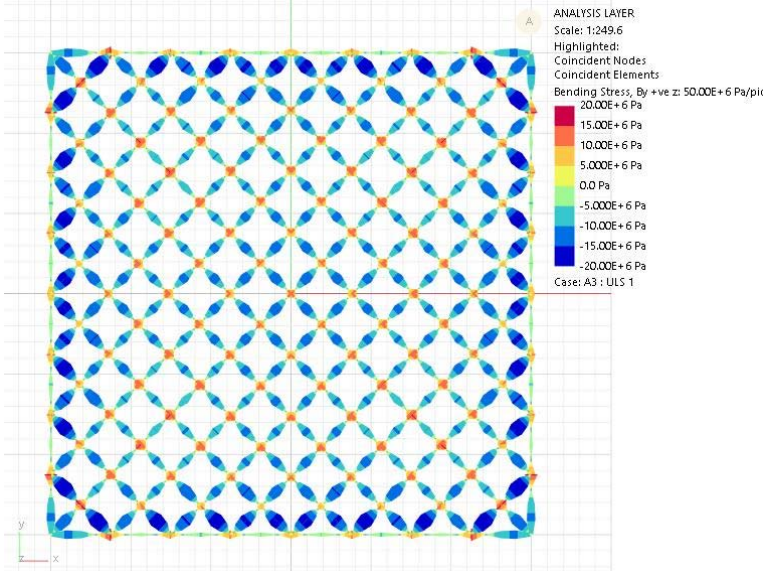
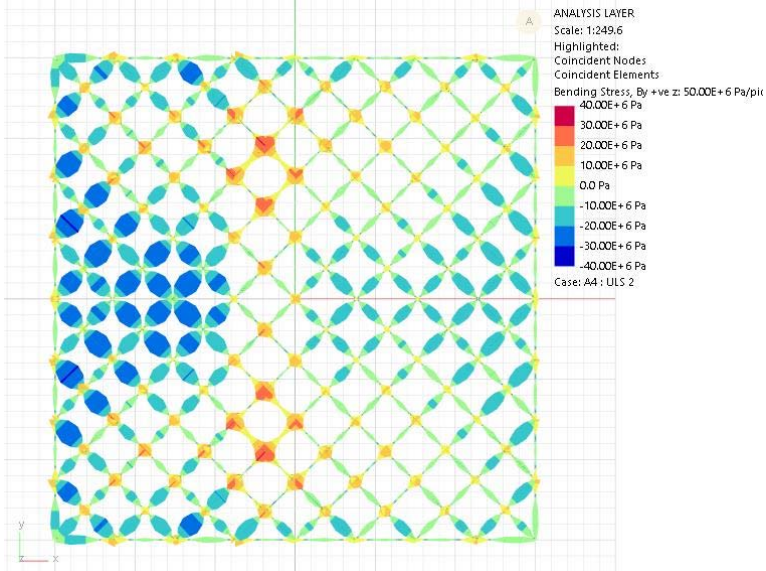
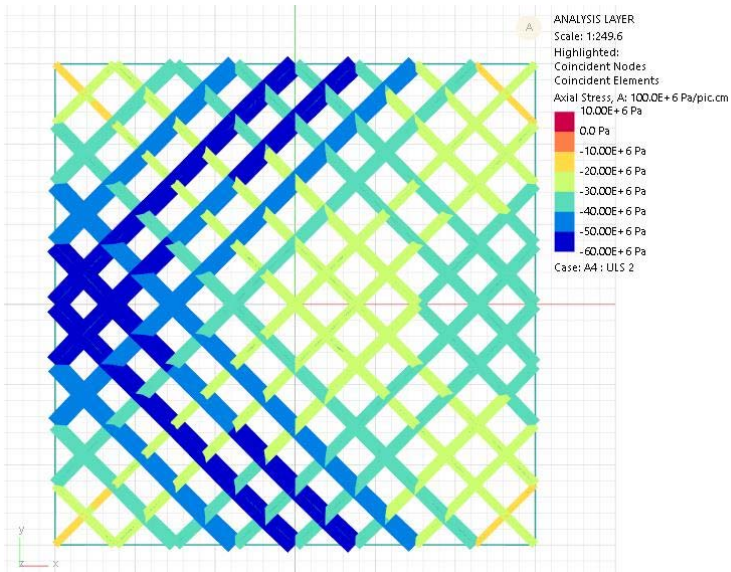




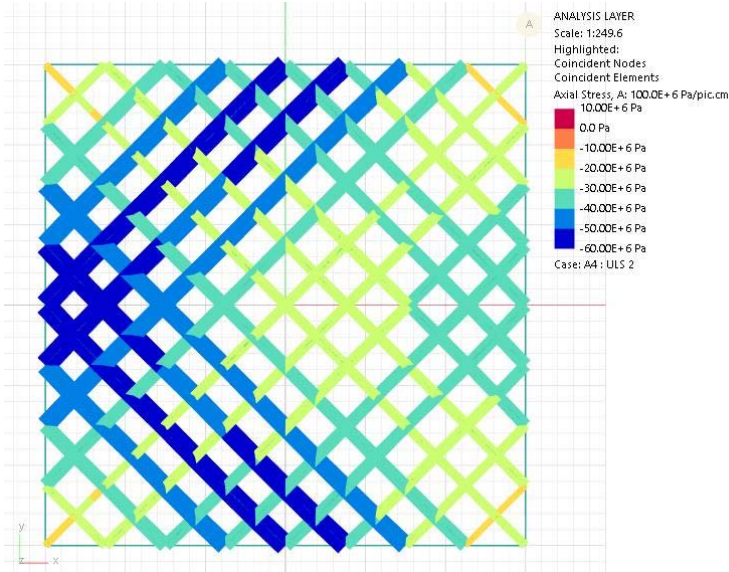
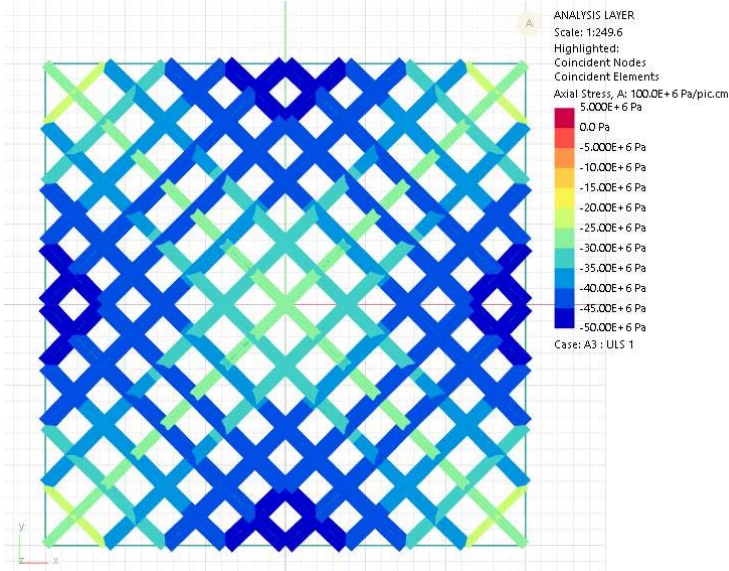
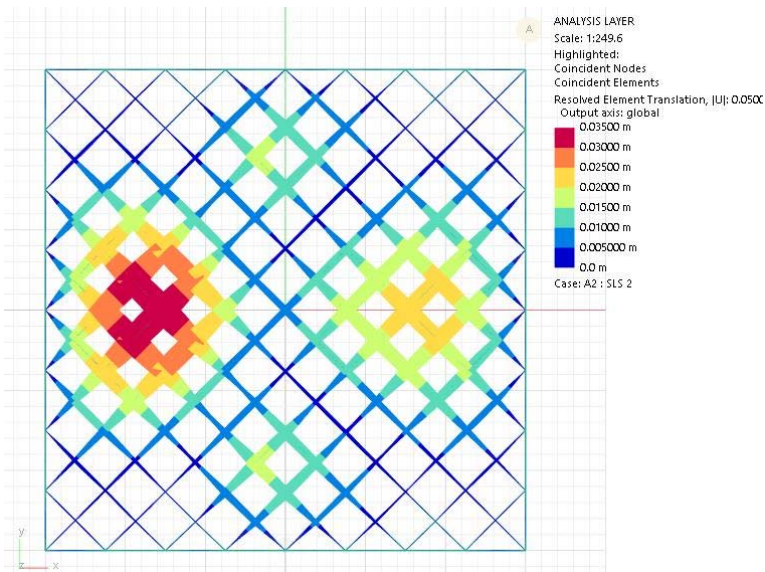


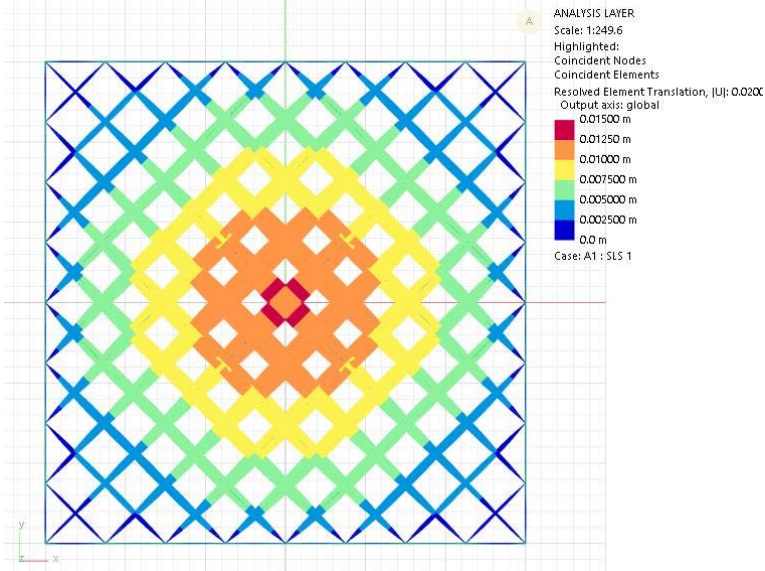
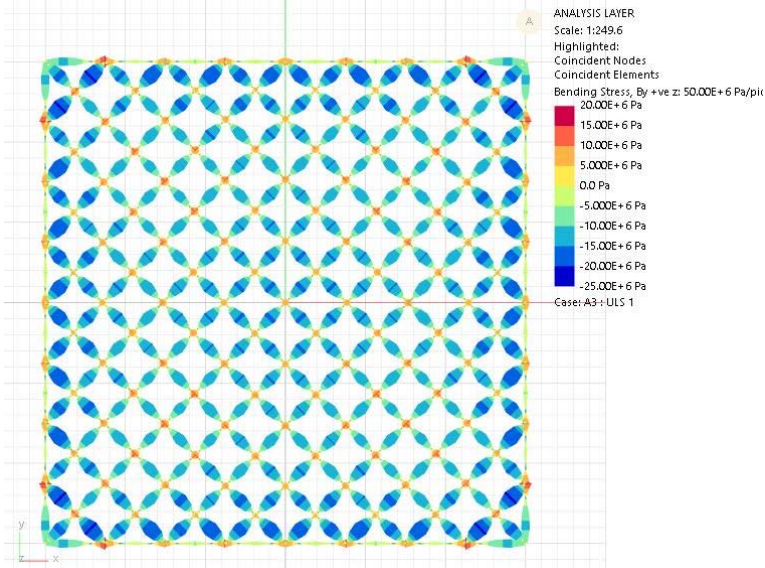
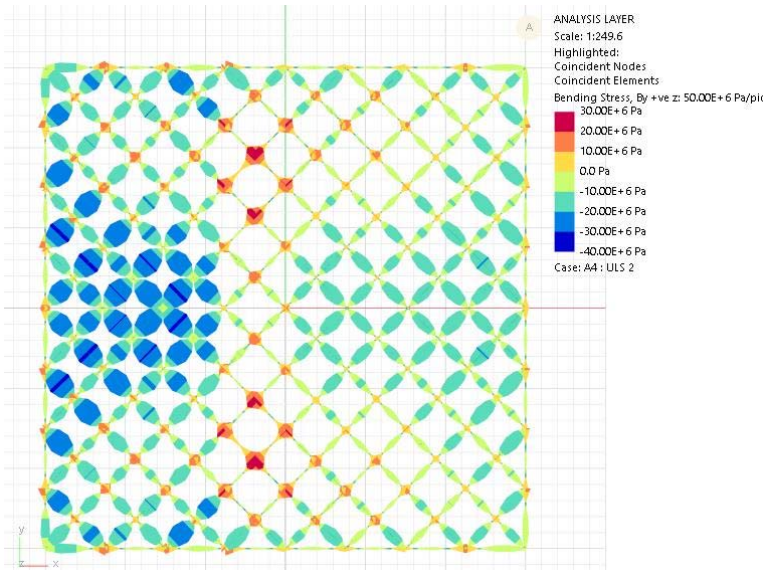
Stiffness: $0.114EI/L$



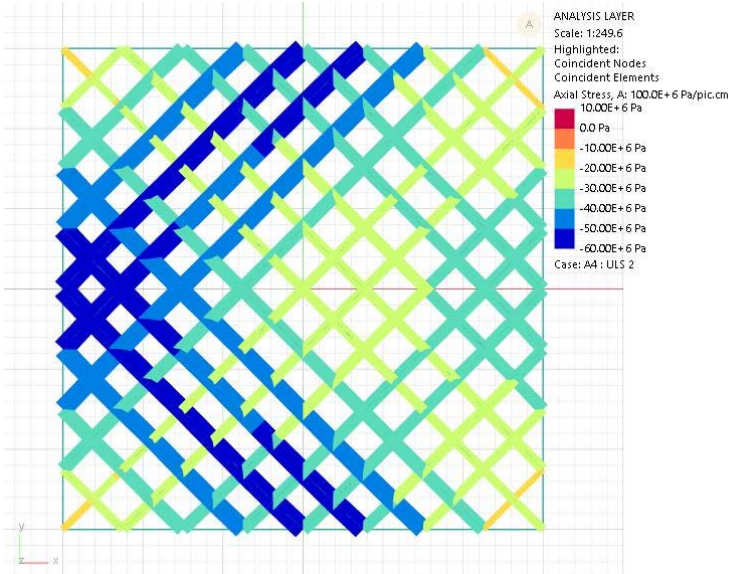
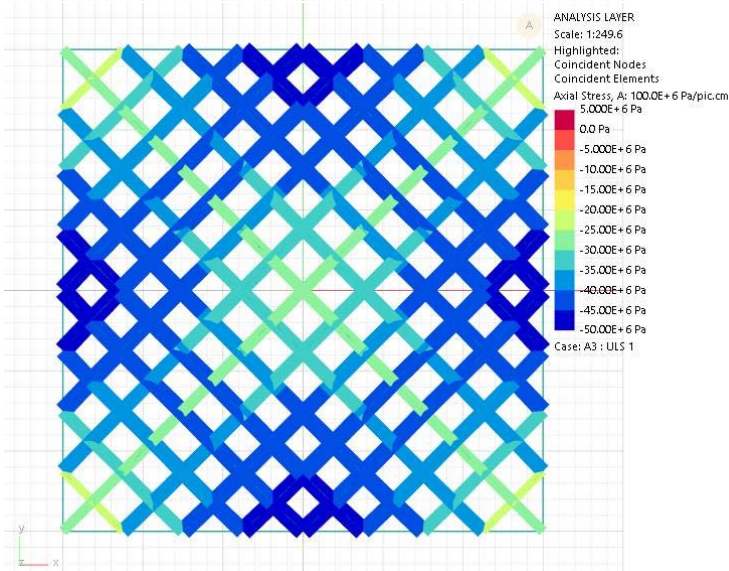
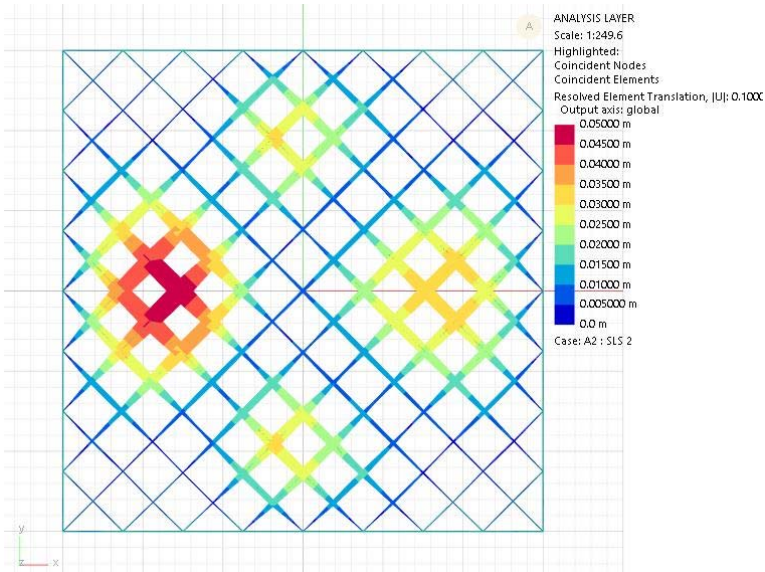


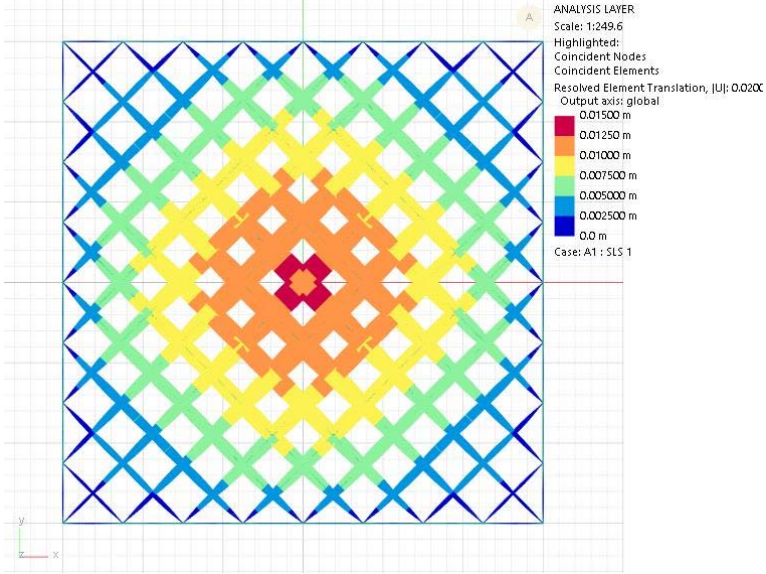
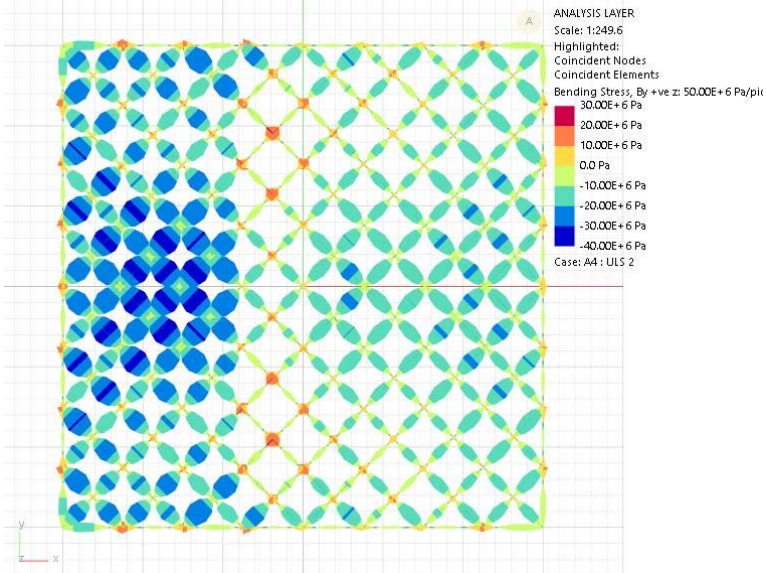
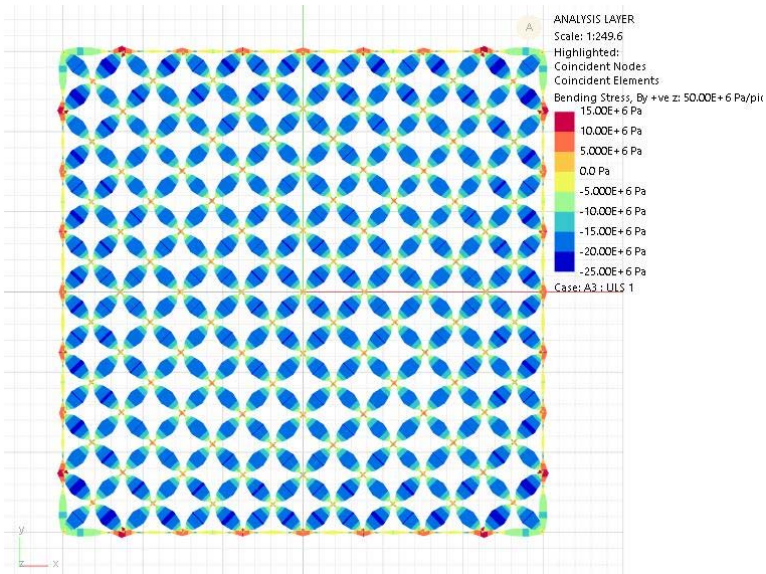
Stiffness: 0.0389EI/L



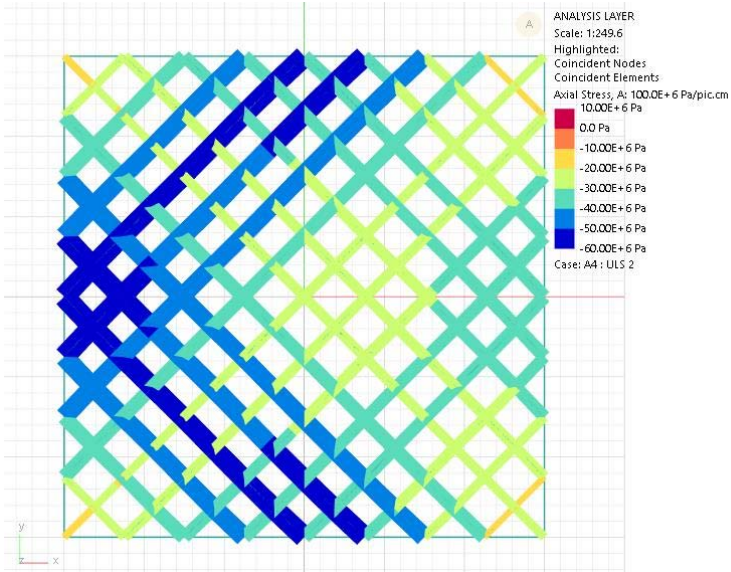
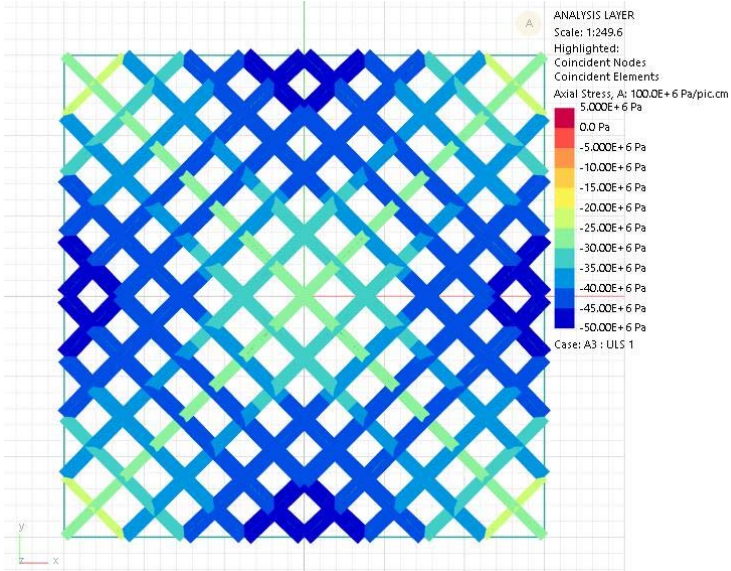
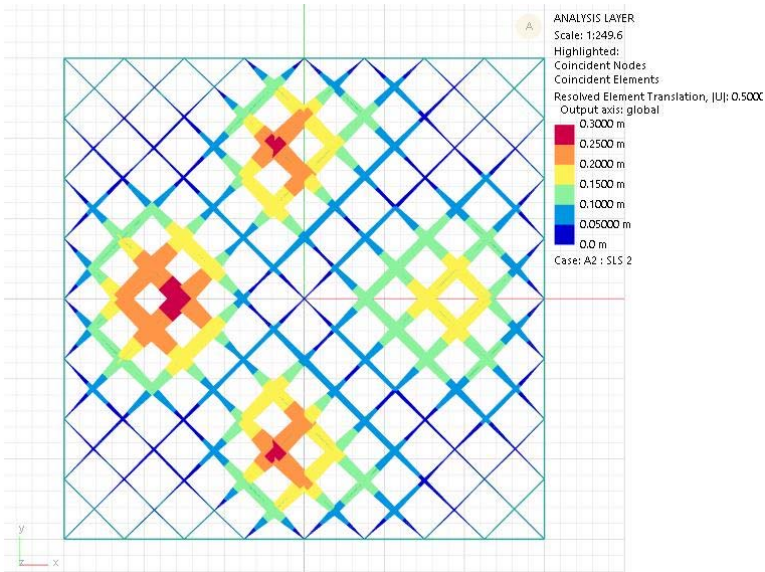


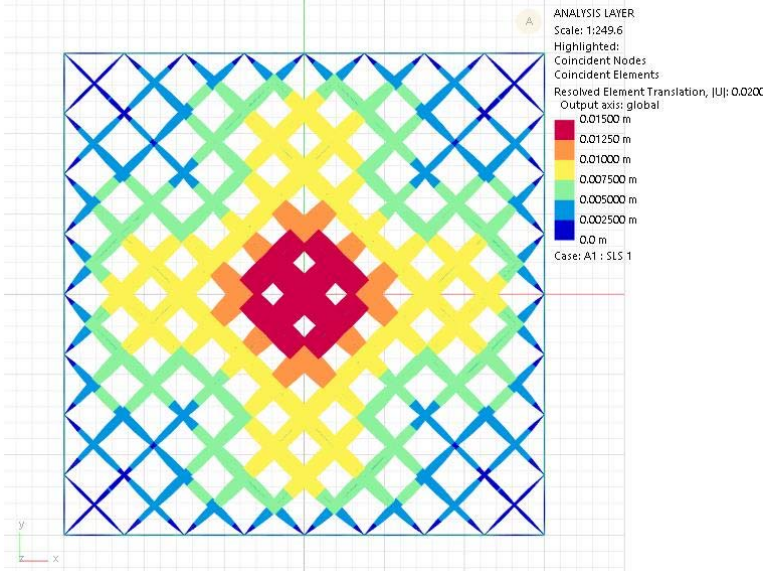
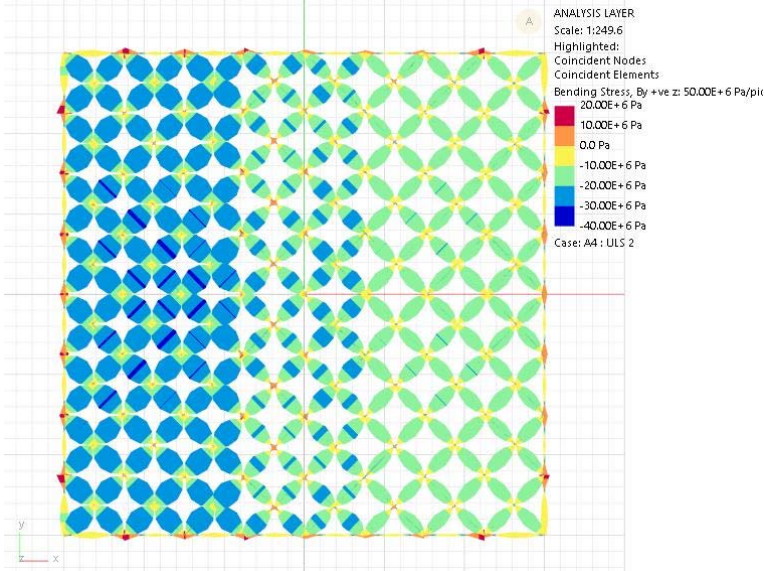
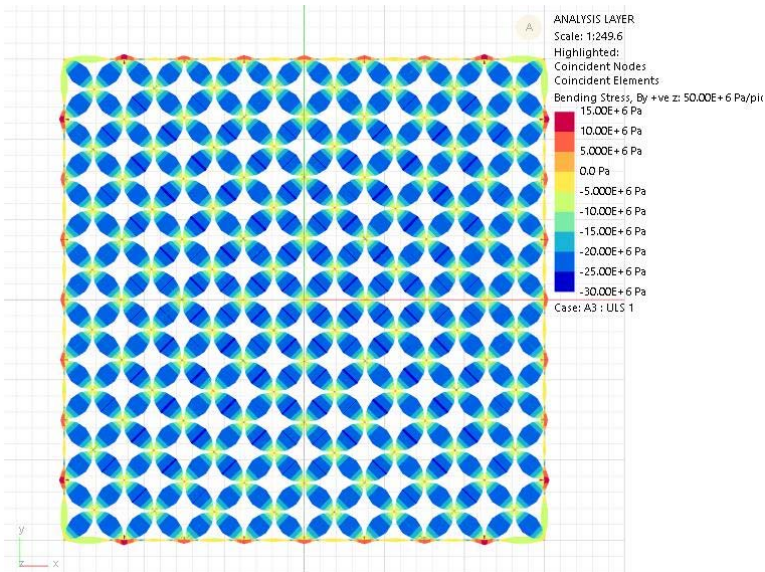
Stiffness: $0.0114EI/L$





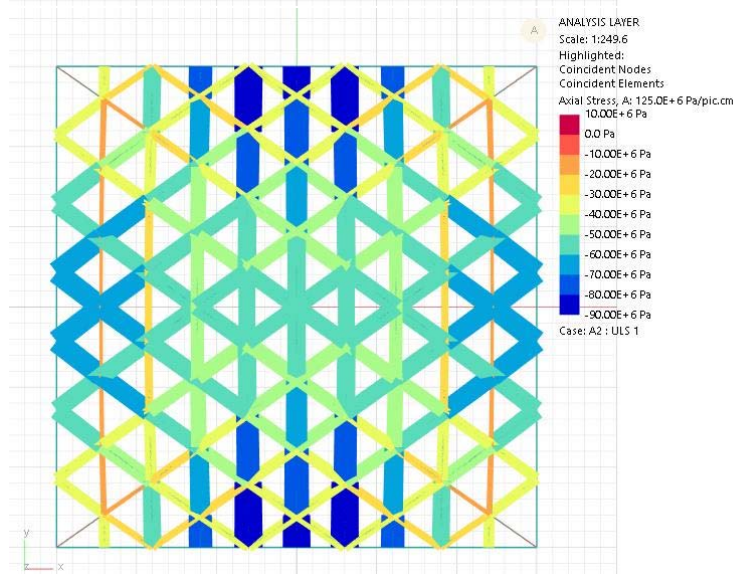
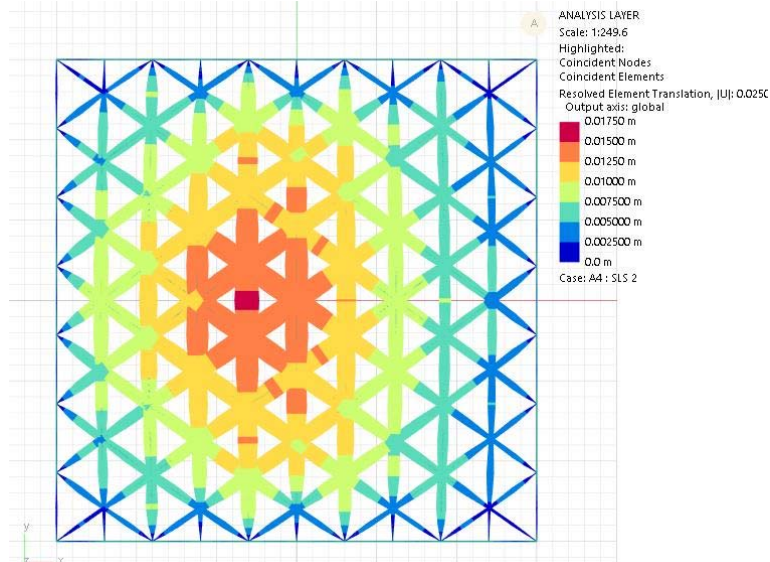
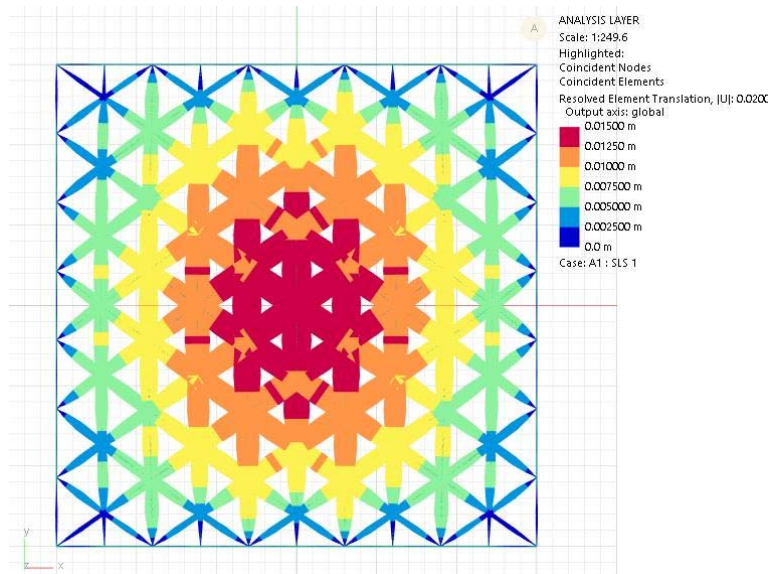
Pinned:

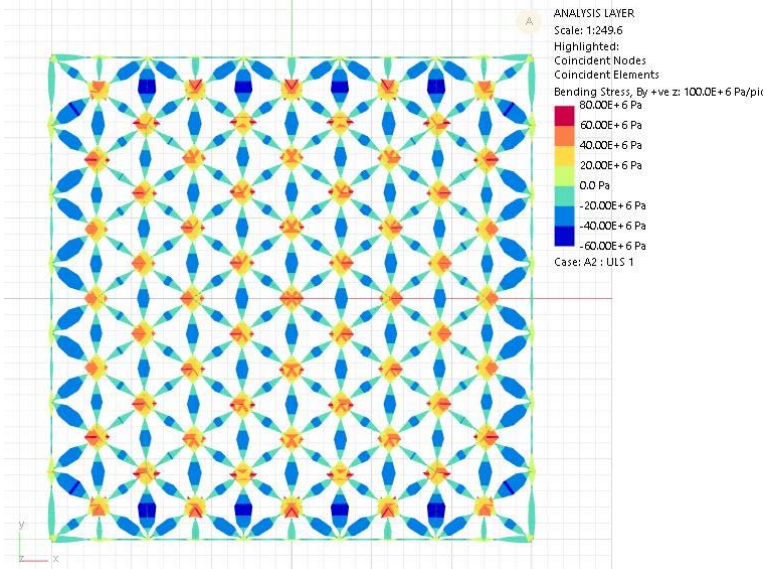
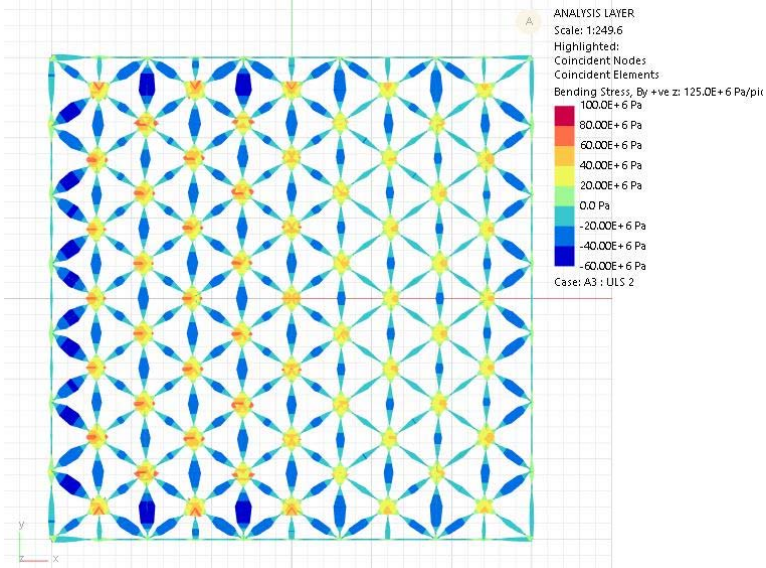
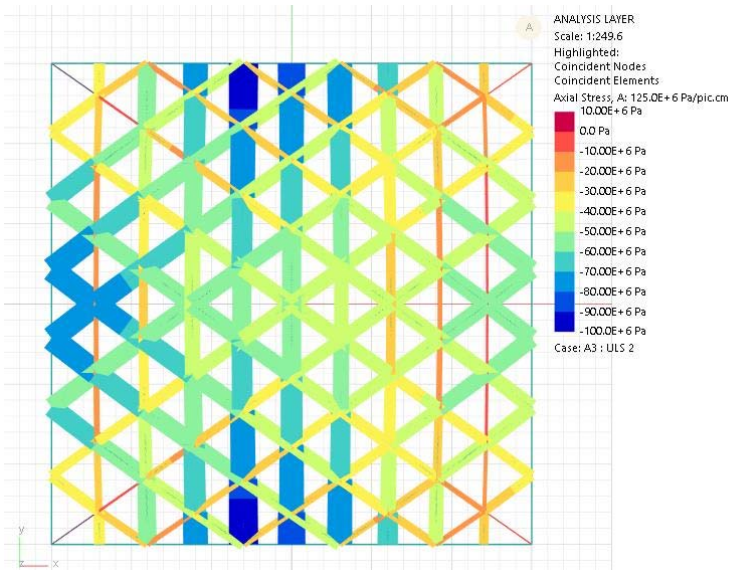




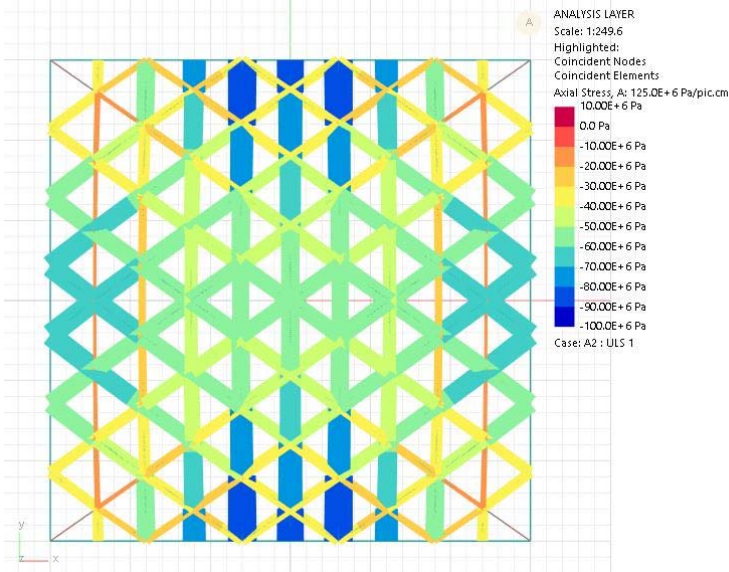
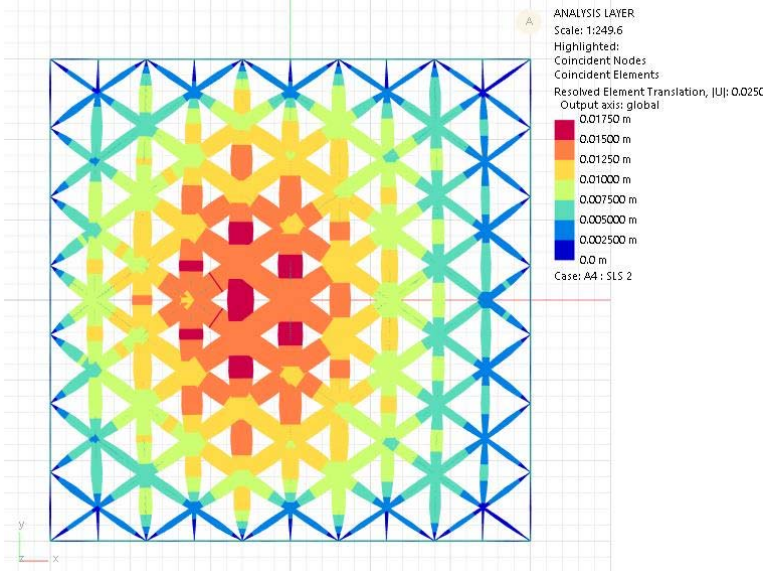
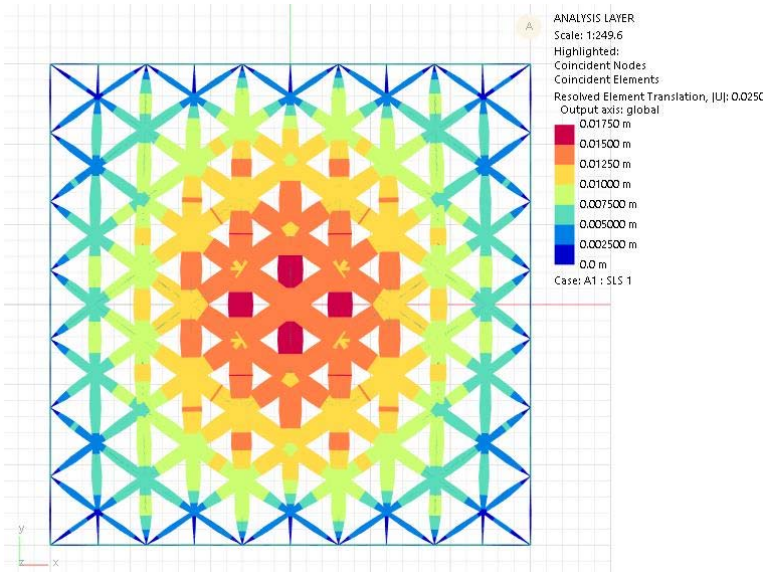
Triangle pattern:

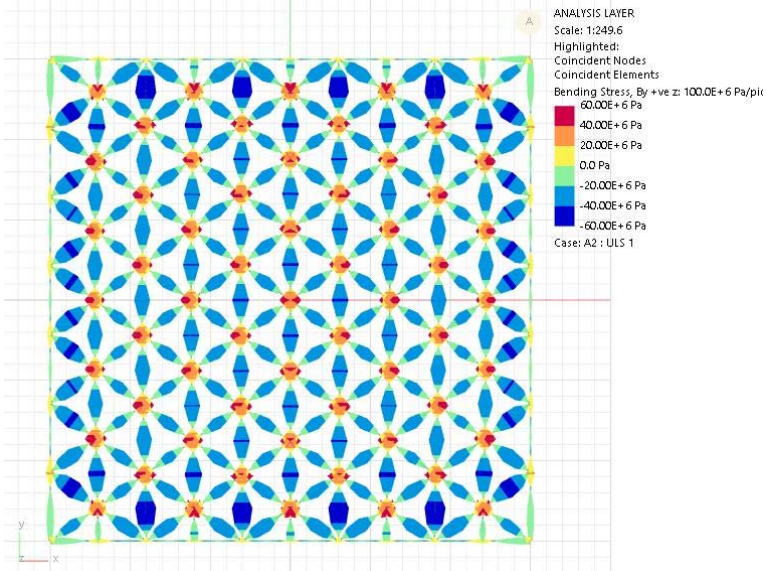
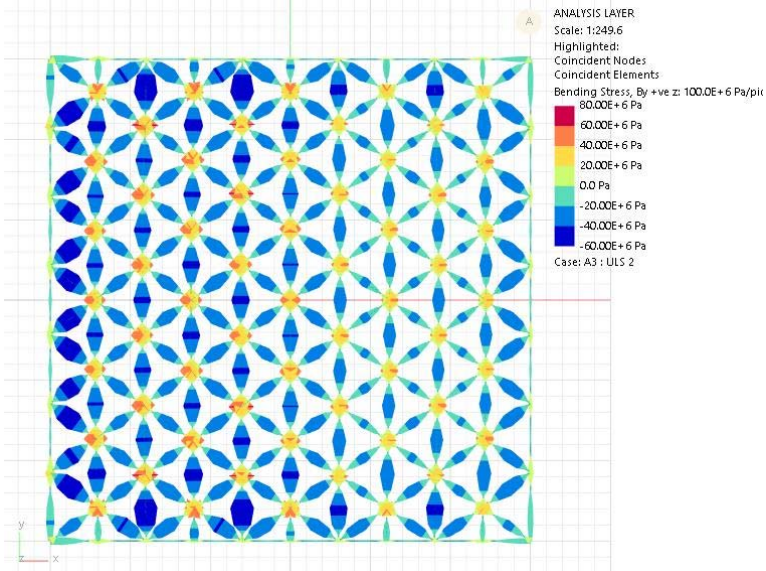
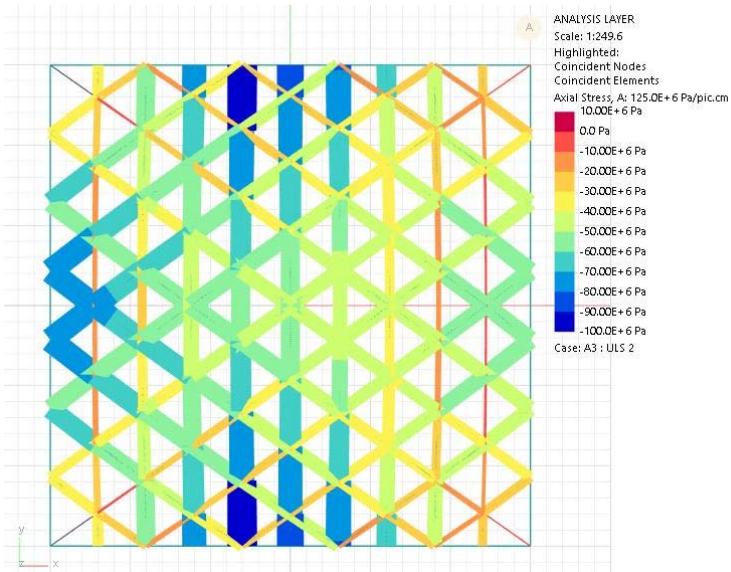
Rigid



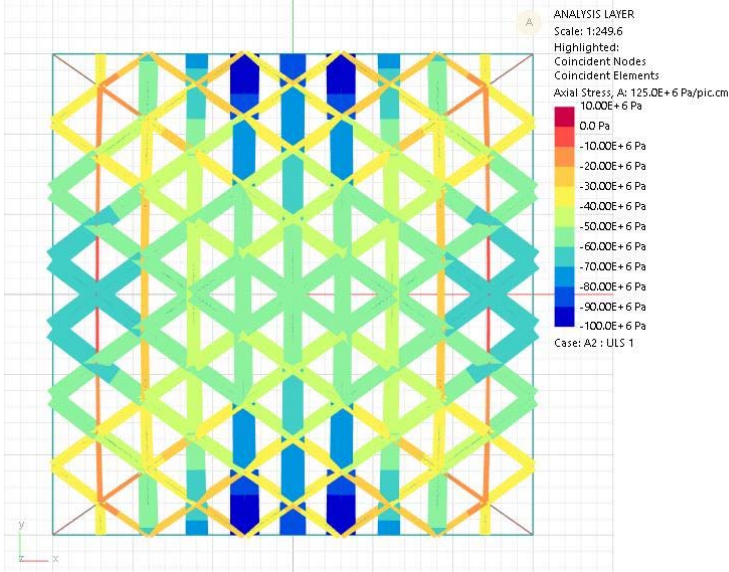
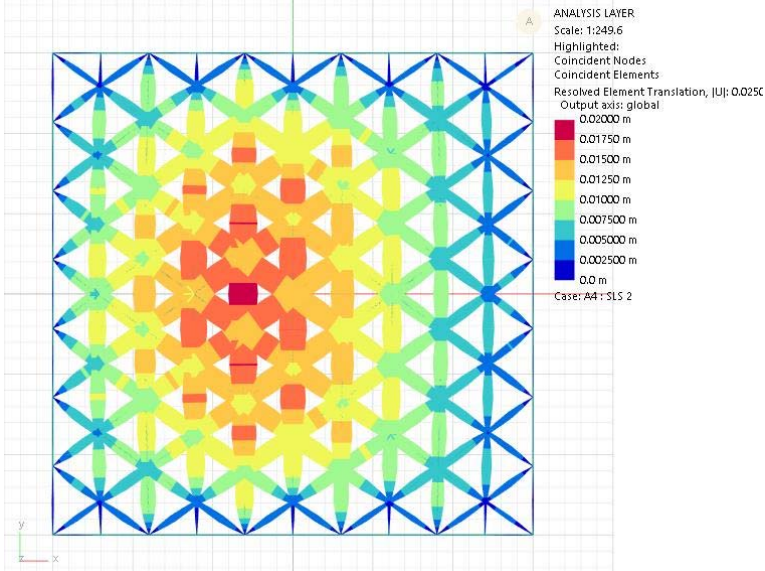
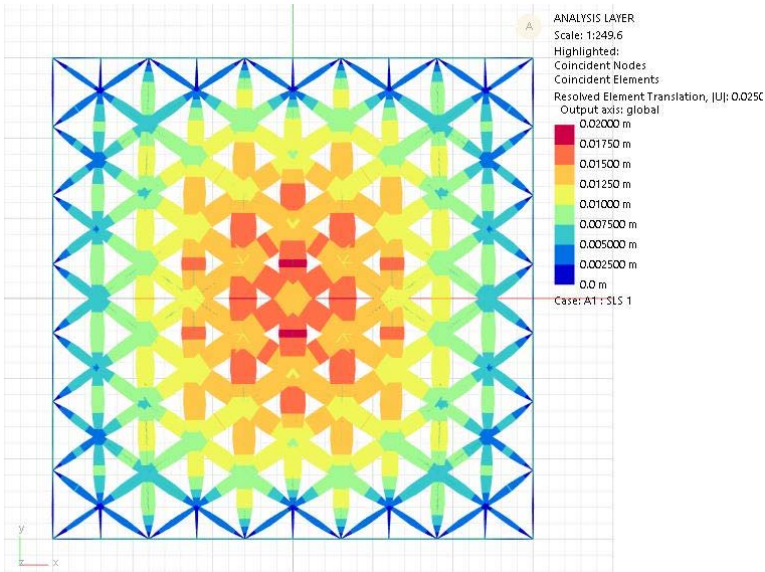


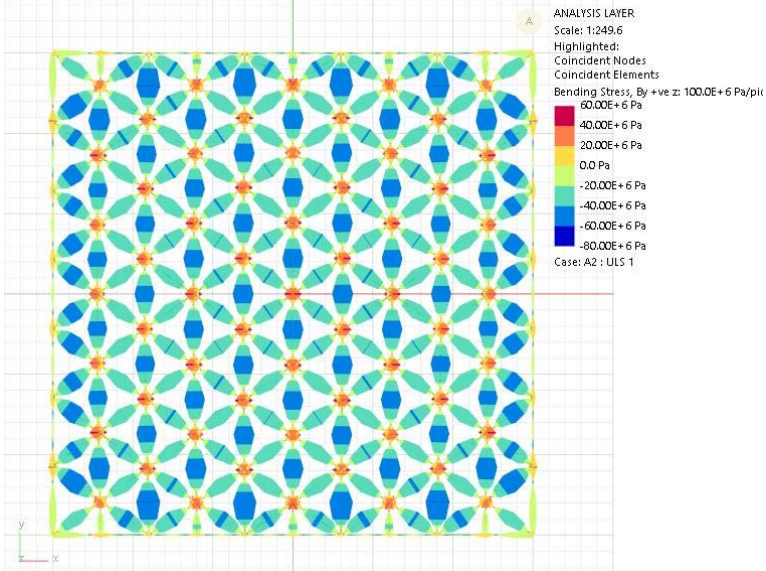
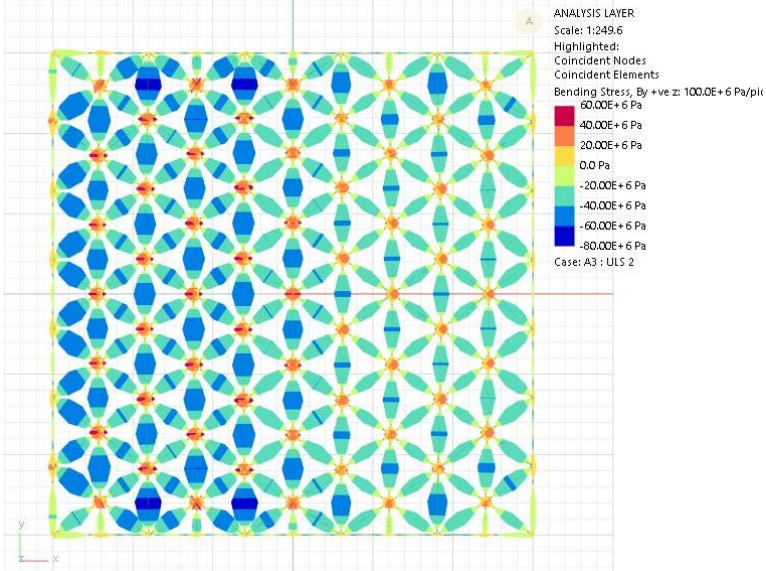
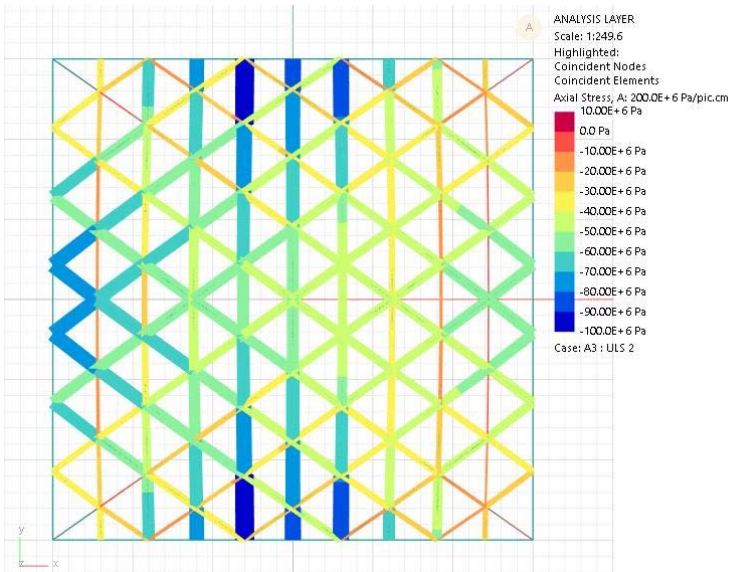
Stiffness: $0.114EI/L$



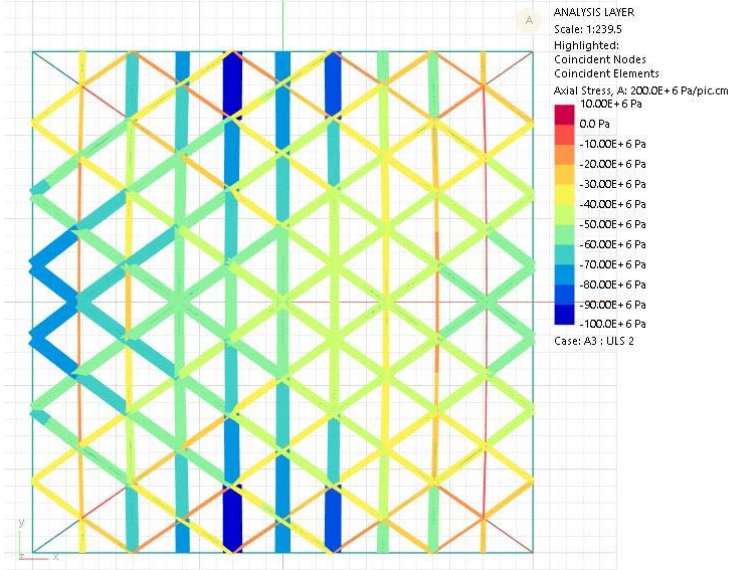
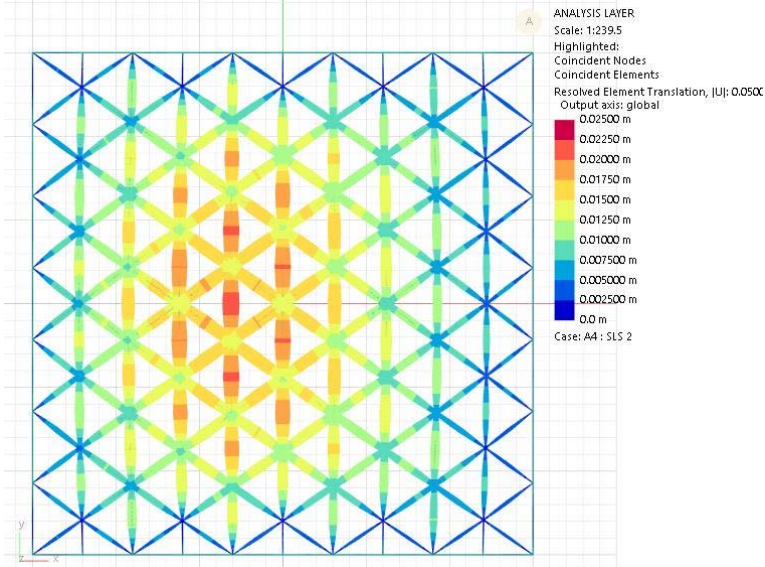
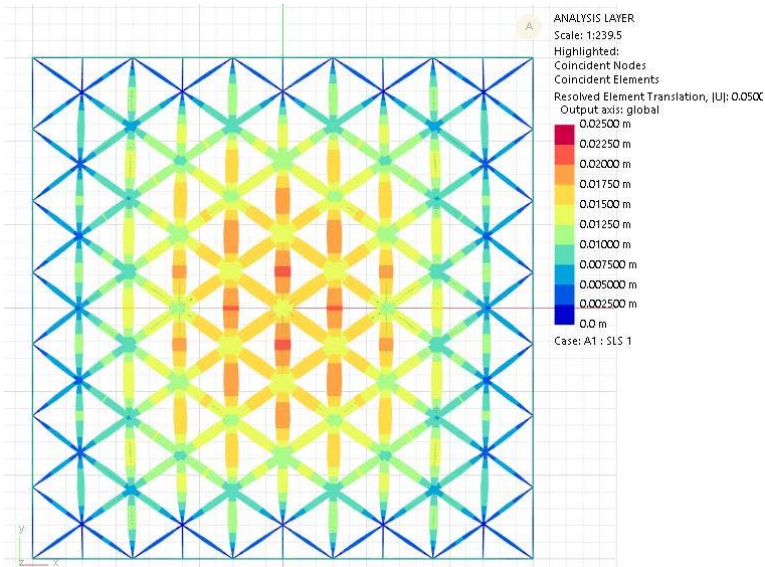


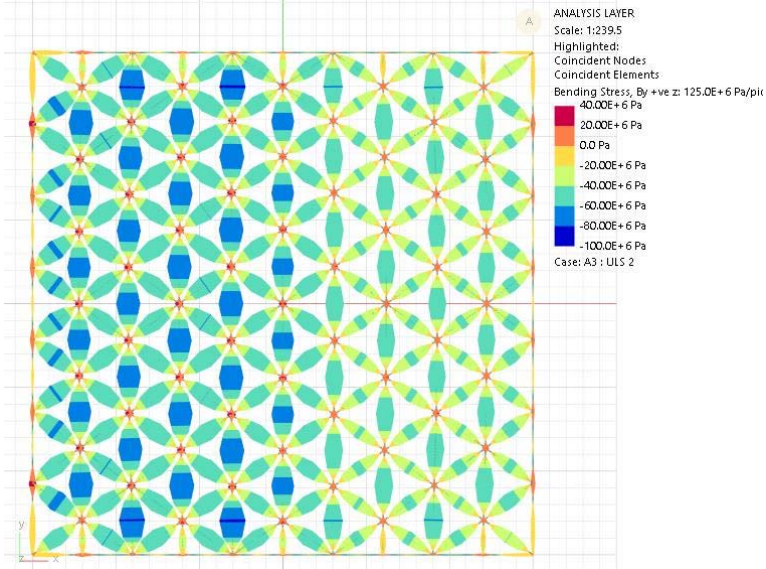
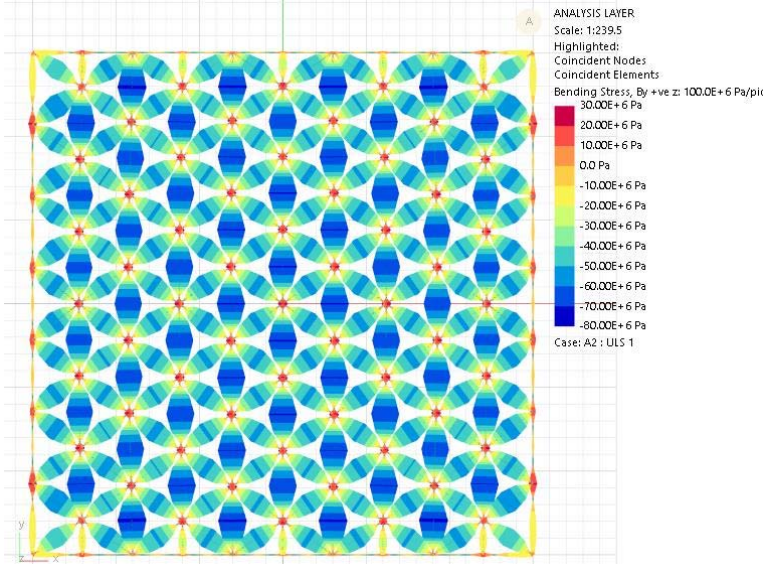
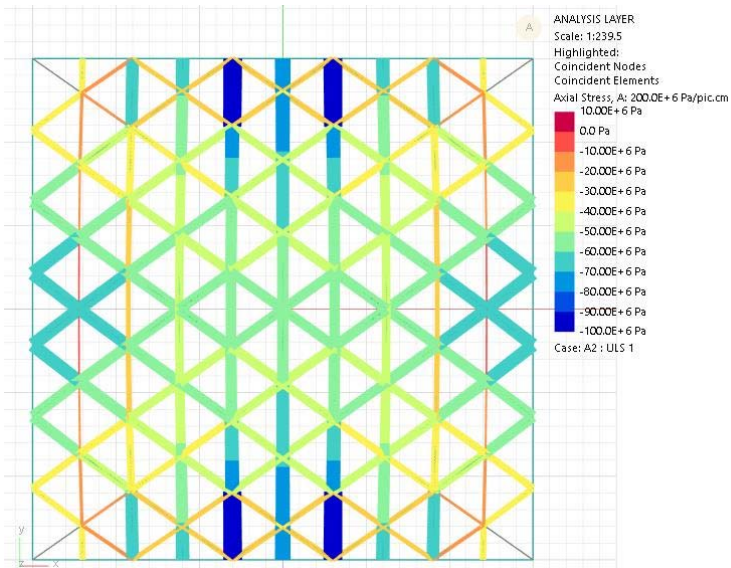
Stiffness: 0.0389 EI/L



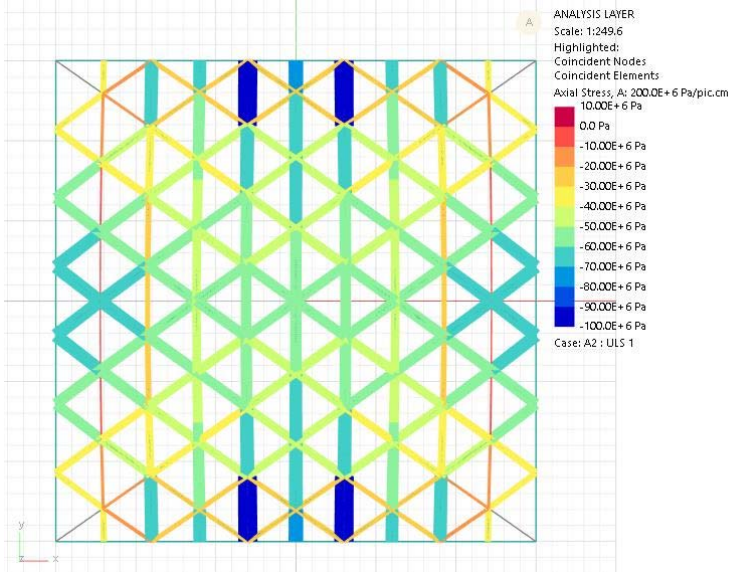
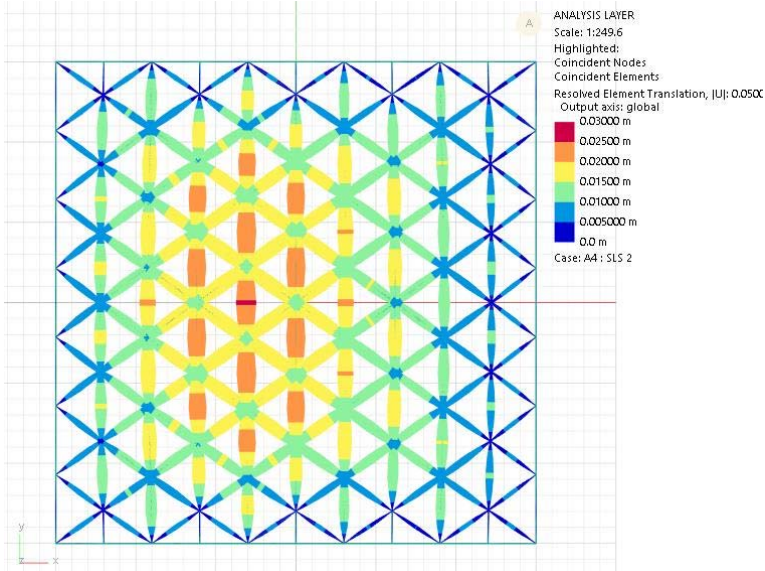
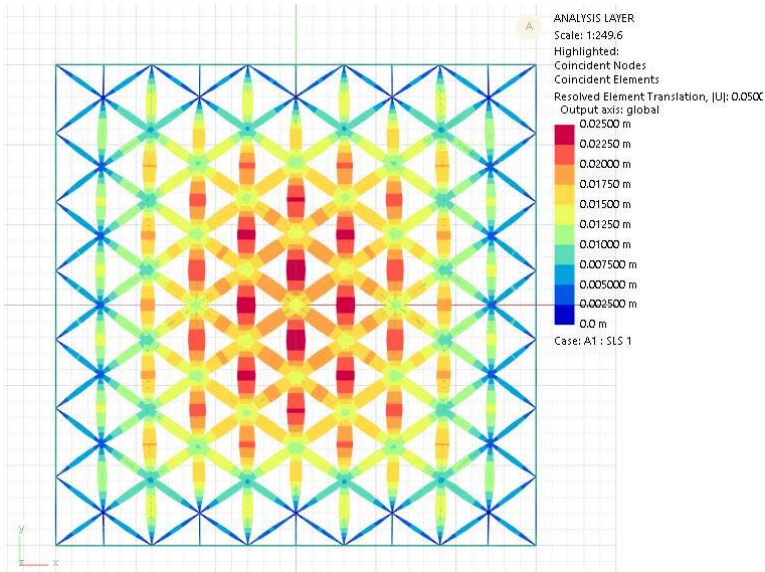


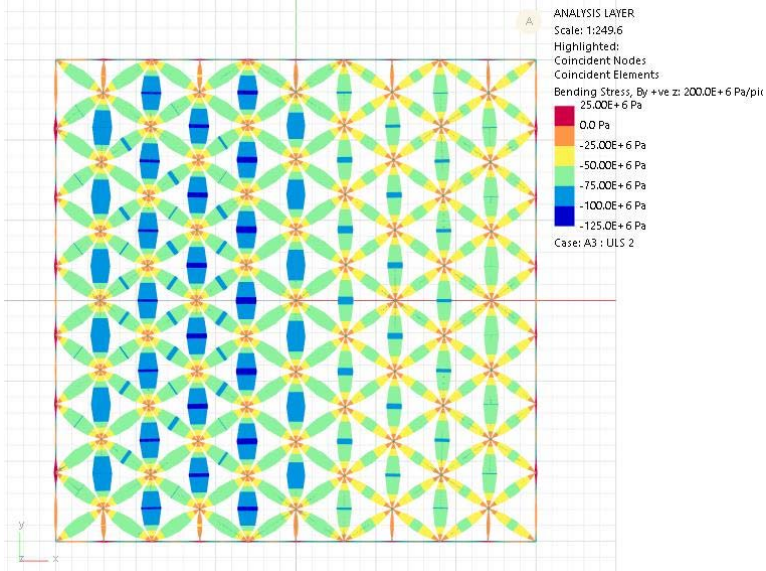
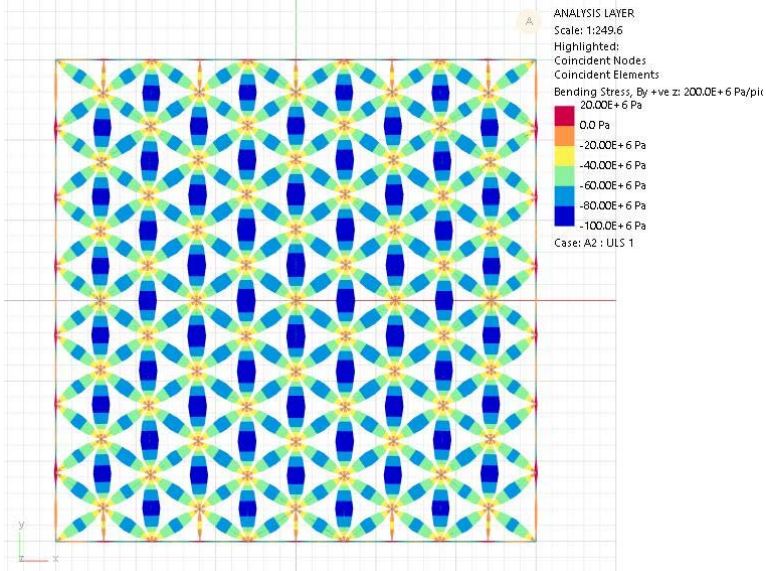
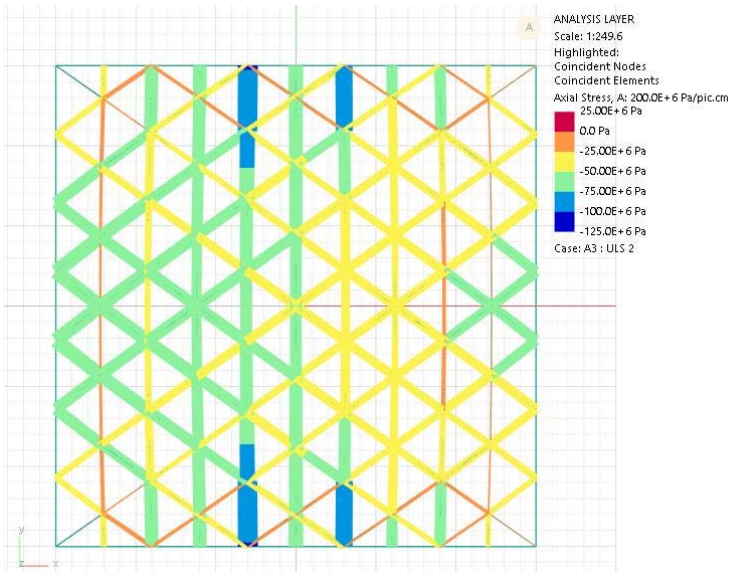
Stiffness: 0.0114 EI/L





Pinned:





E | APPENDIX E. CONNECTION DESIGN

E.1 RIGID CONNECTION

Project:
Project no:
Author:

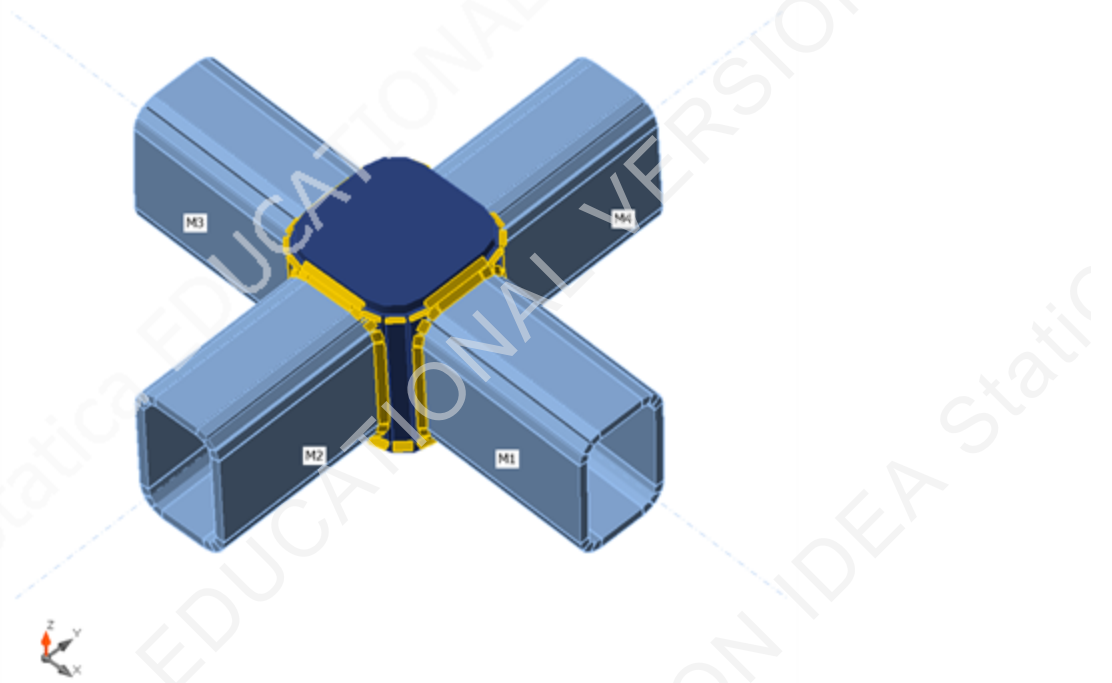
Project item Final design_Thesis

Design

Name Final design_Thesis
Description
Analysis Stress, strain/ simplified loading

Beams and columns

Name	Cross-section	β - Direction [°]	γ - Pitch [°]	α - Rotation [°]	Offset ex [mm]	Offset ey [mm]	Offset ez [mm]	Forces in
M1	1 - RHS150/100/10.0	0.0	2.8	3.4	0	0	0	Node
M2	1 - RHS150/100/10.0	-90.0	3.4	0.0	0	0	0	Node
M3	1 - RHS150/100/10.0	-180.0	-2.8	-3.4	0	0	0	Node
M4	1 - RHS150/100/10.0	90.0	-3.4	0.0	0	0	0	Node



Cross-sections

Name	Material
1 - RHS150/100/10.0	Edit of S 235
5 - SHS150/150/16.0	S 355

Project:
Project no:
Author:

Load effects (equilibrium not required)

Name	Member	N [kN]	Vy [kN]	Vz [kN]	Mx [kNm]	My [kNm]	Mz [kNm]
LE1	M2	-160.0	0.0	0.0	0.0	4.4	0.0
	M3	160.0	0.0	0.0	0.0	4.4	0.0
	M4	-160.0	0.0	0.0	0.0	4.4	0.0

Check

Summary

Name	Value	Status
Analysis	100.0%	OK
Plates	0.0 < 5.0%	OK
Welds	97.2 < 100%	OK
Buckling	Not calculated	
GMNA	Calculated	

Plates

Name	Material	Thickness [mm]	Loads	σ_{Ed} [MPa]	ϵ_{Pl} [%]	σ_{cEd} [MPa]	Status
M1	Edit of S 235	10.0	LE1	113.7	0.0	0.0	OK
M2	Edit of S 235	10.0	LE1	128.7	0.0	0.0	OK
M3	Edit of S 235	10.0	LE1	99.0	0.0	0.0	OK
M4	Edit of S 235	10.0	LE1	130.0	0.0	0.0	OK
SM1	S 355	16.0	LE1	144.4	0.0	0.0	OK
STIFF2	S 355	12.0	LE1	112.2	0.0	0.0	OK
STIFF3	S 355	12.0	LE1	123.1	0.0	0.0	OK

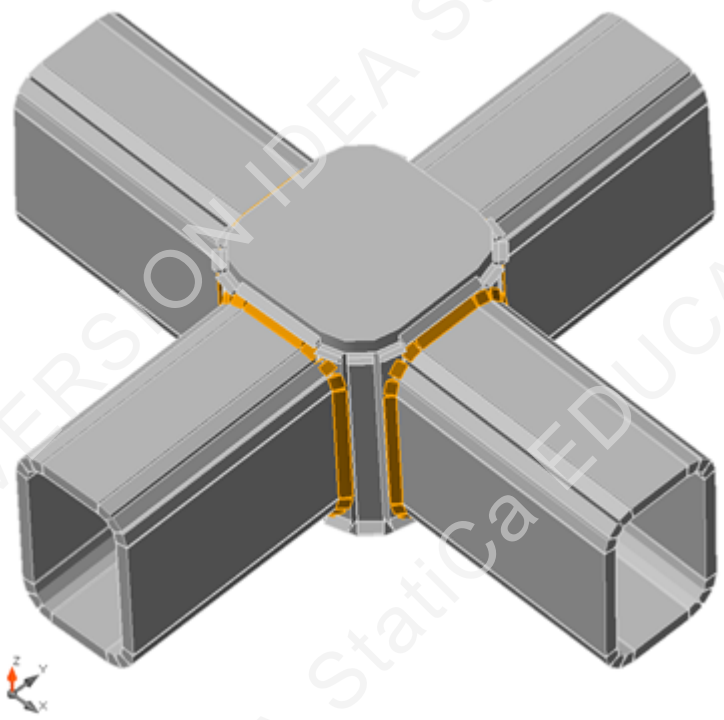
Design data

Material	f_y [MPa]	ϵ_{lim} [%]
Edit of S 235	235.0	5.0
S 355	355.0	5.0

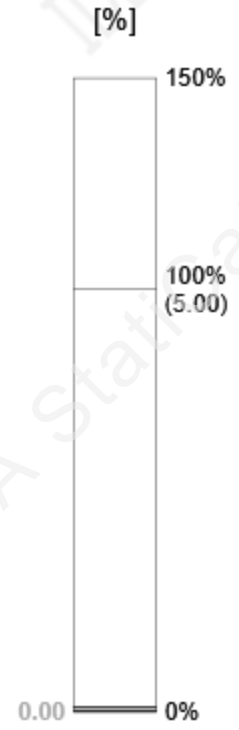
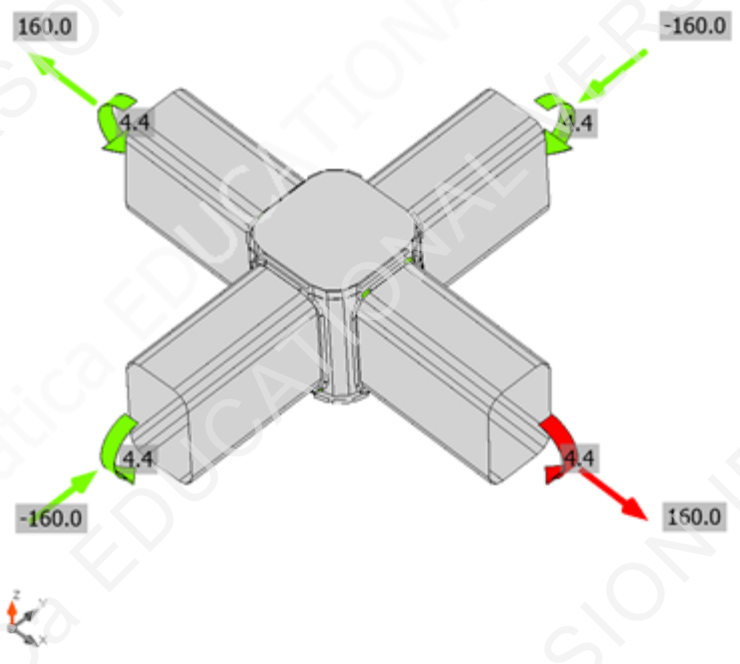
Symbol explanation

ϵ_{Pl}	Strain
σ_{Ed}	Eq. stress
σ_{cEd}	Contact stress
f_y	Yield strength
ϵ_{lim}	Limit of plastic strain

Project:
Project no:
Author:

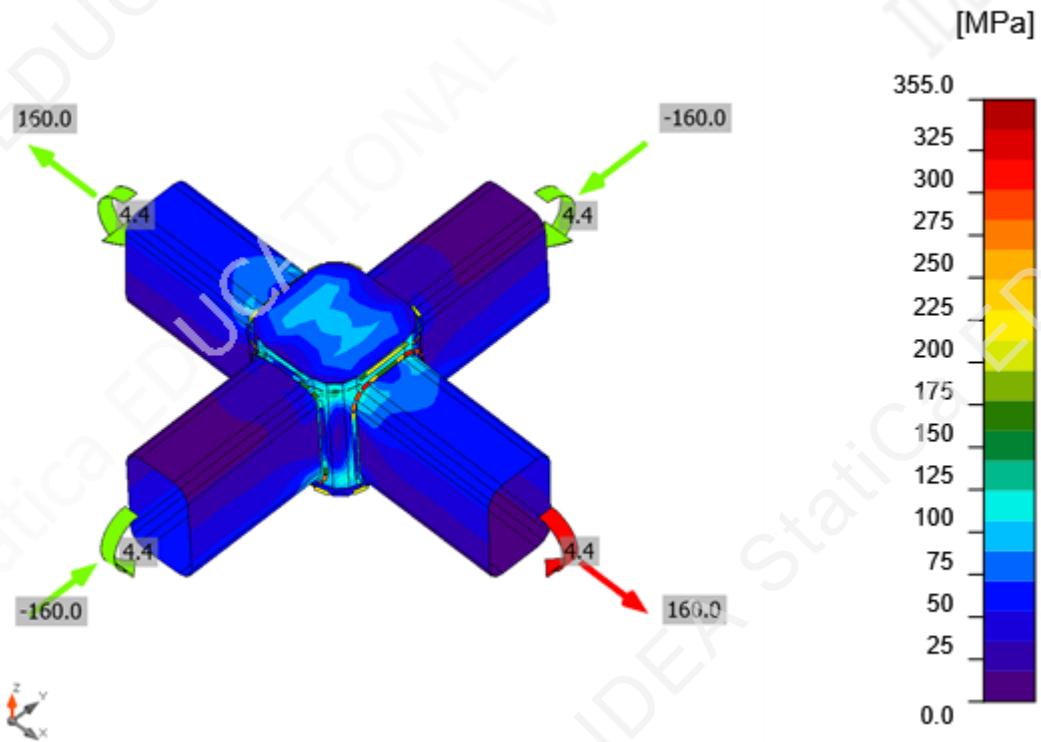


Overall check, LE1



Strain check, LE1

Project:
Project no:
Author:



Equivalent stress, LE1

Welds (Plastic redistribution)

Item	Edge	Material	Throat th. [mm]	Length [mm]	Loads	$\sigma_{w,Ed}$ [MPa]	ϵ_{pl} [%]	σ_{\perp} [MPa]	τ_{\parallel} [MPa]	τ_{\perp} [MPa]	Ut [%]	Ut _c [%]	Status
SM1-w 4	M1	Edit of S 235	4.0	425	LE1	323.1	0.0	252.0	47.4	-106.7	97.2	36.7	OK
STIFF2	SM1	S 355	4.0	479	LE1	249.2	0.0	164.6	-11.8	-107.4	57.2	36.7	OK
STIFF3	SM1	S 355	4.0	479	LE1	242.2	0.0	88.5	-31.0	126.4	55.6	37.2	OK
SM1-w 3	M2	Edit of S 235	4.0	416	LE1	334.1	0.0	-252.0	102.0	75.1	97.2	35.6	OK
SM1-w 2	M3	Edit of S 235	4.0	425	LE1	332.7	0.0	252.0	41.7	-118.2	97.2	36.2	OK
SM1-w 1	M4	Edit of S 235	4.0	416	LE1	333.5	0.0	-252.0	101.9	74.4	97.2	35.6	OK

Design data

	β_w [-]	$\sigma_{w,Rd}$ [MPa]	0.9 σ [MPa]
Edit of S 235	0.80	360.0	259.2
S 355	0.90	435.6	352.8

Project:
Project no:
Author:

Symbol explanation

ϵ_{PI}	Strain
$\sigma_{w,Ed}$	Equivalent stress
$\sigma_{w,Rd}$	Equivalent stress resistance
σ_{\perp}	Perpendicular stress
τ_{\parallel}	Shear stress parallel to weld axis
τ_{\perp}	Shear stress perpendicular to weld axis
0.9σ	Perpendicular stress resistance - $0.9 \cdot f_u / \gamma_{M2}$
β_w	Corelation factor EN 1993-1-8 tab. 4.1
U_t	Utilization
U_{tc}	Weld capacity utilization

Buckling

Buckling analysis was not calculated.

Code settings

Item	Value	Unit	Reference
Y_{M0}	1.00	-	EN 1993-1-1: 6.1
Y_{M1}	1.00	-	EN 1993-1-1: 6.1
Y_{M2}	1.25	-	EN 1993-1-1: 6.1
Y_{M3}	1.25	-	EN 1993-1-8: 2.2
Y_C	1.50	-	EN 1992-1-1: 2.4.2.4
Y_{Inst}	1.20	-	EN 1992-4: Table 4.1
Joint coefficient β_j	0.67	-	EN 1993-1-8: 6.2.5
Effective area - influence of mesh size	0.10	-	
Friction coefficient - concrete	0.25	-	EN 1993-1-8
Friction coefficient in slip-resistance	0.30	-	EN 1993-1-8 tab 3.7
Limit plastic strain	0.05	-	EN 1993-1-5
Weld stress evaluation	Plastic redistribution		
Detailing	No		
Distance between bolts [d]	2.20	-	EN 1993-1-8: tab 3.3
Distance between bolts and edge [d]	1.20	-	EN 1993-1-8: tab 3.3
Concrete breakout resistance check	Both		EN 1992-4: 7.2.1.4 and 7.2.2.5
Use calculated a_b in bearing check.	Yes		EN 1993-1-8: tab 3.4
Cracked concrete	Yes		EN 1992-4
Local deformation check	No		CIDECT DG 1, 3 - 1.1
Local deformation limit	0.03	-	CIDECT DG 1, 3 - 1.1
Geometrical nonlinearity (GMNA)	Yes		Analysis with large deformations for hollow section joints
Braced system	No		EN 1993-1-8: 5.2.2.5

Project:
 Project no:
 Author:

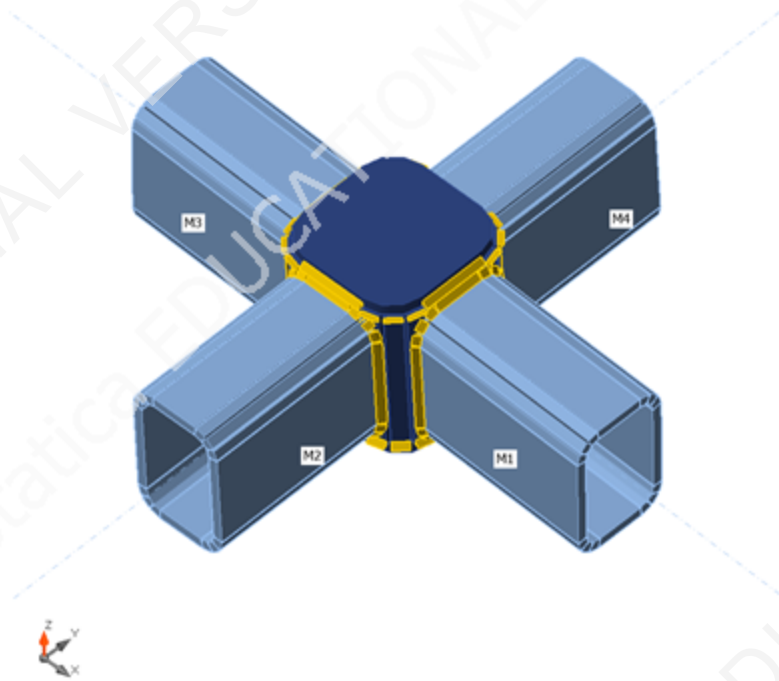
Project item Final design_Thesis

Design

Name Final design_Thesis
 Description
 Analysis Stiffness

Beams and columns

Name	Cross-section	β - Direction [°]	γ - Pitch [°]	α - Rotation [°]	Offset ex [mm]	Offset ey [mm]	Offset ez [mm]	Forces in
M1	1 - RHS150/100/10.0	0.0	2.8	3.4	0	0	0	Node
M2	1 - RHS150/100/10.0	-90.0	3.4	0.0	0	0	0	Node
M3	1 - RHS150/100/10.0	-180.0	-2.8	-3.4	0	0	0	Node
M4	1 - RHS150/100/10.0	90.0	-3.4	0.0	0	0	0	Node



Cross-sections

Name	Material
1 - RHS150/100/10.0	Edit of S 235
5 - SHS150/150/16.0	S 355

Load effects

Name	Member	N [kN]	Vy [kN]	Vz [kN]	Mx [kNm]	My [kNm]	Mz [kNm]
LE1	M1	160.0	0.0	0.0	0.0	4.4	0.0

Project:
Project no:
Author:

Check

Rotational stiffness

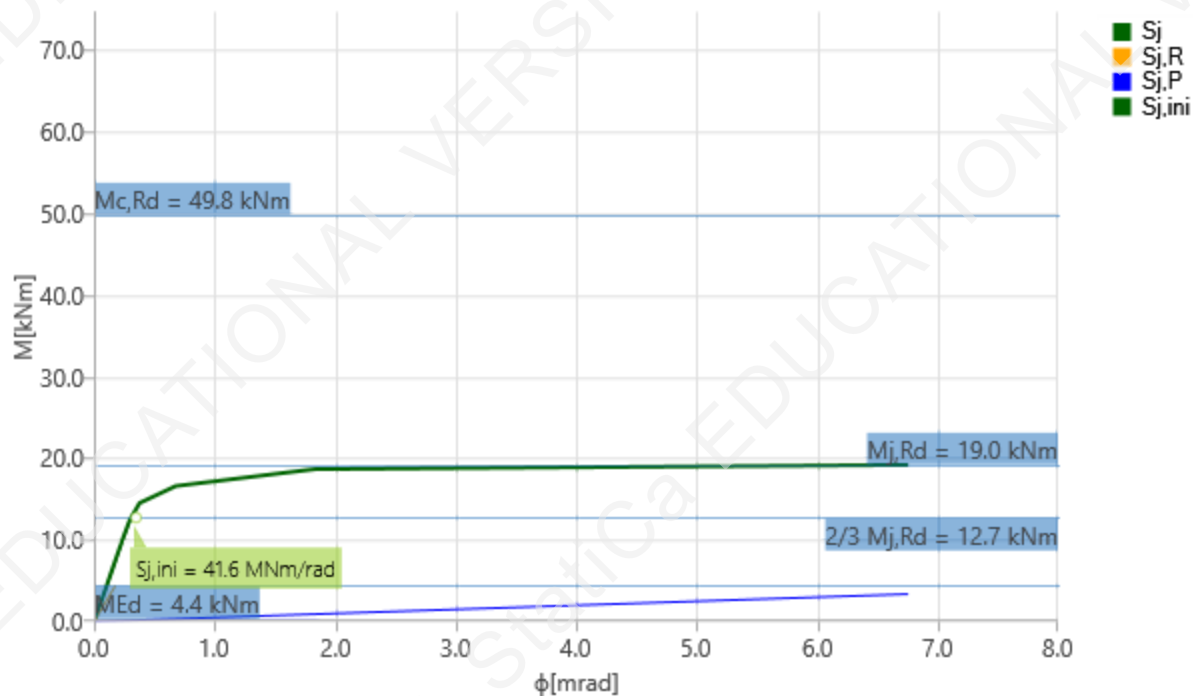
Name	Comp.	Loads	$M_{j,Rd}$ [kNm]	$S_{j,ini}$ [MNm/rad]	Φ_c [mrad]	L [m]	$S_{j,R}$ [MNm/rad]	$S_{j,P}$ [MNm/rad]	Class.
M1	My	LE1	19.0	41.6	3.4	2.70	24.9	0.5	Rigid

Secant rotational stiffness

Name	Comp.	Loads	M [kNm]	$S_{j,s}$ [MNm/rad]	Φ [mrad]
M1	My	LE1	4.4	42.3	0.1

Symbol explanation

- $M_{j,Rd}$ Bending resistance
- $S_{j,ini}$ Initial rotational stiffness
- $S_{j,s}$ Secant rotational stiffness
- Φ Rotational deformation
- Φ_c Rotational capacity
- $S_{j,R}$ Limit value - rigid joint
- $S_{j,P}$ Limit value - nominally pinned joint



Stiffness diagram My - ϕ_y , LE1

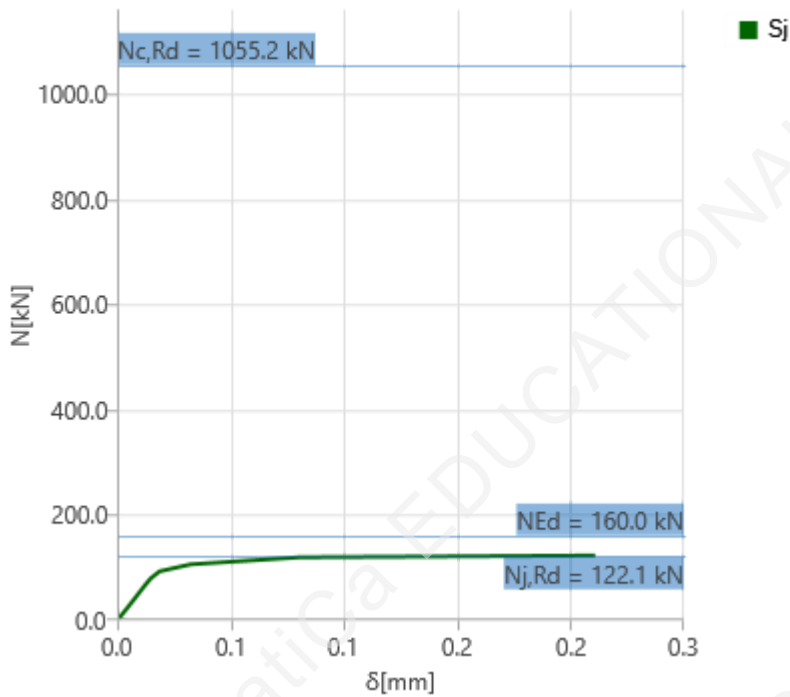
Axial stiffness

Name	Component	Loads	N [kN]	$N_{j,Rd}$ [kN]	dx [mm]	St [MN/m]
M1	N	LE1	160.0	122.1	0	503

Project:
Project no:
Author:

Symbol explanation

$N_{j,Rd}$ Tension (compression) resistance
 S_t Secant axial stiffness
 δ Longitudinal deformation



Stiffness diagram N - δ , LE1

Code settings

Item	Value	Unit	Reference
Y_{M0}	1.00	-	EN 1993-1-1: 6.1
Y_{M1}	1.00	-	EN 1993-1-1: 6.1
Y_{M2}	1.25	-	EN 1993-1-1: 6.1
Y_{M3}	1.25	-	EN 1993-1-8: 2.2
Y_C	1.50	-	EN 1992-1-1: 2.4.2.4
Y_{Inst}	1.20	-	EN 1992-4: Table 4.1
Joint coefficient β_j	0.67	-	EN 1993-1-8: 6.2.5
Effective area - influence of mesh size	0.10	-	
Friction coefficient - concrete	0.25	-	EN 1993-1-8
Friction coefficient in slip-resistance	0.30	-	EN 1993-1-8 tab 3.7
Limit plastic strain	0.05	-	EN 1993-1-5
Weld stress evaluation	Plastic redistribution		
Detailing	No		
Distance between bolts [d]	2.20	-	EN 1993-1-8: tab 3.3
Distance between bolts and edge [d]	1.20	-	EN 1993-1-8: tab 3.3
Concrete breakout resistance check	Both		EN 1992-4: 7.2.1.4 and 7.2.2.5

Project:
Project no:
Author:

Item	Value	Unit	Reference
Use calculated α_b in bearing check.	Yes		EN 1993-1-8: tab 3.4
Cracked concrete	Yes		EN 1992-4
Local deformation check	No		CIDECT DG 1, 3 - 1.1
Local deformation limit	0.03	-	CIDECT DG 1, 3 - 1.1
Geometrical nonlinearity (GMNA)	Yes		Analysis with large deformations for hollow section joints
Braced system	No		EN 1993-1-8: 5.2.2.5

E.2 SEMI-RIGID 1 CONNECTION

Project:
 Project no:
 Author:

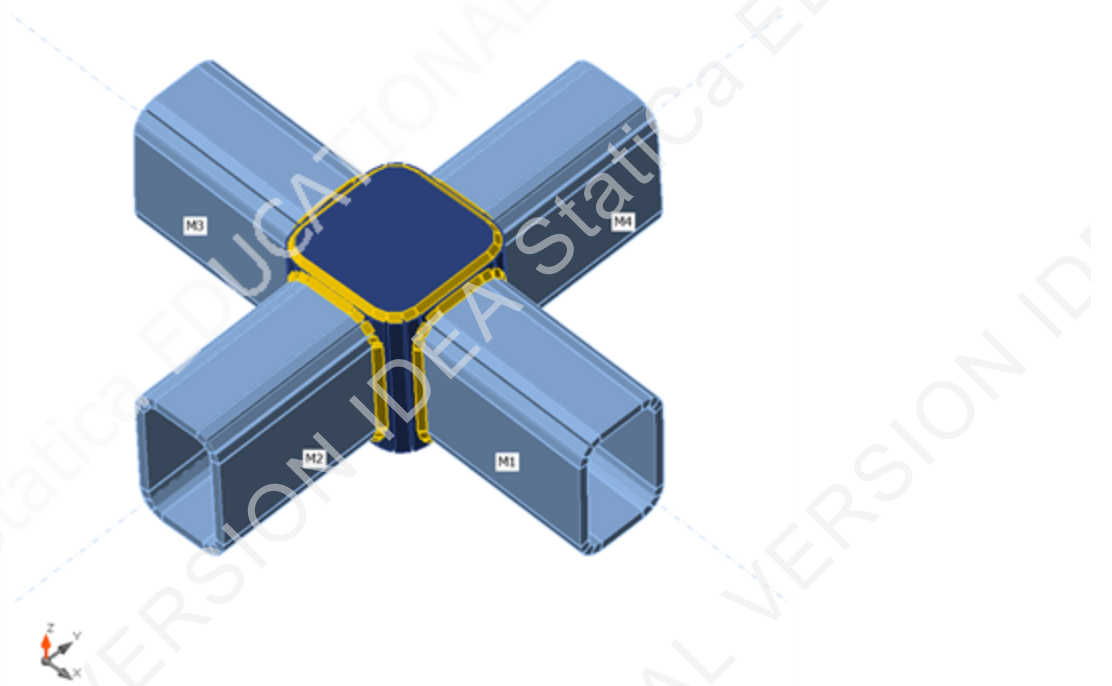
Project item Final design_Thesis

Design

Name Final design_Thesis
 Description
 Analysis Stress, strain/ loads in equilibrium

Beams and columns

Name	Cross-section	β - Direction [°]	γ - Pitch [°]	α - Rotation [°]	Offset ex [mm]	Offset ey [mm]	Offset ez [mm]	Forces in
M1	1 - RHS150/100/10.0	0.0	2.8	3.4	0	0	0	Node
M2	1 - RHS150/100/10.0	-90.0	3.4	0.0	0	0	0	Node
M3	1 - RHS150/100/10.0	-180.0	-2.8	-3.4	0	0	0	Node
M4	1 - RHS150/100/10.0	90.0	-3.4	0.0	0	0	0	Node



Cross-sections

Name	Material
1 - RHS150/100/10.0	Edit of S 235
6 - SHS150/150/12.5	S 355

Project:
Project no:
Author:

Load effects (forces in equilibrium)

Name	Member	N [kN]	Vy [kN]	Vz [kN]	Mx [kNm]	My [kNm]	Mz [kNm]
LE1	M1	160.0	0.0	0.0	0.0	4.3	0.0
	M2	-160.0	0.0	0.0	0.0	4.3	0.0
	M3	160.0	0.0	0.0	0.0	4.3	0.0
	M4	-160.0	0.0	0.0	0.0	4.3	0.0

Check

Summary

Name	Value	Status
Analysis	100.0%	OK
Plates	0.0 < 5.0%	OK
Welds	98.0 < 100%	OK
Buckling	Not calculated	
GMNA	Calculated	

Plates

Name	Material	Thickness [mm]	Loads	σ_{Ed} [MPa]	ϵ_{pl} [%]	σ_{cEd} [MPa]	Status
M1	Edit of S 235	10.0	LE1	160.8	0.0	0.0	OK
M2	Edit of S 235	10.0	LE1	139.5	0.0	0.0	OK
M3	Edit of S 235	10.0	LE1	139.9	0.0	0.0	OK
M4	Edit of S 235	10.0	LE1	139.1	0.0	0.0	OK
SM1	S 355	12.5	LE1	251.8	0.0	0.0	OK
STIFF2	S 355	5.0	LE1	245.5	0.0	0.0	OK
STIFF3	S 355	5.0	LE1	249.4	0.0	0.0	OK

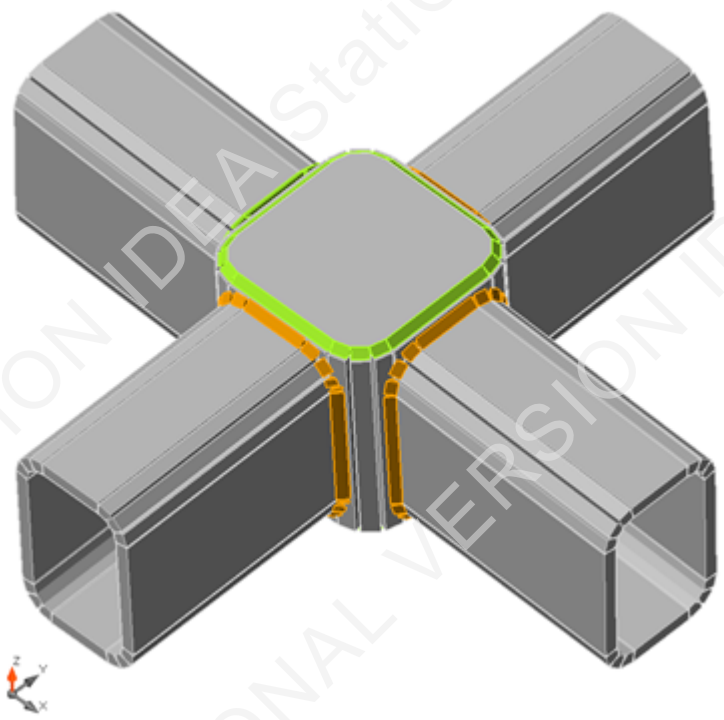
Design data

Material	f_y [MPa]	ϵ_{lim} [%]
Edit of S 235	235.0	5.0
S 355	355.0	5.0

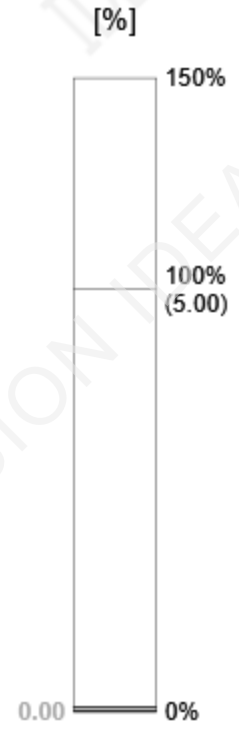
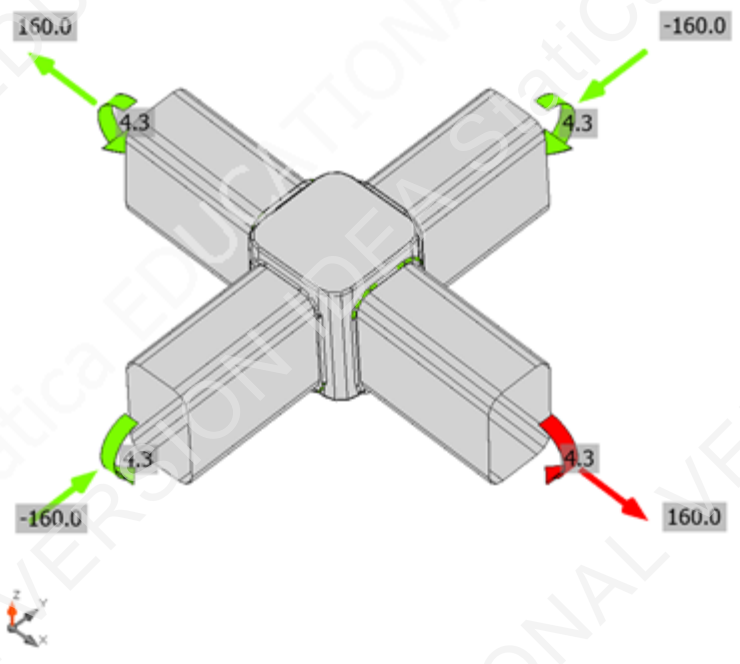
Symbol explanation

ϵ_{pl}	Strain
σ_{Ed}	Eq. stress
σ_{cEd}	Contact stress
f_y	Yield strength
ϵ_{lim}	Limit of plastic strain

Project:
Project no:
Author:

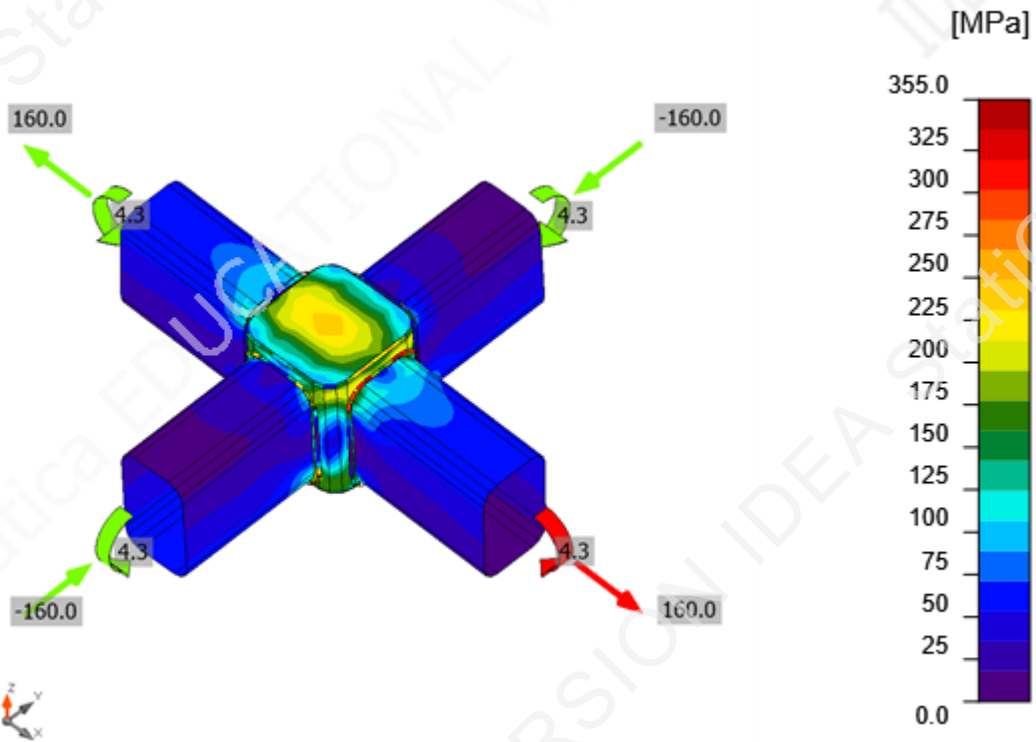


Overall check, LE1



Strain check, LE1

Project:
Project no:
Author:



Equivalent stress, LE1

Welds (Plastic redistribution)

Item	Edge	Material	Throat th. [mm]	Length [mm]	Loads	$\sigma_{w,Ed}$ [MPa]	ϵ_{pl} [%]	σ_{\perp} [MPa]	τ_{\parallel} [MPa]	τ_{\perp} [MPa]	Ut [%]	Ut _c [%]	Status
SM1-w 4	M1	Edit of S 235	▲4.0	425	LE1	348.3	0.0	252.0	19.0	-137.5	97.2	37.2	OK
STIFF2	SM1	S 355	▲4.0	494	LE1	310.9	0.0	159.8	17.6	-153.0	71.4	38.1	OK
STIFF3	SM1	S 355	▲4.0	494	LE1	293.0	0.0	-149.5	23.4	143.6	67.3	38.2	OK
SM1-arc 6	M2	Edit of S 235	▲4.0	412	LE1	352.9	0.0	-222.7	122.2	100.2	98.0	38.3	OK
SM1-w 2	M3	Edit of S 235	▲4.0	425	LE1	325.6	0.0	208.7	-24.2	-142.3	90.5	36.7	OK
SM1-arc 12	M4	Edit of S 235	▲4.0	412	LE1	352.9	0.1	-236.2	109.4	104.7	98.0	38.2	OK

Design data

	β_w [-]	$\sigma_{w,Rd}$ [MPa]	0.9 σ [MPa]
Edit of S 235	0.80	360.0	259.2
S 355	0.90	435.6	352.8

Project:
Project no:
Author:

Symbol explanation

ϵ_{Pl}	Strain
$\sigma_{w,Ed}$	Equivalent stress
$\sigma_{w,Rd}$	Equivalent stress resistance
σ_{\perp}	Perpendicular stress
τ_{\parallel}	Shear stress parallel to weld axis
τ_{\perp}	Shear stress perpendicular to weld axis
0.9σ	Perpendicular stress resistance - $0.9 \cdot f_u / \gamma_{M2}$
β_w	Corelation factor EN 1993-1-8 tab. 4.1
U_t	Utilization
U_{tc}	Weld capacity utilization

Buckling

Buckling analysis was not calculated.

Code settings

Item	Value	Unit	Reference
γ_{M0}	1.00	-	EN 1993-1-1: 6.1
γ_{M1}	1.00	-	EN 1993-1-1: 6.1
γ_{M2}	1.25	-	EN 1993-1-1: 6.1
γ_{M3}	1.25	-	EN 1993-1-8: 2.2
γ_C	1.50	-	EN 1992-1-1: 2.4.2.4
γ_{Inst}	1.20	-	EN 1992-4: Table 4.1
Joint coefficient β_j	0.67	-	EN 1993-1-8: 6.2.5
Effective area - influence of mesh size	0.10	-	
Friction coefficient - concrete	0.25	-	EN 1993-1-8
Friction coefficient in slip-resistance	0.30	-	EN 1993-1-8 tab 3.7
Limit plastic strain	0.05	-	EN 1993-1-5
Weld stress evaluation	Plastic redistribution		
Detailing	No		
Distance between bolts [d]	2.20	-	EN 1993-1-8: tab 3.3
Distance between bolts and edge [d]	1.20	-	EN 1993-1-8: tab 3.3
Concrete breakout resistance check	Both		EN 1992-4: 7.2.1.4 and 7.2.2.5
Use calculated a_b in bearing check.	Yes		EN 1993-1-8: tab 3.4
Cracked concrete	Yes		EN 1992-4
Local deformation check	No		CIDECT DG 1, 3 - 1.1
Local deformation limit	0.03	-	CIDECT DG 1, 3 - 1.1
Geometrical nonlinearity (GMNA)	Yes		Analysis with large deformations for hollow section joints
Braced system	No		EN 1993-1-8: 5.2.2.5

Project:
 Project no:
 Author:

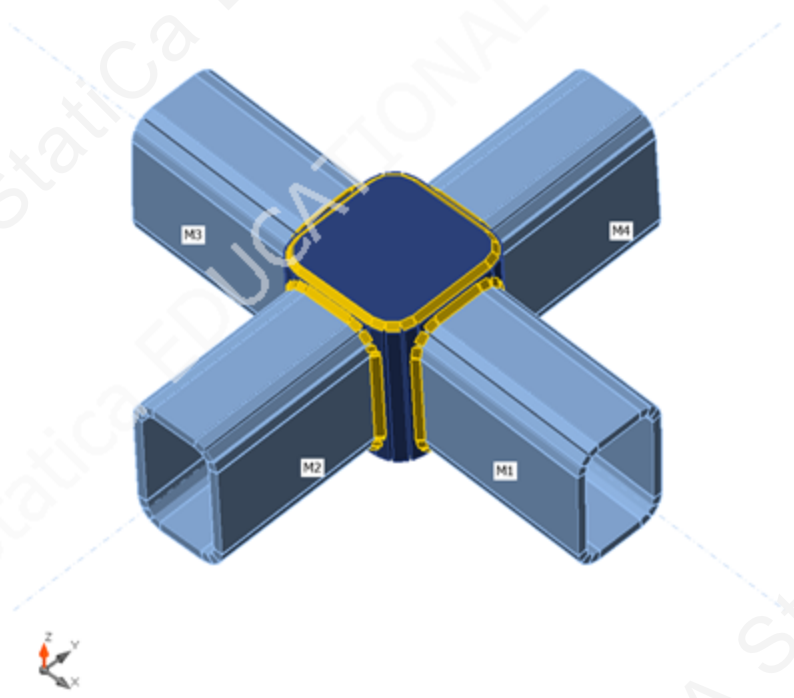
Project item Final design_Thesis

Design

Name Final design_Thesis
 Description
 Analysis Stiffness

Beams and columns

Name	Cross-section	β - Direction [°]	γ - Pitch [°]	α - Rotation [°]	Offset ex [mm]	Offset ey [mm]	Offset ez [mm]	Forces in
M1	1 - RHS150/100/10.0	0.0	2.8	3.4	0	0	0	Node
M2	1 - RHS150/100/10.0	-90.0	3.4	0.0	0	0	0	Node
M3	1 - RHS150/100/10.0	-180.0	-2.8	-3.4	0	0	0	Node
M4	1 - RHS150/100/10.0	90.0	-3.4	0.0	0	0	0	Node



Cross-sections

Name	Material
1 - RHS150/100/10.0	Edit of S 235
6 - SHS150/150/12.5	S 355

Project:
Project no:
Author:

Load effects

Name	Member	N [kN]	Vy [kN]	Vz [kN]	Mx [kNm]	My [kNm]	Mz [kNm]
LE1	M1	160.0	0.0	0.0	0.0	4.3	0.0
	M2	-160.0	0.0	0.0	0.0	4.3	0.0
	M3	160.0	0.0	0.0	0.0	4.3	0.0
	M4	-160.0	0.0	0.0	0.0	4.3	0.0

Check

Rotational stiffness

Name	Comp.	Loads	Mj,Rd [kNm]	Sj,ini [MNm/rad]	Φc [mrad]	L [m]	Sj,R [MNm/rad]	Sj,P [MNm/rad]	Class.
M1	My	LE1	0.0	13.3	0.0	2.70	24.9	0.5	Semi-rigid

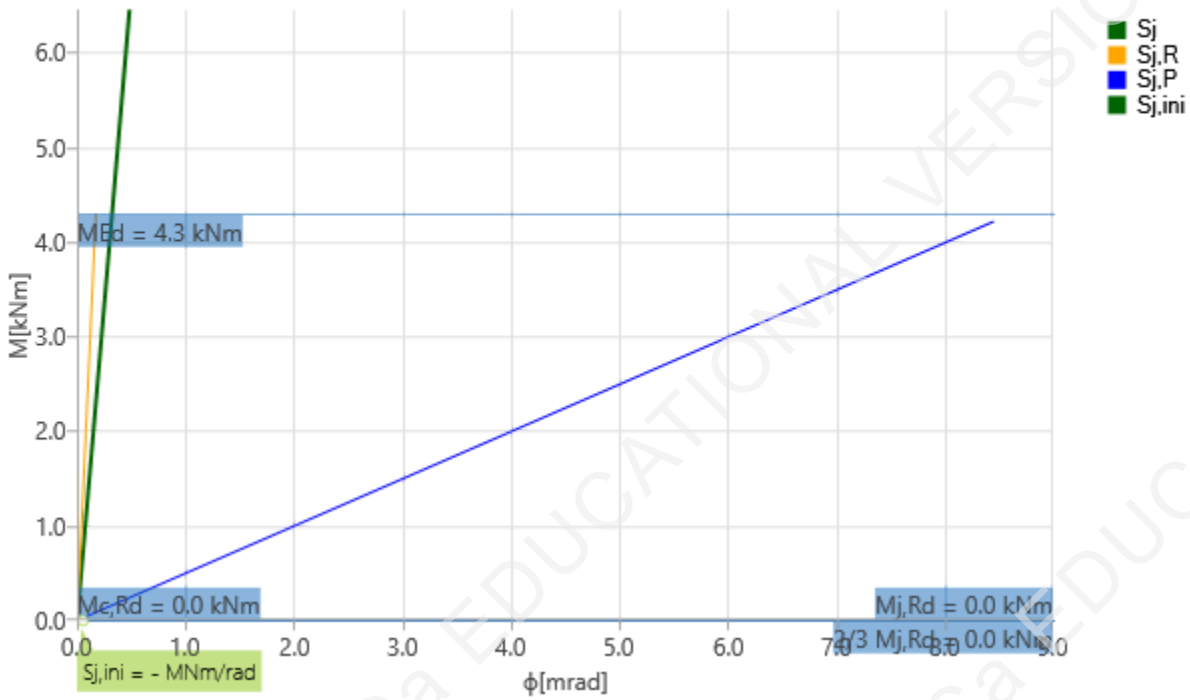
Secant rotational stiffness

Name	Comp.	Loads	M [kNm]	Sjs [MNm/rad]	Φ [mrad]
M1	My	LE1	4.3	13.3	0.3

Symbol explanation

$M_{j,Rd}$	Bending resistance
$S_{j,ini}$	Initial rotational stiffness
$S_{j,s}$	Secant rotational stiffness
Φ	Rotational deformation
Φ_c	Rotational capacity
$S_{j,R}$	Limit value - rigid joint
$S_{j,P}$	Limit value - nominally pinned joint

Project:
 Project no:
 Author:



Stiffness diagram My - ϕ_y , LE1

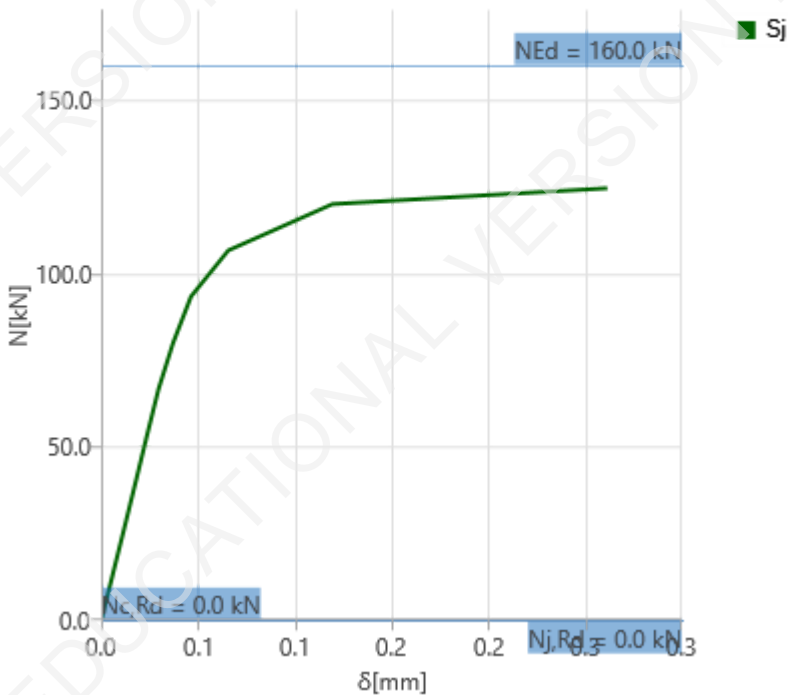
Axial stiffness

Name	Component	Loads	N [kN]	N _{j,Rd} [kN]	dx [mm]	St [MN/m]
M1	N	LE1	160.0	0.0	0	431

Symbol explanation

- N_{j,Rd} Tension (compression) resistance
- S_t Secant axial stiffness
- δ Longitudinal deformation

Project:
Project no:
Author:



Stiffness diagram N - δ , LE1

Code settings

Item	Value	Unit	Reference
Y _{M0}	1.00	-	EN 1993-1-1: 6.1
Y _{M1}	1.00	-	EN 1993-1-1: 6.1
Y _{M2}	1.25	-	EN 1993-1-1: 6.1
Y _{M3}	1.25	-	EN 1993-1-8: 2.2
Y _C	1.50	-	EN 1992-1-1: 2.4.2.4
Y _{Inst}	1.20	-	EN 1992-4: Table 4.1
Joint coefficient β_j	0.67	-	EN 1993-1-8: 6.2.5
Effective area - influence of mesh size	0.10	-	
Friction coefficient - concrete	0.25	-	EN 1993-1-8
Friction coefficient in slip-resistance	0.30	-	EN 1993-1-8 tab 3.7
Limit plastic strain	0.05	-	EN 1993-1-5
Weld stress evaluation	Plastic redistribution		
Detailing	No		
Distance between bolts [d]	2.20	-	EN 1993-1-8: tab 3.3
Distance between bolts and edge [d]	1.20	-	EN 1993-1-8: tab 3.3
Concrete breakout resistance check	Both		EN 1992-4: 7.2.1.4 and 7.2.2.5
Use calculated a_b in bearing check.	Yes		EN 1993-1-8: tab 3.4
Cracked concrete	Yes		EN 1992-4
Local deformation check	No		CIDECT DG 1, 3 - 1.1
Local deformation limit	0.03	-	CIDECT DG 1, 3 - 1.1

Project:
Project no:
Author:

Item	Value	Unit	Reference
Geometrical nonlinearity (GMNA)	Yes		Analysis with large deformations for hollow section joints
Braced system	No		EN 1993-1-8: 5.2.2.5

E.3 SEMI-RIGID 2 CONNECTION

Project:
 Project no:
 Author:

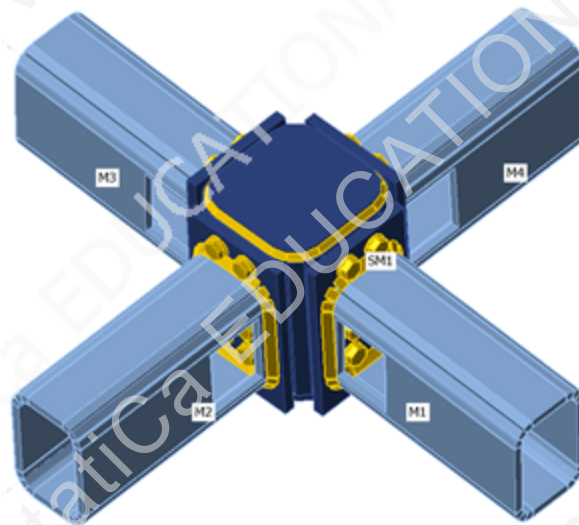
Project item Final design_Thesis

Design

Name Final design_Thesis
 Description
 Analysis Stress, strain/ loads in equilibrium

Beams and columns

Name	Cross-section	β - Direction [°]	γ - Pitch [°]	α - Rotation [°]	Offset ex [mm]	Offset ey [mm]	Offset ez [mm]	Forces in
M1	1 - RHS150/100/10.0	0.0	2.8	3.4	0	0	0	Node
M2	1 - RHS150/100/10.0	-90.0	3.4	0.0	0	0	0	Node
M3	1 - RHS150/100/10.0	-180.0	-2.8	-3.4	0	0	0	Node
M4	1 - RHS150/100/10.0	90.0	-3.4	0.0	0	0	0	Node



Cross-sections

Name	Material
1 - RHS150/100/10.0	Edit of S 235
5 - SHS160/160/16.0	S 355

Bolts

Name	Bolt assembly	Diameter [mm]	f_u [MPa]	Gross area [mm ²]
M12 10.9	M12 10.9	12	1000.0	113

Project:
Project no:
Author:

Load effects (forces in equilibrium)

Name	Member	N [kN]	Vy [kN]	Vz [kN]	Mx [kNm]	My [kNm]	Mz [kNm]
LE1	M1	160.0	0.0	0.0	0.0	3.8	0.0
	M2	-160.0	0.0	0.0	0.0	3.8	0.0
	M3	160.0	0.0	0.0	0.0	3.8	0.0
	M4	-160.0	0.0	0.0	0.0	3.8	0.0

Check

Summary

Name	Value	Status
Analysis	100.0%	OK
Plates	0.0 < 5.0%	OK
Bolts	58.6 < 100%	OK
Welds	66.2 < 100%	OK
Buckling	Not calculated	
GMNA	Calculated	

Plates

Name	Material	Thickness [mm]	Loads	σ_{Ed} [MPa]	ϵ_{pl} [%]	σ_{cEd} [MPa]	Status
M1	Edit of S 235	10.0	LE1	204.5	0.0	0.0	OK
M2	Edit of S 235	10.0	LE1	232.9	0.0	0.0	OK
M3	Edit of S 235	10.0	LE1	214.5	0.0	0.0	OK
M4	Edit of S 235	10.0	LE1	232.8	0.0	0.0	OK
SM1	S 355	16.0	LE1	304.0	0.0	113.7	OK
STIFF2	S 355	10.0	LE1	198.8	0.0	0.0	OK
STIFF3	S 355	16.0	LE1	166.8	0.0	0.0	OK
EP1	S 355	12.0	LE1	321.9	0.0	26.9	OK
EP2	S 355	12.0	LE1	87.2	0.0	47.4	OK
EP3	S 355	12.0	LE1	296.7	0.0	27.3	OK
EP4	S 355	12.0	LE1	86.8	0.0	47.4	OK

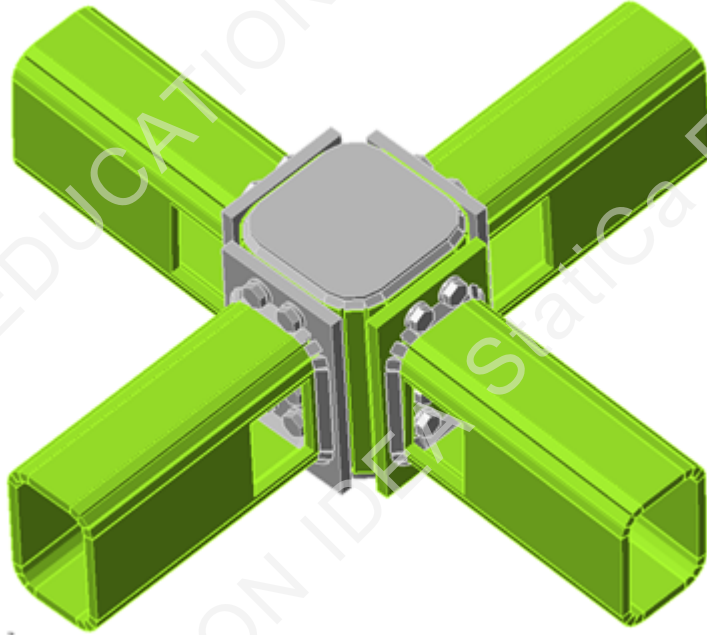
Design data

Material	f_y [MPa]	ϵ_{lim} [%]
Edit of S 235	235.0	5.0
S 355	355.0	5.0

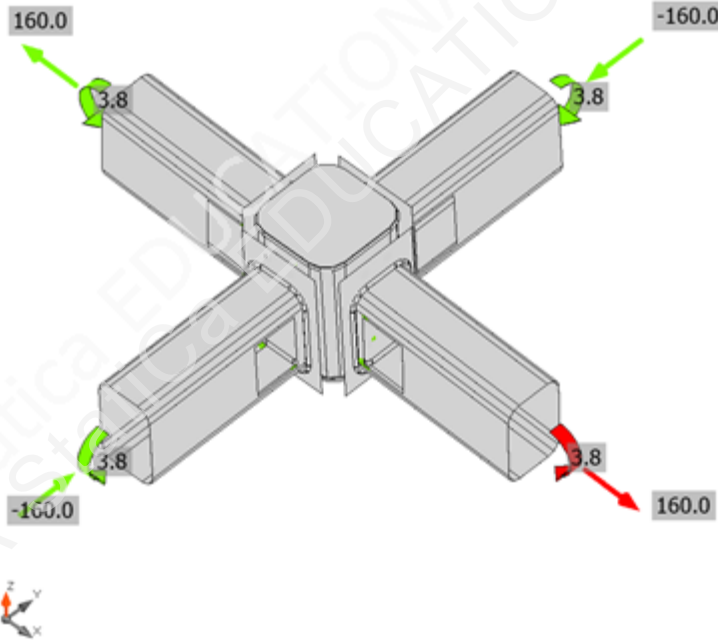
Symbol explanation

ϵ_{pl}	Strain
σ_{Ed}	Eq. stress
σ_{cEd}	Contact stress
f_y	Yield strength
ϵ_{lim}	Limit of plastic strain

Project:
Project no:
Author:

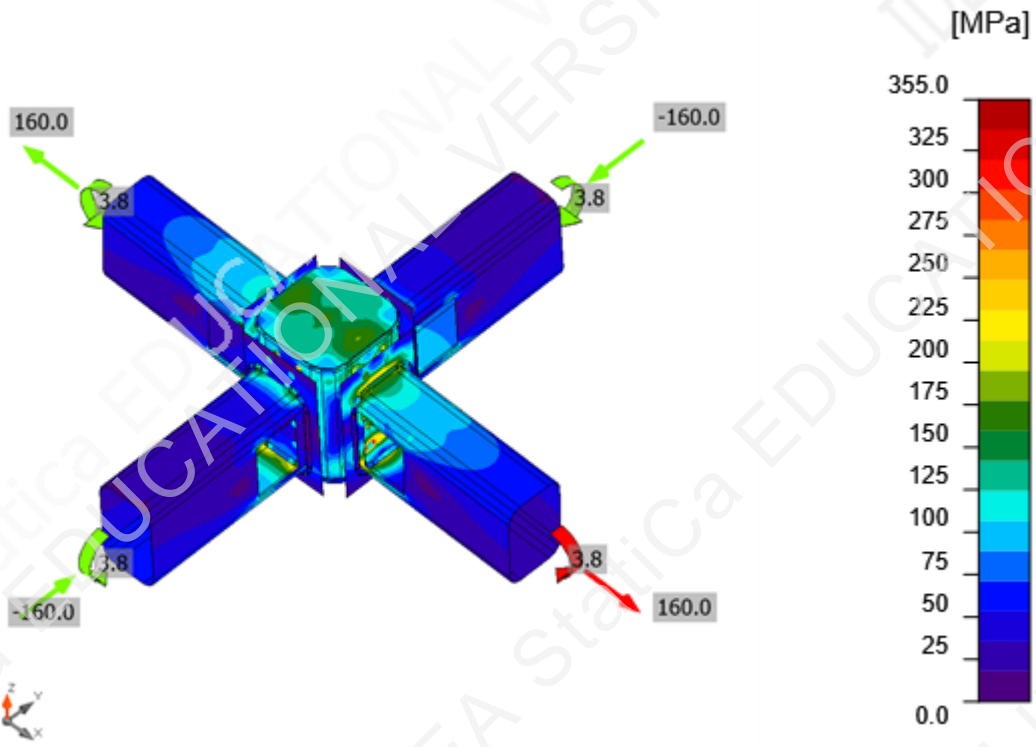


Overall check, LE1



Strain check, LE1

Project:
Project no:
Author:



Equivalent stress, LE1

Project:
Project no:
Author:

Bolts

	Name	Loads	$F_{t,Ed}$ [kN]	V [kN]	U_{t_t} [%]	$F_{b,Rd}$ [kN]	U_{t_s} [%]	U_{t_s} [%]	Status
	B5	LE1	20.8	0.6	34.3	141.1	1.7	26.2	OK
	B6	LE1	20.7	0.5	34.2	141.1	1.5	25.9	OK
	B7	LE1	8.5	0.3	14.1	141.1	0.9	11.0	OK
	B8	LE1	8.5	0.2	14.0	141.1	0.6	10.6	OK
	B9	LE1	35.4	0.4	58.5	109.5	1.2	43.0	OK
	B10	LE1	35.2	0.4	58.1	109.5	1.2	42.7	OK
	B11	LE1	27.4	3.1	45.3	70.6	9.3	41.7	OK
B12	LE1	27.3	3.1	45.1	70.6	9.2	41.5	OK	
	B17	LE1	3.1	0.4	5.0	96.5	1.2	4.8	OK
	B18	LE1	3.0	0.4	5.0	96.5	1.2	4.8	OK
	B19	LE1	4.4	0.6	7.2	103.1	1.9	7.0	OK
	B20	LE1	4.4	0.7	7.2	103.5	2.0	7.1	OK
	B21	LE1	1.9	1.3	3.2	109.5	3.9	6.2	OK
	B22	LE1	1.9	1.3	3.2	109.5	3.8	6.1	OK
	B23	LE1	0.0	1.5	0.0	96.2	4.6	4.6	OK
B24	LE1	0.0	1.6	0.0	96.2	4.7	4.7	OK	
	B29	LE1	20.5	1.7	33.9	109.5	5.1	29.3	OK
	B30	LE1	20.4	1.7	33.8	109.5	5.0	29.1	OK
	B31	LE1	8.3	1.8	13.7	109.5	5.3	15.1	OK
	B32	LE1	8.2	1.8	13.6	109.5	5.3	15.0	OK
	B33	LE1	35.4	1.5	58.6	141.1	4.4	46.3	OK
	B34	LE1	35.3	1.5	58.4	141.1	4.4	46.1	OK
	B35	LE1	27.5	1.0	45.5	74.8	2.9	35.4	OK
B36	LE1	27.7	1.0	45.8	74.8	3.0	35.7	OK	
	B41	LE1	3.0	0.4	5.0	96.5	1.3	4.8	OK
	B42	LE1	3.1	0.4	5.1	96.5	1.3	4.9	OK
	B43	LE1	4.4	0.6	7.2	102.2	1.9	7.0	OK
	B44	LE1	4.3	0.6	7.2	101.8	1.8	7.0	OK
	B45	LE1	1.9	1.2	3.2	109.5	3.7	6.0	OK
	B46	LE1	1.9	1.3	3.2	109.5	3.8	6.0	OK
	B47	LE1	0.0	1.6	0.0	96.8	4.7	4.7	OK
B48	LE1	0.0	1.6	0.0	96.8	4.8	4.8	OK	

Design data

Name	$F_{t,Rd}$ [kN]	$B_{p,Rd}$ [kN]	$F_{v,Rd}$ [kN]
M12 10.9 - 1	60.5	203.9	33.6

Project:
Project no:
Author:

Symbol explanation

$F_{t,Rd}$	Bolt tension resistance EN 1993-1-8 tab. 3.4
$F_{t,Ed}$	Tension force
$B_{p,Rd}$	Punching shear resistance
V	Resultant of shear forces V_y, V_z in bolt
$F_{v,Rd}$	Bolt shear resistance EN_1993-1-8 table 3.4
$F_{b,Rd}$	Plate bearing resistance EN 1993-1-8 tab. 3.4
U_t	Utilization in tension
U_s	Utilization in shear

Welds (Plastic redistribution)

Item	Edge	Material	Throat th. [mm]	Length [mm]	Loads	$\sigma_{w,Ed}$ [MPa]	ϵ_{pl} [%]	σ_{\perp} [MPa]	τ_{\parallel} [MPa]	τ_{\perp} [MPa]	U_t [%]	U_c [%]	Status
STIFF2	SM1	S 355	▲4.0▲	519	LE1	194.8	0.0	147.5	-70.6	20.6	44.7	30.9	OK
STIFF3	SM1	S 355	▲4.0▲	519	LE1	271.9	0.0	233.7	-6.3	80.0	66.2	43.4	OK
EP1	M1	Edit of S 235	▲6.0▲	425	LE1	142.4	0.0	32.5	-0.4	80.1	39.6	23.5	OK
EP2	M2	Edit of S 235	▲6.0▲	424	LE1	162.7	0.0	-49.0	-25.9	-85.7	45.2	12.0	OK
EP3	M3	Edit of S 235	▲6.0▲	425	LE1	132.5	0.0	34.7	-3.6	73.8	36.8	23.2	OK
EP4	M4	Edit of S 235	▲6.0▲	424	LE1	162.3	0.0	-49.1	25.9	-85.5	45.1	11.9	OK
		S 355	▲4.0▲	519	LE1	147.1	0.0	14.3	61.5	-58.0	33.8	26.0	OK
		S 355	▲4.0▲	519	LE1	195.5	0.0	-1.9	-0.5	112.9	44.9	35.6	OK
		Edit of S 235	▲6.0▲	425	LE1	170.2	0.0	96.5	-60.2	-54.1	47.3	16.4	OK
		Edit of S 235	▲6.0▲	424	LE1	196.8	0.0	-124.4	-5.0	87.9	54.7	18.0	OK
		Edit of S 235	▲6.0▲	425	LE1	172.5	0.0	97.5	-62.0	-54.0	47.9	16.1	OK
		Edit of S 235	▲6.0▲	424	LE1	196.8	0.0	-124.2	4.7	88.0	54.7	17.9	OK

Design data

	β_w [-]	$\sigma_{w,Rd}$ [MPa]	0.9σ [MPa]
S 355	0.90	435.6	352.8
Edit of S 235	0.80	360.0	259.2

Symbol explanation

ϵ_{pl}	Strain
$\sigma_{w,Ed}$	Equivalent stress
$\sigma_{w,Rd}$	Equivalent stress resistance
σ_{\perp}	Perpendicular stress
τ_{\parallel}	Shear stress parallel to weld axis
τ_{\perp}	Shear stress perpendicular to weld axis
0.9σ	Perpendicular stress resistance - $0.9 \cdot f_u / \gamma_{M2}$
β_w	Corelation factor EN 1993-1-8 tab. 4.1
U_t	Utilization
U_c	Weld capacity utilization

Project:
Project no:
Author:

Buckling

Buckling analysis was not calculated.

Code settings

Item	Value	Unit	Reference
YM0	1.00	-	EN 1993-1-1: 6.1
YM1	1.00	-	EN 1993-1-1: 6.1
YM2	1.25	-	EN 1993-1-1: 6.1
YM3	1.25	-	EN 1993-1-8: 2.2
YC	1.50	-	EN 1992-1-1: 2.4.2.4
YInst	1.20	-	EN 1992-4: Table 4.1
Joint coefficient β_j	0.67	-	EN 1993-1-8: 6.2.5
Effective area - influence of mesh size	0.10	-	
Friction coefficient - concrete	0.25	-	EN 1993-1-8
Friction coefficient in slip-resistance	0.30	-	EN 1993-1-8 tab 3.7
Limit plastic strain	0.05	-	EN 1993-1-5
Weld stress evaluation	Plastic redistribution		
Detailing	No		
Distance between bolts [d]	2.20	-	EN 1993-1-8: tab 3.3
Distance between bolts and edge [d]	1.20	-	EN 1993-1-8: tab 3.3
Concrete breakout resistance check	Both		EN 1992-4: 7.2.1.4 and 7.2.2.5
Use calculated a_b in bearing check.	Yes		EN 1993-1-8: tab 3.4
Cracked concrete	Yes		EN 1992-4
Local deformation check	No		CIDECT DG 1, 3 - 1.1
Local deformation limit	0.03	-	CIDECT DG 1, 3 - 1.1
Geometrical nonlinearity (GMNA)	Yes		Analysis with large deformations for hollow section joints
Braced system	No		EN 1993-1-8: 5.2.2.5

Project:
 Project no:
 Author:

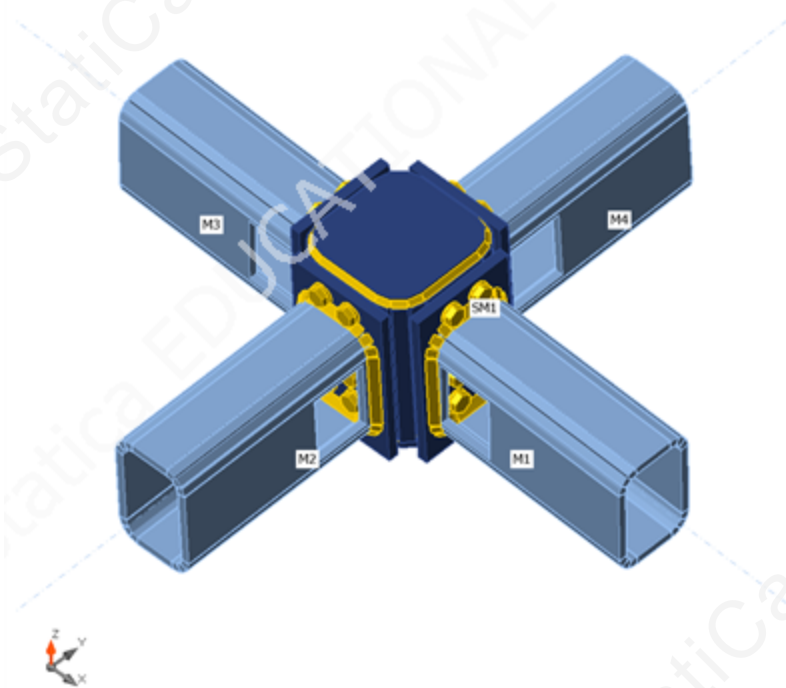
Project item Final design_Thesis

Design

Name Final design_Thesis
 Description
 Analysis Stiffness

Beams and columns

Name	Cross-section	β - Direction [°]	γ - Pitch [°]	α - Rotation [°]	Offset ex [mm]	Offset ey [mm]	Offset ez [mm]	Forces in
M1	1 - RHS150/100/10.0	0.0	2.8	3.4	0	0	0	Node
M2	1 - RHS150/100/10.0	-90.0	3.4	0.0	0	0	0	Node
M3	1 - RHS150/100/10.0	-180.0	-2.8	-3.4	0	0	0	Node
M4	1 - RHS150/100/10.0	90.0	-3.4	0.0	0	0	0	Node



Cross-sections

Name	Material
1 - RHS150/100/10.0	Edit of S 235
5 - SHS160/160/16.0	S 355

Bolts

Name	Bolt assembly	Diameter [mm]	f_u [MPa]	Gross area [mm ²]
M12 10.9	M12 10.9	12	1000.0	113

Project:
Project no:
Author:

Load effects

Name	Member	N [kN]	Vy [kN]	Vz [kN]	Mx [kNm]	My [kNm]	Mz [kNm]
LE1	M1	160.0	0.0	0.0	0.0	3.8	0.0
	M2	-160.0	0.0	0.0	0.0	3.8	0.0
	M3	160.0	0.0	0.0	0.0	3.8	0.0
	M4	-160.0	0.0	0.0	0.0	3.8	0.0

Check

Rotational stiffness

Name	Comp.	Loads	Mj,Rd [kNm]	Sj,ini [MNm/rad]	Φ_c [mrad]	L [m]	Sj,R [MNm/rad]	Sj,P [MNm/rad]	Class.
M1	My	LE1	24.1	4.0	9.1	2.70	24.9	0.5	Semi-rigid

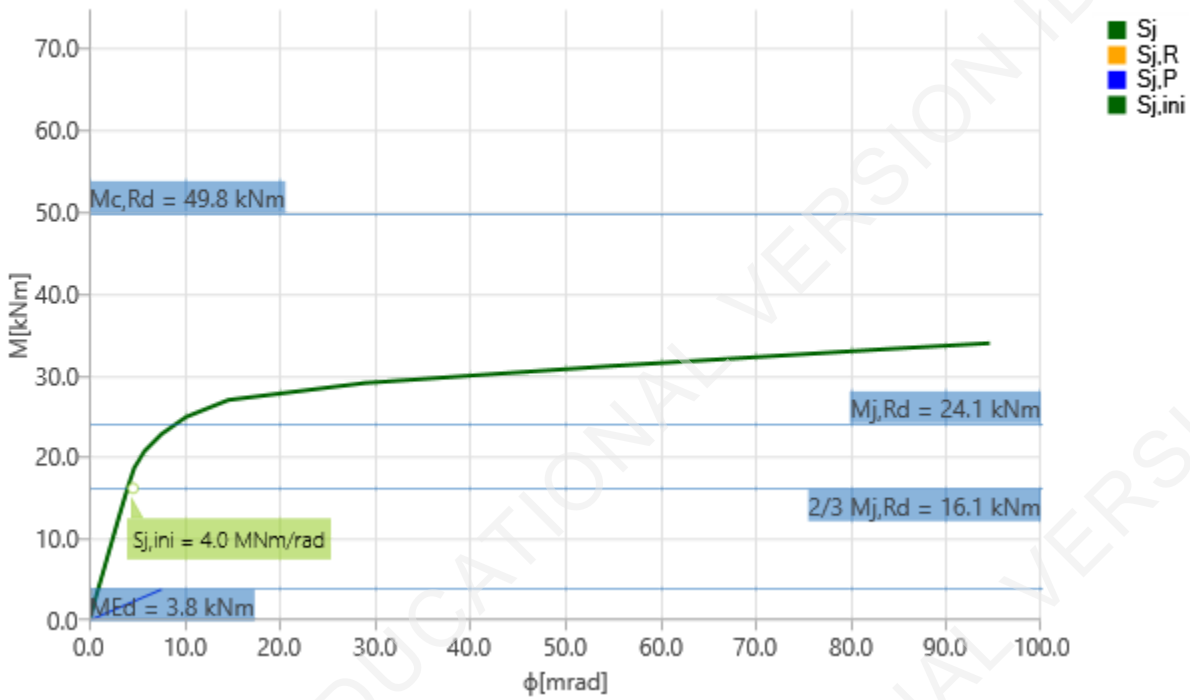
Secant rotational stiffness

Name	Comp.	Loads	M [kNm]	Sjs [MNm/rad]	Φ [mrad]
M1	My	LE1	3.8	4.0	0.9

Symbol explanation

$M_{j,Rd}$	Bending resistance
$S_{j,ini}$	Initial rotational stiffness
$S_{j,s}$	Secant rotational stiffness
Φ	Rotational deformation
Φ_c	Rotational capacity
$S_{j,R}$	Limit value - rigid joint
$S_{j,P}$	Limit value - nominally pinned joint

Project:
Project no:
Author:



Stiffness diagram My - ϕ , LE1

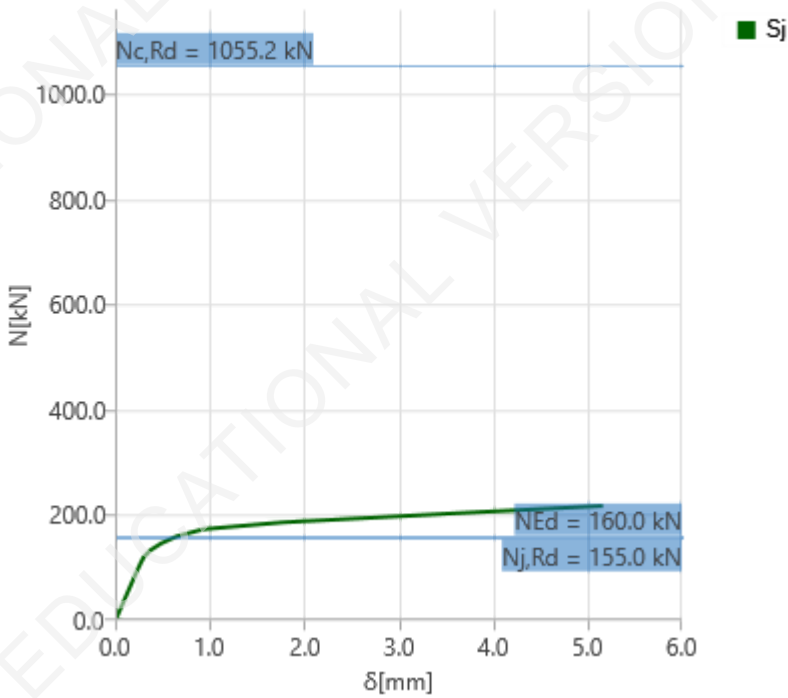
Axial stiffness

Name	Component	Loads	N [kN]	Nj,Rd [kN]	dx [mm]	St [MN/m]
M1	N	LE1	160.0	155.0	1	191

Symbol explanation

- $N_{j,Rd}$ Tension (compression) resistance
- S_t Secant axial stiffness
- δ Longitudinal deformation

Project:
Project no:
Author:



Stiffness diagram N - δ , LE1

Code settings

Item	Value	Unit	Reference
Y _{M0}	1.00	-	EN 1993-1-1: 6.1
Y _{M1}	1.00	-	EN 1993-1-1: 6.1
Y _{M2}	1.25	-	EN 1993-1-1: 6.1
Y _{M3}	1.25	-	EN 1993-1-8: 2.2
Y _C	1.50	-	EN 1992-1-1: 2.4.2.4
Y _{Inst}	1.20	-	EN 1992-4: Table 4.1
Joint coefficient β_j	0.67	-	EN 1993-1-8: 6.2.5
Effective area - influence of mesh size	0.10	-	
Friction coefficient - concrete	0.25	-	EN 1993-1-8
Friction coefficient in slip-resistance	0.30	-	EN 1993-1-8 tab 3.7
Limit plastic strain	0.05	-	EN 1993-1-5
Weld stress evaluation	Plastic redistribution		
Detailing	No		
Distance between bolts [d]	2.20	-	EN 1993-1-8: tab 3.3
Distance between bolts and edge [d]	1.20	-	EN 1993-1-8: tab 3.3
Concrete breakout resistance check	Both		EN 1992-4: 7.2.1.4 and 7.2.2.5
Use calculated a_b in bearing check.	Yes		EN 1993-1-8: tab 3.4
Cracked concrete	Yes		EN 1992-4
Local deformation check	No		CIDECT DG 1, 3 - 1.1
Local deformation limit	0.03	-	CIDECT DG 1, 3 - 1.1

Project:
Project no:
Author:

Item	Value	Unit	Reference
Geometrical nonlinearity (GMNA)	Yes		Analysis with large deformations for hollow section joints
Braced system	No		EN 1993-1-8: 5.2.2.5

E.4 SEMI-RIGID 3 CONNECTION

Project:
Project no:
Author:

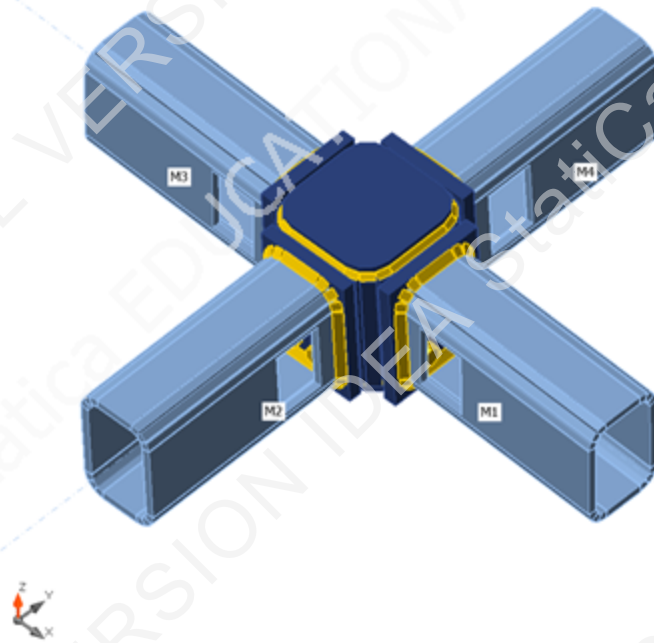
Project item Final design_Thesis

Design

Name Final design_Thesis
Description
Analysis Stress, strain/ loads in equilibrium

Beams and columns

Name	Cross-section	β - Direction [°]	γ - Pitch [°]	α - Rotation [°]	Offset ex [mm]	Offset ey [mm]	Offset ez [mm]	Forces in
M1	1 - RHS150/100/10.0	0.0	2.8	3.4	0	0	0	Node
M2	1 - RHS150/100/10.0	-90.0	3.4	0.0	0	0	0	Node
M3	1 - RHS150/100/10.0	-180.0	-2.8	-3.4	0	0	0	Node
M4	1 - RHS150/100/10.0	90.0	-3.4	0.0	0	0	0	Node



Cross-sections

Name	Material
1 - RHS150/100/10.0	Edit of S 235
5 - SHS160/160/16.0	S 355

Bolts

Name	Bolt assembly	Diameter [mm]	f_u [MPa]	Gross area [mm ²]
M12 10.9	M12 10.9	12	1000.0	113

Project:
Project no:
Author:

Load effects (forces in equilibrium)

Name	Member	N [kN]	Vy [kN]	Vz [kN]	Mx [kNm]	My [kNm]	Mz [kNm]
LE1	M1	159.0	0.0	0.0	0.0	1.7	0.0
	M2	-159.0	0.0	0.0	0.0	1.7	0.0
	M3	159.0	0.0	0.0	0.0	1.7	0.0
	M4	-159.0	0.0	0.0	0.0	1.7	0.0

Check

Summary

Name	Value	Status
Analysis	100.0%	OK
Plates	0.0 < 5.0%	OK
Bolts	81.7 < 100%	OK
Welds	69.1 < 100%	OK
Buckling	Not calculated	
GMNA	Calculated	

Plates

Name	Material	Thickness [mm]	Loads	σ_{Ed} [MPa]	ϵ_{pl} [%]	σ_{cEd} [MPa]	Status
M1	Edit of S 235	10.0	LE1	208.3	0.0	0.0	OK
M2	Edit of S 235	10.0	LE1	142.6	0.0	0.0	OK
M3	Edit of S 235	10.0	LE1	219.9	0.0	0.0	OK
M4	Edit of S 235	10.0	LE1	141.8	0.0	0.0	OK
SM1	S 355	16.0	LE1	339.5	0.0	120.8	OK
STIFF2	S 355	15.0	LE1	169.0	0.0	0.0	OK
STIFF3	S 355	15.0	LE1	159.0	0.0	0.0	OK
EP1	S 355	16.0	LE1	289.5	0.0	0.0	OK
EP2	S 355	16.0	LE1	46.3	0.0	59.5	OK
EP3	S 355	16.0	LE1	301.1	0.0	0.0	OK
EP4	S 355	16.0	LE1	45.7	0.0	59.5	OK

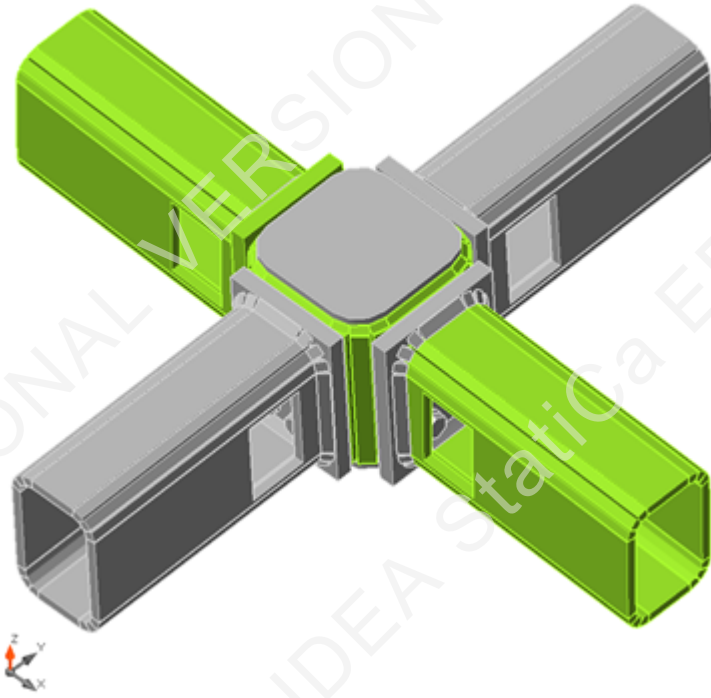
Design data

Material	f_y [MPa]	ϵ_{lim} [%]
Edit of S 235	235.0	5.0
S 355	355.0	5.0

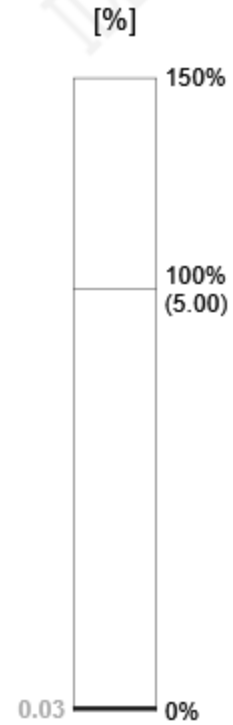
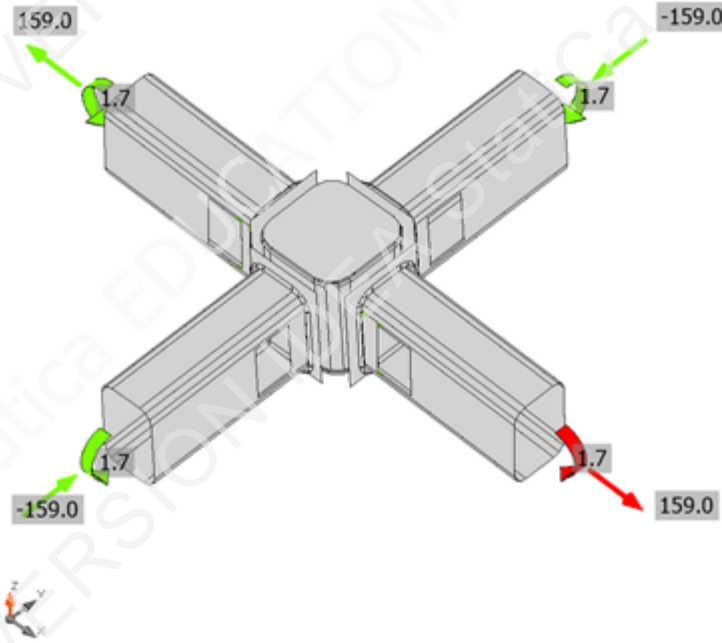
Symbol explanation

ϵ_{pl}	Strain
σ_{Ed}	Eq. stress
σ_{cEd}	Contact stress
f_y	Yield strength
ϵ_{lim}	Limit of plastic strain

Project:
Project no:
Author:

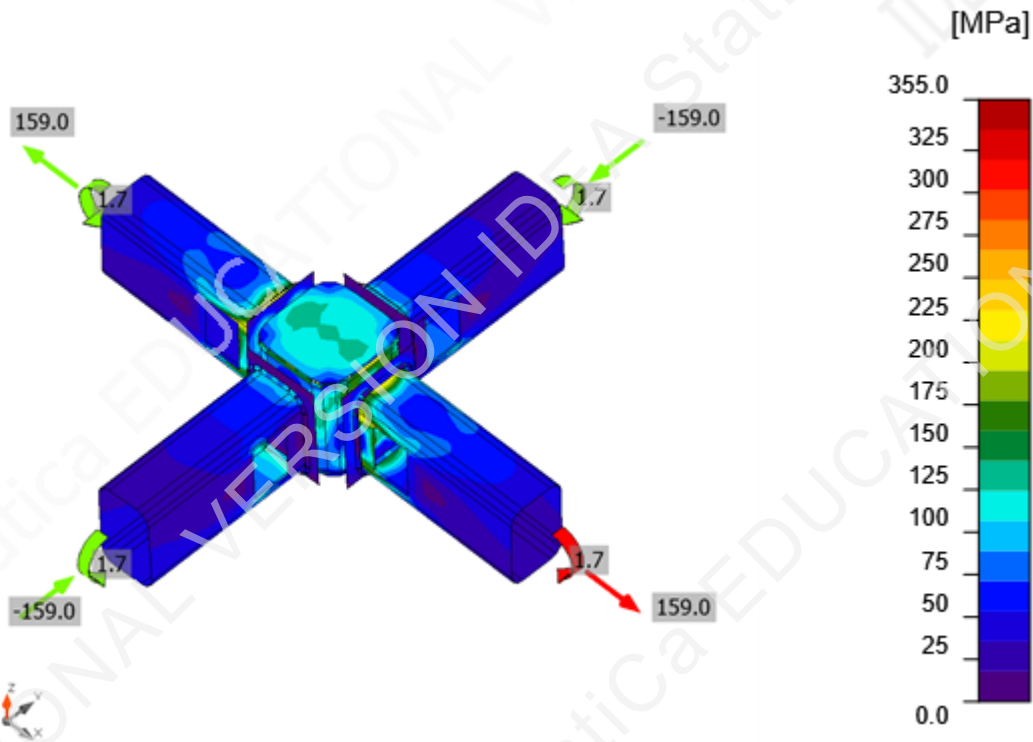


Overall check, LE1



Strain check, LE1

Project:
Project no:
Author:



Equivalent stress, LE1

Bolts

	Name	Loads	$F_{t,Ed}$ [kN]	V [kN]	$U_{t,t}$ [%]	$F_{b,Rd}$ [kN]	$U_{t,s}$ [%]	$U_{t,s}$ [%]	Status
	B5	LE1	49.1	2.1	81.2	188.2	6.2	64.3	OK
	B6	LE1	49.1	2.1	81.2	188.2	6.2	64.3	OK
	B7	LE1	30.2	1.8	50.0	174.1	5.3	41.0	OK
	B8	LE1	30.2	1.8	49.9	174.1	5.4	41.0	OK
	B13	LE1	3.7	0.8	6.1	156.6	2.2	6.6	OK
	B14	LE1	3.7	0.7	6.1	159.4	2.1	6.5	OK
	B15	LE1	3.6	0.8	5.9	140.3	2.5	6.7	OK
	B16	LE1	3.5	0.8	5.8	141.8	2.4	6.5	OK
	B21	LE1	49.4	1.9	81.7	174.1	5.5	63.9	OK
	B22	LE1	49.4	1.8	81.7	174.1	5.4	63.7	OK
	B23	LE1	29.9	2.1	49.4	188.2	6.2	41.5	OK
	B24	LE1	29.9	2.1	49.4	188.2	6.1	41.4	OK
	B29	LE1	3.7	0.8	6.1	161.7	2.3	6.6	OK
	B30	LE1	3.8	0.8	6.3	159.0	2.4	7.0	OK
	B31	LE1	3.5	0.7	5.8	138.7	2.2	6.3	OK
	B32	LE1	3.4	0.8	5.7	137.1	2.3	6.3	OK

Project:
Project no:
Author:

Design data

Name	$F_{t,Rd}$ [kN]	$B_{p,Rd}$ [kN]	$F_{v,Rd}$ [kN]
M12 10.9 - 1	60.5	271.9	33.6

Symbol explanation

$F_{t,Rd}$	Bolt tension resistance EN 1993-1-8 tab. 3.4
$F_{t,Ed}$	Tension force
$B_{p,Rd}$	Punching shear resistance
V	Resultant of shear forces V_y, V_z in bolt
$F_{v,Rd}$	Bolt shear resistance EN_1993-1-8 table 3.4
$F_{b,Rd}$	Plate bearing resistance EN 1993-1-8 tab. 3.4
U_t	Utilization in tension
U_s	Utilization in shear

Welds (Plastic redistribution)

Item	Edge	Material	Throat th. [mm]	Length [mm]	Loads	$\sigma_{w,Ed}$ [MPa]	ϵ_{pl} [%]	σ_{\perp} [MPa]	τ_{\parallel} [MPa]	τ_{\perp} [MPa]	U_t [%]	U_c [%]	Status
STIFF2	SM1	S 355	▲4.0▲	519	LE1	275.2	0.0	243.9	10.2	72.9	69.1	40.1	OK
STIFF3	SM1	S 355	▲4.0▲	519	LE1	235.3	0.0	208.2	-6.7	63.0	59.0	36.9	OK
EP1	M1	Edit of S 235	▲6.0▲	425	LE1	158.6	0.0	67.2	69.5	45.2	44.1	23.8	OK
EP2	M2	Edit of S 235	▲6.0▲	424	LE1	128.9	0.0	-52.5	-6.2	-67.7	35.8	13.3	OK
EP3	M3	Edit of S 235	▲6.0▲	425	LE1	159.7	0.0	67.5	-70.5	44.9	44.3	24.1	OK
EP4	M4	Edit of S 235	▲6.0▲	424	LE1	128.3	0.0	-52.5	5.6	-67.3	35.6	13.3	OK
		S 355	▲4.0▲	519	LE1	218.4	0.0	-64.6	3.6	-120.4	50.1	33.6	OK
		S 355	▲4.0▲	519	LE1	175.5	0.0	-61.2	-0.5	-95.0	40.3	31.4	OK
		Edit of S 235	▲6.0▲	425	LE1	69.7	0.0	7.3	-6.1	-39.5	19.4	9.8	OK
		Edit of S 235	▲6.0▲	424	LE1	137.1	0.0	-79.5	-3.1	64.4	38.1	14.8	OK
		Edit of S 235	▲6.0▲	425	LE1	69.8	0.0	3.0	16.5	-36.7	19.4	9.4	OK
		Edit of S 235	▲6.0▲	424	LE1	136.6	0.0	-78.9	3.6	64.3	37.9	14.8	OK

Design data

	β_w [-]	$\sigma_{w,Rd}$ [MPa]	0.9σ [MPa]
S 355	0.90	435.6	352.8
Edit of S 235	0.80	360.0	259.2

Project:
Project no:
Author:

Symbol explanation

ϵ_{pl}	Strain
$\sigma_{w,Ed}$	Equivalent stress
$\sigma_{w,Rd}$	Equivalent stress resistance
σ_{\perp}	Perpendicular stress
$\tau_{ }$	Shear stress parallel to weld axis
τ_{\perp}	Shear stress perpendicular to weld axis
0.9σ	Perpendicular stress resistance - $0.9 \cdot f_u / \gamma_{M2}$
β_w	Corelation factor EN 1993-1-8 tab. 4.1
U_t	Utilization
U_{tc}	Weld capacity utilization

Buckling

Buckling analysis was not calculated.

Code settings

Item	Value	Unit	Reference
Y _{M0}	1.00	-	EN 1993-1-1: 6.1
Y _{M1}	1.00	-	EN 1993-1-1: 6.1
Y _{M2}	1.25	-	EN 1993-1-1: 6.1
Y _{M3}	1.25	-	EN 1993-1-8: 2.2
Y _C	1.50	-	EN 1992-1-1: 2.4.2.4
Y _{Inst}	1.20	-	EN 1992-4: Table 4.1
Joint coefficient β_j	0.67	-	EN 1993-1-8: 6.2.5
Effective area - influence of mesh size	0.10	-	
Friction coefficient - concrete	0.25	-	EN 1993-1-8
Friction coefficient in slip-resistance	0.30	-	EN 1993-1-8 tab 3.7
Limit plastic strain	0.05	-	EN 1993-1-5
Weld stress evaluation	Plastic redistribution		
Detailing	No		
Distance between bolts [d]	2.20	-	EN 1993-1-8: tab 3.3
Distance between bolts and edge [d]	1.20	-	EN 1993-1-8: tab 3.3
Concrete breakout resistance check	Both		EN 1992-4: 7.2.1.4 and 7.2.2.5
Use calculated a_b in bearing check.	Yes		EN 1993-1-8: tab 3.4
Cracked concrete	Yes		EN 1992-4
Local deformation check	No		CIDECT DG 1, 3 - 1.1
Local deformation limit	0.03	-	CIDECT DG 1, 3 - 1.1
Geometrical nonlinearity (GMNA)	Yes		Analysis with large deformations for hollow section joints
Braced system	No		EN 1993-1-8: 5.2.2.5

Project:
 Project no:
 Author:

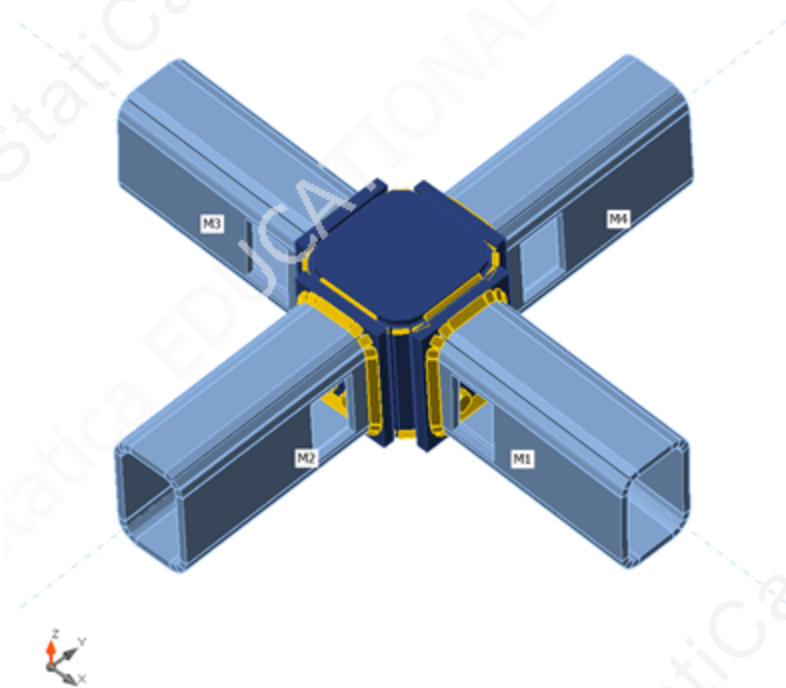
Project item Final design_Thesis

Design

Name Final design_Thesis
 Description
 Analysis Stiffness

Beams and columns

Name	Cross-section	β - Direction [°]	γ - Pitch [°]	α - Rotation [°]	Offset ex [mm]	Offset ey [mm]	Offset ez [mm]	Forces in
M1	1 - RHS150/100/10.0	0.0	2.8	3.4	0	0	0	Node
M2	1 - RHS150/100/10.0	-90.0	3.4	0.0	0	0	0	Node
M3	1 - RHS150/100/10.0	-180.0	-2.8	-3.4	0	0	0	Node
M4	1 - RHS150/100/10.0	90.0	-3.4	0.0	0	0	0	Node



Cross-sections

Name	Material
1 - RHS150/100/10.0	Edit of S 235
5 - SHS160/160/16.0	S 355

Bolts

Name	Bolt assembly	Diameter [mm]	f_u [MPa]	Gross area [mm ²]
M12 10.9	M12 10.9	12	1000.0	113

Project:
Project no:
Author:

Load effects

Name	Member	N [kN]	Vy [kN]	Vz [kN]	Mx [kNm]	My [kNm]	Mz [kNm]
LE1	M1	159.0	0.0	0.0	0.0	1.7	0.0
	M2	-159.0	0.0	0.0	0.0	1.7	0.0
	M3	159.0	0.0	0.0	0.0	1.7	0.0
	M4	-159.0	0.0	0.0	0.0	1.7	0.0

Check

Rotational stiffness

Name	Comp.	Loads	Mj,Rd [kNm]	Sj,ini [MNm/rad]	Φ_c [mrad]	L [m]	Sj,R [MNm/rad]	Sj,P [MNm/rad]	Class.
M1	My	LE1	10.5	1.4	11.5	2.70	24.9	0.5	Semi-rigid

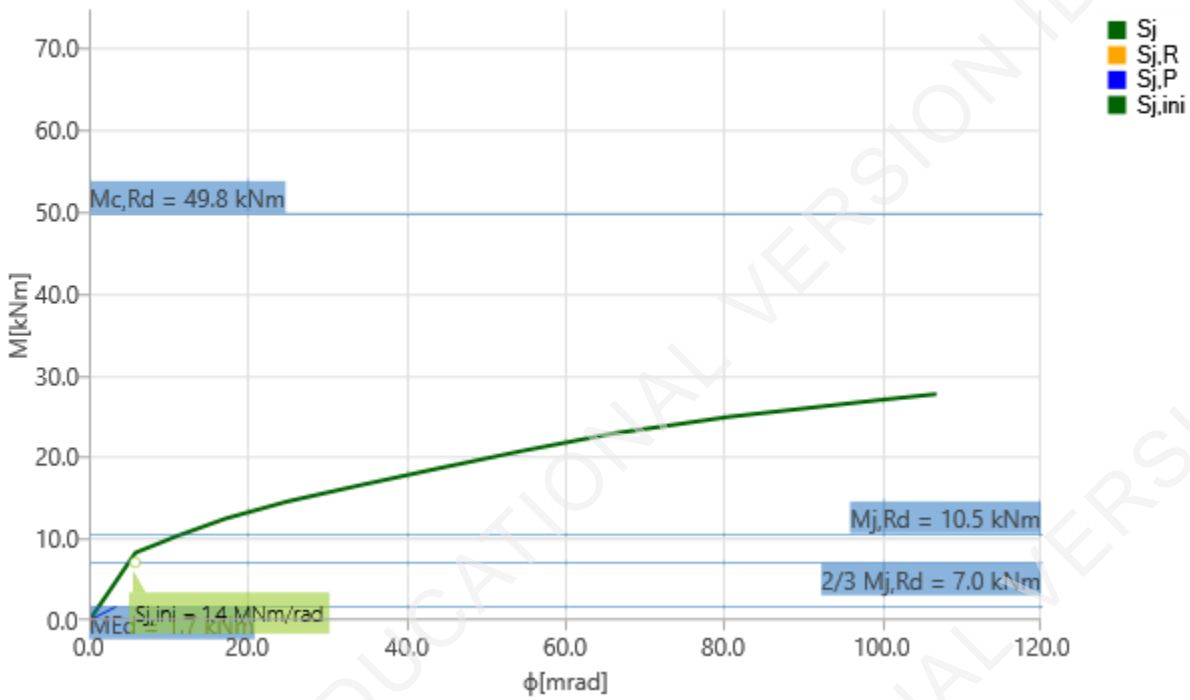
Secant rotational stiffness

Name	Comp.	Loads	M [kNm]	Sjs [MNm/rad]	Φ [mrad]
M1	My	LE1	1.7	1.4	1.2

Symbol explanation

$M_{j,Rd}$	Bending resistance
$S_{j,ini}$	Initial rotational stiffness
$S_{j,s}$	Secant rotational stiffness
Φ	Rotational deformation
Φ_c	Rotational capacity
$S_{j,R}$	Limit value - rigid joint
$S_{j,P}$	Limit value - nominally pinned joint

Project:
 Project no:
 Author:



Stiffness diagram $M_y - \phi_y$, LE1

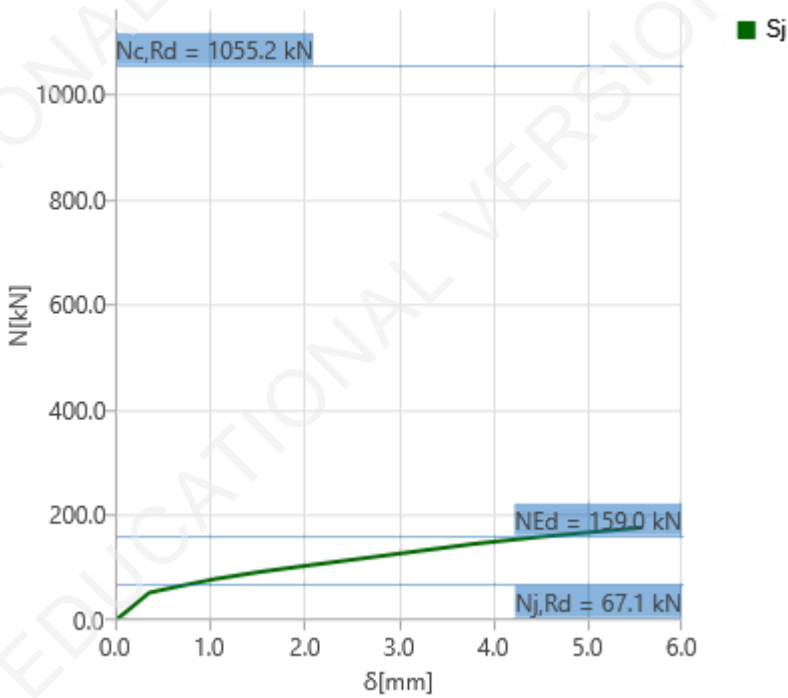
Axial stiffness

Name	Component	Loads	N [kN]	Nj,Rd [kN]	dx [mm]	St [MN/m]
M1	N	LE1	159.0	67.1	1	160

Symbol explanation

- $N_{j,Rd}$ Tension (compression) resistance
- S_t Secant axial stiffness
- δ Longitudinal deformation

Project:
Project no:
Author:



Stiffness diagram N - δ , LE1

Code settings

Item	Value	Unit	Reference
Y _{M0}	1.00	-	EN 1993-1-1: 6.1
Y _{M1}	1.00	-	EN 1993-1-1: 6.1
Y _{M2}	1.25	-	EN 1993-1-1: 6.1
Y _{M3}	1.25	-	EN 1993-1-8: 2.2
Y _C	1.50	-	EN 1992-1-1: 2.4.2.4
Y _{Inst}	1.20	-	EN 1992-4: Table 4.1
Joint coefficient β_j	0.67	-	EN 1993-1-8: 6.2.5
Effective area - influence of mesh size	0.10	-	
Friction coefficient - concrete	0.25	-	EN 1993-1-8
Friction coefficient in slip-resistance	0.30	-	EN 1993-1-8 tab 3.7
Limit plastic strain	0.05	-	EN 1993-1-5
Weld stress evaluation	Plastic redistribution		
Detailing	No		
Distance between bolts [d]	2.20	-	EN 1993-1-8: tab 3.3
Distance between bolts and edge [d]	1.20	-	EN 1993-1-8: tab 3.3
Concrete breakout resistance check	Both		EN 1992-4: 7.2.1.4 and 7.2.2.5
Use calculated a_b in bearing check.	Yes		EN 1993-1-8: tab 3.4
Cracked concrete	Yes		EN 1992-4
Local deformation check	No		CIDECT DG 1, 3 - 1.1
Local deformation limit	0.03	-	CIDECT DG 1, 3 - 1.1

Project:
Project no:
Author:

Item	Value	Unit	Reference
Geometrical nonlinearity (GMNA)	Yes		Analysis with large deformations for hollow section joints
Braced system	No		EN 1993-1-8: 5.2.2.5

E.5 PINNED CONNECTION

Project:
 Project no:
 Author:

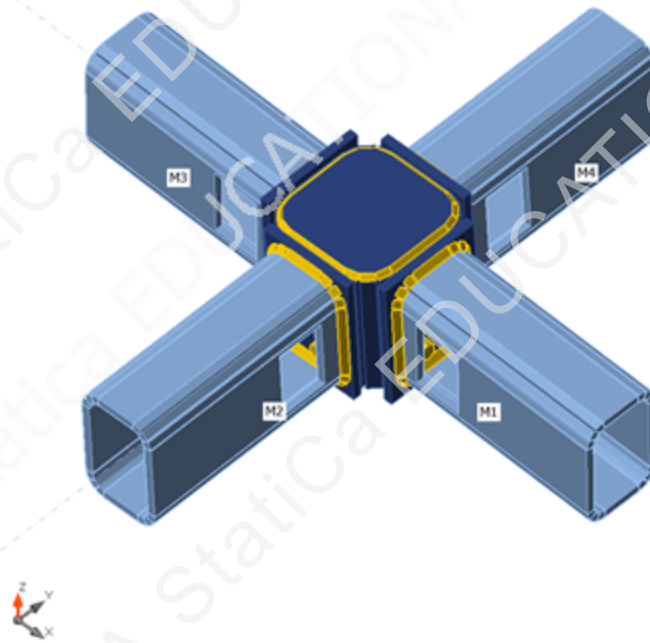
Project item Final design_Thesis

Design

Name Final design_Thesis
 Description
 Analysis Stress, strain/ loads in equilibrium

Beams and columns

Name	Cross-section	β - Direction [°]	γ - Pitch [°]	α - Rotation [°]	Offset ex [mm]	Offset ey [mm]	Offset ez [mm]	Forces in
M1	1 - RHS150/100/10.0	0.0	2.8	3.4	0	0	0	Node
M2	1 - RHS150/100/10.0	-90.0	3.4	0.0	0	0	0	Node
M3	1 - RHS150/100/10.0	-180.0	-2.8	-3.4	0	0	0	Node
M4	1 - RHS150/100/10.0	90.0	-3.4	0.0	0	0	0	Node



Cross-sections

Name	Material
1 - RHS150/100/10.0	Edit of S 235
5 - SHS160/160/16.0	S 355

Bolts

Name	Bolt assembly	Diameter [mm]	f_u [MPa]	Gross area [mm ²]
M12 8.8	M12 8.8	12	800.0	113

Project:
Project no:
Author:

Load effects (forces in equilibrium)

Name	Member	N [kN]	Vy [kN]	Vz [kN]	Mx [kNm]	My [kNm]	Mz [kNm]
LE1	M1	84.9	0.0	0.0	0.0	1.2	0.0
	M2	-84.9	0.0	0.0	0.0	1.2	0.0
	M3	84.9	0.0	0.0	0.0	1.2	0.0
	M4	-84.9	0.0	0.0	0.0	1.2	0.0

Check

Summary

Name	Value	Status
Analysis	100.0%	OK
Plates	0.0 < 5.0%	OK
Bolts	66.7 < 100%	OK
Welds	43.8 < 100%	OK
Buckling	Not calculated	
GMNA	Calculated	

Plates

Name	Material	Thickness [mm]	Loads	σ_{Ed} [MPa]	ϵ_{pl} [%]	σ_{cEd} [MPa]	Status
M1	Edit of S 235	10.0	LE1	217.6	0.0	0.0	OK
M2	Edit of S 235	10.0	LE1	106.9	0.0	0.0	OK
M3	Edit of S 235	10.0	LE1	197.0	0.0	0.0	OK
M4	Edit of S 235	10.0	LE1	106.5	0.0	0.0	OK
SM1	S 355	16.0	LE1	263.4	0.0	77.7	OK
STIFF2	S 355	5.0	LE1	134.2	0.0	0.0	OK
STIFF3	S 355	5.0	LE1	143.4	0.0	0.0	OK
EP1	S 355	10.0	LE1	325.1	0.0	23.3	OK
EP2	S 355	10.0	LE1	49.3	0.0	37.3	OK
EP3	S 355	10.0	LE1	336.3	0.0	20.9	OK
EP4	S 355	10.0	LE1	49.4	0.0	37.3	OK

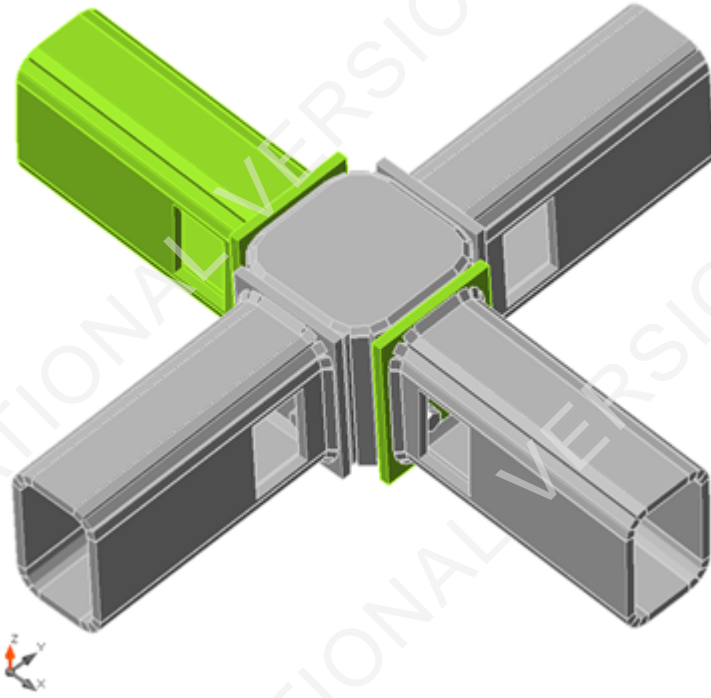
Design data

Material	f_y [MPa]	ϵ_{lim} [%]
Edit of S 235	235.0	5.0
S 355	355.0	5.0

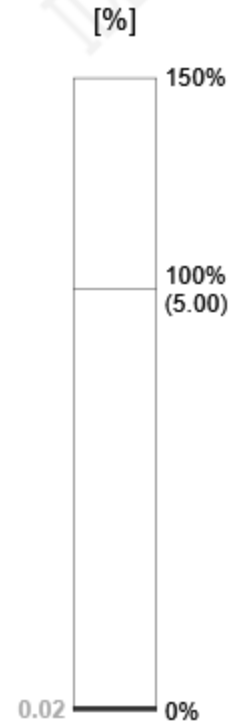
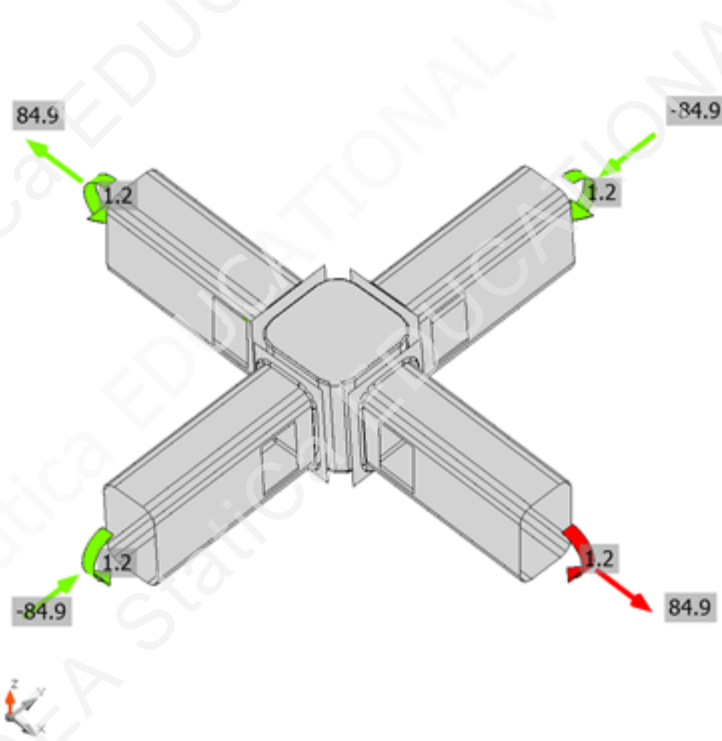
Symbol explanation

ϵ_{pl}	Strain
σ_{Ed}	Eq. stress
σ_{cEd}	Contact stress
f_y	Yield strength
ϵ_{lim}	Limit of plastic strain

Project:
Project no:
Author:

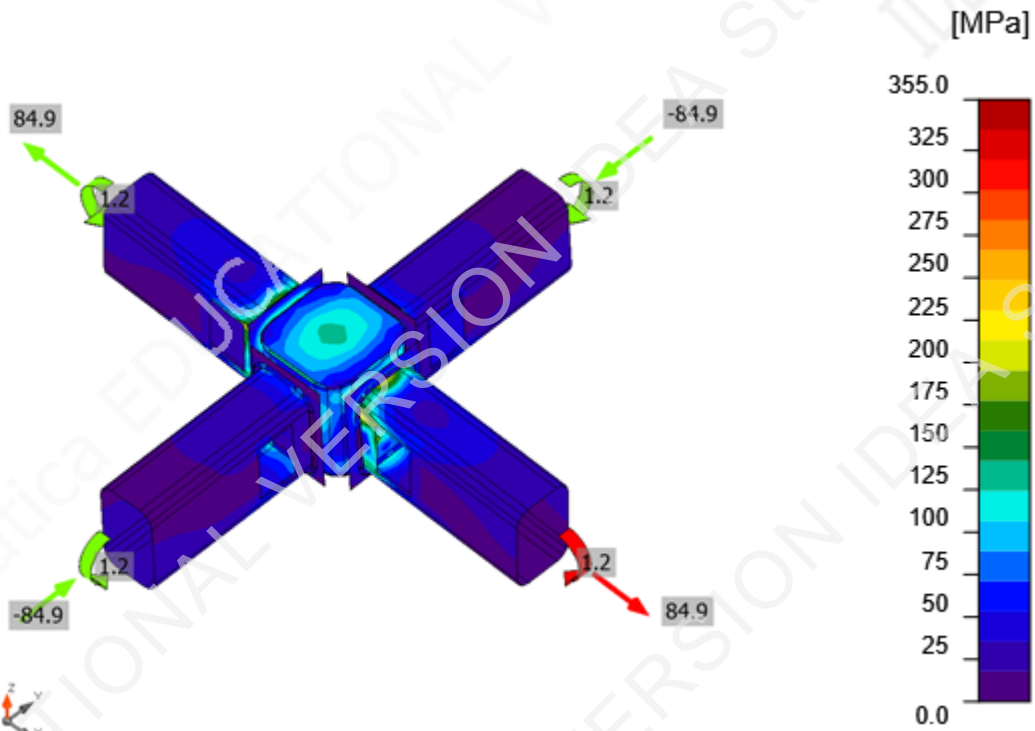


Overall check, LE1



Strain check, LE1

Project:
 Project no:
 Author:



Equivalent stress, LE1

Bolts

	Name	Loads	$F_{t,Ed}$ [kN]	V [kN]	U_t [%]	$F_{b,Rd}$ [kN]	U_s [%]	U_{ts} [%]	Status
	B5	LE1	32.1	0.8	66.4	117.6	2.4	49.8	OK
	B6	LE1	16.1	1.3	33.2	117.6	3.9	27.7	OK
	B7	LE1	32.2	0.8	66.5	117.6	2.6	50.1	OK
	B8	LE1	16.1	1.3	33.2	117.6	4.0	27.8	OK
	B13	LE1	2.9	0.3	6.0	109.5	1.0	5.3	OK
	B14	LE1	2.7	0.3	5.5	107.0	1.1	5.0	OK
	B15	LE1	2.6	0.4	5.4	106.9	1.1	5.0	OK
	B16	LE1	2.9	0.3	6.0	109.0	0.9	5.2	OK
	B21	LE1	16.0	0.8	33.1	117.6	2.5	26.1	OK
	B22	LE1	32.3	1.3	66.7	117.6	4.0	51.6	OK
	B23	LE1	16.0	0.8	33.2	117.6	2.4	26.1	OK
	B24	LE1	32.3	1.3	66.7	117.6	4.0	51.6	OK
	B29	LE1	2.9	0.3	6.0	113.1	1.1	5.4	OK
	B30	LE1	2.7	0.3	5.5	104.0	1.0	4.9	OK
	B31	LE1	2.6	0.3	5.4	104.0	1.0	4.9	OK
	B32	LE1	2.9	0.3	6.0	112.7	1.0	5.3	OK

Project:
Project no:
Author:

Design data

Name	$F_{t,Rd}$ [kN]	$B_{p,Rd}$ [kN]	$F_{v,Rd}$ [kN]
M12 8.8 - 1	48.4	147.8	32.3

Symbol explanation

$F_{t,Rd}$	Bolt tension resistance EN 1993-1-8 tab. 3.4
$F_{t,Ed}$	Tension force
$B_{p,Rd}$	Punching shear resistance
V	Resultant of shear forces V_y, V_z in bolt
$F_{v,Rd}$	Bolt shear resistance EN_1993-1-8 table 3.4
$F_{b,Rd}$	Plate bearing resistance EN 1993-1-8 tab. 3.4
U_t	Utilization in tension
U_t_s	Utilization in shear

Welds (Plastic redistribution)

Item	Edge	Material	Throat th. [mm]	Length [mm]	Loads	$\sigma_{w,Ed}$ [MPa]	ϵ_{pl} [%]	σ_{\perp} [MPa]	τ_{\parallel} [MPa]	τ_{\perp} [MPa]	U_t [%]	$U_{t,c}$ [%]	Status
STIFF2	SM1	S 355	▲4.0	519	LE1	137.2	0.0	-71.2	-0.9	67.7	31.5	19.9	OK
STIFF3	SM1	S 355	▲4.0	519	LE1	168.8	0.0	-87.3	1.3	83.4	38.8	20.2	OK
EP1	M1	Edit of S 235	▲5.0▲	425	LE1	144.7	0.0	60.6	66.9	35.7	40.2	22.6	OK
EP2	M2	Edit of S 235	▲5.0▲	424	LE1	94.4	0.0	-33.2	12.4	-49.5	26.2	8.5	OK
EP3	M3	Edit of S 235	▲5.0▲	425	LE1	157.8	0.0	58.8	-76.7	35.5	43.8	23.3	OK
EP4	M4	Edit of S 235	▲5.0▲	424	LE1	94.4	0.0	-33.4	-12.5	-49.4	26.2	8.5	OK
		Edit of S 235	▲5.0▲	425	LE1	59.3	0.0	-12.1	8.9	-32.3	16.5	8.2	OK
		Edit of S 235	▲5.0▲	424	LE1	115.2	0.0	-69.3	-0.4	53.1	32.0	11.1	OK
		Edit of S 235	▲5.0▲	425	LE1	61.0	0.0	-12.1	-1.9	-34.5	16.9	8.2	OK
		Edit of S 235	▲5.0▲	424	LE1	115.0	0.0	-69.2	-0.6	53.0	31.9	11.1	OK

Design data

	β_w [-]	$\sigma_{w,Rd}$ [MPa]	0.9σ [MPa]
S 355	0.90	435.6	352.8
Edit of S 235	0.80	360.0	259.2

Project:
Project no:
Author:

Symbol explanation

ϵ_{pl}	Strain
$\sigma_{w,Ed}$	Equivalent stress
$\sigma_{w,Rd}$	Equivalent stress resistance
σ_{\perp}	Perpendicular stress
τ_{\parallel}	Shear stress parallel to weld axis
τ_{\perp}	Shear stress perpendicular to weld axis
0.9σ	Perpendicular stress resistance - $0.9 \cdot f_u / \gamma_{M2}$
β_w	Corelation factor EN 1993-1-8 tab. 4.1
U_t	Utilization
U_{tc}	Weld capacity utilization

Buckling

Buckling analysis was not calculated.

Code settings

Item	Value	Unit	Reference
Y _{M0}	1.00	-	EN 1993-1-1: 6.1
Y _{M1}	1.00	-	EN 1993-1-1: 6.1
Y _{M2}	1.25	-	EN 1993-1-1: 6.1
Y _{M3}	1.25	-	EN 1993-1-8: 2.2
Y _C	1.50	-	EN 1992-1-1: 2.4.2.4
Y _{Inst}	1.20	-	EN 1992-4: Table 4.1
Joint coefficient β_j	0.67	-	EN 1993-1-8: 6.2.5
Effective area - influence of mesh size	0.10	-	
Friction coefficient - concrete	0.25	-	EN 1993-1-8
Friction coefficient in slip-resistance	0.30	-	EN 1993-1-8 tab 3.7
Limit plastic strain	0.05	-	EN 1993-1-5
Weld stress evaluation	Plastic redistribution		
Detailing	No		
Distance between bolts [d]	2.20	-	EN 1993-1-8: tab 3.3
Distance between bolts and edge [d]	1.20	-	EN 1993-1-8: tab 3.3
Concrete breakout resistance check	Both		EN 1992-4: 7.2.1.4 and 7.2.2.5
Use calculated a_b in bearing check.	Yes		EN 1993-1-8: tab 3.4
Cracked concrete	Yes		EN 1992-4
Local deformation check	No		CIDECT DG 1, 3 - 1.1
Local deformation limit	0.03	-	CIDECT DG 1, 3 - 1.1
Geometrical nonlinearity (GMNA)	Yes		Analysis with large deformations for hollow section joints
Braced system	No		EN 1993-1-8: 5.2.2.5

Project:
Project no:
Author:

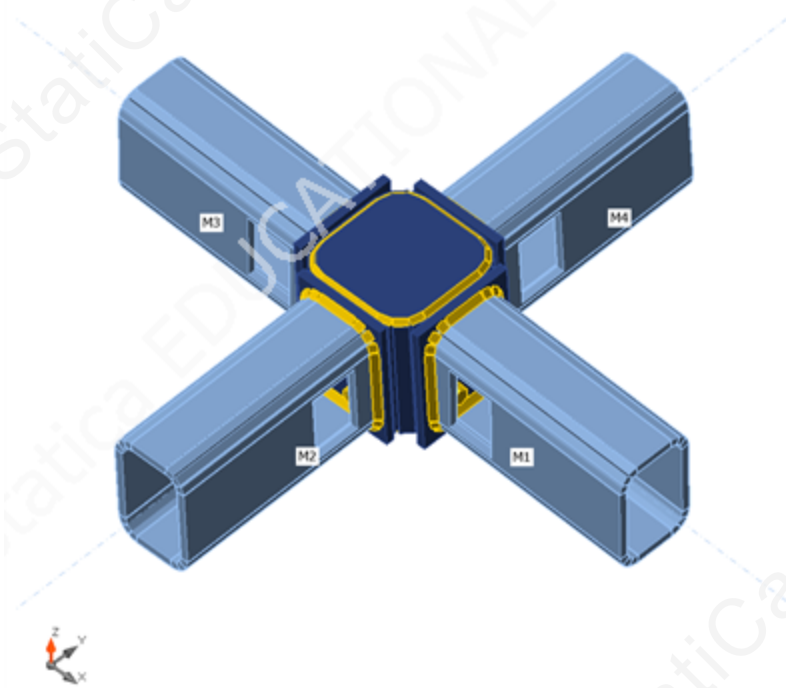
Project item Final design_Thesis

Design

Name Final design_Thesis
Description
Analysis Stiffness

Beams and columns

Name	Cross-section	β - Direction [°]	γ - Pitch [°]	α - Rotation [°]	Offset ex [mm]	Offset ey [mm]	Offset ez [mm]	Forces in
M1	1 - RHS150/100/10.0	0.0	2.8	3.4	0	0	0	Node
M2	1 - RHS150/100/10.0	-90.0	3.4	0.0	0	0	0	Node
M3	1 - RHS150/100/10.0	-180.0	-2.8	-3.4	0	0	0	Node
M4	1 - RHS150/100/10.0	90.0	-3.4	0.0	0	0	0	Node



Cross-sections

Name	Material
1 - RHS150/100/10.0	Edit of S 235
5 - SHS160/160/16.0	S 355

Bolts

Name	Bolt assembly	Diameter [mm]	f_u [MPa]	Gross area [mm ²]
M12 8.8	M12 8.8	12	800.0	113

Project:
Project no:
Author:

Load effects

Name	Member	N [kN]	Vy [kN]	Vz [kN]	Mx [kNm]	My [kNm]	Mz [kNm]
LE1	M1	84.9	0.0	0.0	0.0	1.2	0.0
	M2	-84.9	0.0	0.0	0.0	1.2	0.0
	M3	84.9	0.0	0.0	0.0	1.2	0.0
	M4	-84.9	0.0	0.0	0.0	1.2	0.0

Check

Rotational stiffness

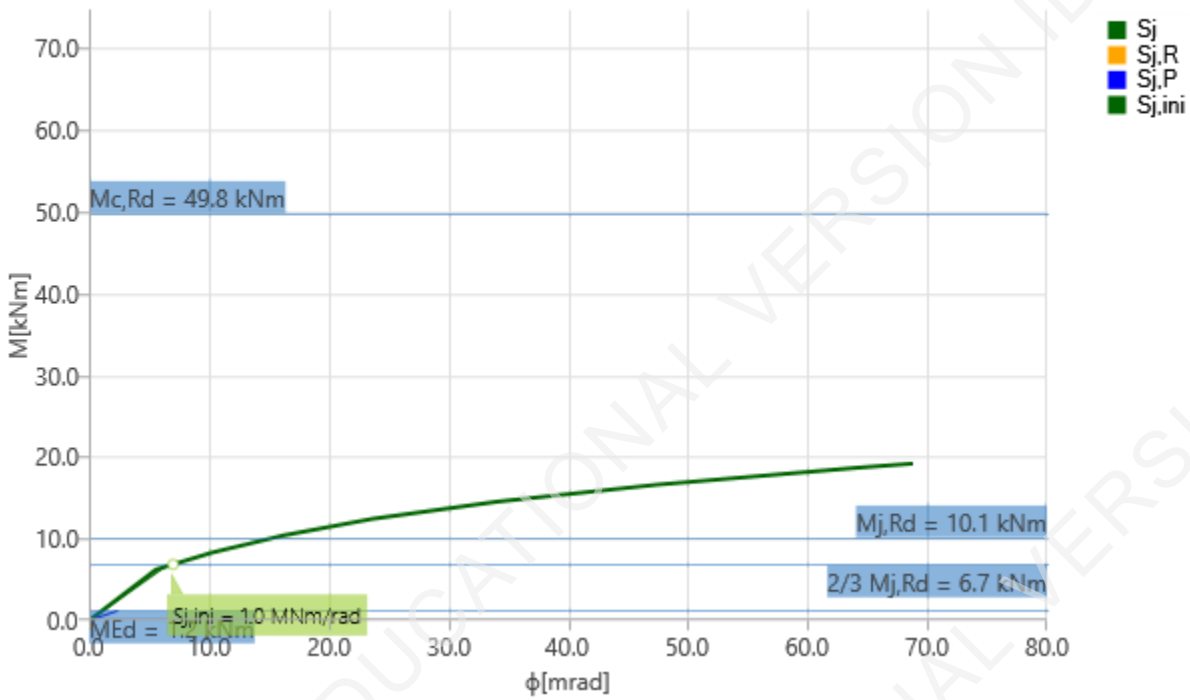
Name	Comp.	Loads	Mj,Rd [kNm]	Sj,ini [MNm/rad]	Φ_c [mrad]	L [m]	Sj,R [MNm/rad]	Sj,P [MNm/rad]	Class.
M1	My	LE1	10.1	1.0	15.2	2.70	24.9	0.5	Semi-rigid

Secant rotational stiffness

Name	Comp.	Loads	M [kNm]	Sjs [MNm/rad]	Φ [mrad]
M1	My	LE1	1.2	1.1	1.1

Symbol explanation

$M_{j,Rd}$	Bending resistance
$S_{j,ini}$	Initial rotational stiffness
$S_{j,s}$	Secant rotational stiffness
Φ	Rotational deformation
Φ_c	Rotational capacity
$S_{j,R}$	Limit value - rigid joint
$S_{j,P}$	Limit value - nominally pinned joint



Stiffness diagram $M_y - \phi_y$, LE1

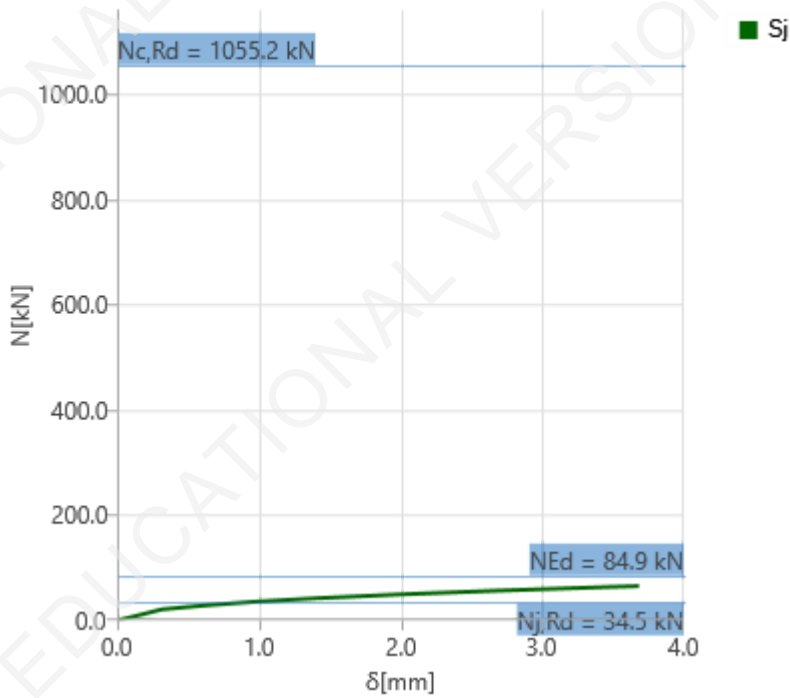
Axial stiffness

Name	Component	Loads	N [kN]	$N_{j,Rd}$ [kN]	dx [mm]	S_t [MN/m]
M1	N	LE1	84.9	34.5	1	130

Symbol explanation

$N_{j,Rd}$	Tension (compression) resistance
S_t	Secant axial stiffness
δ	Longitudinal deformation

Project:
Project no:
Author:



Stiffness diagram N - δ , LE1

Code settings

Item	Value	Unit	Reference
Y _{M0}	1.00	-	EN 1993-1-1: 6.1
Y _{M1}	1.00	-	EN 1993-1-1: 6.1
Y _{M2}	1.25	-	EN 1993-1-1: 6.1
Y _{M3}	1.25	-	EN 1993-1-8: 2.2
Y _C	1.50	-	EN 1992-1-1: 2.4.2.4
Y _{Inst}	1.20	-	EN 1992-4: Table 4.1
Joint coefficient β_j	0.67	-	EN 1993-1-8: 6.2.5
Effective area - influence of mesh size	0.10	-	
Friction coefficient - concrete	0.25	-	EN 1993-1-8
Friction coefficient in slip-resistance	0.30	-	EN 1993-1-8 tab 3.7
Limit plastic strain	0.05	-	EN 1993-1-5
Weld stress evaluation	Plastic redistribution		
Detailing	No		
Distance between bolts [d]	2.20	-	EN 1993-1-8: tab 3.3
Distance between bolts and edge [d]	1.20	-	EN 1993-1-8: tab 3.3
Concrete breakout resistance check	Both		EN 1992-4: 7.2.1.4 and 7.2.2.5
Use calculated a_b in bearing check.	Yes		EN 1993-1-8: tab 3.4
Cracked concrete	Yes		EN 1992-4
Local deformation check	No		CIDECT DG 1, 3 - 1.1
Local deformation limit	0.03	-	CIDECT DG 1, 3 - 1.1

Project:
Project no:
Author:

Item	Value	Unit	Reference
Geometrical nonlinearity (GMNA)	Yes		Analysis with large deformations for hollow section joints
Braced system	No		EN 1993-1-8: 5.2.2.5

F | APPENDIX F. OPTIMAL CONNECTION DESIGN

F.1 CONNECTION DESIGN WITH OPTIMAL CROSS SECTION AND FULLY RIGID STIFFNESS

Project:
Project no:
Author:

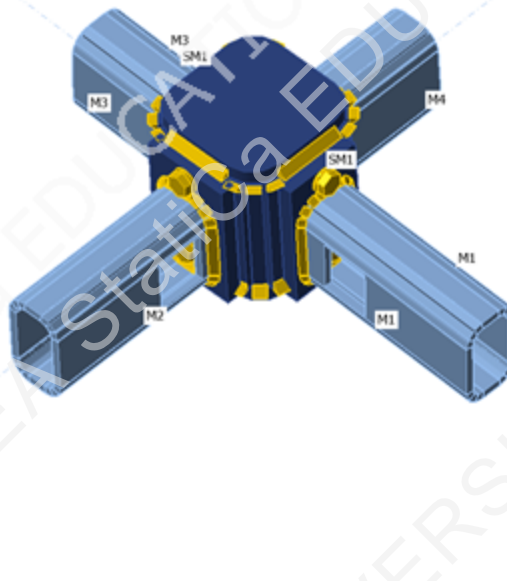
Project item Final design_Thesis

Design

Name Final design_Thesis
Description
Analysis Stress, strain/ loads in equilibrium

Beams and columns

Name	Cross-section	β - Direction [°]	γ - Pitch [°]	α - Rotation [°]	Offset ex [mm]	Offset ey [mm]	Offset ez [mm]	Forces in
M1	1 - RHS100/60/8.0	0.0	2.8	3.4	0	0	0	Node
M2	1 - RHS100/60/8.0	-90.0	3.4	0.0	0	0	0	Node
M3	1 - RHS100/60/8.0	-180.0	-2.8	-3.4	0	0	0	Node
M4	1 - RHS100/60/8.0	90.0	-3.4	0.0	0	0	0	Node



Cross-sections

Name	Material
1 - RHS100/60/8.0	Edit of S 235
7 - 120x120(RHS140x140)	S 355

Bolts

Name	Bolt assembly	Diameter [mm]	f_u [MPa]	Gross area [mm ²]
M12 10.9	M12 10.9	12	1000.0	113

Project:
Project no:
Author:

Load effects (forces in equilibrium)

Name	Member	N [kN]	Vy [kN]	Vz [kN]	Mx [kNm]	My [kNm]	Mz [kNm]
LE1	M1	117.0	0.0	0.0	0.0	3.1	0.0
	M2	-117.0	0.0	0.0	0.0	3.1	0.0
	M3	117.0	0.0	0.0	0.0	3.1	0.0
	M4	-117.0	0.0	0.0	0.0	3.1	0.0

Check

Summary

Name	Value	Status
Analysis	100.0%	OK
Plates	0.1 < 5.0%	OK
Bolts	73.3 < 100%	OK
Welds	98.0 < 100%	OK
Buckling	Not calculated	
GMNA	Calculated	

Plates

Name	Material	Thickness [mm]	Loads	σ_{Ed} [MPa]	ϵ_{pl} [%]	σ_{cEd} [MPa]	Status
M1	Edit of S 235	8.0	LE1	235.1	0.1	0.0	OK
M2	Edit of S 235	8.0	LE1	227.8	0.0	0.0	OK
M3	Edit of S 235	8.0	LE1	234.7	0.0	0.0	OK
M4	Edit of S 235	8.0	LE1	225.2	0.0	0.0	OK
SM1	S 355	20.0	LE1	237.2	0.0	0.0	OK
STIFF2	S 355	15.0	LE1	111.4	0.0	0.0	OK
STIFF3	S 355	15.0	LE1	130.0	0.0	0.0	OK
EP1	S 355	15.0	LE1	218.6	0.0	0.0	OK
EP2	S 355	15.0	LE1	48.6	0.0	52.6	OK

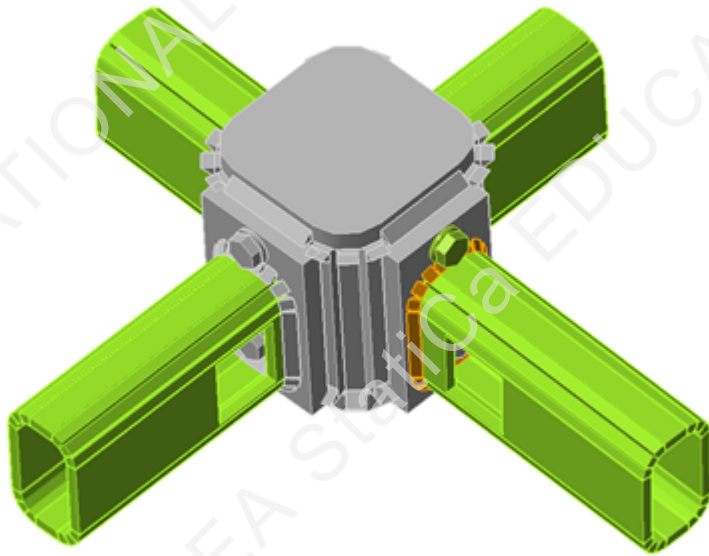
Design data

Material	f_y [MPa]	ϵ_{lim} [%]
Edit of S 235	235.0	5.0
S 355	355.0	5.0

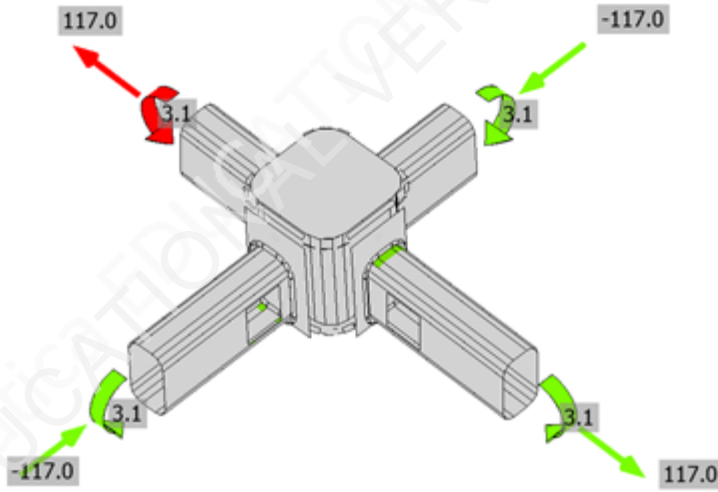
Symbol explanation

ϵ_{pl}	Strain
σ_{Ed}	Eq. stress
σ_{cEd}	Contact stress
f_y	Yield strength
ϵ_{lim}	Limit of plastic strain

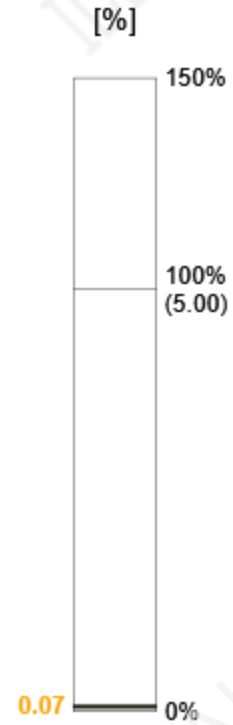
Project:
Project no:
Author:



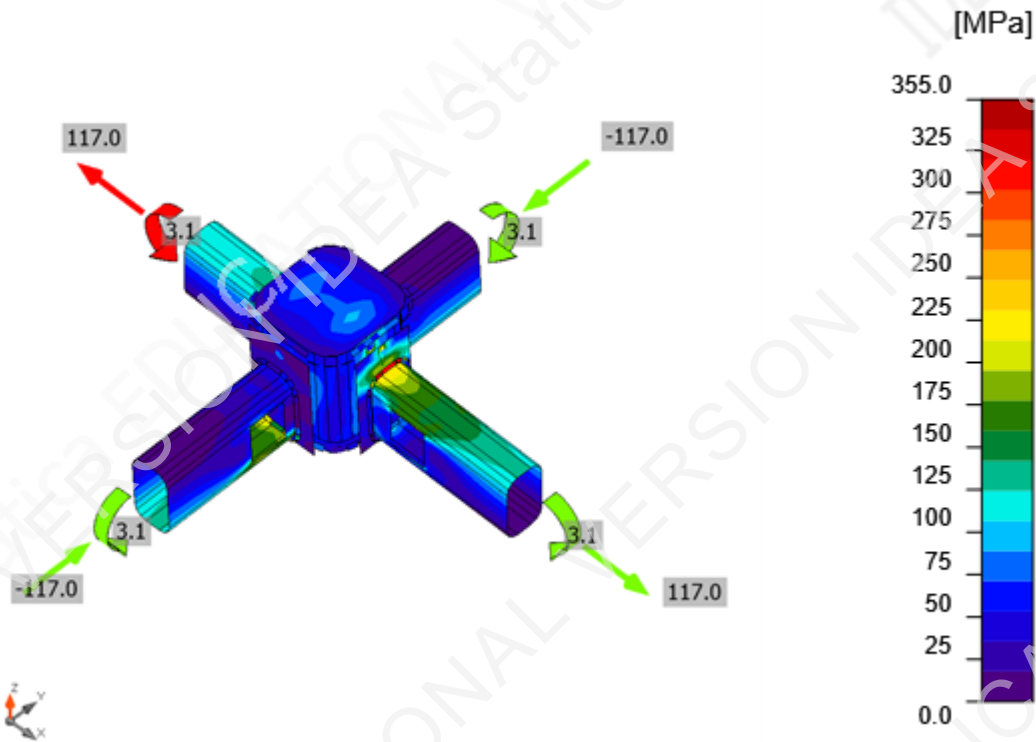
Overall check, LE1



Strain check, LE1


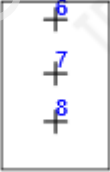


Project:
 Project no:
 Author:



Equivalent stress, LE1

Bolts

	Name	Grade	Loads	$F_{t,Ed}$ [kN]	V [kN]	$U_{t,t}$ [%]	$F_{b,Rd}$ [kN]	$U_{t,s}$ [%]	$U_{t,s}$ [%]	Status
	B2	M12 10.9 - 1	LE1	38.8	1.2	64.1	159.4	2.1	47.9	OK
	B3	M12 10.9 - 1	LE1	33.6	1.0	55.6	136.8	1.8	41.5	OK
	B4	M12 10.9 - 1	LE1	44.3	3.6	73.3	64.8	6.6	59.0	OK
	B6	M12 10.9 - 2	LE1	0.0	0.5	0.0	90.1	1.5	1.5	OK
	B7	M12 10.9 - 2	LE1	1.3	0.1	2.1	159.4	0.2	1.7	OK
	B8	M12 10.9 - 2	LE1	0.0	0.5	0.0	136.8	1.6	1.6	OK

Design data

Name	$F_{t,Rd}$ [kN]	$B_{p,Rd}$ [kN]	$F_{v,Rd}$ [kN]
M12 10.9 - 1	60.5	254.9	54.2
M12 10.9 - 2	60.5	254.9	33.6

Project:
Project no:
Author:

Symbol explanation

$F_{t,Rd}$	Bolt tension resistance EN 1993-1-8 tab. 3.4
$F_{t,Ed}$	Tension force
$B_{p,Rd}$	Punching shear resistance
V	Resultant of shear forces V_y, V_z in bolt
$F_{v,Rd}$	Bolt shear resistance EN_1993-1-8 table 3.4
$F_{b,Rd}$	Plate bearing resistance EN 1993-1-8 tab. 3.4
U_t	Utilization in tension
U_s	Utilization in shear

Welds (Plastic redistribution)

Item	Edge	Material	Throat th. [mm]	Length [mm]	Loads	$\sigma_{w,Ed}$ [MPa]	ϵ_{pl} [%]	σ_{\perp} [MPa]	τ_{\parallel} [MPa]	τ_{\perp} [MPa]	U_t [%]	$U_{t,c}$ [%]	Status
STIFF2	SM1	S 355	▲6.0▲	435	LE1	96.4	0.0	85.0	-26.2	2.2	24.1	13.1	OK
STIFF3	SM1	S 355	▲6.0▲	435	LE1	106.3	0.0	-85.7	11.3	34.5	24.4	16.0	OK
SM1-w 2	M3	Edit of S 235	▲6.0▲	260	LE1	151.4	0.0	24.5	-2.4	86.2	42.1	17.2	OK
SM1-w 1	M4	Edit of S 235	▲5.5▲	259	LE1	165.1	0.0	-49.8	18.1	-89.1	45.9	17.7	OK
EP1	M1	Edit of S 235	▲4.0▲	260	LE1	352.8	0.0	119.5	-16.5	190.9	98.0	30.9	OK
EP2	M2	Edit of S 235	▲5.0▲	259	LE1	214.3	0.0	-84.4	-14.7	-112.8	59.5	18.3	OK
		S 355	▲6.0▲	435	LE1	88.9	0.0	20.5	-26.5	-42.3	20.4	10.1	OK
		S 355	▲6.0▲	435	LE1	109.4	0.0	-64.4	12.2	49.6	25.1	14.4	OK
		Edit of S 235	▲6.0▲	260	LE1	157.5	0.0	113.5	11.8	-61.9	43.8	17.8	OK
		Edit of S 235	▲5.5▲	259	LE1	179.1	0.0	-117.0	-9.9	77.7	49.8	20.2	OK
		Edit of S 235	▲4.0▲	260	LE1	344.8	0.0	208.9	68.5	-142.7	95.8	25.5	OK
		Edit of S 235	▲5.0▲	259	LE1	212.3	0.0	-125.0	20.2	97.0	59.0	20.0	OK

Design data

	β_w [-]	$\sigma_{w,Rd}$ [MPa]	0.9σ [MPa]
S 355	0.90	435.6	352.8
Edit of S 235	0.80	360.0	259.2

Project:
Project no:
Author:

Symbol explanation

ϵ_{Pl}	Strain
$\sigma_{w,Ed}$	Equivalent stress
$\sigma_{w,Rd}$	Equivalent stress resistance
σ_{\perp}	Perpendicular stress
τ_{\parallel}	Shear stress parallel to weld axis
τ_{\perp}	Shear stress perpendicular to weld axis
0.9σ	Perpendicular stress resistance - $0.9 \cdot f_u / \gamma_{M2}$
β_w	Corelation factor EN 1993-1-8 tab. 4.1
U_t	Utilization
U_{tc}	Weld capacity utilization

Buckling

Buckling analysis was not calculated.

Cost estimation

Steel

Steel grade	Total weight [kg]	Unit cost [€/kg]	Cost [€]
S 355	15.92	2.00	31.83

Bolts

Bolt assembly	Total weight [kg]	Unit cost [€/kg]	Cost [€]
M12 10.9	0.73	5.00	3.65

Welds

Weld type	Throat thickness [mm]	Leg size [mm]	Total weight [kg]	Unit cost [€/kg]	Cost [€]
Double fillet	6.0	8.5	0.64	40.00	25.55
Double fillet	5.5	7.8	0.12	40.00	4.93
Double fillet	4.0	5.7	0.07	40.00	2.61
Double fillet	5.0	7.1	0.10	40.00	4.07

Hole drilling

Bolt assembly cost [€]	Percentage of bolt assembly cost [%]	Cost [€]
3.65	30.0	1.10

Cost summary

Cost estimation summary	Cost [€]
Total estimated cost	73.74

Code settings

Project:
 Project no:
 Author:

Item	Value	Unit	Reference
Y _{M0}	1.00	-	EN 1993-1-1: 6.1
Y _{M1}	1.00	-	EN 1993-1-1: 6.1
Y _{M2}	1.25	-	EN 1993-1-1: 6.1
Y _{M3}	1.25	-	EN 1993-1-8: 2.2
Y _C	1.50	-	EN 1992-1-1: 2.4.2.4
Y _{Inst}	1.20	-	EN 1992-4: Table 4.1
Joint coefficient β _j	0.67	-	EN 1993-1-8: 6.2.5
Effective area - influence of mesh size	0.10	-	
Friction coefficient - concrete	0.25	-	EN 1993-1-8
Friction coefficient in slip-resistance	0.30	-	EN 1993-1-8 tab 3.7
Limit plastic strain	0.05	-	EN 1993-1-5
Weld stress evaluation	Plastic redistribution		
Detailing	No		
Distance between bolts [d]	2.20	-	EN 1993-1-8: tab 3.3
Distance between bolts and edge [d]	1.20	-	EN 1993-1-8: tab 3.3
Concrete breakout resistance check	Both		EN 1992-4: 7.2.1.4 and 7.2.2.5
Use calculated α _b in bearing check.	Yes		EN 1993-1-8: tab 3.4
Cracked concrete	Yes		EN 1992-4
Local deformation check	No		CIDECT DG 1, 3 - 1.1
Local deformation limit	0.03	-	CIDECT DG 1, 3 - 1.1
Geometrical nonlinearity (GMNA)	Yes		Analysis with large deformations for hollow section joints
Braced system	No		EN 1993-1-8: 5.2.2.5

Project:
 Project no:
 Author:

Project item Final design_Thesis

Design

Name Final design_Thesis
 Description
 Analysis Stiffness

Beams and columns

Name	Cross-section	β - Direction [°]	γ - Pitch [°]	α - Rotation [°]	Offset ex [mm]	Offset ey [mm]	Offset ez [mm]	Forces in
M1	1 - RHS100/60/8.0	0.0	2.8	3.4	0	0	0	Node
M2	1 - RHS100/60/8.0	-90.0	3.4	0.0	0	0	0	Node
M3	1 - RHS100/60/8.0	-180.0	-2.8	-3.4	0	0	0	Node
M4	1 - RHS100/60/8.0	90.0	-3.4	0.0	0	0	0	Node



Cross-sections

Name	Material
1 - RHS100/60/8.0	Edit of S 235
7 - 120x120(RHS140x140)	S 355

Bolts

Name	Bolt assembly	Diameter [mm]	f_u [MPa]	Gross area [mm ²]
M12 10.9	M12 10.9	12	1000.0	113

Project:
Project no:
Author:

Load effects

Name	Member	N [kN]	Vy [kN]	Vz [kN]	Mx [kNm]	My [kNm]	Mz [kNm]
LE1	M1	117.0	0.0	0.0	0.0	3.1	0.0
	M2	-117.0	0.0	0.0	0.0	3.1	0.0
	M3	117.0	0.0	0.0	0.0	3.1	0.0
	M4	-117.0	0.0	0.0	0.0	3.1	0.0

Check

Rotational stiffness

Name	Comp.	Loads	Mj,Rd [kNm]	Sj,ini [MNm/rad]	Φ_c [mrad]	L [m]	Sj,R [MNm/rad]	Sj,P [MNm/rad]	Class.
M3	My	LE1	12.9	7.6	41.4	2.70	5.1	0.1	Rigid

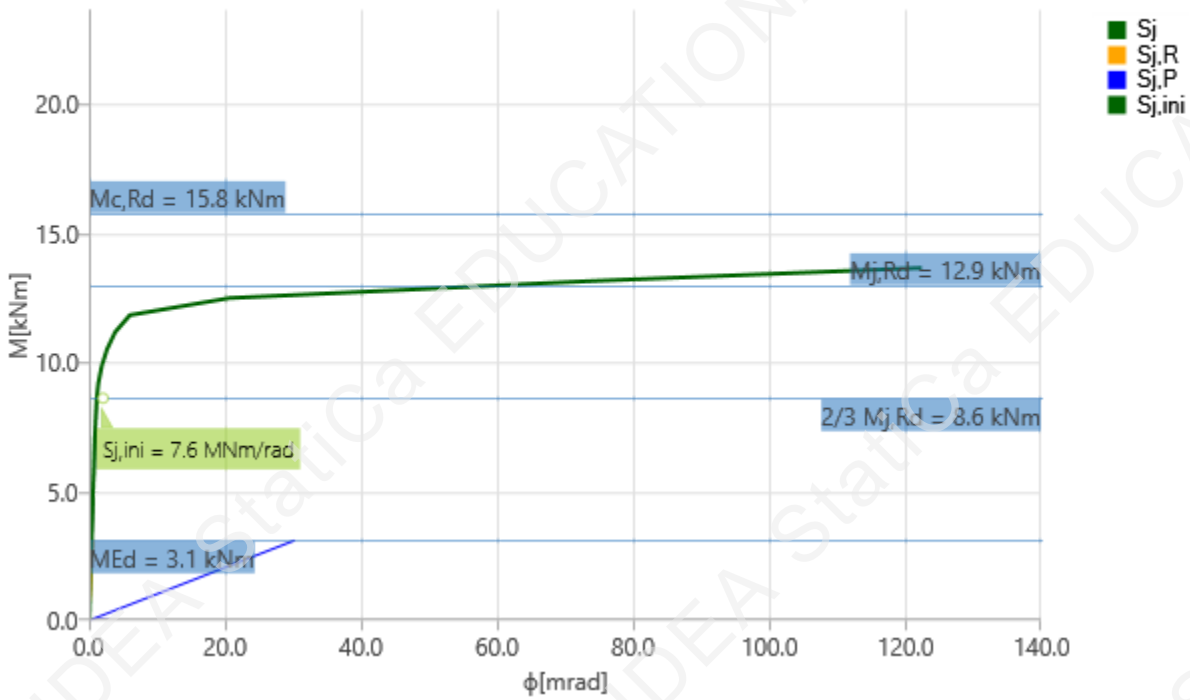
Secant rotational stiffness

Name	Comp.	Loads	M [kNm]	Sjs [MNm/rad]	Φ [mrad]
M3	My	LE1	3.1	8.4	0.4

Symbol explanation

$M_{j,Rd}$	Bending resistance
$S_{j,ini}$	Initial rotational stiffness
$S_{j,s}$	Secant rotational stiffness
Φ	Rotational deformation
Φ_c	Rotational capacity
$S_{j,R}$	Limit value - rigid joint
$S_{j,P}$	Limit value - nominally pinned joint

Project:
 Project no:
 Author:



Stiffness diagram My - ϕ , LE1

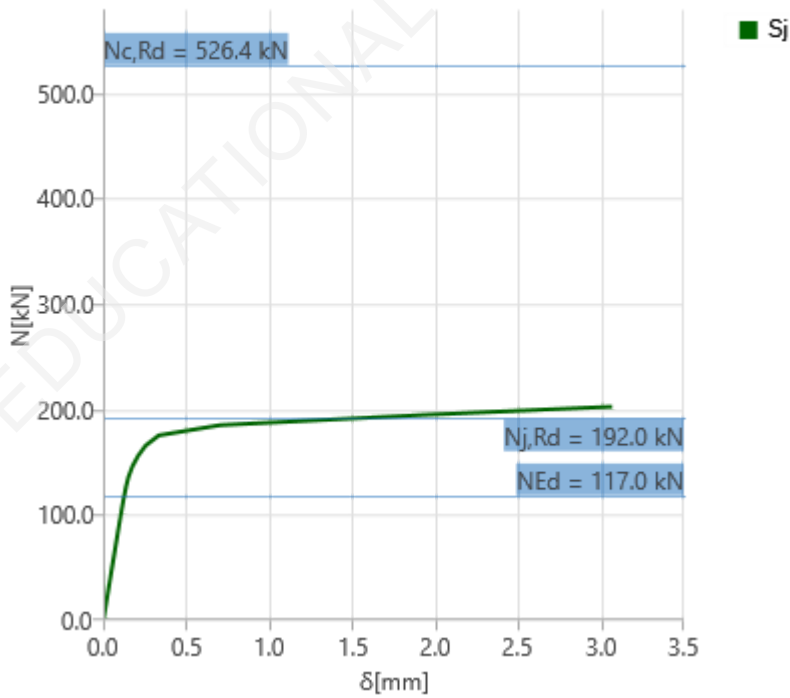
Axial stiffness

Name	Component	Loads	N [kN]	Nj,Rd [kN]	dx [mm]	St [MN/m]
M3	N	LE1	117.0	192.0	0	246

Symbol explanation

- $N_{j,Rd}$ Tension (compression) resistance
- S_t Secant axial stiffness
- δ Longitudinal deformation

Project:
Project no:
Author:



Stiffness diagram N - δ , LE1

Cost estimation

Steel

Steel grade	Total weight [kg]	Unit cost [€/kg]	Cost [€]
S 355	15.92	2.00	31.83

Bolts

Bolt assembly	Total weight [kg]	Unit cost [€/kg]	Cost [€]
M12 10.9	0.73	5.00	3.65

Welds

Weld type	Throat thickness [mm]	Leg size [mm]	Total weight [kg]	Unit cost [€/kg]	Cost [€]
Double fillet	6.0	8.5	0.64	40.00	25.55
Double fillet	5.5	7.8	0.12	40.00	4.93
Double fillet	4.0	5.7	0.07	40.00	2.61
Double fillet	5.0	7.1	0.10	40.00	4.07

Hole drilling

Bolt assembly cost [€]	Percentage of bolt assembly cost [%]	Cost [€]
3.65	30.0	1.10

Project:
Project no:
Author:

Cost summary

Cost estimation summary	Cost [€]
Total estimated cost	73.74

Code settings

Item	Value	Unit	Reference
Y _{M0}	1.00	-	EN 1993-1-1: 6.1
Y _{M1}	1.00	-	EN 1993-1-1: 6.1
Y _{M2}	1.25	-	EN 1993-1-1: 6.1
Y _{M3}	1.25	-	EN 1993-1-8: 2.2
Y _C	1.50	-	EN 1992-1-1: 2.4.2.4
Y _{Inst}	1.20	-	EN 1992-4: Table 4.1
Joint coefficient β _j	0.67	-	EN 1993-1-8: 6.2.5
Effective area - influence of mesh size	0.10	-	
Friction coefficient - concrete	0.25	-	EN 1993-1-8
Friction coefficient in slip-resistance	0.30	-	EN 1993-1-8 tab 3.7
Limit plastic strain	0.05	-	EN 1993-1-5
Weld stress evaluation	Plastic redistribution		
Detailing	No		
Distance between bolts [d]	2.20	-	EN 1993-1-8: tab 3.3
Distance between bolts and edge [d]	1.20	-	EN 1993-1-8: tab 3.3
Concrete breakout resistance check	Both		EN 1992-4: 7.2.1.4 and 7.2.2.5
Use calculated α _b in bearing check.	Yes		EN 1993-1-8: tab 3.4
Cracked concrete	Yes		EN 1992-4
Local deformation check	No		CIDECT DG 1, 3 - 1.1
Local deformation limit	0.03	-	CIDECT DG 1, 3 - 1.1
Geometrical nonlinearity (GMNA)	Yes		Analysis with large deformations for hollow section joints
Braced system	No		EN 1993-1-8: 5.2.2.5

F.2 CONNECTION DESIGN WITH OPTIMAL STIFFNESS AND CROSS SECTION

F.2.1 Connection with bolts

Project:
Project no:
Author:

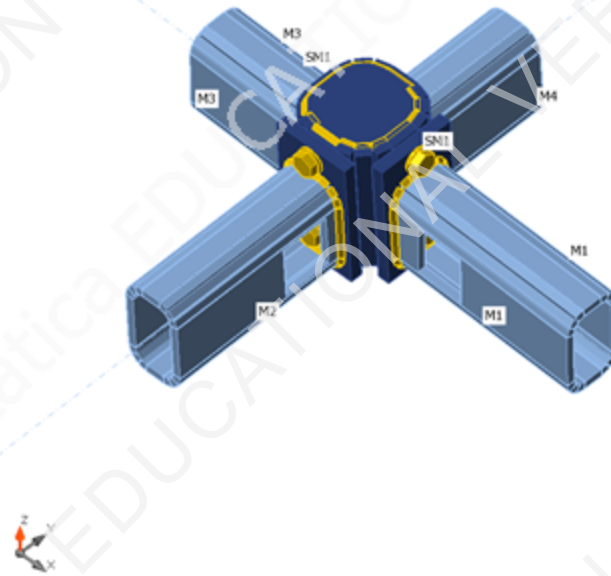
Project item Final design_Thesis

Design

Name Final design_Thesis
Description
Analysis Stress, strain/ loads in equilibrium

Beams and columns

Name	Cross-section	β - Direction [°]	γ - Pitch [°]	α - Rotation [°]	Offset ex [mm]	Offset ey [mm]	Offset ez [mm]	Forces in
M1	1 - RHS100/60/8.0	0.0	2.8	3.4	0	0	0	Node
M2	1 - RHS100/60/8.0	-90.0	3.4	0.0	0	0	0	Node
M3	1 - RHS100/60/8.0	-180.0	-2.8	-3.4	0	0	0	Node
M4	1 - RHS100/60/8.0	90.0	-3.4	0.0	0	0	0	Node



Cross-sections

Name	Material
1 - RHS100/60/8.0	Edit of S 235
7 - 120x120(RHS100x100)	S 355

Bolts

Name	Bolt assembly	Diameter [mm]	f_u [MPa]	Gross area [mm ²]
M12 10.9	M12 10.9	12	1000.0	113

Project:
Project no:
Author:

Load effects (forces in equilibrium)

Name	Member	N [kN]	Vy [kN]	Vz [kN]	Mx [kNm]	My [kNm]	Mz [kNm]
LE1	M1	117.0	0.0	0.0	0.0	3.1	0.0
	M2	-117.0	0.0	0.0	0.0	3.1	0.0
	M3	117.0	0.0	0.0	0.0	3.1	0.0
	M4	-117.0	0.0	0.0	0.0	3.1	0.0

Check

Summary

Name	Value	Status
Analysis	100.0%	OK
Plates	0.0 < 5.0%	OK
Bolts	77.5 < 100%	OK
Welds	98.6 < 100%	OK
Buckling	Not calculated	
GMNA	Calculated	

Plates

Name	Material	Thickness [mm]	Loads	σ_{Ed} [MPa]	ϵ_{pl} [%]	σ_{cEd} [MPa]	Status
M1	Edit of S 235	8.0	LE1	235.0	0.0	0.0	OK
M2	Edit of S 235	8.0	LE1	231.5	0.0	0.0	OK
M3	Edit of S 235	8.0	LE1	133.0	0.0	0.0	OK
M4	Edit of S 235	8.0	LE1	157.8	0.0	0.0	OK
SM1	S 355	16.0	LE1	353.1	0.0	0.0	OK
STIFF2	S 355	2.0	LE1	232.3	0.0	0.0	OK
STIFF3	S 355	3.0	LE1	355.0	0.0	0.0	OK
EP1	S 355	12.0	LE1	325.5	0.0	0.0	OK
EP2	S 355	12.0	LE1	225.1	0.0	127.2	OK

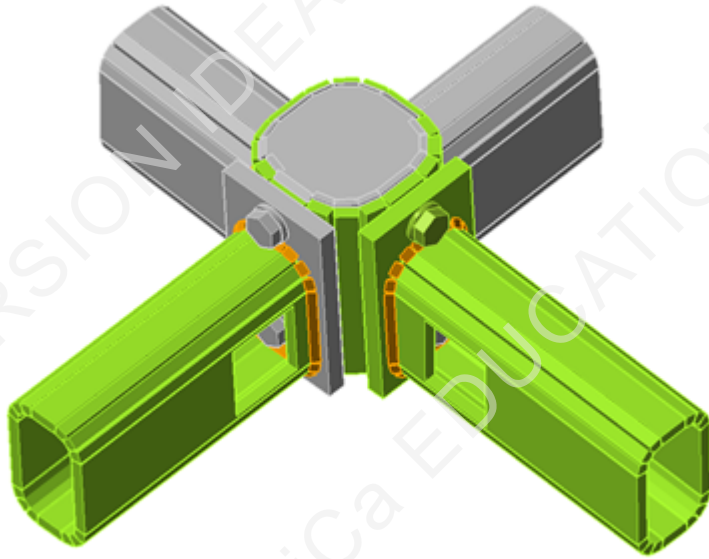
Design data

Material	f_y [MPa]	ϵ_{lim} [%]
Edit of S 235	235.0	5.0
S 355	355.0	5.0

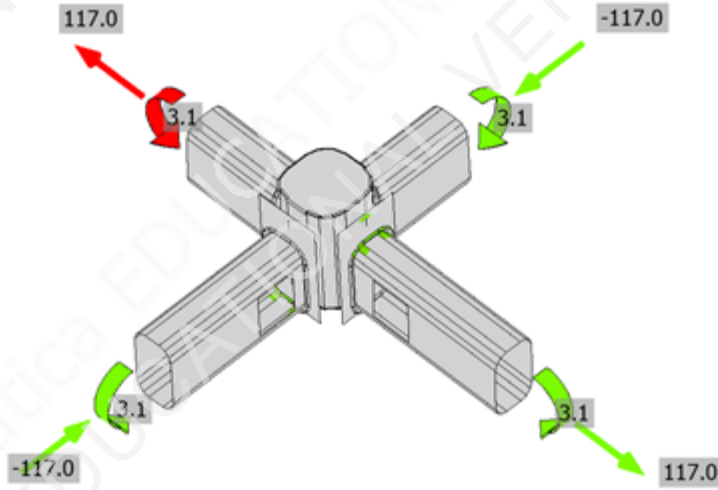
Symbol explanation

ϵ_{pl}	Strain
σ_{Ed}	Eq. stress
σ_{cEd}	Contact stress
f_y	Yield strength
ϵ_{lim}	Limit of plastic strain

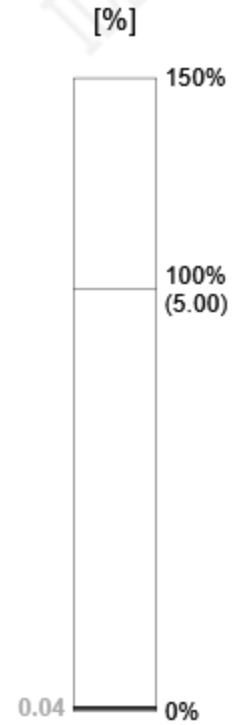
Project:
Project no:
Author:



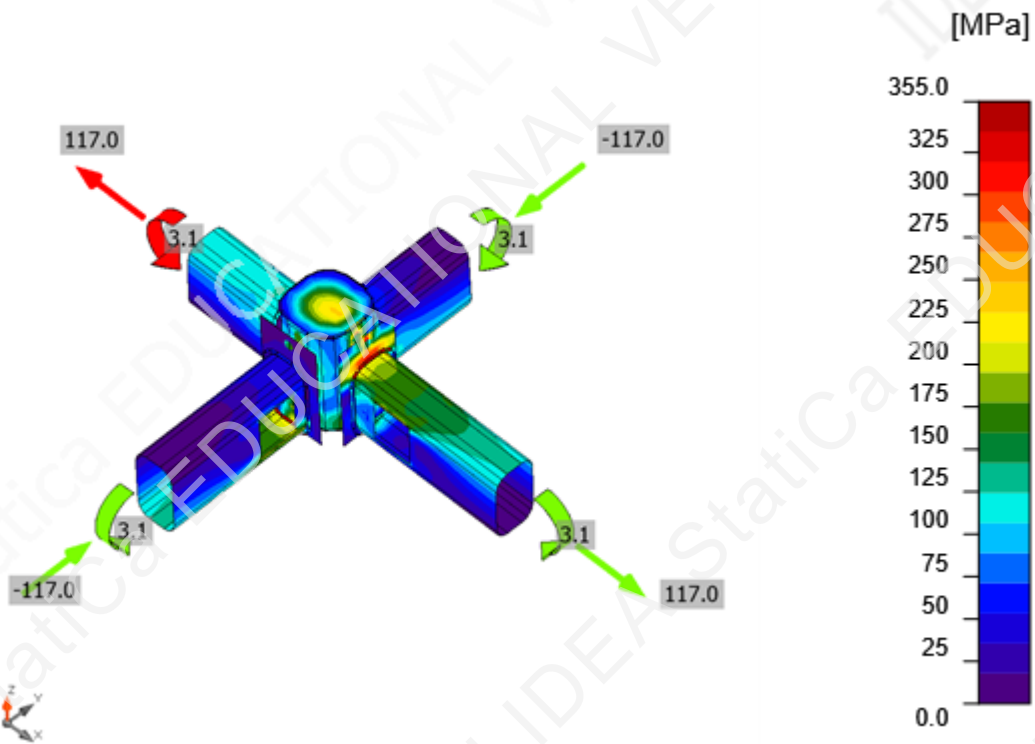
Overall check, LE1



Strain check, LE1



Project:
Project no:
Author:



Equivalent stress, LE1

Bolts

	Name	Loads	$F_{t,Ed}$ [kN]	V [kN]	U_{t_t} [%]	$F_{b,Rd}$ [kN]	U_{t_s} [%]	$U_{t_{ts}}$ [%]	Status
	B2	LE1	46.9	1.1	77.5	61.5	3.2	58.5	OK
	B3	LE1	29.6	1.1	49.0	58.0	3.2	38.2	OK
	B4	LE1	40.3	3.6	66.7	52.4	10.6	58.3	OK
	B6	LE1	0.0	0.3	0.0	38.0	1.0	1.0	OK
	B7	LE1	1.0	0.3	1.6	57.6	0.8	1.9	OK
	B8	LE1	0.0	0.2	0.0	61.1	0.6	0.6	OK

Design data

Name	$F_{t,Rd}$ [kN]	$B_{p,Rd}$ [kN]	$F_{v,Rd}$ [kN]
M12 10.9 - 1	60.5	203.9	33.6

Project:
Project no:
Author:

Symbol explanation

$F_{t,Rd}$	Bolt tension resistance EN 1993-1-8 tab. 3.4
$F_{t,Ed}$	Tension force
$B_{p,Rd}$	Punching shear resistance
V	Resultant of shear forces V_y, V_z in bolt
$F_{v,Rd}$	Bolt shear resistance EN_1993-1-8 table 3.4
$F_{b,Rd}$	Plate bearing resistance EN 1993-1-8 tab. 3.4
U_t	Utilization in tension
U_s	Utilization in shear

Welds (Plastic redistribution)

Item	Edge	Throat th. [mm]	Length [mm]	Loads	$\sigma_{w,Ed}$ [MPa]	ϵ_{pl} [%]	σ_{\perp} [MPa]	τ_{\parallel} [MPa]	τ_{\perp} [MPa]	U_t [%]	U_{tc} [%]	Status
STIFF2	SM1	▲3.0	286	LE1	200.9	0.0	-96.4	1.2	101.7	55.8	23.7	OK
STIFF3	SM1	▲3.0	286	LE1	353.8	0.7	-172.8	-1.2	178.2	98.3	55.6	OK
SM1-w 2	M3	▲3.0	260	LE1	353.6	0.6	250.2	-1.4	-144.2	98.2	65.6	OK
SM1-w 1	M4	▲3.0	252	LE1	354.5	1.2	-222.2	-21.6	158.0	98.5	70.8	OK
EP1	M1	▲3.0▲	260	LE1	353.9	0.8	154.5	-14.8	183.3	98.3	47.0	OK
EP2	M2	▲3.0▲	259	LE1	353.8	0.7	-180.1	13.8	-175.3	98.3	40.6	OK
		▲3.0▲	260	LE1	354.9	1.5	188.8	20.5	-172.3	98.6	36.1	OK
		▲3.0▲	259	LE1	353.8	0.7	-170.1	-18.2	178.2	98.3	31.3	OK

Design data

	β_w [-]	$\sigma_{w,Rd}$ [MPa]	0.9σ [MPa]
Edit of S 235	0.80	360.0	259.2

Symbol explanation

ϵ_{pl}	Strain
$\sigma_{w,Ed}$	Equivalent stress
$\sigma_{w,Rd}$	Equivalent stress resistance
σ_{\perp}	Perpendicular stress
τ_{\parallel}	Shear stress parallel to weld axis
τ_{\perp}	Shear stress perpendicular to weld axis
0.9σ	Perpendicular stress resistance - $0.9 \cdot f_u / \gamma_{M2}$
β_w	Corelation factor EN 1993-1-8 tab. 4.1
U_t	Utilization
U_{tc}	Weld capacity utilization

Buckling

Buckling analysis was not calculated.

Project:
Project no:
Author:

Cost estimation

Steel

Steel grade	Total weight [kg]	Unit cost [€/kg]	Cost [€]
S 355	7.13	2.00	14.26

Bolts

Bolt assembly	Total weight [kg]	Unit cost [€/kg]	Cost [€]
M12 10.9	0.68	5.00	3.41

Welds

Weld type	Throat thickness [mm]	Leg size [mm]	Total weight [kg]	Unit cost [€/kg]	Cost [€]
Fillet rear	3.0	4.2	0.15	40.00	5.99

Hole drilling

Bolt assembly cost [€]	Percentage of bolt assembly cost [%]	Cost [€]
3.41	30.0	1.02

Cost summary

Cost estimation summary	Cost [€]
Total estimated cost	24.69

Code settings

Item	Value	Unit	Reference
YM0	1.00	-	EN 1993-1-1: 6.1
YM1	1.00	-	EN 1993-1-1: 6.1
YM2	1.25	-	EN 1993-1-1: 6.1
YM3	1.25	-	EN 1993-1-8: 2.2
YC	1.50	-	EN 1992-1-1: 2.4.2.4
YInst	1.20	-	EN 1992-4: Table 4.1
Joint coefficient β_j	0.67	-	EN 1993-1-8: 6.2.5
Effective area - influence of mesh size	0.10	-	
Friction coefficient - concrete	0.25	-	EN 1993-1-8
Friction coefficient in slip-resistance	0.30	-	EN 1993-1-8 tab 3.7
Limit plastic strain	0.05	-	EN 1993-1-5
Weld stress evaluation	Plastic redistribution		
Detailing	No		
Distance between bolts [d]	2.20	-	EN 1993-1-8: tab 3.3
Distance between bolts and edge [d]	1.20	-	EN 1993-1-8: tab 3.3

Project:
Project no:
Author:

Item	Value	Unit	Reference
Concrete breakout resistance check	Both		EN 1992-4: 7.2.1.4 and 7.2.2.5
Use calculated α_b in bearing check.	Yes		EN 1993-1-8: tab 3.4
Cracked concrete	Yes		EN 1992-4
Local deformation check	No		CIDECT DG 1, 3 - 1.1
Local deformation limit	0.03	-	CIDECT DG 1, 3 - 1.1
Geometrical nonlinearity (GMNA)	Yes		Analysis with large deformations for hollow section joints
Braced system	No		EN 1993-1-8: 5.2.2.5

Project:
 Project no:
 Author:

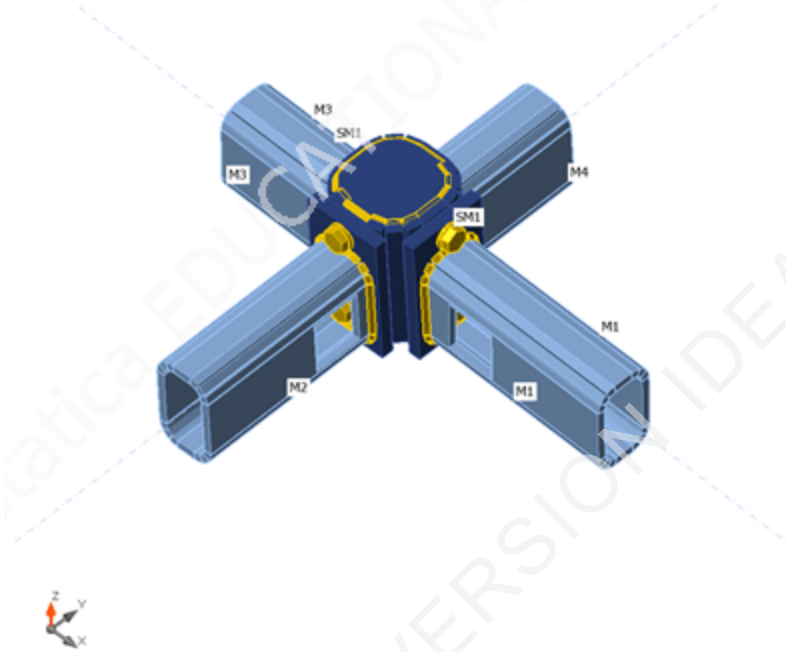
Project item Final design_Thesis

Design

Name Final design_Thesis
 Description
 Analysis Stiffness

Beams and columns

Name	Cross-section	β - Direction [°]	γ - Pitch [°]	α - Rotation [°]	Offset ex [mm]	Offset ey [mm]	Offset ez [mm]	Forces in
M1	1 - RHS100/60/8.0	0.0	2.8	3.4	0	0	0	Node
M2	1 - RHS100/60/8.0	-90.0	3.4	0.0	0	0	0	Node
M3	1 - RHS100/60/8.0	-180.0	-2.8	-3.4	0	0	0	Node
M4	1 - RHS100/60/8.0	90.0	-3.4	0.0	0	0	0	Node



Cross-sections

Name	Material
1 - RHS100/60/8.0	Edit of S 235
7 - 120x120(RHS100x100)	S 355

Bolts

Name	Bolt assembly	Diameter [mm]	f_u [MPa]	Gross area [mm ²]
M12 10.9	M12 10.9	12	1000.0	113

Project:
Project no:
Author:

Load effects

Name	Member	N [kN]	Vy [kN]	Vz [kN]	Mx [kNm]	My [kNm]	Mz [kNm]
LE1	M1	117.0	0.0	0.0	0.0	3.1	0.0
	M2	-117.0	0.0	0.0	0.0	3.1	0.0
	M3	117.0	0.0	0.0	0.0	3.1	0.0
	M4	-117.0	0.0	0.0	0.0	3.1	0.0

Check

Rotational stiffness

Name	Comp.	Loads	Mj,Rd [kNm]	Sj,ini [MNm/rad]	Φ_c [mrad]	L [m]	Sj,R [MNm/rad]	Sj,P [MNm/rad]	Class.
M3	My	LE1	5.1	3.9	4.9	2.70	5.1	0.1	Semi-rigid

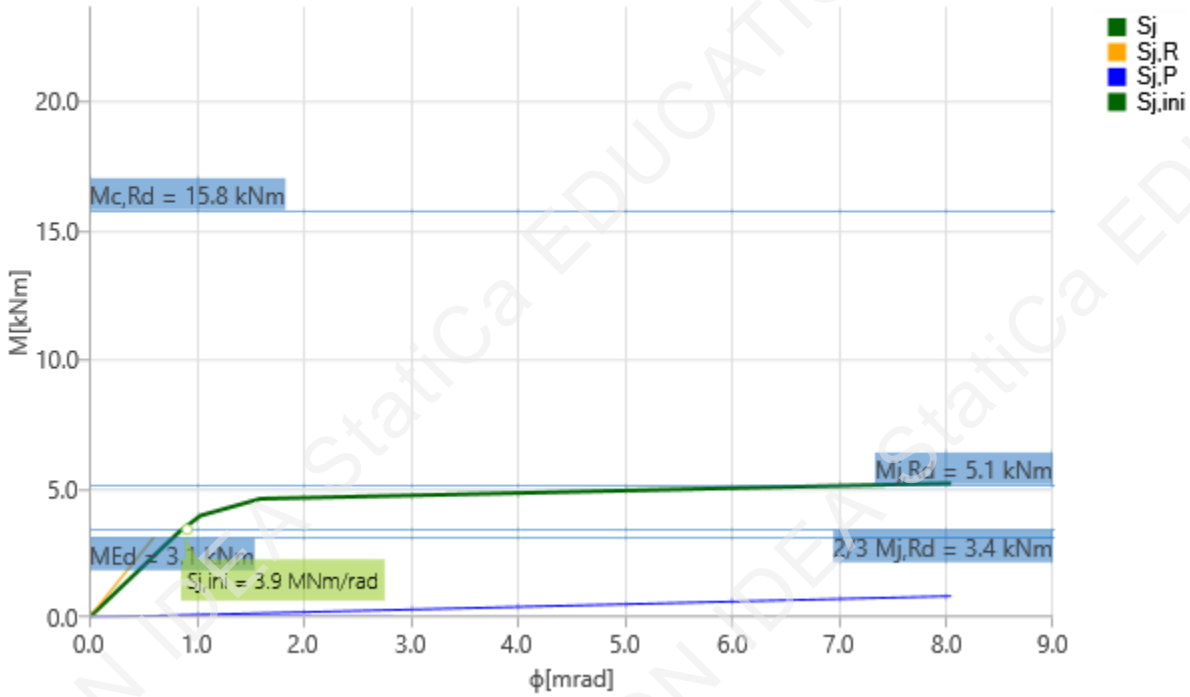
Secant rotational stiffness

Name	Comp.	Loads	M [kNm]	Sjs [MNm/rad]	Φ [mrad]
M3	My	LE1	3.1	3.9	0.8

Symbol explanation

$M_{j,Rd}$	Bending resistance
$S_{j,ini}$	Initial rotational stiffness
$S_{j,s}$	Secant rotational stiffness
Φ	Rotational deformation
Φ_c	Rotational capacity
$S_{j,R}$	Limit value - rigid joint
$S_{j,P}$	Limit value - nominally pinned joint

Project:
 Project no:
 Author:



Stiffness diagram $M_y - \phi_y$, LE1

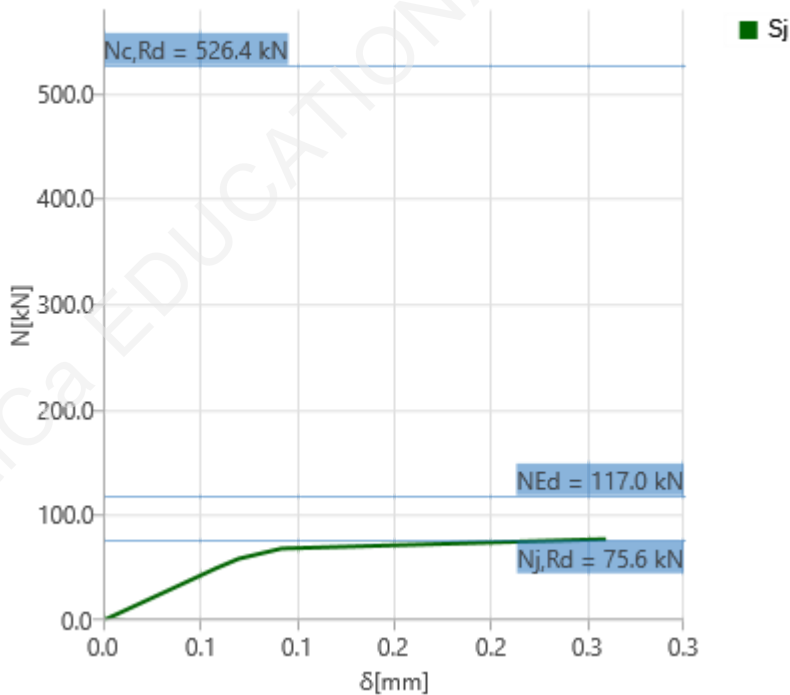
Axial stiffness

Name	Component	Loads	N [kN]	$N_{j,Rd}$ [kN]	dx [mm]	S_t [MN/m]
M3	N	LE1	117.0	75.6	0	236

Symbol explanation

- $N_{j,Rd}$ Tension (compression) resistance
- S_t Secant axial stiffness
- δ Longitudinal deformation

Project:
Project no:
Author:



Stiffness diagram N - δ , LE1

Cost estimation

Steel

Steel grade	Total weight [kg]	Unit cost [€/kg]	Cost [€]
S 355	7.13	2.00	14.26

Bolts

Bolt assembly	Total weight [kg]	Unit cost [€/kg]	Cost [€]
M12 10.9	0.68	5.00	3.41

Welds

Weld type	Throat thickness [mm]	Leg size [mm]	Total weight [kg]	Unit cost [€/kg]	Cost [€]
Fillet rear	3.0	4.2	0.15	40.00	5.99

Hole drilling

Bolt assembly cost [€]	Percentage of bolt assembly cost [%]	Cost [€]
3.41	30.0	1.02

Cost summary

Cost estimation summary	Cost [€]
Total estimated cost	24.69

Project:
Project no:
Author:

Code settings

Item	Value	Unit	Reference
Y _{M0}	1.00	-	EN 1993-1-1: 6.1
Y _{M1}	1.00	-	EN 1993-1-1: 6.1
Y _{M2}	1.25	-	EN 1993-1-1: 6.1
Y _{M3}	1.25	-	EN 1993-1-8: 2.2
Y _C	1.50	-	EN 1992-1-1: 2.4.2.4
Y _{Inst}	1.20	-	EN 1992-4: Table 4.1
Joint coefficient β _j	0.67	-	EN 1993-1-8: 6.2.5
Effective area - influence of mesh size	0.10	-	
Friction coefficient - concrete	0.25	-	EN 1993-1-8
Friction coefficient in slip-resistance	0.30	-	EN 1993-1-8 tab 3.7
Limit plastic strain	0.05	-	EN 1993-1-5
Weld stress evaluation	Plastic redistribution		
Detailing	No		
Distance between bolts [d]	2.20	-	EN 1993-1-8: tab 3.3
Distance between bolts and edge [d]	1.20	-	EN 1993-1-8: tab 3.3
Concrete breakout resistance check	Both		EN 1992-4: 7.2.1.4 and 7.2.2.5
Use calculated a _b in bearing check.	Yes		EN 1993-1-8: tab 3.4
Cracked concrete	Yes		EN 1992-4
Local deformation check	No		CIDECT DG 1, 3 - 1.1
Local deformation limit	0.03	-	CIDECT DG 1, 3 - 1.1
Geometrical nonlinearity (GMNA)	Yes		Analysis with large deformations for hollow section joints
Braced system	No		EN 1993-1-8: 5.2.2.5

F.2.2 Connection with welding

Project:
 Project no:
 Author:

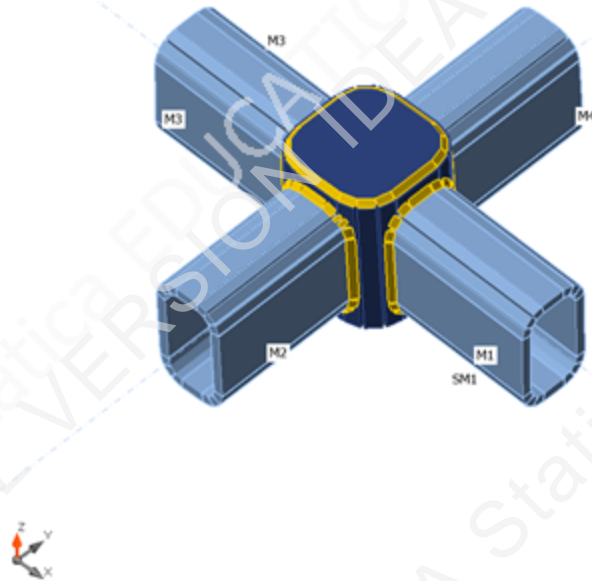
Project item Final design_Thesis

Design

Name Final design_Thesis
 Description
 Analysis Stress, strain/ loads in equilibrium

Beams and columns

Name	Cross-section	β - Direction [°]	γ - Pitch [°]	α - Rotation [°]	Offset ex [mm]	Offset ey [mm]	Offset ez [mm]	Forces in
M1	1 - RHS100/60/8.0	0.0	2.8	3.4	0	0	0	Node
M2	1 - RHS100/60/8.0	-90.0	3.4	0.0	0	0	0	Node
M3	1 - RHS100/60/8.0	-180.0	-2.8	-3.4	0	0	0	Node
M4	1 - RHS100/60/8.0	90.0	-3.4	0.0	0	0	0	Node



Cross-sections

Name	Material
1 - RHS100/60/8.0	Edit of S 235
6 - RHS100x100	S 355

Project:
Project no:
Author:

Load effects (forces in equilibrium)

Name	Member	N [kN]	Vy [kN]	Vz [kN]	Mx [kNm]	My [kNm]	Mz [kNm]
LE1	M1	117.0	0.0	0.0	0.0	3.1	0.0
	M2	-117.0	0.0	0.0	0.0	3.1	0.0
	M3	117.0	0.0	0.0	0.0	3.1	0.0
	M4	-117.0	0.0	0.0	0.0	3.1	0.0

Check

Summary

Name	Value	Status
Analysis	100.0%	OK
Plates	0.0 < 5.0%	OK
Welds	99.3 < 100%	OK
Buckling	Not calculated	
GMNA	Calculated	

Plates

Name	Material	Thickness [mm]	Loads	σ_{Ed} [MPa]	ϵ_{pl} [%]	σ_{CEd} [MPa]	Status
M1	Edit of S 235	8.0	LE1	151.9	0.0	0.0	OK
M2	Edit of S 235	8.0	LE1	151.6	0.0	0.0	OK
M3	Edit of S 235	8.0	LE1	158.4	0.0	0.0	OK
M4	Edit of S 235	8.0	LE1	151.7	0.0	0.0	OK
SM1	S 355	10.0	LE1	355.0	0.0	0.0	OK
STIFF2	S 355	3.0	LE1	306.9	0.0	0.0	OK
STIFF3	S 355	3.0	LE1	355.0	0.0	0.0	OK

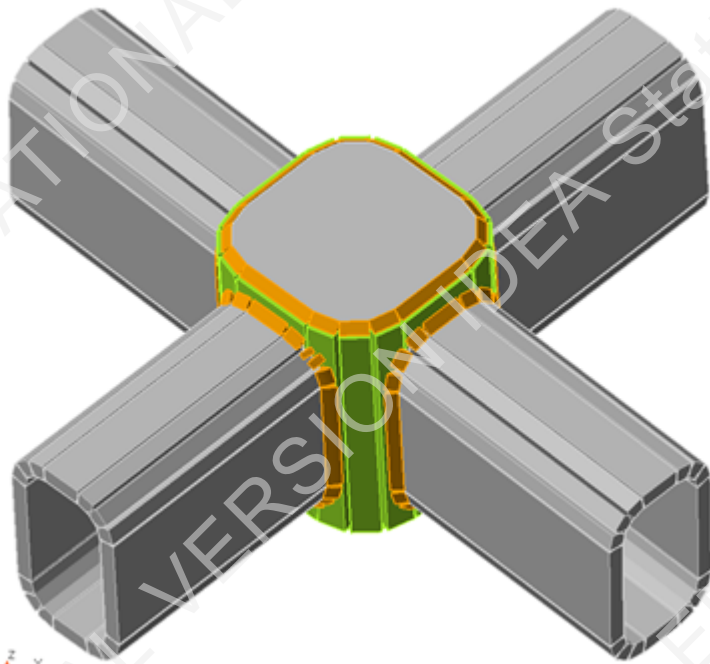
Design data

Material	f_y [MPa]	ϵ_{lim} [%]
Edit of S 235	235.0	5.0
S 355	355.0	5.0

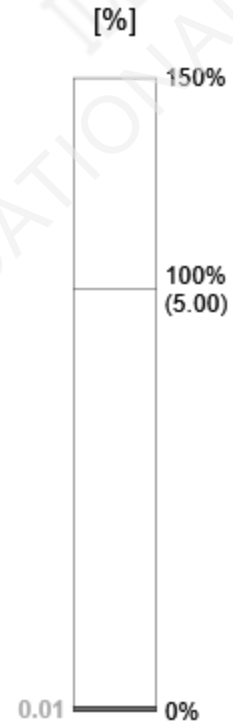
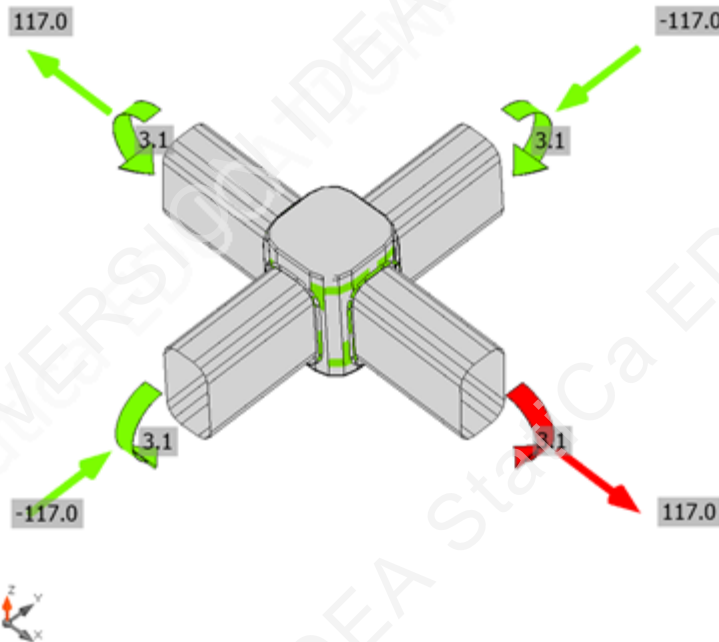
Symbol explanation

ϵ_{pl}	Strain
σ_{Ed}	Eq. stress
σ_{CEd}	Contact stress
f_y	Yield strength
ϵ_{lim}	Limit of plastic strain

Project:
Project no:
Author:

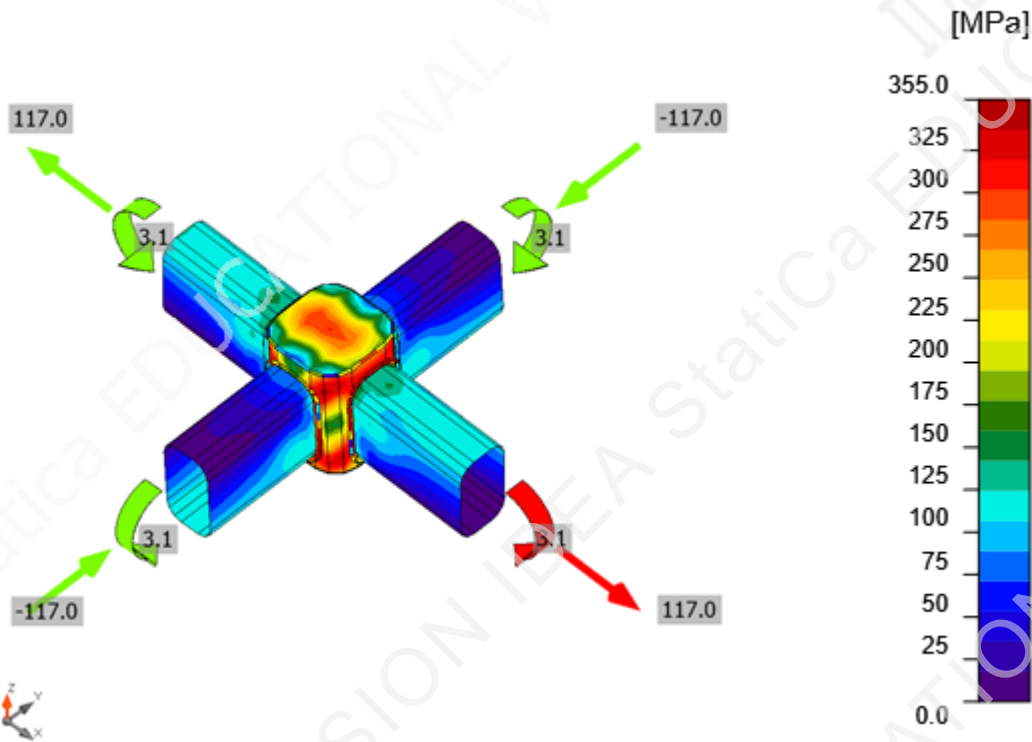


Overall check, LE1



Strain check, LE1

Project:
Project no:
Author:



Equivalent stress, LE1

Welds (Plastic redistribution)

Item	Edge	Throat th. [mm]	Length [mm]	Loads	$\sigma_{w,Ed}$ [MPa]	ϵ_{pl} [%]	σ_{\perp} [MPa]	τ_{\parallel} [MPa]	τ_{\perp} [MPa]	Ut [%]	Ut _c [%]	Status
SM1-w 4	M1	▲3.0	260	LE1	355.8	2.1	252.1	46.4	-137.3	98.8	75.0	OK
STIFF2	SM1	▲3.0	309	LE1	352.8	0.0	177.8	-4.2	-175.9	98.0	46.4	OK
STIFF3	SM1	▲3.0	309	LE1	324.7	0.0	-159.2	21.2	162.0	90.2	48.5	OK
SM1-w 3	M2	▲3.0	252	LE1	357.3	3.1	-245.9	17.0	148.7	99.3	73.6	OK
SM1-w 2	M3	▲3.0	260	LE1	355.7	2.0	253.8	13.0	-143.3	98.8	73.4	OK
SM1-w 1	M4	▲3.0	252	LE1	357.3	3.1	-245.4	-17.3	149.0	99.3	73.6	OK

Design data

	β_w [-]	$\sigma_{w,Rd}$ [MPa]	0.9σ [MPa]
Edit of S 235	0.80	360.0	259.2

Project:
Project no:
Author:

Symbol explanation

ϵ_{pl}	Strain
$\sigma_{w,Ed}$	Equivalent stress
$\sigma_{w,Rd}$	Equivalent stress resistance
σ_{\perp}	Perpendicular stress
$\tau_{ }$	Shear stress parallel to weld axis
τ_{\perp}	Shear stress perpendicular to weld axis
0.9σ	Perpendicular stress resistance - $0.9 \cdot f_u / \gamma_{M2}$
β_w	Corelation factor EN 1993-1-8 tab. 4.1
U_t	Utilization
U_{tc}	Weld capacity utilization

Buckling

Buckling analysis was not calculated.

Cost estimation

Steel

Steel grade	Total weight [kg]	Unit cost [€/kg]	Cost [€]
S 355	3.31	2.00	6.61

Bolts

Bolt assembly	Total weight [kg]	Unit cost [€/kg]	Cost [€]

Welds

Weld type	Throat thickness [mm]	Leg size [mm]	Total weight [kg]	Unit cost [€/kg]	Cost [€]
Fillet rear	3.0	4.2	0.12	40.00	4.64

Hole drilling

Bolt assembly cost [€]	Percentage of bolt assembly cost [%]	Cost [€]

Cost summary

Cost estimation summary	Cost [€]
Total estimated cost	11.25

Code settings

Item	Value	Unit	Reference
YM0	1.00	-	EN 1993-1-1: 6.1
YM1	1.00	-	EN 1993-1-1: 6.1
YM2	1.25	-	EN 1993-1-1: 6.1

Project:
 Project no:
 Author:

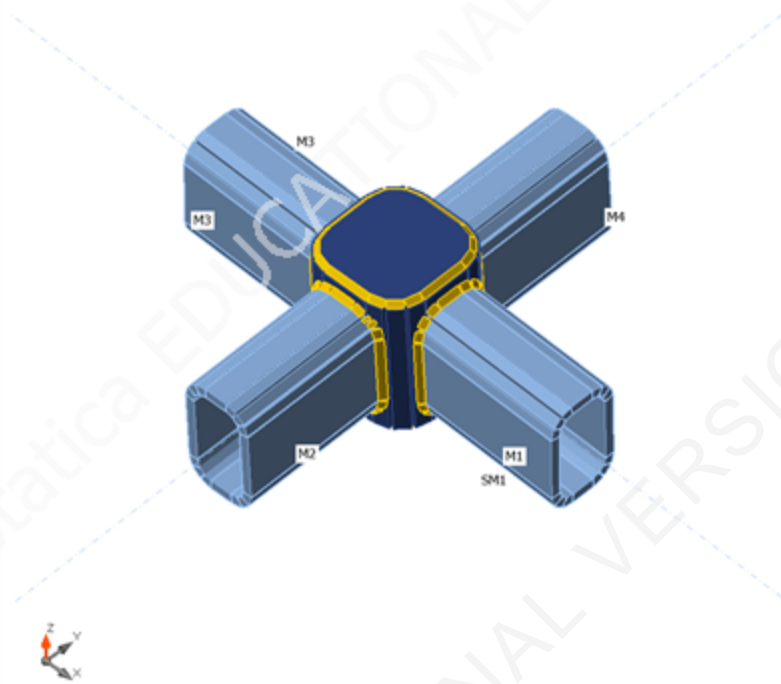
Project item Final design_Thesis

Design

Name Final design_Thesis
 Description
 Analysis Stiffness

Beams and columns

Name	Cross-section	β - Direction [°]	γ - Pitch [°]	α - Rotation [°]	Offset ex [mm]	Offset ey [mm]	Offset ez [mm]	Forces in
M1	1 - RHS100/60/8.0	0.0	2.8	3.4	0	0	0	Node
M2	1 - RHS100/60/8.0	-90.0	3.4	0.0	0	0	0	Node
M3	1 - RHS100/60/8.0	-180.0	-2.8	-3.4	0	0	0	Node
M4	1 - RHS100/60/8.0	90.0	-3.4	0.0	0	0	0	Node



Cross-sections

Name	Material
1 - RHS100/60/8.0	Edit of S 235
6 - RHS100x100	S 355

Project:
Project no:
Author:

Load effects

Name	Member	N [kN]	Vy [kN]	Vz [kN]	Mx [kNm]	My [kNm]	Mz [kNm]
LE1	M1	117.0	0.0	0.0	0.0	3.1	0.0
	M2	-117.0	0.0	0.0	0.0	3.1	0.0
	M3	117.0	0.0	0.0	0.0	3.1	0.0
	M4	-117.0	0.0	0.0	0.0	3.1	0.0

Check

Rotational stiffness

Name	Comp.	Loads	Mj,Rd [kNm]	Sj,ini [MNm/rad]	Φ_c [mrad]	L [m]	Sj,R [MNm/rad]	Sj,P [MNm/rad]	Class.
M1	My	LE1	5.2	4.1	6.1	2.70	5.1	0.1	Semi-rigid

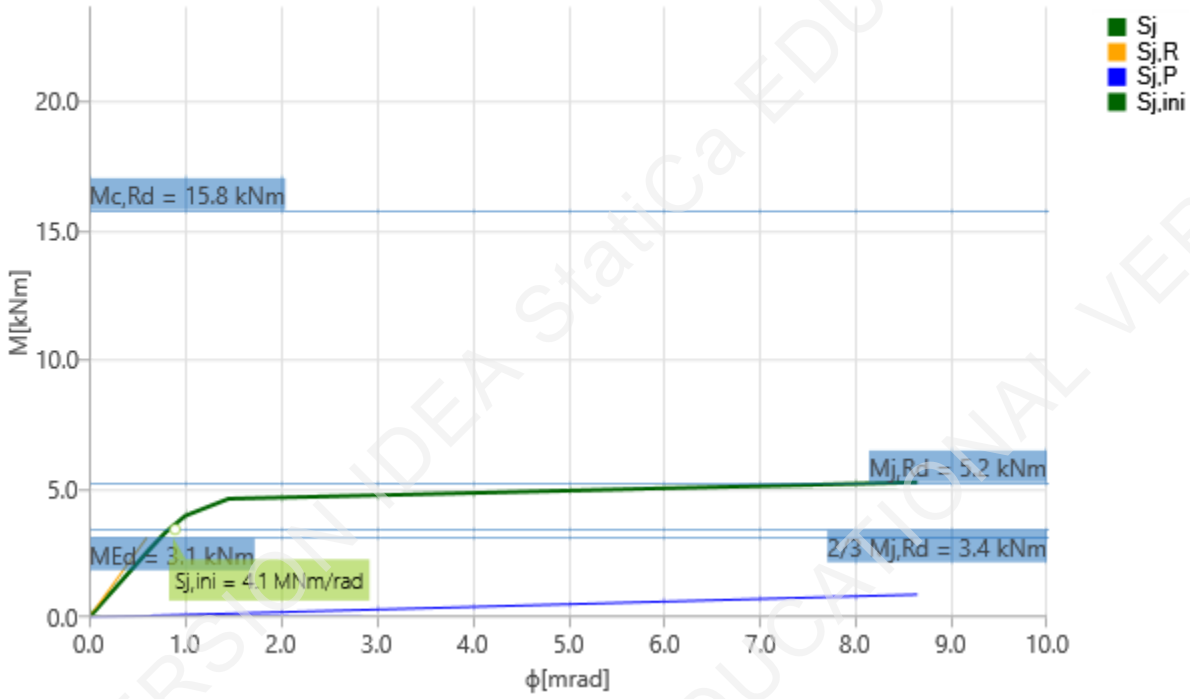
Secant rotational stiffness

Name	Comp.	Loads	M [kNm]	Sjs [MNm/rad]	Φ [mrad]
M1	My	LE1	3.1	4.2	0.7

Symbol explanation

$M_{j,Rd}$	Bending resistance
$S_{j,ini}$	Initial rotational stiffness
$S_{j,s}$	Secant rotational stiffness
Φ	Rotational deformation
Φ_c	Rotational capacity
$S_{j,R}$	Limit value - rigid joint
$S_{j,P}$	Limit value - nominally pinned joint

Project:
 Project no:
 Author:



Stiffness diagram My - ϕ , LE1

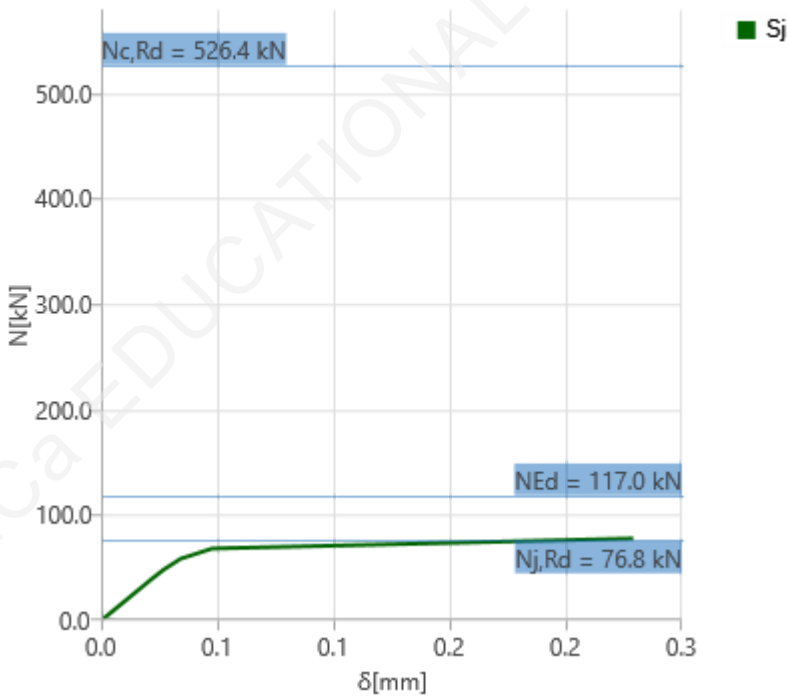
Axial stiffness

Name	Component	Loads	N [kN]	N _{j,Rd} [kN]	dx [mm]	St [MN/m]
M1	N	LE1	117.0	76.8	0	321

Symbol explanation

- N_{j,Rd} Tension (compression) resistance
- S_t Secant axial stiffness
- δ Longitudinal deformation

Project:
Project no:
Author:



Stiffness diagram N - δ , LE1

Cost estimation

Steel

Steel grade	Total weight [kg]	Unit cost [€/kg]	Cost [€]
S 355	3.31	2.00	6.61

Bolts

Bolt assembly	Total weight [kg]	Unit cost [€/kg]	Cost [€]

Welds

Weld type	Throat thickness [mm]	Leg size [mm]	Total weight [kg]	Unit cost [€/kg]	Cost [€]
Fillet rear	3.0	4.2	0.12	40.00	4.64

Hole drilling

Bolt assembly cost [€]	Percentage of bolt assembly cost [%]	Cost [€]

Cost summary

Cost estimation summary	Cost [€]
Total estimated cost	11.25

Project:
 Project no:
 Author:

Code settings

Item	Value	Unit	Reference
YM0	1.00	-	EN 1993-1-1: 6.1
YM1	1.00	-	EN 1993-1-1: 6.1
YM2	1.25	-	EN 1993-1-1: 6.1
YM3	1.25	-	EN 1993-1-8: 2.2
YC	1.50	-	EN 1992-1-1: 2.4.2.4
YInst	1.20	-	EN 1992-4: Table 4.1
Joint coefficient β_j	0.67	-	EN 1993-1-8: 6.2.5
Effective area - influence of mesh size	0.10	-	
Friction coefficient - concrete	0.25	-	EN 1993-1-8
Friction coefficient in slip-resistance	0.30	-	EN 1993-1-8 tab 3.7
Limit plastic strain	0.05	-	EN 1993-1-5
Weld stress evaluation	Plastic redistribution		
Detailing	No		
Distance between bolts [d]	2.20	-	EN 1993-1-8: tab 3.3
Distance between bolts and edge [d]	1.20	-	EN 1993-1-8: tab 3.3
Concrete breakout resistance check	Both		EN 1992-4: 7.2.1.4 and 7.2.2.5
Use calculated a_b in bearing check.	Yes		EN 1993-1-8: tab 3.4
Cracked concrete	Yes		EN 1992-4
Local deformation check	No		CIDECT DG 1, 3 - 1.1
Local deformation limit	0.03	-	CIDECT DG 1, 3 - 1.1
Geometrical nonlinearity (GMNA)	Yes		Analysis with large deformations for hollow section joints
Braced system	No		EN 1993-1-8: 5.2.2.5

